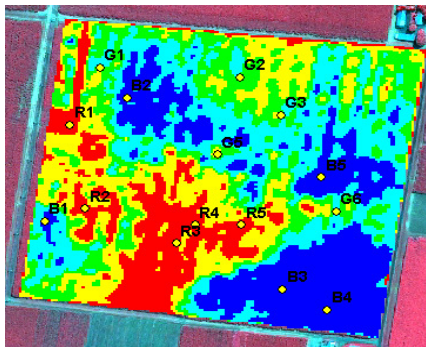


**FINAL REPORT- SRDC PROJECT DPI021
REMOTE SENSING- BASED PRECISION AGRICULTURE TOOLS
FOR THE SUGAR INDUSTRY**

BY

ANDREW ROBSON, CHRIS ABBOTT, ROB BRAMLEY, DAVID LAMB





Australian Government

**Sugar Research and
Development Corporation**

Final Report

SRDC Project DPI021

Remote Sensing- based Precision Agriculture Tools for the Sugar Industry

ANDREW ROBSON¹, CHRIS ABBOTT¹, ROB BRAMLEY², DAVID LAMB³

¹Department Agriculture, Fisheries and Forestry, Queensland. Kingaroy. 4610.

²CSIRO Ecosystem Sciences, Adelaide. SA. 5064.

³Precision Agriculture Research Group, University of New England. Armidale NSW. 2351.

Project commencement date: August 2009
Project completion date: March 2013
SRDC Program: Regional Futures
SRDC Strategy: Farming and harvesting systems

Administrator: Helen Kamel
Organisation: Dept. of Agriculture, Fisheries and Forestry, Qld
Postal Address: PO Box 241 Darling Heights Qld 4350.
Ph: +61 7 4631 5380 **Fax:** +61 7 44631 5378 **E-mail:** Helen.kamel@daff.qld.gov.au

Principal Researcher: Dr Andrew Robson (Senior Research Scientist)
Organisation: Dept. of Agriculture, Fisheries and Forestry, Qld
Postal Address: PO Box 23 Kingaroy Queensland 4610.
Ph: +61 7 41600735 **Fax:** +61 7 41623238 **E-mail:** andrew.robson@daff.qld.gov.au

Additional Researchers:
Chris Abbott (DAAF Qld): chris.abbott@daff.qld.gov.au
David Lamb (UNE): dlamb@une.edu.au
Rob Bramley (CSIRO): Rob.Bramley@CSIRO.au

Table of Contents

1. Executive Summary.	5
2. Publications/ Project extension.	7
3. Background.	9
4. Objectives.	10
5. Methodology.	11
5.1. Site locations.	11
5.2. Image pre-processing.	15
5.2.1. Converting ‘At Sensor’ digital numbers to ‘Top of Atmosphere’ reflectance values.	15
5.2.2. Geographic registration of imagery and vector data.	15
5.3. Extracting spectral data from imagery using mill vector data.	15
5.4. Derivation of vegetation indices.	16
5.5. Collection of field data for ground truthing imagery.	17
5.6. Developing image based yield maps from field sampled data:	20
5.7. Development of a generic yield algorithm:	20
5.8. Regional predictions of average yield using a ‘generic’ algorithm:	21
5.9. Derivation and distribution of yield maps at the regional scale using yield prediction algorithms.	21
5.10. Validation of image derived yield maps.	21
5.11. Correlating image results against harvester derived yield maps (CSE022).	22
6. Results.	23
6.1. Benchmarking and identifying the most feasible and suitable commercial imagery (i.e. spatial resolution, repeat time and economic feasibility) for identifying crop variability and thus directing targeted mid-season management within the Australian cane industry.	23
6.1.1. Evaluation of the Raptor sensor.	24
6.2. Identifying the optimum time of image capture that will accurately depict mid- season crop variability whilst avoiding seasonal times most prone to cloud cover, across key Australian cane farming regions. ³⁴	
6.2.1. Using spatial technologies to identify growth variability in cane crops, likely constraints to production and suggested remedial action.	35
6.3. Assess the utility of this imagery for explaining the yield variability measured through the CSE022 “A coordinated approach to Precision Agriculture RDE for the Australian Sugar Industry’ project.	46
6.3.1. CSEO22 sites.	47
6.3.2. Additional yield validation sites.	52
6.3.3. Derivation of a generic algorithm.	55
6.3.4. Validation of the generic algorithm at the regional level.	56
6.3.5. Validation of the generic algorithm at the block and within block level.	65
6.3.6. Production of classified yield maps using the generic algorithms.	68

6.4. Implement optimal image processing and delivery protocols for the rapid distribution of classified imagery to agronomists, growers etc.	71
6.5. Provide recommendations to participating growers, consultants and industry representatives on the potential cost / benefit of implementing RS technologies into current agronomic management practices.	72
7. Conclusion.	75
8. Acknowledgements.	76
9. References.	76
10. Appendix 1: Tutorials.	80
Tutorial 1: ENVI: Converting 'At Sensor' Digital Numbers to 'Top of Atmosphere' reflectance values	80
Tutorial 2: ENVI: Georectification of satellite imagery using an orthorectified base layer and derivation of a GNDVI image.	87
Tutorial 3: ArcGIS: Conversion of Mapinfo (.TAB) files into ArcGIS (.SHP) files.	91
Tutorial 4: ArcGIS: Buffering of polygons and removal of those affected by cloud before the extraction of spectral data.	92
Tutorial 5: Starspan GUI: Extracting average spectral values and associated attribute information for multiple blocks.	95
Tutorial 6: ENVI: Producing a classified vegetation index map of a cane crop from a 4 band satellite image.	97
Tutorial 7: ENVI: Extracting point source spectral information from imagery using regions of interest (ROI's).	100
Tutorial 8: ENVI: Converting VI pixel values into yield (TCH) using an exponential linear algorithm.	101
Tutorial 9: ENVI: Creating Google Earth KMZ files from Geotiffs.	102
11. Appendix 2: Media/ Publications.	105
2012 ASSCT presentation.	105
Article in Australian Sugarcane. February- March 2011.	115
2011 ASSCT Poster presentation.	119
2010 ASSCT Poster presentation.	122
Article in the Burdekin 'The Advocate' Newspaper promoting the presentation at Burdekin Productivity Services Annual General Meeting 16 th August 2011.	124
SRDC promotion of DPI021 involvement in the Herbert Resource Information Centre Spatial Community in Action Conference. Ingham (18-19 August 2011)	124
Hand out for BSES cane talks	125
The SRDC sugar cane project (DPI021) featured in a Department of Innovation, Industry, Science, and Research (DIISR): Space Policy Unit (SPU) handout promoting Earth Observation R&D being conducted in Australia	126
Article in the Australian Canegrower, December 2010: 16."Cane monitoring made easy with new sensor"	127
Flier promoting SRDC Webinar conducted 22 February 2013.	128
12. Appendix 3: Project contracts and variations.	129

1. Executive Summary

This project aimed to develop remote sensing applications that were both relevant and of commercial benefit to the Australian sugar industry and therefore adoptable. Such applications included the in season mapping of crop vigour so as to guide future management strategies, the identification of specific abiotic and biotic cropping constraints, and the conversion of GNDVI variability maps into yield at the block, farm and regional level. In order to achieve these applications the project team reviewed an array of remote sensing platforms, timing of imagery capture, software and analysis protocols; as well as distribution formats of derived imagery products, to a range of end users. The project developed strong collaborative linkages with all levels of the industry including mills, productivity services, agronomists, growers and researchers and increased its initial coverage from three individual farms in Bundaberg, Burdekin and the Herbert, coinciding with project CSE022, to include over 33,000 crops grown across 6 growing regions (Mulgrave, Herbert, Burdekin, Bundaberg, ISIS and Condong) during the 2011/2012 season.

The remote sensing systems evaluated throughout this project included ALOS (1 capture), SPOT5 (12), SPOT4 (1), RapidEYE (4), IKONOS (21), GeoEYE (1) and Raptor aerial active sensor (3). These systems provided a range of passive and active sensors, spatial and spectral resolutions, revisit times, cost and processing requirements. Overall, imagery from the French owned SPOT5 satellite, supplied by Astrium (<http://www.astrium-geo.com/>), was identified to be the most suitable for a range of applications. A single SPOT5 scene (3600km²) encompassed the majority of cane crops within a particular growing region therefore eliminating the need for additional image processing such as mosaicing and colour balancing. The imagery was shown to be cost effective at ~AUS\$1 per km² and owing to its 2-3 day revisit time, provide sufficient operational flexibility to acquire cloud free imagery during periods of continual cloud cover. The spectral resolution of SPOT5 (green, red, near and mid infrared) allowed most accepted vegetation indices to be derived, with a greenness normalised difference vegetation index (GNDVI) exhibiting the strongest correlation with yield in terms of tonnes of cane per hectare (TCH). At the block level, the classified GNDVI 'zonal' vigour maps produced from the 10 metre spatial resolution images were comparable to that generated from the higher spatial resolution systems. However they proved unable to discern sub metre constraints such as weed infestations and damage resulting from grubs, soldier fly, rat and feral pig. The pan sharpened IKONOS product (0.8 metre spatial resolution) was shown to be effective in identifying such sub metre constraints and was the most cost effective at AUS\$22 per km² when purchased as three 50 km² areas of interest, as supplied by Geoimage (<http://www.geoimage.com.au/geoimage/>) and AAM (<http://aamgroup.com/>).

The active airborne Raptor sensor was also evaluated, with a number of tests conducted to identify the optimal image capture protocols for sugar cane. The optimal flying height was identified to be between 100 and 135 ft above ground level with data collected at transects not exceeding 50 metres apart. Although the direction in which the data was collected i.e. along or across cane rows was shown to have little influence, an internal buffer of 15m was

required to remove 'edge' effects from non cane specific targets. The crop vigour maps derived from the Raptor sensor were found to be highly comparable to those produced from IKONOS imagery, supporting the recommendation that the Raptor sensor, once commercialised could be an effective option for the Australian cane industry.

Through this project, remote sensing was demonstrated to be an accurate tool for identifying the spatial variability of crop vigour at the individual block and farm level. By deriving 5 colour class NDVI maps, growers were able to identify the extent of low performing regions and through targeted plant and soil testing determine the likely nature of the constraint. It was initially envisaged that growers supplied with this information could implement remedial action within that growing season. However, consistent cloud cover over most Queensland growing regions between January and March greatly limited the availability of this information within the crucial vegetative stage of the crop. This delay meant that when the information was provided, the crop was at a growth stage and height that made remedial action of little value or mechanically impossible. Imagery captured during the early vegetative growth stage, i.e. during December, may provide useful and timely information that can assist within season remedial action but this was not evaluated through this project. The mid season variability maps that were generated through this project did support alternative management strategies post-harvest, such as the zonal applications of silica, fertilizer, mill mud as well as re- land forming of blocks. It is

For the prediction of yield, strong correlations between GNDVI and tonnes of cane per hectare were achieved from imagery acquired between March and May. This time frame was believed to coincide with a stabilisation period of cane growth between vegetative development and maturation, a hypothesis supported by other research. The derivation of a non cultivar and non class specific algorithm for converting GNDVI values into yield achieved regional predictions to within 5% agreement to what was actually achieved for the Bundaberg, Isis, Herbert and Condong growing regions. An additional algorithm was developed for the Burdekin region to account for the vastly different climatic conditions. Although the yield estimates were encouraging, additional research is required to understand and then account for the impact of variable seasonal conditions. This may require the integration of an agro-meteorological model to normalise the seasonal trends or more simply the development of slightly refined algorithms that represent 'good' and 'bad' years.

In an attempt to extrapolate the accuracies of the yield predictions to the sub block level, the project team developed methodologies for the derivation of image based yield maps from both high and mid spatial resolution imagery. Using comprehensive GIS vector data layers provided by each mill and the freeware software Starspan GUI, spectral information for the majority of cane crops within each growing region was extracted. For the 2012 growing season each pixel value (GNDVI) was converted into TCH using the appropriate regional GNDVI algorithm, with each block then segregated into 8 yield classes. These surrogate yield maps were then distributed to industry via a number of formats including GoogleEarth (kmz) files, GeoTiffs, static images or embedded in documents. Although the predictions of average block yield and the spatial trends of crop performance were shown to

be accurate across some locations, others were highly inaccurate. This varied result indicates that further research is required to ensure a greater degree of precision is achieved. This will likely require the development of algorithms for specific class and variety and possibly sub-growing regions.

The software ENVI (<http://www.exelisvis.com/ProductsServices/ENVI.aspx>) was identified to be suitable for remote sensing data analysis, whilst for the querying and manipulation of vector data ArcGIS (<http://www.esri.com/software/arcgis>) was used. To assist with the future adoption of these technologies analysis protocols developed through this project are provided as training tutorials within the appendices of this report.

The Department of Agriculture, Fisheries and Forestry, Queensland (DAAF Qld) with CSIRO and UNE greatly appreciate the opportunity provided by the SRDC to undertake this research and acknowledge the input and collaboration from a number of industry partners. It is believed that the results of this research will support the increased adoption of remote sensing technologies by the Australian sugar industry.

2. Publications/Project Extension

Publications:

- Andrew Robson, Chris Abbott, David Lamb, Rob Bramley and Mary Barnes (2012). Deriving sugar cane yield maps from SPOT 5 satellite imagery at a regional scale. Poster Abstract. Proceedings of the International Society of Sugar Cane Technologists workshop. Townsville, Qld. 10 – 14 September 2012.
- Andrew Robson, Chris Abbott, David Lamb and Rob Bramley (2012). Developing sugar cane yield algorithms from satellite imagery. Proceedings of the Australian Society of Sugar Cane Technologists. 34th Conference, Cairns, Qld. 1- 4 May 2012.
- Andrew Robson, Chris Abbott, David Lamb and Rob Bramley (2011). Paddock and regional scale yield prediction of cane using satellite imagery. Poster Abstract. Proceedings of the Australian Society of Sugar Cane Technologists. 33rd Conference, Mackay, Qld. 4 -6 May 2011.
- Andrew Robson, Chris Abbott, David Lamb and Rob Bramley (2011). Satellite remote sensing of sugarcane- some FAQs. Australian Sugarcane. February- March 2011.
- A. Robson, J.R. Hughes and R.J. Coventry (2010). Using spatial layers to understand variability in precision agricultural systems for sugarcane production. Poster abstract. In Proceedings of the 32nd conference of the Australian Society of Sugar Cane Technologists. Bundaberg. Qld. 11 – 14 May 2010.
- Robson, A.J., Wright, G.W., Bell, M.J., Medway, J., Hatfield, P., and Rao. C.N. Rachaputi (2009). Practical remote sensing applications for the Peanut, Sugar cane

and Cotton Farming Systems. Poster presentation and abstract. 13th Annual Symposium of Precision Agriculture in Australasia. Armidale, NSW. 10- 11th September 2009.

Research referred to in:

- Bramley RGV, Trengove S. 2012. Precision Agriculture in Australia: present status and recent developments. In ConBap 2012 - Proceedings Congresso Brasileiro de Agricultura de Precisão, Ribeirão Preto - SP, Brasil. 24 to 26 September.
- Bramley RGV. 2012. Precision Agriculture: Opportunities for Improved Management of Sugarcane Production. In: RA Gilbert (Ed) Sustainable sugarcane production. Proceedings of the International Society of Sugar Cane Technologists workshop. Townsville, Qld. 10 – 14 September 2012.
- Mike Bell, Steve Walker, Andrew Robson, David Jordan and Dave Murray (2009). The evolution of modern cropping systems *In National Water and Environment Bulletin*. Spring 2009. Page 43- 47.

Project extension/ Professional engagements:

- 2013 (22 February): SRDC Webinar presentation of project results.
- 2012 (24 October): Project results presented at Sugar Research and Development Corporation (SRDC) seminar series. Queensland University of Technology (QUT), Brisbane.
- 2012 (14- 15 May): Project results presented at Sugar Research and Development Corporation (SRDC) research exposition: Mackay, Proserpine.
- 2012 (9- 11 May): Project results presented at Sugar Research and Development Corporation (SRDC) research exposition: Maryborough, Murwillumbah and MacLean.
- 2012 (1- 4 May): Project results presented at the 34th conference of the Australian Society of Sugar Cane Technologists. Cairns, QLD.
- 2011 (25 November): Project results presented to growers/ ISIS mill and Canegrowers representatives at Childers.
- 2011 (1 October): Project results presented to a World Congress of Conservation Agriculture (WACCA) tour group, Kingaroy, Qld.
- 2011 (31 August): Project meeting phone conference.
- 2011 (18- 19 August): Project results presented at Herbert Resource Information Centre Spatial Community in Action Conference. Ingham. Qld.
- 2011 (16 August): Guest speaker at Burdekin Productivity Service annual general meeting. Ayr.
- 2011 (4- 6May): Poster presentation at the 33rd Conference of the Australian Society of Sugar Cane Technologists. Mackay, Qld.
- 2011 (14- 16 March): Project results presented at 6 BSES CPI meetings in the Burdekin region (115 participants).
- 2011 (15- 22 February): Project results presented at 6 BSES CPI meetings in the Bundaberg region (81 participants).

- 2010 (3 September): Poster presentation at the 14th Annual Symposium of Precision Agriculture in Australasia. Albury, NSW. 2- 3 September 2010
- 2010 (11- 14 May): Poster presentation at the 32nd conference of the Australian Society of Sugar Cane Technologists. Bundaberg. Qld.
- 2010 (4 March): Project meeting at SRDC head Office, Brisbane.
- 2009 (1 December): ENVI training course for industry collaborators, Mackay (5 participants).
- 2009 (26 November): Project results presented at 'Southern Queensland Farming Systems' field day. Kingsthorpe, Qld.
- 2009 (3 November): Project introduction meeting for industry collaborators in Bundaberg (19 participants).
- 2009 (16 October): Project introduction meeting for industry collaborators in Townsville (15 participants).
- 2009 (15 October): Project introduction meeting for industry collaborators in Mackay (5 participants).
- 2009 (10- 11 September): Poster presentation at the 13th Annual Symposium on Precision agriculture in Australia. Armidale, NSW.

3. Background

The last decade has seen a major global increase in the development and application of spatial technologies, driven by improved access to high quality, cost efficient remote sensing platforms; intelligent analysis softwares; enhanced computer processing and data storage capacities and image delivery systems including GoogleEarth. In terms of agriculture, decades of research across multiple cropping systems has identified remotely sensed (RS) imagery as an effective tool for identifying mid season spatial variability in crop vigour and yield. This information when incorporated into a Geographic Information System (GIS) has facilitated the adoption of precision agriculture, particularly targeted sampling and then variable rate technologies, applications that can reduce input costs whilst maintaining or increasing productivity. It has also provided an effective tool for in season yield forecasting, supporting decisions regarding harvest management, as well as the handling, storage and forward selling of produce post harvest.

The Australian sugar industry has widely adopted GIS as an essential framework for the recording and managing spatial data (Davis *et al.* 2007). The mills themselves implement comprehensive GIS vector layers that spatially define and detail every crop within their specified growing region. This has greatly increased the integration of mill and productivity datasets, thus enabling greater efficiencies in data retrieval and analysis of client information (Markley *et al.* 2008). A whole-of-community GIS system developed for the Herbert River sugar district has the capacity to record real-time cane harvester operations via GPS. This has improved the coordination and planning of the cane harvest, the identification of consignment errors and been used to improve the safety and efficiency of the rail transport infrastructure (De Lai *et al.* 2011). The establishment of such integrated GIS system supports the use of remote technologies, by allowing the rapid extraction of spectral data via crop

boundaries, data interrogation based on variety and class, and re-distribution of derived imagery products using the existing GIS framework.

Globally, remote sensing has been shown to be an effective yield prediction tool (Fernandes *et al.* 2011; Benvenuti and Weill 2010; Bégué *et al.* 2010; Simões *et al.* 2009; Abdel-Rahman and Ahmed 2008; Bégué *et al.* 2008; Almeida *et al.* 2006; Simões *et al.* 2005; Krishna Rao *et al.* 2002; and Rudorff and Batista 1990). However, research in Australia has been limited (Noonan. 1999; Markley *et al.* 2003; Robson *et al.* 2011; Robson *et al.* 2010; Lee-Lovick and Kirchner 1991). Commercially, Mackay Sugar Ltd has been the predominant adopter of satellite imagery as a commercial yield forecasting tool, by utilising yield prediction algorithms derived from SPOT2 imagery (Markley *et al.* 2003). However, this has not been extrapolated to the other Australian growing regions. This project aimed to address that shortfall. In regards to the use of remote sensing technologies for mid season detection of crop variability there has also been little adoption by the Australian sugar industry. This is believed to be the result of a lack of awareness of the technologies available, insufficient evidence supporting the cost/benefits of adoption, limited expertise to analyse current high resolution data, an inability to image cropping regions due to continued cloud cover or lack of access to the information close to 'near real time'.

This project was developed to produce practical and relevant benchmarks, protocols and recommendations for the adoption of remote sensing technologies for improved in season management and therefore production within the Australian sugar cane industry.

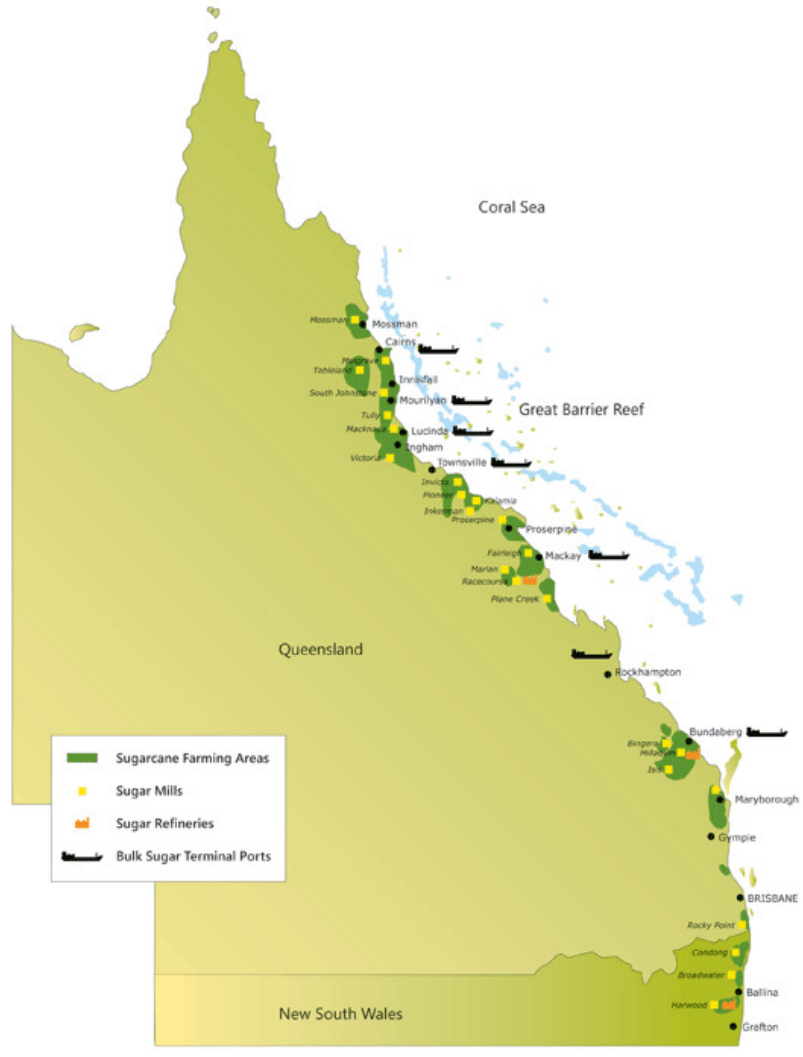
4. Objectives

1. Benchmarking and identifying the most feasible and suitable commercial imagery (i.e. spatial resolution, repeat time and economic feasibility) for identifying crop variability and thus directing targeted mid-season management within the Australian cane industry.
2. Also the optimum time of image capture that will accurately depict mid- season crop variability whilst avoiding seasonal times most prone to cloud cover, across key Australian cane farming regions.
3. Assess the utility of this imagery for explaining the yield variability measured through the CSE022 'A coordinated approach to Precision Agriculture RDE for the Australian Sugar Industry' project.
4. Implement optimal image processing and delivery protocols for the rapid distribution of classified imagery to agronomists, growers etc.
5. Provide recommendations to participating growers, consultants and industry representatives on the potential cost / benefit of implementing RS technologies into current agronomic management practices.

5. Methodology

The following section details a number of methodologies and analysis protocols developed by this project in order to deliver on its objectives.

5.1. Site locations.



http://www.canegrowers.com.au/page/Industry_Centre/about-sugarcane/Statistics_facts_figures/

Figure 1. Location of Australian sugar growing regions and associated mills.

This project had an initial focus area of one individual farm within each of the Australian intensive cropping regions of Bundaberg, Burdekin and the Herbert (Figure 1). The three farms Pozzebon (Burdekin) (Figure 2a), Hubert (Bundaberg) (Figure 2b), and Tabone (Herbert) (Figure 2c) coincided with SRDC project (CSE022) 'A collaborative approach to Precision Agriculture RDE for the Australian Sugar Industry'. The rationale behind the mutual site selections was that this project would supply image derived vigour maps indicating within crop spatial variability that could be compared to the spatial trends produced from the yield monitors being evaluated by CSE022. In return the field sampled yield data collected by CSE022 would assist in the calibration of imagery to yield.

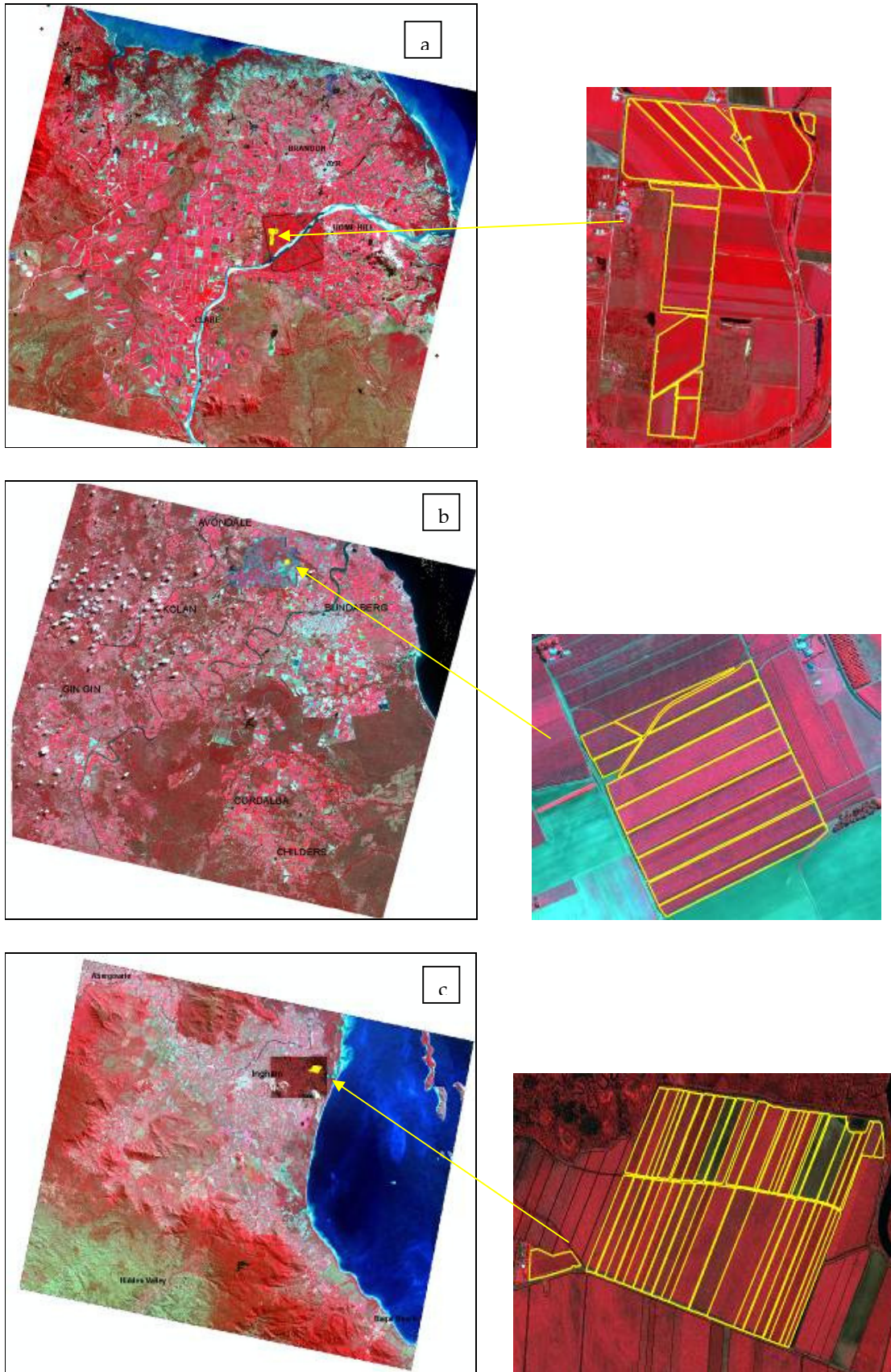


Figure 2. False colour SPOT5 image coverage (3600km²) of three Australian cane growing regions, with each of the CSE022 sites highlighted in yellow a. Pozzebon: Burdekin; b. Bundaberg: Hubert; c. Tabone; Herbert.

The false colour images presented in Figure 2, are three band composite image (green, red, and near infrared) with the brighter the red/ pink colour the more vigorous the vegetative growth.

As well as image analysis undertaken on the individual farms identified in Figure 2, a number of additional properties were also investigated. Classified GNDVI vigour maps were derived for each of the 974 can blocks (Table 1), and distributed to growers via GoogleEarth or as static documents.

Table 1: GNDVI vigour and derived yield maps distributed to growers during the project.

Grower	Location	Blocks	Grower	Location	Blocks
Bullseye Farming	Bundaberg	30	Fiamingo	Burdekin	2
Cayley	Bundaberg	29	Fowler	Burdekin	6
Halpin	Bundaberg	26	Haigh	Burdekin	28
Hubert	Bundaberg	32	Linton JK	Burdekin	20
Lewis	Bundaberg	13	Lyons	Burdekin	27
Pegg	Bundaberg	9	Luckel	Burdekin	52
Relmay Farming	Bundaberg	56	Mann A	Burdekin	6
Scott	Bundaberg	12	Mann B	Burdekin	12
Russo	Childers	88	Mann K	Burdekin	18
Kangas	Herbert	18	Populin	Burdekin	48
Morley	Herbert	3	Pozzebon	Burdekin	11
Tabone	Herbert	20	Setter	Burdekin	7
BSES trials	Gordnonvale	2	Scarbossa	Burdekin	24
Bugeja	Mackay	1	SISI farming	Burdekin	40
Attard	Burdekin	24	Sorbella	Burdekin	12
Burrows	Burdekin	97	Strathdee	Burdekin	14
BSES trials	Burdekin	20	Ianmurb	Burdekin	11
Cacciola	Burdekin	11	Jordan	Burdekin	12
Catalano	Burdekin	30	Kelly	Burdekin	9
Darween	Burdekin	19	Linton A	Burdekin	9
Davco	Burdekin	53	Linton J	Burdekin	15
<i>Total</i>					974

In order to deliver on the first project objective, imagery from an array of platforms was acquired on multiple occasions over the Burdekin, Herbert and Bundaberg growing regions. Some additional Australian cane growing regions were also included (Table 2).

Table 2. Inventory of imagery:

Location	Sensor	Spatial resolution	Acquisition date	Area covered
Herbert	LIDAR		9-Aug-09	sample area
Bundaberg	RapidEYE	5m	1-Mar-09	sample area
Bundaberg	RapidEYE	5m	30-Jun-09	sample area
Bundaberg	ALOS	10m	17-Jan-10	5000km2
Bundaberg	SPOT5	10m	10-May-10	3600km2
Bundaberg	SPOT5	10m	14-Apr-10	3600km2
Bundaberg (CSE022 sites)	IKONOS	0.8m PS	14-May-10	50km2
Burdekin	SPOT5	10m	14-May-10	3600km2
Burdekin	TerraSAR-X	3m	28-Jun-10	sample area
Burdekin (CSE022 site)	IKONOS	0.8m PS	28-May-10	50km2
Burdekin	IKONOS	0.8m PS	11-Jun-10	50km2
Herbert	IKONOS	0.8m PS	16-Aug-10	50km2
Herbert	IKONOS	0.8m PS	22-Jun-10	50km2
Gordonvale	IKONOS	0.8m PS	18-Mar-10	50km2
Mackay	RapidEYE	5m	6-Mar-10	sample area
Mackay	IKONOS	0.8m PS	19-Jun-10	50km2
Mackay	SPOT4	20m	11-Apr-10	3600km2
Mackay	TerraSAR-X	3m	May-10	sample area
Bundaberg (CSE022 sites)	IKONOS	0.8m PS	23-Mar-11	50km2
Bundaberg (CSE022 sites)	IKONOS	0.8m PS	30-Apr-11	50km2
South Bundaberg	IKONOS	0.8m PS	23-Mar-11	50km2
South Bundaberg	IKONOS	0.8m PS	30-Apr-11	50km2
Farnsfield (Bundaberg)	IKONOS	0.8m PS	25-May-11	50km2
Herbert (CSE022 site)	IKONOS	0.8m PS	1-May-11	50km2
Burdekin (CSE022 site)	IKONOS	0.8m PS	12-May-11	50km2
Burdekin	IKONOS	0.8m PS	20-Apr-11	50km2
Mona Park (Burdekin)	IKONOS	0.8m PS	28-May-11	50km2
Bundaberg	SPOT5	10m	27-Mar-11	3600km2
Burdekin	SPOT5	10m	22-Apr-11	3600km2
Herbert	SPOT5	10m	5-May-11	3600km2
Bundaberg (CSE022 sites)	UNE Raptor system	Varying	23-Feb-11	3 individual crops
Bundaberg (CSE022 sites)	UNE Raptor system	Varying	23-Mar-11	3 individual crops
Bundaberg (CSE022 sites)	UNE Raptor system	Varying	2-May-11	3 individual crops
Gordonvale	RapidEYE	5m	12-Apr-11	sample area
Mackay	IKONOS	0.8m PS	25-May-11	50km2
Herbert (CSE022 site)	IKONOS	0.8m PS	11-Apr-12	50km2
Herbert	SPOT5	10m	4-Apr-12	3600km2
Bundaberg (CSE022 site)	IKONOS	0.8m PS	6-Apr-12	50km2
Bundaberg	SPOT5	10m	1-Apr-12	3600km2
Mulgrave	GeoEYE	0.5m PS	4-May-12	50km2
Burdekin	SPOT5	10m	16-May-12	3600km2
Burdekin	IKONOS	0.8m PS	11-Apr-12	50km2
Burdekin	IKONOS	0.8m PS	25-Mar-12	50km2
Burdekin (CSE022 site)	IKONOS	0.8m PS	28-Mar-12	68km2
Northern NSW	SPOT5	10m	29-Feb-12	3600km2

* PS refers to pan sharpening, where the spatial resolution of a multispectral imagery can be increased by using an additional panchromatic band. Pan-sharpened images were not used for algorithm development.

At the time of this project, an individual SPOT5 image (3600km²) supplied by Astrium (<http://www.astrium-geo.com/>) cost AU\$3465 per scene (AU\$0.96/km²), with additional processing such as orthorectification attracting an additional fee (AU\$500). The cost of an IKONOS image was US\$1100 (US\$22/km²) per scene when purchased under a three * 50km² image capture deal; again, additional processing attracted additional fees (AU\$687.50). The evaluation RapidEYE data was provided by AAM (<http://aamgroup.com/>): The airborne Raptor data acquired by the University of New England cost on average AU\$8,000 per flight. However 75% of the cost covered the ferry of the aircraft/sensor to site locations (~ return flight time from Armidale to Bundaberg). The sensor and flight specifications are as follows: Dual wavelength Red (658 nm: 17 nm fwhm) and NIR (850 nm: 32 nm fwhm);

irradiance footprint divergence angle of $\sim 14^\circ \times 8^\circ$ from source; 5 Hz GPS (Garmin GPS18x5 Hz, Olathe KA USA) plus interpolation setting on GeoScout providing ~ 17 Hz position calculation rate. The data was collected at an airspeed of ~ 100 knots with a flight transect width of 3m. Data was collected on three occasions (Table 2) with multiple flights over the Relmay site (23 Feb 2011) to assess the impact of height (100 ft, 135 ft and 180 ft Above Ground Level (AGL)) and flight direction (across rows and with cane rows) on the resultant kriged NDVI image.

5.2. Image pre-processing.

5.2.1. Converting 'At Sensor' digital numbers to 'Top of Atmosphere' reflectance values.

To allow temporal comparison, all satellite imagery was corrected for variable atmospheric conditions using a 'top of atmosphere' (TOA) correction. To assist in the future adoption of these analysis protocols, the theory and methodology for applying this correction to a number of commercial satellites is detailed below. An ENVI tutorial for undertaking this correction is also supplied as *Appendix 1: Tutorial 1: ENVI: Converting 'At Sensor' Digital Numbers to 'Top of Atmosphere' reflectance values.*

5.2.2. Geographic registration of imagery and vector data.

So that all vector and raster data obtained throughout this project could be spatially compared and subsequently analysed it was reprojected to: *Projection:* Transverse Mercator; *Datum:* Geocentric Datum of Australia 1994 (GDA94).

For the raster data, the initial image for each site was purchased as an orthorectified product. This is an image with high spatial integrity as it has been corrected for both topographic relief (provided by a digital elevation model: DEM) and vertical aspect. The orthorectified images were used as base layers, in which all subsequent imagery for each respective region was 'warped' to, using an image-to-image rectification process, refer to *Appendix 1: Tutorial 2: ENVI: Georectification of satellite imagery using an orthorectified base layer and derivation of a GNDVI image.* This process was suitable for most growing areas investigated due to their relatively flat topography. However, for more undulating regions such as Mulgrave, it is recommended that all images should be orthorectified.

The registration accuracy of mill vector data, was generally high. However some exceptions indicated the need for a degree of quality assurance before further analysis. One issue identified was the compatibility of information when transferred from one GIS software to another. The Mills generally use the MapINFO, whilst the project team used ArcGIS. The obvious solution is for all parties to use the same software. However where this issue does occur a tutorial has been included in this report for the importing of MapINFO Tab files into ArcGIS as SHP files (*Appendix 1: Tutorial 3: ArcGIS: Conversion of Mapinfo (.TAB) files into ArcGIS (.SHP) files.*)

5.3. Extracting spectral data from imagery using mill vector data.

For the development and then implementation of the generic yield prediction algorithms, a methodology was developed for the rapid extraction of spectral information from each image using the respective mill vector boundaries. Firstly, to ensure the spatial data was specific to cane, all boundaries outside of the image extent were removed, as well as those obscured by cloud or cloud shadows. An internal buffer was then applied to each crop boundary to ensure the image pixels used to extract spectral information did not include spectral data specific to headlands, roads, buildings etc. A tutorial has been included for undertaking these processing steps with the software ArcGIS (*Appendix 1: Tutorial 4: ArcGIS: Buffering of polygons and removal of those effected by cloud before the extraction of spectral data*).

The freeware Starspan GUI was used to extract the average spectral information for the 4 band widths for each selected crop. These average values were exported in a .CSV file format along with the Mill attribute data corresponding to each crop, and interrogated within Microsoft Excel. A tutorial detailing the use of Starspan GUI is provided in the appendices of this report (*Appendix 1: Tutorial 5: Starspan GUI: Extracting average spectral values and associated attribute information for multiple blocks*).

5.4. Derivation of vegetation indices.

Vegetation indices or band ratios are highly effective for identifying variations in plant vigour whilst also minimising errors associated with atmospheric attenuation, plant shading and interference from soil reflectance. The commonly used Normalised Difference Vegetation Index (NDVI) does address some atmospheric attenuation and shading. However it can saturate in large biomass crops such as sugar cane with a leaf area index (LAI) greater than 3 (Benvenuti and Weill 2010; Bégué *et al.* 2010; Xiao 2005; Xiao *et al.* 2004b; Xiao *et al.* 2004a; Huete *et al.* 2002; Huete *et al.* 1997). Therefore, following a review of published literature, a number of structural and pigment based indices were investigated to identify which one consistently produced a higher correlation with sugar cane yield (TCH) (Table 3).

Table 3: Vegetation indices assessed for their correlation to sugar yield (TCH)

Normalised Difference Vegetation Index (NDVI)	$R_{NIR} - R_{Red} / R_{NIR} + R_{Red}$
GreenNDVI	$R_{NIR} - R_{Green} / R_{NIR} + R_{Green}$
MidIRNDVI	$R_{MIR} - R_{Red} / R_{MIR} - R_{Red}$
Plant Cell Density (PCD)	R_{NIR} / R_{Red}
MidIRPCD	R_{MIR} / R_{Red}
NDVIPCD	$NDVI / R_{Red}$
MidIRNDVIPCD	$MidIRNDVI / R_{Red}$
Transformed chlorophyll absorption reflectance index (TCARI)	$-3*(R_{Red} - R_{Green}) - 0.2*(R_{Red} - R_{Green}) *(R_{Red} / R_{NIR} + Red))$
Two-band Enhance Vegetation Index (EVI_2)	$2.5*((R_{NIR} - R_{Red}) / (R_{NIR} + (2.4* R_{Red}) + 1))$

where for SPOT5:

Green = wavelengths 0.5 - 0.59µm

Red = wavelengths 0.61 – 0.68µm

NIR = 'Near-Infrared' wavelengths 0.78 – 0.89µm

MIR = 'Mid-Infrared' wavelengths 1.58 – 1.75µm; and

for IKONOS:

Blue = wavelengths 0.45 - 0.516 µm

Green = wavelengths 0.506 -0.595µm

Red = wavelengths 0.632 – 0.698µm

NIR = 'Near-Infrared' wavelengths 0.757 – 0.853µm

5.5. Collection of field data for ground truthing imagery.

To determine the relationship between the spectral reflectance characteristics of the sugar cane canopy and a corresponding measure of productivity in terms of yield (TCH) and CCS, field sampling was undertaken within a number of crops at strategic locations (Table 4).

Table 4. Field sampling undertaken for the ground truthing of imagery.

Sample Date	Sample location
21 August 2009	Herbert (H2) with BPS001
6 July 2010	Burdekin (A Mann)
24 October 2010	Bundaberg (Relmay)
2 November 2010	Bundaberg (Bullseye)
27 September 2011	Bundaberg (Relmay)
18 July 2011	Bundaberg (Bullseye)
26 November 2011	Burdekin (Pozzebon)

Each sample location was selected to represent a range of spectral values as defined by the 5 colour class classified NDVI image (Figure 3). At least three replicate samples were chosen to represent the high (Blue), medium (Green) and low (Red) NDVI zones. A tutorial for undertaking this process in ENVI is supplied in the appendices of this report (*Appendix 1: Tutorial 6: ENVI: Producing a classified vegetation index map of a cane crop from a 4 band satellite image*).

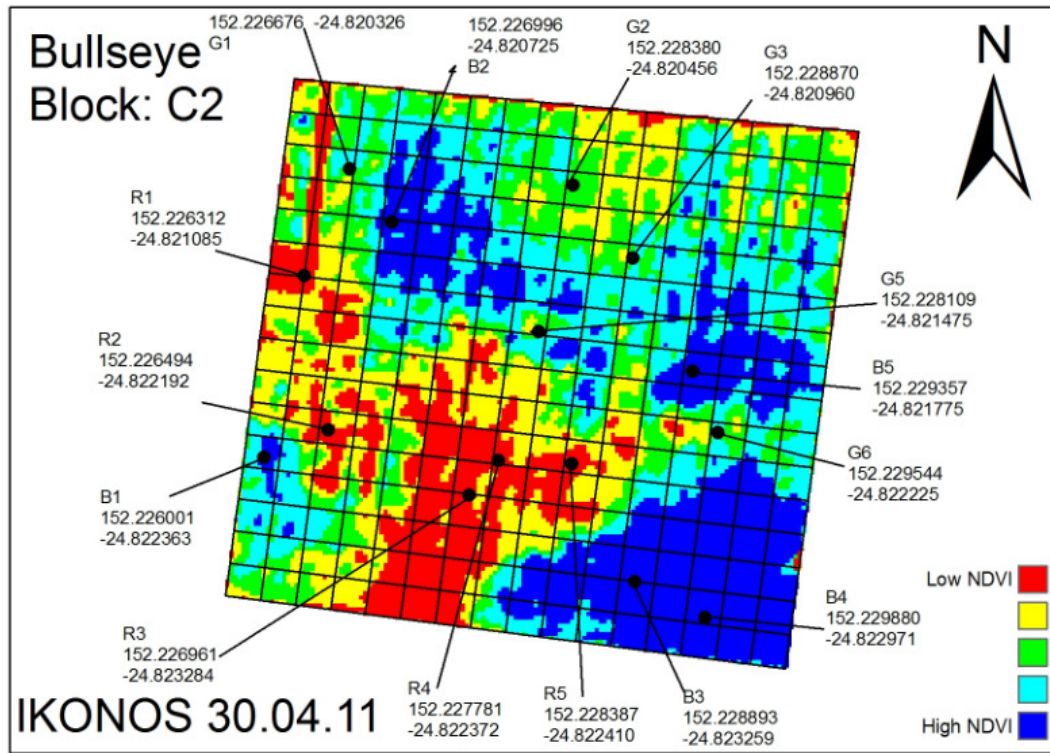


Figure 3. Example of a classified NDVI image of a sugar cane crop with sampling coordinates representing a range of homogenous colour zones indicated.

Field sampling coincided with the commercial harvesting of each respective crop (Figure 4a and c), so as to reduce the need of locating, cutting and then dragging samples through nearly impenetrable cane. The samples were located with a non-differential Garmin GPS (model: *etrex LEGEND*) with an accuracy +/- 6 m and marked with flagging tape (Figure 4b). A 5 m linear row of cane was measured with the number of stalks counted to provide an estimate of stalk density. Once exposed by the commercial harvester, the 5 m row was manually cut with a cane knife at ground level (Figure 4c) and then weighed on a trailer mounted load cell (Figure 4d).



Figure 4. Photos of field sampling (a) burning of a Burdekin cane crop prior to harvest; (b) sampling lodged burnt cane; (c) coinciding the field sampling with commercial harvester and (d) cutting samples from a green Bundaberg crop, with samples then weighed on a portable trailer load cell.

The weight of 5 m samples provided an estimate of total biomass whilst the additional weighing of a 20 stalks sub-sample, with and without its top leaf, provided an estimate of percent millable stalk. Using the known row spacing of the crop, the weight of the 5 m total biomass sample and percentage of millable stalk a measure of Tonnes of Cane per Hectare (TCH) was calculated. 6 stalks from each sample location were also retained and tested for Brix, Temp, Pol, Purity %, Fibre and CCS by the respective BSES station in each sampling region.

To verify if soil health and structure were driving crop variability, 10 cm soil cores were also manually collected at depths of 0- 20 cm and 40 -60 cm from high and low NDVI sample sites. The samples were dried and sent to CSBP soil and plant analysis laboratory (<http://www.csbp-fertilisers.com.au/nutrition-services/soil-and-plant-analysis-laboratory>) for a 'comprehensive' soil analysis including Colwell P and K, KCl 40 S, organic carbon, Nitrate N, Ammonium N, EC, pH- water, pH-CaCl₂, DTPA trace elements (Cu, ZN, Mn, Fe) and exchangeable cations (Ca, Mg, Na, K, Al), Boron, Acid P (BSES), and Chloride. From these sample results Estimated Cation Exchange Capacity (Est. CEC), Exchangeable Sodium Percentage (ESP) and Exchangeable Sodium to Potassium ratio (Na:K ratio) were calculated. Correlations were undertaken between all soil parameters with yield (TCH) and CCS to identify any likely drivers of reduced production.

5.6. Developing image based yield maps from field sampled data.

The spectral data corresponding to each sampling location was extracted using small areas of interest (average of 2 SPOT5 pixels 10 * 20 m; and the average of 9 IKONOS pixels 3.2 * 3.2 m, note the pan-sharpened images were not used for algorithm development). SPOT5 imagery warped to an orthorectified image had a RMS of less than 10 m, whilst for IKONOS an RMS less than 2 m was achieved. A tutorial for undertaking this process in ENVI is supplied in the appendices of this report (*Appendix 1: Tutorial 7: ENVI: Extracting point source spectral information from imagery using regions of interest (ROI's)*).

Once extracted, the average 4 band spectral data was entered into a Microsoft Excel spreadsheet along with the corresponding field measurements and soil chemistry results. To identify the best correlations between satellite imagery and crop yield (TCH), a number of vegetation indices (VI) (refer to section 5.4.) were examined, with the index that provided the highest correlation coefficient selected for further analysis. The average yield for the sampled crop was calculated by substituting the average VI value into the linear algorithm produced from the correlation. Total crop yield was then calculated by multiplying the average crop yield by the crop area, with the prediction accuracies validated against mill reports following harvest.

Coinciding with the prediction of average and total yield, the algorithm developed for each sampled crop was applied to each corresponding image to convert the VI pixel values into yield. A tutorial for undertaking this process in ENVI is supplied in the appendices of this report (*Appendix 1: Tutorial 8: ENVI: Converting VI pixel values into yield (TCH) using an exponential linear algorithm*). By further classifying these converted images into a graduated scaling of yield via a density slice, a surrogate yield map was produced.

5.7. Development of a generic yield algorithm.

Following the accuracies achieved in the prediction of sampled crops using field samples and site specific algorithms, the project team investigated the accuracies of a non cultivar, crop class and regionally specific yield prediction algorithm. The initial algorithm was developed from the correlation between the average GNDVI values of 112 Bundaberg cane blocks extracted from a TOA corrected SPOT5 image (acquired 10 May 2010), to average 2010 harvest yields for the corresponding blocks. This initial algorithm was applied to a 2008 SPOT5 image (acquired 31 March 2008) to predict the average and total yield of 39 cane blocks (600 ha) grown within the same Bundaberg region during the 2008 season. A 'generic' Bundaberg algorithm was subsequently developed from the combined 2008 and 2010 data sets. It was hypothesised that combined data set would make the algorithm less seasonally specific. Further statistical analysis of this algorithm in terms of predictive accuracy of yield was undertaken by Mary Barnes (CSIRO Mathematics Informatics and Statistics), where upper and lower 95% confidence intervals were calculated to show error on individual predictions. The standard 95% confidence intervals around the line of best fit were

calculated on the log scale (i.e. $\log(\text{TCH})$ a straight line relationship), with the resultant prediction intervals back transformed to an exponential relationship.

5.8. Regional predictions of average yield using a 'generic' algorithm.

To further assess the accuracy of the 'Bundaberg generic algorithm', retrospective predictions of average regional yield were derived for the Bundaberg (3544 crops), Isis (2772 crops) and Burdekin (4573 crops) growing regions, following the 2010 harvest. Comprehensive vector layers defining crop boundaries, cultivar, class etc. provided from each respective mill, were used to extract spectral data from SPOT5 imagery captured acquired 10 May 2010 (Bundaberg and Isis) and 14 May 2010 (Burdekin). For the 2011 season, predictions of average yield were again made for the Bundaberg (3824 crops), Isis (4204 crops), Burdekin (4999 crops) and Herbert (8596 crops) regions with imagery captured on the 27 March 2011 (Bundaberg and Isis), 22 April 2011 (Burdekin) and 5 May 2011 (Herbert). For the 2012 season predictions were made for the Bundaberg (3217 crops), Isis (4000 crops), Burdekin (6921 crops) and Herbert (15463 crops) regions with imagery captured on the 1 April 2012 (Bundaberg and Isis), 16 May 2012 (Burdekin) and 4 April 2012 (Herbert). Additional estimates were made for the Condong Mill region (New South Wales) (2087 crop) by applying the 'generic' algorithm to a SPOT5 image captured on the 29 February 2012.

Due to the poor predictive accuracy of the generic algorithm for the Burdekin region during both the 2010 and 2011 season, a Burdekin specific algorithm was derived from the correlation between the 2010 Burdekin crop GNDVI values and harvested yield. The new algorithm was evaluated during the 2011 and 2012 growing seasons. For the Mulgrave region, a scoping study was undertaken using an algorithm developed from the correlation of average block yield from 832 crops and GNDVI derived from an IKONOS image captured on the 26 May 2010. This algorithm was applied to 1324 crops captured by GeoEYE imagery on 4 May 2012.

5.9. Derivation and distribution of yield maps at the regional scale using yield prediction algorithms.

Coinciding with the prediction of average regional yield, the project team evaluated the accuracies of producing yield maps for all crops defined in section 5.8. Using the process defined in section 5.6, the algorithms applicable for each region were applied to each sub-setted crop, converting GNDVI values for each pixel into yield (TCH). The yield maps were classified into 8 yield classes via a density slice and distributed to industry as Google Earth files (KMZ). A tutorial detailing how to produce these files using ENVI is provided in the appendices of this report (*Appendix 1: Tutorial 9: ENVI: Creating Google Earth KMZ files from Geotiffs*).

5.10. Validation of image derived yield maps.

The accuracy of prediction at the block level was validated against Mill data following the 2010, 2011 and 2012 harvest. This analysis was conducted by DAFF Qld biometricians and included 8 data sets (Bundaberg 2010, 2011, 2012; Isis 2010; Herbert 2011 and 2012 and

Burdekin 2011 and 2012). Using the software GenStat, a simple regression was fitted between actual (y variable) and predicted yield (x variable) for each data set. For the initial analysis no data was excluded in spite of there being evidence of data with high leverage and or residuals. Following a t-test, the accuracy of prediction was identified by the closeness of the R-squared value to 100%, the intercept being not significantly different to zero, and the slope not significantly different to 1. As well as the validation of predicted yield at the whole crop level, predictive accuracies were also undertaken at the within the crop level, using point source field samples from two crops as defined in section 5.5.

Additional analysis of all data sets in terms of seasonal conditions, growing year, cultivar and class will be undertaken in a follow on SRDC project (Developing remote sensing as an industry wide yield forecasting, nitrogen mapping and research aide).

5.11. Correlating image results against harvester derived yield maps (CSE022).

In order to meet objective 3 (Section 4) of this project, classified VI images and image derived yield maps were correlated against those produced from harvester yield monitors (CSE022). At the time of this report, the 2011 yield data collected for the Bundaberg (Hubert-6.7 ha) and Burdekin (Pozzebon- 26.8 ha) was available and subsequently analysed against the corresponding imagery for each site, IKONOS imagery captured 12 May 2011 (Burdekin) and 23 March 2011 (Bundaberg).

The 4 band imagery was georectified, with pixel data within the boundary of CSE022 each site, extracted. Pixel values were then converted into GNDVI, and converted to text format. To remain consistent with the harvester derived yield maps the GNDVI images were re-sampled to a 2 metre grid by multiplying the 3.2 metre pixel resolution IKONOS images by a floating point 2 metre raster, with all values set to unity. The resultant 2 m GNDVI images were then smoothed using a moving average on a 5 x 5 array (= 10 m x 10 m) of pixels centred on the pixel of interest, this was achieved using the 'focal statistics' function (Spatial Analyst).

The yield monitor data were kriged on to the same 2 m grid as the imagery using the software Vesper. The data was reduced to 3 second logging intervals with any points exceeding 3 standard deviations from the mean also removed prior to map interpolation. The data was then adjusted to match mill harvest data on a per- harvest event basis. At the Bundaberg site, the yield map was derived from a roller opening sensor, whilst at the Burdekin site data was provided by a Solinftec yield monitor. Note that the Solinftec yield monitor also relies on sensing of the roller opening, with data adjusted to yield (TCH) using a proprietary algorithm. Clustering of the various map layers was done using *k*-means clustering in JMP 8 (SAS, Cary, North Carolina, USA).

6. Results

The following section details the results of the project in terms of the 5 objectives.

6.1. Benchmarking and identifying the most feasible and suitable commercial imagery (i.e. spatial resolution, repeat time and economic feasibility) for identifying crop variability and thus directing targeted mid-season management within the Australian cane industry.

As listed in Table 2 of this report, the project team obtained imagery from a wide range of active and passive sensors. With all passive multispectral platforms capable of producing VI images, the recommendation of the most suitable came down to cost, the most appropriate minimum purchase area, repeat capture time, appropriate spatial resolution, and overall ability to be easily manipulated in terms of georectification etc.

Overall, imagery from the French owned SPOT5 satellite, supplied by Astrium (<http://www.astrium-geo.com/>), was identified to be the most suitable for a range of applications. A single SPOT5 scene (3600km²) encompassed the majority of cane crops within a particular growing region therefore eliminating the need for additional image processing such as mosaicing and colour balancing. The imagery was shown to be cost effective at \$1AUS per km² and due to its 2-3 day revisit interval, reliable in terms of providing cloud-free scenes. The spectral resolution of SPOT5 (green, red, near and mid infrared) allowed most accepted vegetation indices to be derived. At the block level, the classified GNDVI 'zonal' vigour maps produced from the 10 metre spatial resolution images were comparable to those produced by the higher resolution platforms. However, were unable to discern sub metre constraints such as weed infestations and damage resulting from grubs, soldier fly, rat and pig. The pan sharpened IKONOS product (0.8 metre) was shown to be effective in identifying such sub metre constraints. It is acknowledged that a number of commercially available satellites could have supplied similar high quality sub-metre imagery. However, at the time of this project, IKONOS imagery was available under a three * 50 km² capture deal that equated to \$22AUS per km² as supplied by Geoimage (<http://www.geoimage.com.au/geoimage/>) and AAM (<http://aamgroup.com/>).

The RapidEYE (RE) imagery held great promise as a optimal image source for the development of sugarcane applications due to its 5 m spatial resolution, 5 spectral bands (blue, green, red, red-edge and near infrared) and 5 satellites in the constellation meaning a high revisit rate, ideal for cloud prone areas. Unfortunately a number of issues limited the ability to fully assess the suitability of this imagery. Initially the minimum RE scene was \$5000km² scene and at AU\$9850 (including the mosaicing of 14 tiles), which was cost prohibitive at the research level when compared to SPOT5. There were also issues in communication between the Australian distributors and German owners of the satellite. I understand that at the completion of this research, the minimum RE scene size has been reduced to 3500km² and communications with the German owners has improved. As such this may be identified as an option for the future along with new generation platforms such as SPOT6 with 6 metre spatial resolution and Pleiades'.

In regards to the active sensors, imagery from Terra SAR X and Lidar was obtained by other agencies for a number of the project sites. However, a lack of time to access and then correctly process the data meant that it could not be effectively evaluated. It is envisaged that radar sensors may play a future part in directing in season management due to their ability to provide data during the cloud prone early vegetative growth stage (February to March). Additional research is required to validate this. The 'Raptor' active, airborne optical reflectance sensor was considered to be a possible future source of crop vigour data for the cane industry due to its ability to operate under variable cloud cover and at night, and as such was evaluated through this project.

6.1.1. Evaluation of the Raptor sensor.

Prior to this project, the Raptor sensor's capacity to produce accurate measures of sugar cane vigour had not been assessed. As such a number of tests were undertaken to identify the impact that variables such as flying height (Figure 5) and direction (Figure 6) had on the accuracies of derived vigour maps.

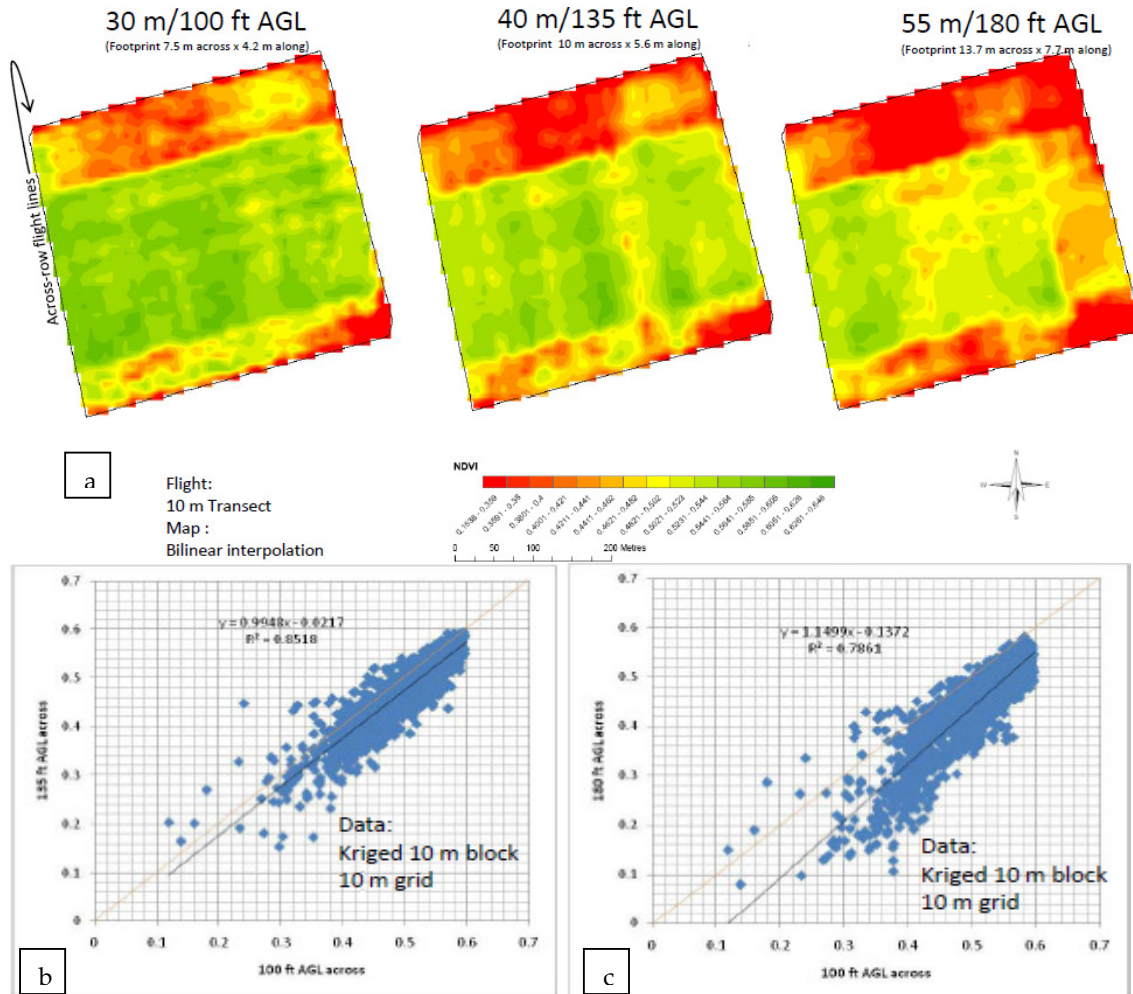
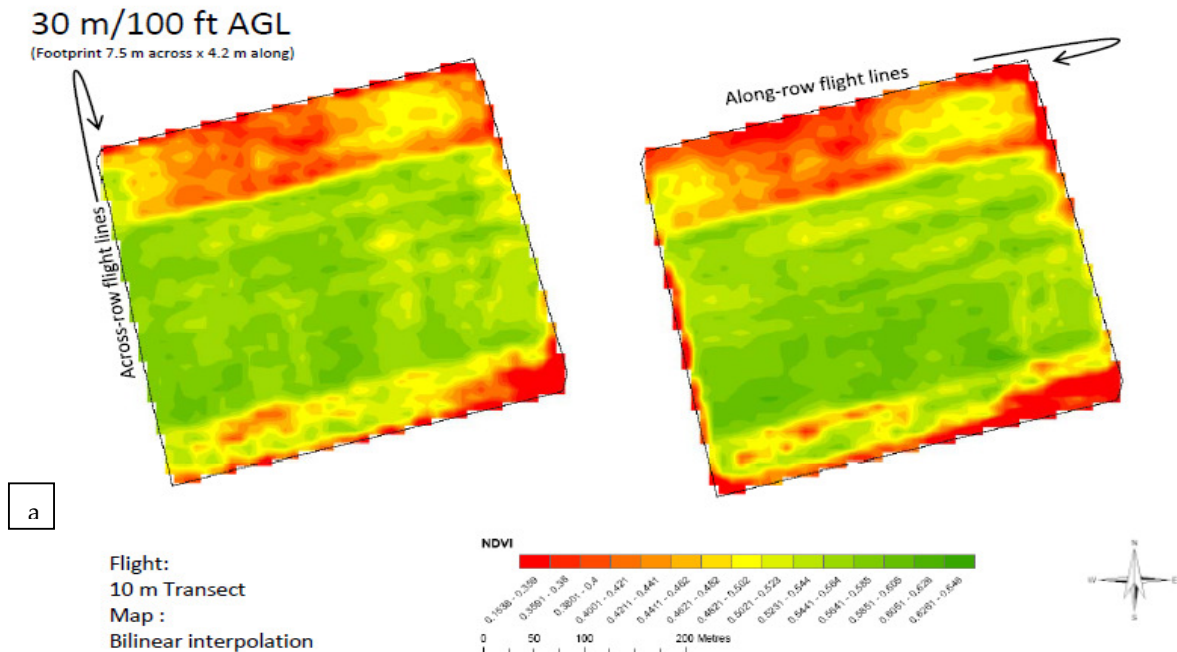


Figure 5. a. Classified NDVI images identifying the spatial trends of crop vigour measured at three different flying heights (100, 135 and 180 ft AGL). b. correlation between NDVI

measured at 100 ft AGL and 135 ft AGL. c. correlation between NDVI measured at 100 ft AGL and 180 ft AGL.

The collection of NDVI data at the three different flying heights identified little difference between 100 and 135 ft above ground level (AGL), producing an $R^2 = 0.85$, a slope close to 1 (0.995) and an intercept close to 0 (0.02). A lower correlation was identified between 100 ft AGL and 180 ft AGL, producing an $R^2 = 0.79$, slope of 1.15 and intercept of 1.137. This result indicates that there is some flexibility in the flying height at which Raptor imagery is collected although erroneous results may occur if the height exceeds 135 ft AGL. This result is consistent with those identified by the University of New England in the capturing of Raptor imagery where the signal, particularly within the Red band decays beyond a sensor-canopy distance of approximately 60 metres.

Given the row structure of cane, it was considered prudent to evaluate the impact of flying direction, namely across or along cane rows, on the derived maps. In Figure 6, it can be seen that similar spatial trends are present in the classified NDVI images from data collected from both flying directions (Figure 6 a), as well as a high correlation ($R^2 = 0.78$), slope 0.98 and intercept of 0.005 produced when comparing the two (Figure 6 b). These results indicate that flying direction had little influence on data integrity, a result most likely attributed to the large footprint of the Raptor sensor and the fact that the sugar cane plants were close to full canopy at the timing of data collection, therefore reducing the visibility of inter row soil.



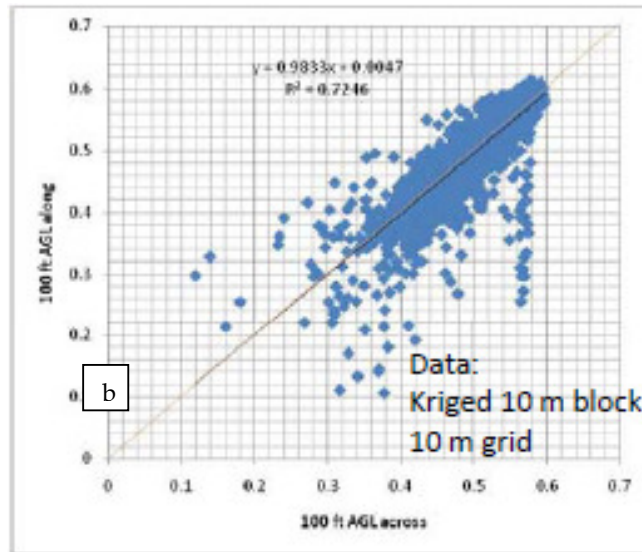
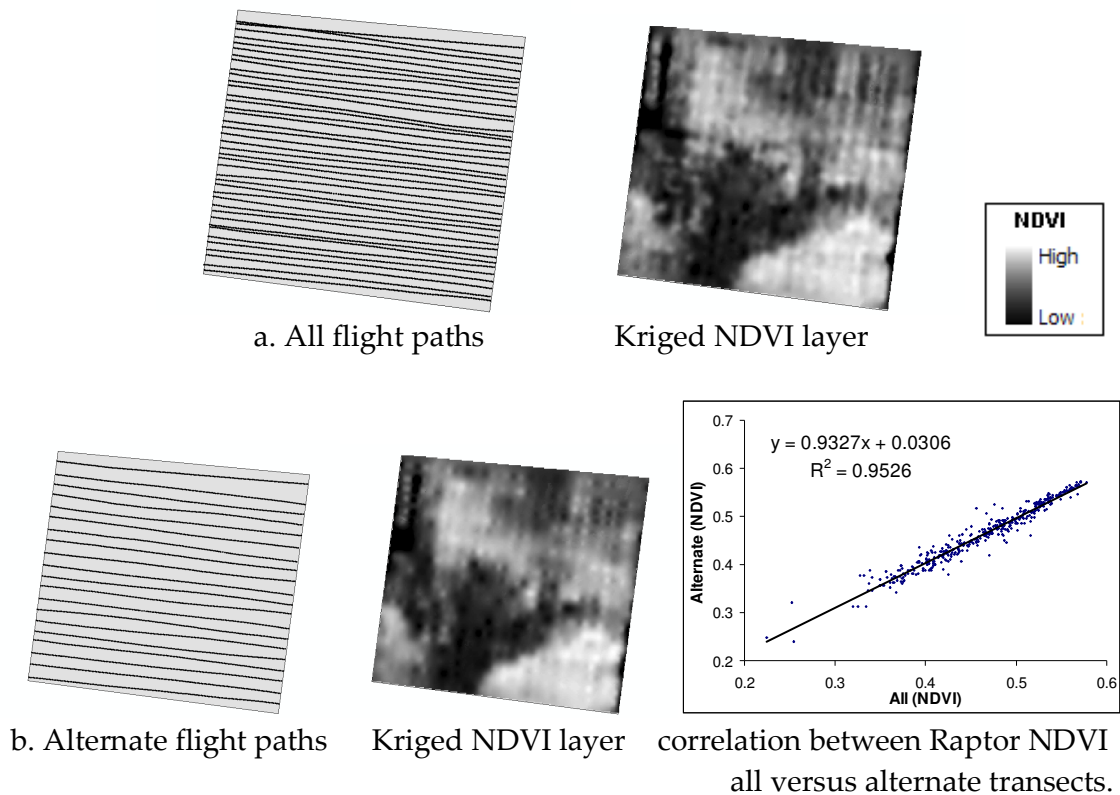


Figure 6. a. Classified NDVI images of a cane crop derived from the Raptor sensor being flown across and along the cane rows. b. correlation between NDVI derived from data collected from the different flying directions.

The Raptor data was initially collected at ~10m (on ground) transect spacing and a desk top study was undertaken to determine if the flight paths could be minimised without altering the spatial pattern of the resultant NDVI map (Figure 7).



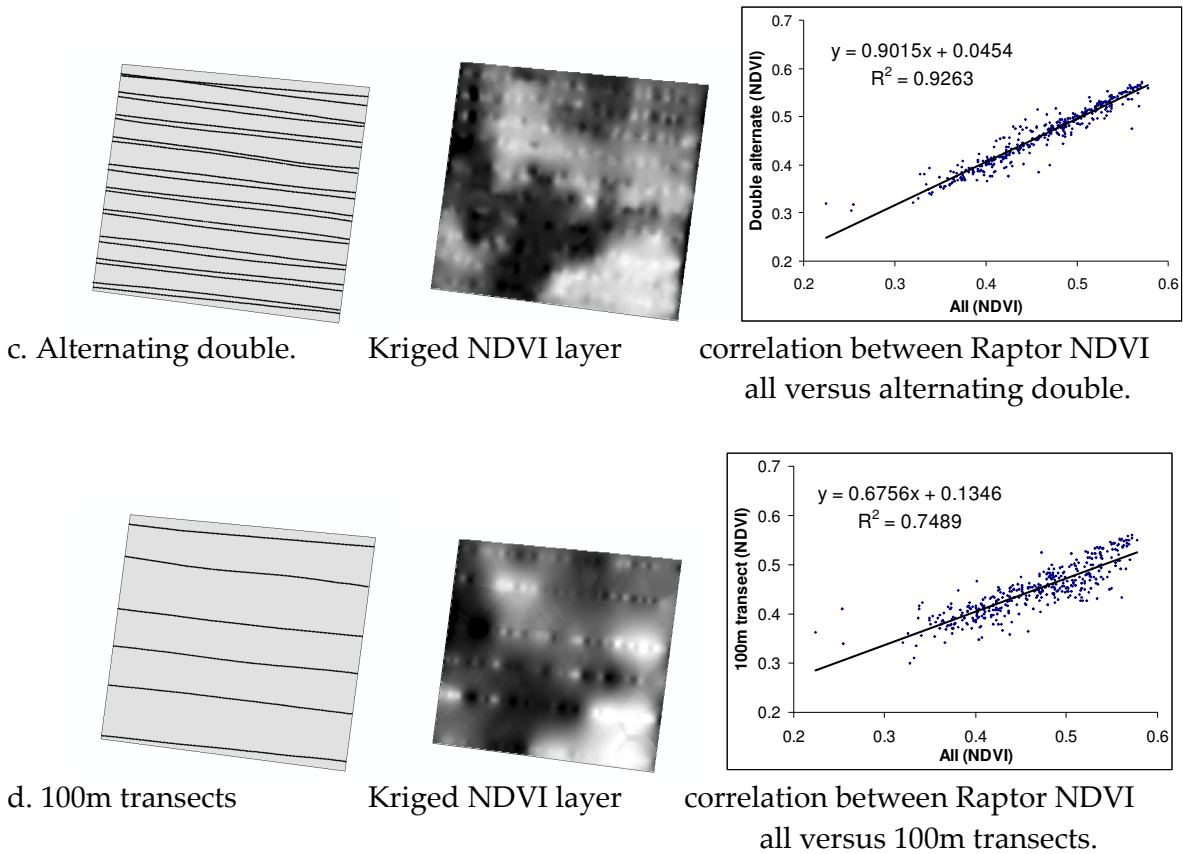


Figure 7. Assessing optimal frequency of flight paths for creating a representative NDVI layer from Raptor data.

As seen in Figure 7, similar zonal paddock trends (kriged NDVI layers) were obtained from a range of flight transect configurations. Figure 7 b identifies very little variation between the original ~10 m transects to one using every second transect i.e. ~ 20 m producing a strong $R^2 = 0.96$, slope of 0.93 and intercept of 0.034. A similar result was produced in Figure 7 c, using alternating transects of two retained and two removed ($R^2 = 0.93$, slope of 0.90 and intercept of 0.05). Even with transects reduced to every ~100 m (Figure 7 d), the correlation remains relatively strong ($R^2 = 0.75$). However, the slope (0.68) and intercept (0.134) indicate a greater separation from original ~ 10 m model. This result indicates that the ~ 10m flown transects may be excessive and that data collection may only be required at relatively wide transect intervals (i.e. 50 m) thereby saving flight time and associated costs.

The temporal comparison of Raptor data captured across each of the three test crops identified a number of erroneous points that were believed to be associated with non cane spectral information or an 'edge' effect. With the on-ground footprint of Raptor being 7.5 m * 4.2 m (at 100 ft AGL) it was decided that an internal 15 m buffer be applied. The implementation of the buffer not only removed the spurious points (Figures 8), but for Block 3 (CSE022 Hubert site) resulted in a greater separation of data representing different cultivars with in the sub blocks. This clear segregation of data supports the potential future application of remote sensing for the rapid screening of varieties for plant breeding rights (PBR) auditing, if required.

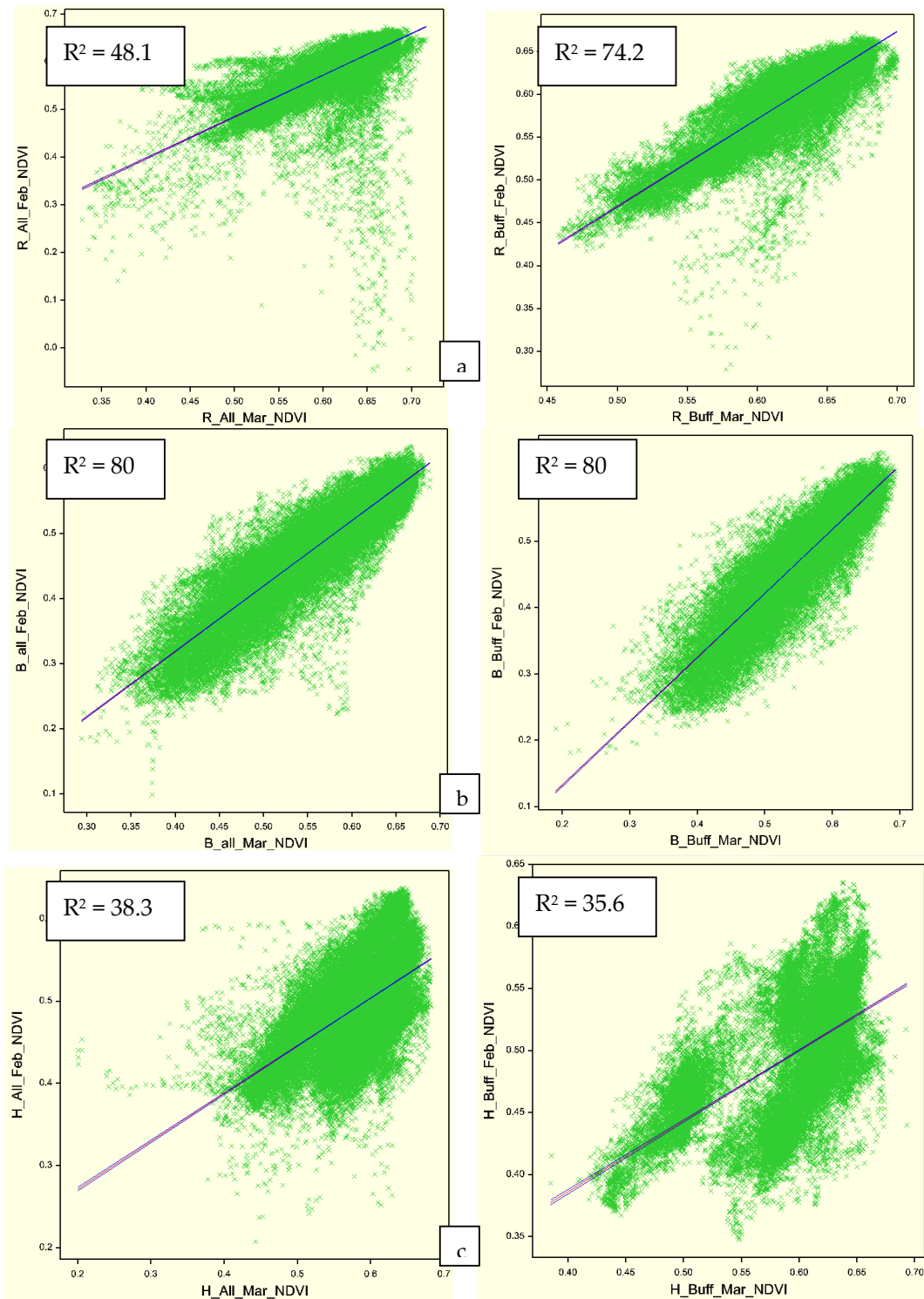


Figure 8. Correlations between Raptor data captured on two occasions (February and March) over the three test crops, Block a (Bullseye), Block b (Hubert) and Block c (Relmay), before and after the implementation of an internal 15 m buffer (H-Buffer).

To validate the accuracy of Raptor derived NDVI maps, imagery captured over three Bundaberg crops on three occasions (23 Feb, 23 March and 2 May 2011) was compared against IKONOS NDVI images captured on two occasions (23 March 2011 and 30 March 2011) (Figure 9) as well as a SPOT5 image captured on the 27 March 2011 (Table 5).

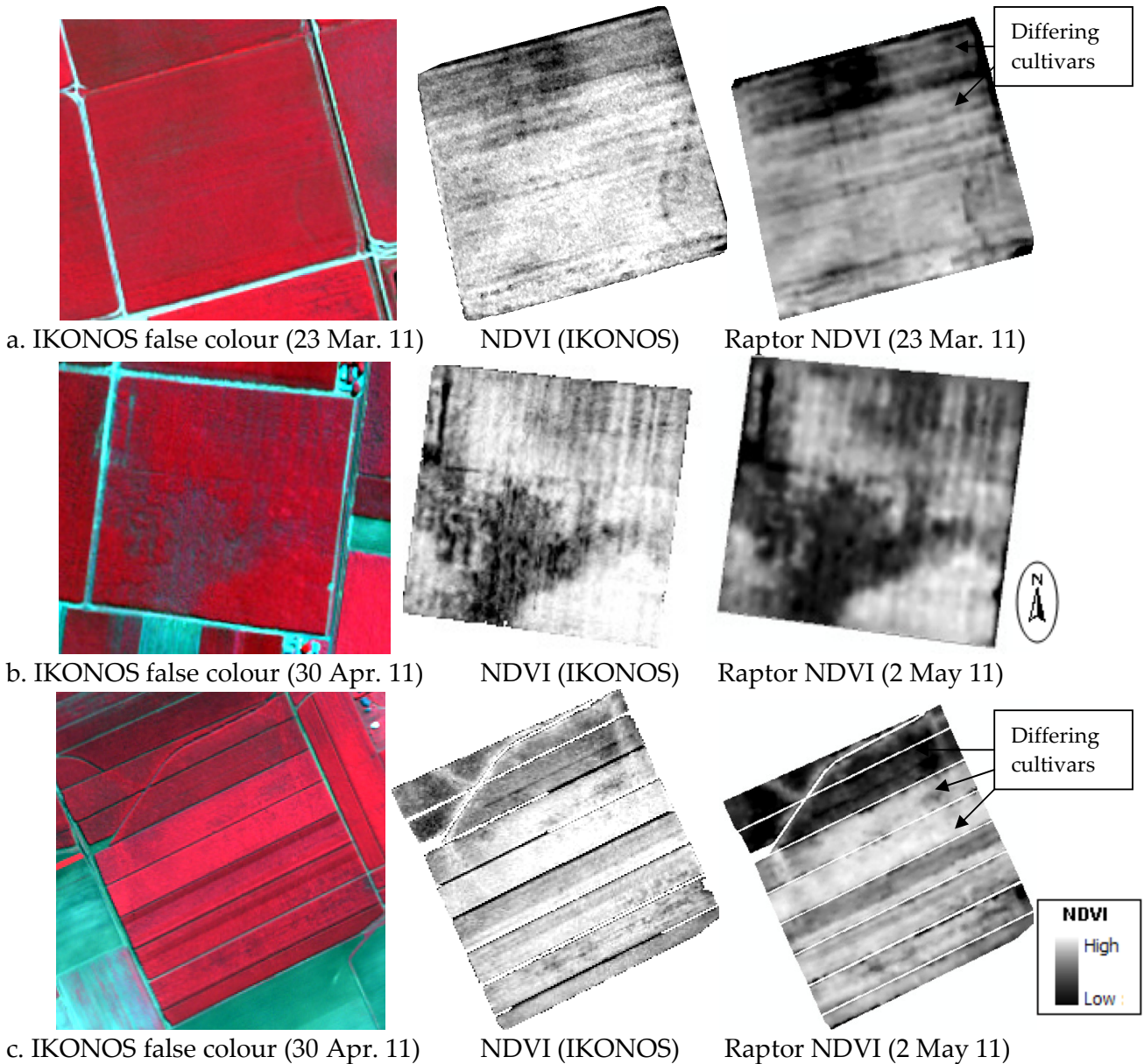
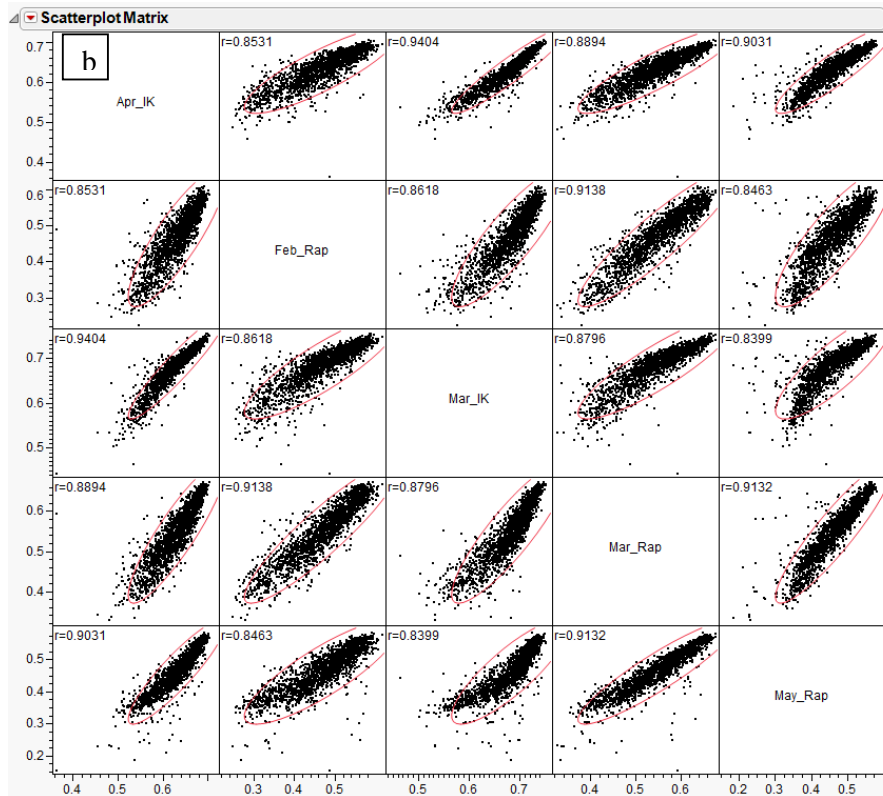
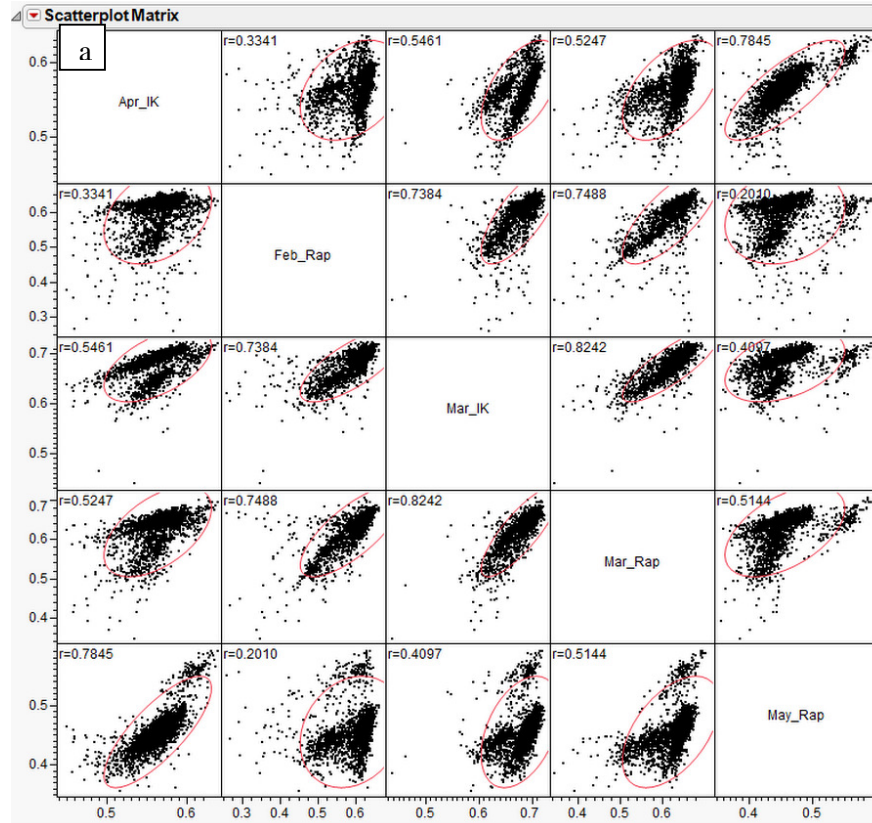


Figure 9. IKONOS False colour and NDVI images of the three Bundaberg crops Relmay (a), Bullseye (b) and Hubert (c). Also NDVI images derived for from the Raptor sensor.

The spatial NDVI patterns displayed in the IKONOS and Raptor images were visually comparable in Figure 9 a, b and c, with different cultivars grown within the sub blocks evident in Figure 9 c. The NDVI images derived from each platform were also statistically compared, following all data sets being interpolated to 10 metres to reduce the volume of data (Figure 10).



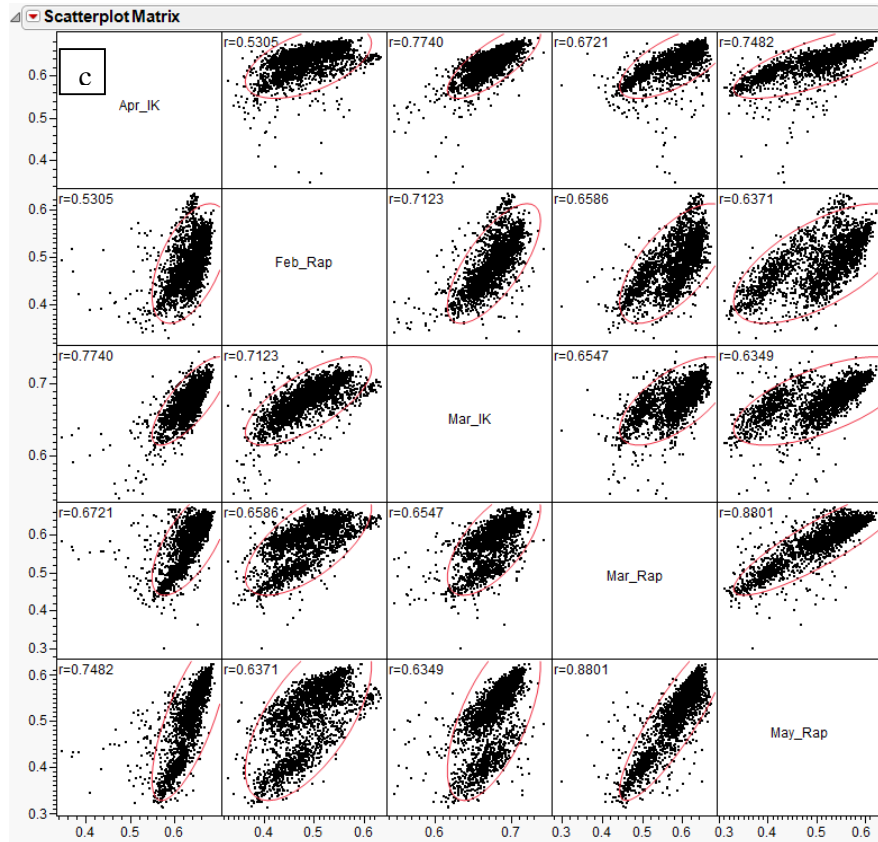


Figure 10. Correlation matrix 'scatter plots' comparing NDVI layers derived from Raptor and IKONOS imagery, collected on a number of occasions over three sites: Relmay (a), Bullseye (b) and Hubert (c).

From the correlation scatter plots the NDVI layers derived for the Bullseye crop (Figure 10 b) produced the highest R^2 values (0.71 to 0.88). The obvious separation in data points for the Hubert crop (Figure 10 c) was attributed to different varieties within the sub blocks. The Relmay crop (Figure 10 a) also exhibited data separation as a result of multiple varieties but a slight malfunction with the Raptor sensor on the 23 February 2011 further confounded the correlations. To further validate the consistency between the sensors and capture dates, NDVI values sampled from 12 specific locations in the Relmay crop (Figure 11 a) and 15 for the Bullseye crop (Figure 11 b) were compared against corresponding values extracted from a SPOT5 image (27 March 2011) and to measured yield and CCS (Table 5).

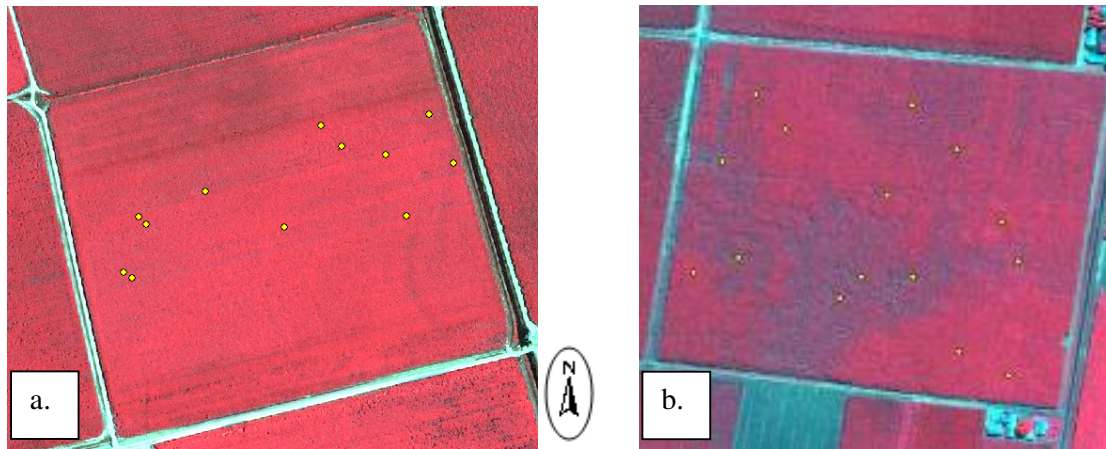


Figure 11. False colour IKONOS images of two Bundaberg crops with field sampling locations highlighted. 12 sample sites for Relmay (a) and 15 for the Bullseye crop (b).

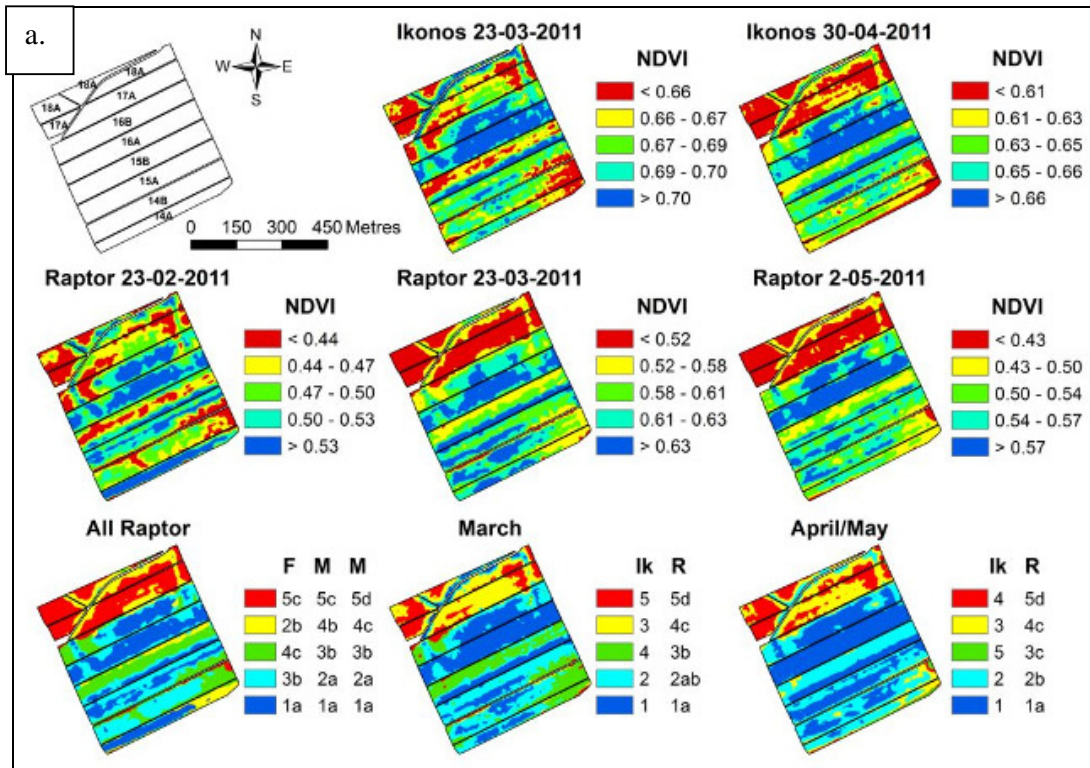
Table 5. Correlation matrix comparing NDVI values derived from imagery captured by the Raptor sensor, SPOT5 and IKONOS to yield and CCS for specific locations within two Bundaberg crops.

Block 1	Raptor 23.02.11	Raptor 23.03.11	IKONOS 23.03.11	SPOT 27.03.11	IKONOS 30.04.11	Raptor 02.05.11	TCH	CCS
Raptor 23.02.11	1	0.8738	0.5380	0.5498	0.4024	0.3436	0.6291	-0.5211
Raptor 23.03.11		1	0.7588	0.8292	0.6264	0.5913	0.7845	-0.3755
IKONOS 23.03.11			1	0.9242	0.9620	0.8501	0.8408	-0.4565
SPOT 27.03.11				1	0.8875	0.8645	0.8460	-0.2630
IKONOS 30.04.11					1	0.9082	0.7510	-0.4206
Raptor 02.05.11						1	0.7474	-0.3440
TCH							1	-0.5614
CCS								1

Block 2	Raptor 23.02.11	Raptor 23.03.11	IKONOS 23.03.11	SPOT 27.03.11	IKONOS 30.04.11	Raptor 02.05.11	TCH	CCS
Raptor 23.02.11	1	0.9845	0.9813	0.9716	0.9774	0.9457	0.9286	-0.7848
Raptor 23.03.11		1	0.9826	0.9787	0.9881	0.9816	0.9429	-0.7628
IKONOS 23.03.11			1	0.9828	0.9948	0.9545	0.9050	-0.7024
SPOT 27.03.11				1	0.9850	0.9564	0.8927	-0.7286
IKONOS 30.04.11					1	0.9763	0.9114	-0.7226
Raptor 02.05.11						1	0.9217	-0.6687
TCH							1	-0.7522
CCS								1

The high correlations (R^2) identified in Table 5, particularly for Block 2 (Bullseye), indicate that at specific sample locations the Raptor is producing a consistent spatial trend in NDVI values to those produced by the satellite platforms. The only exception being the lower R^2 values identified from the 1st Raptor capture to that of the other platforms in Block 1 (Relmay). This indicates a systematic issue with the sensor on that day, with the Raptor performance observed to be degraded owing to suspected moisture infiltration into the sensor head. The high correlations produced between the Raptor data and yield (TCH) for both sites supports the possibility that yield maps could be derived from the Raptor sensor. Interestingly, for Block 2 (Bullseye) consistent negative correlations between NDVI derived from each sensor to CCS was also identified. This may indicate that CCS maps may also be derived from imagery VI values, although further research would be required.

For the CSE022 Hubert site (Block 3) additional k-means clustering analysis was undertaken to compare the consistency of spatial trends in NDVI derived from both sensor types, across the capture dates. This involved the classification of the NDVI layers into 3 and 5 classes (Figure 12). The letters after the cluster rankings indicate whether the means are significantly different. There is no test of significance for the IKONOS data as it was not kriged and to undertake this on the raw data the large number of points would results in everything appearing significant. As with the visual comparisons (Figure 9), the trends identified from both sensors were not totally consistent for any given acquisition date, with the cluster analysis, again identifying the February Raptor image as differing from the other two collection dates.



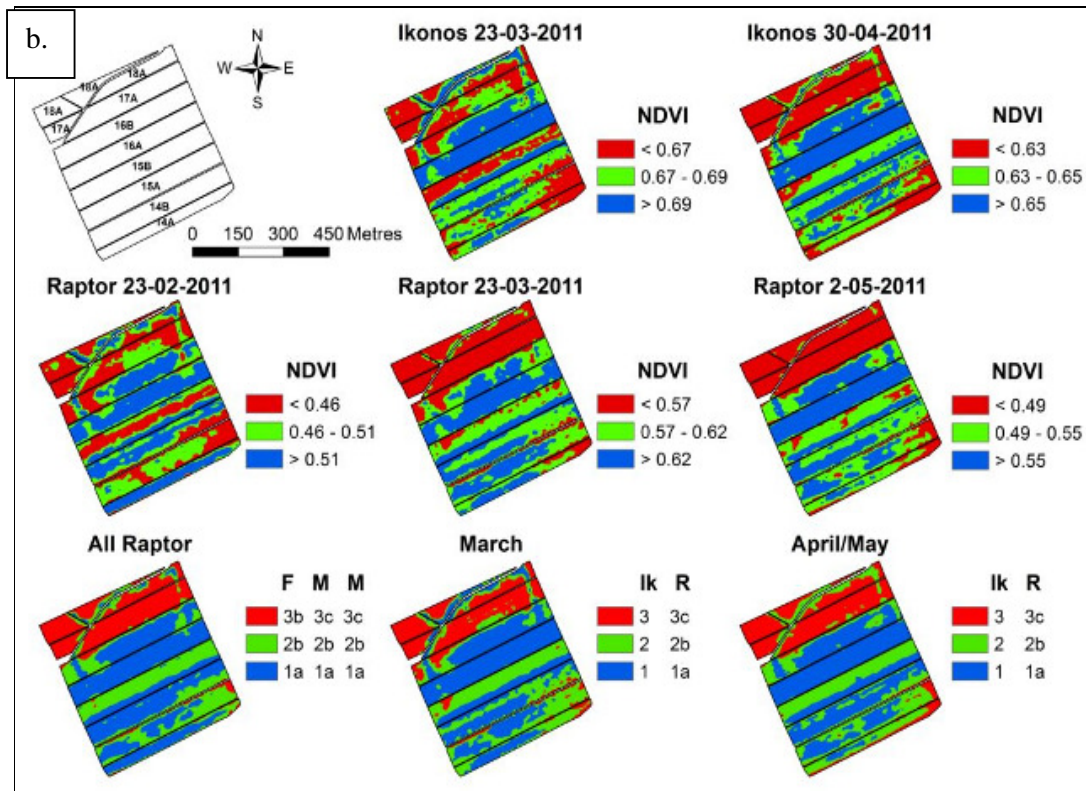


Figure 12. Comparison between classified NDVI layers derived from kriged Raptor data captured on three occasions and IKONOS imagery captured on two occasions. a. demonstrates the analysis of 5 zones, whilst b. includes 3 zones. Legends have been categorised into 20th percentiles. For the NDVI images, 1 indicates a higher value.

From these results it can be seen that the Raptor sensor is providing NDVI maps consistent with those produced by IKONOS, and that there is little difference in NDVI maps derived from imagery captured between February and May.

6.2. Identifying the optimum time of image capture that will accurately depict mid- season crop variability whilst avoiding seasonal times most prone to cloud cover, across key Australian cane farming regions.

For remote sensing to be successfully implemented as a tool for guiding management decisions, imagery has to be available at the appropriate phenological growth stage where the crop can respond to varied management and the management itself can be applied without crop damage. As such, this project attempted to identify that critical window for Australian sugar cane by attempting imagery capture throughout most of the growing season over the Bundaberg, Herbert and Burdekin regions. It was hypothesised that imagery captured early in the growing season i.e. January to March would not only identify variability in crop growth at the required vegetative growth stage, but provide it at a time where applications could still be applied non- destructively. Unfortunately the ability to capture imagery during this time frame was near impossible due to continual cloud cover, a result supported by previous research (Johnson and Kinsley-Henderson, 1997). With successful captures only occurring from March, the ability to implement alternative management strategies based on the imagery within that same season, was negated. This

result indicated either the need for an active sensor such as Radar or the ‘Raptor’ that could provide earlier in the season i.e. January to March, or that alternate management decisions be applied post harvest for the benefit of the following ratoon crop.

6.2.1. Using spatial technologies to identify growth variability in cane crops, likely constraints to production and suggested remedial action.

To demonstrate the capacity of remote sensing as an effective tool for identifying growth variability within a cane crop, 7 individual crops were imaged and intensively samples (refer to methodology section 5.5, Table 4). These included:

Herbert site (H2): variety Q200 planted over 8.2 ha on 7 July 2008; plant-cane harvested on 21 August 2009. 1.83 m spacing.

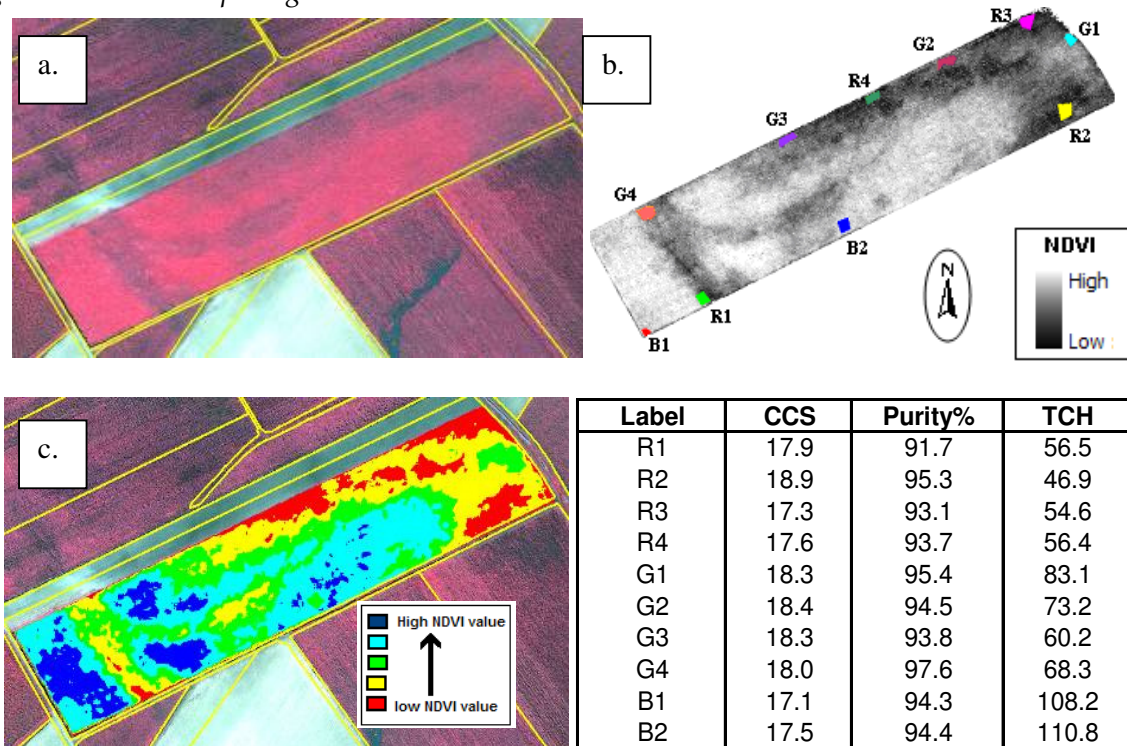


Figure 13. a. False colour IKONOS image of H2 crop (2 August 2009). b. NDVI image of H2 site derived from IKONOS image, with field sampling sites indicated. c. Classified NDVI of H2 site. Table: field sampling results.

From Figure 13, IKONOS imagery of the H2 site clearly identified a large degree of spatial variation of cane vigour, with regions of reduced vigour at the northern end of the crop and within a band extending across the crop at the southern end (red colour in Figure 13 c). Field samples taken at strategic locations within the crop (Figure 13 b) identified the variability in NDVI coincided with similar variations in cane production (TCH) but not to CCS (Figure 13 d.). To identify the likely driver of this reduced vigour the SRDC (BPS001) project team compared the spatial variation to that produced by a soil survey (EM- Veris) undertaken over the block in 2008 (Figure 14).

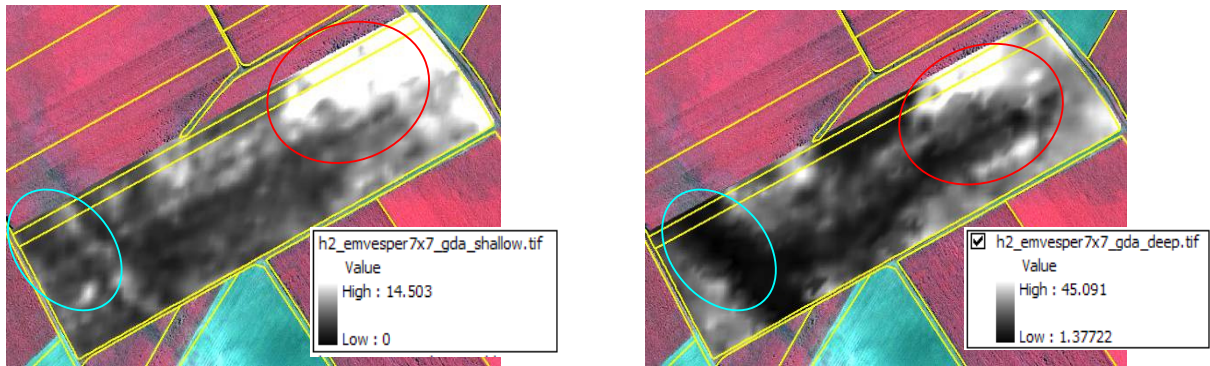
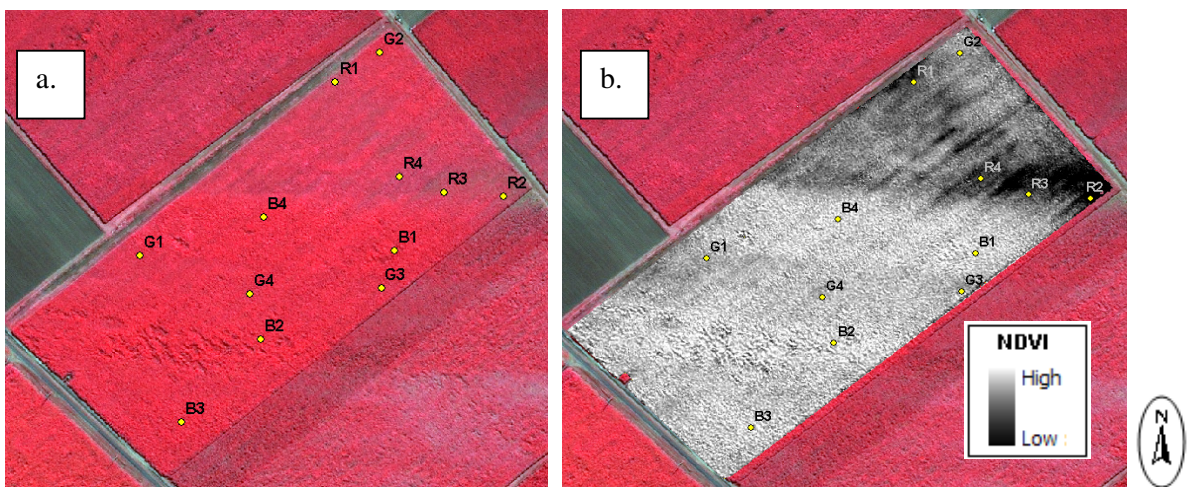


Figure 14. Shallow and deep EM – Veris maps of the H2 site taken in 2008.

As seen in Figure 14, similar spatial trends exist between both the shallow and deep EM maps with the NDVI image (Figure 14b), although low NDVI values occurred in regions of both high EM (red circles) and low EM values (blue circle) measured at both depths. Statistical analysis of these data supported this observation identifying poor correlations between NDVI and shallow electrical conductivity (EC) readings ($R^2 = 0.45$) and NDVI with deep EC readings ($R^2 = 0.08$). This result indicates that the spatial variability in crop performance was unlikely to be the result of factors driving soil conductivity alone. Further evaluation of the crop suggested that topography and soil type may have influenced hill height and ultimately plant establishment, particularly for a seam of heavy clay extending through at the southern end of the crop (blue circle). Further analysis and interpretation of this trial is provided in Coventry *et al.* (2010).

Burdekin site (A. Mann): variety KQ228; Plant cane; 11.5 ha; cane harvested on 6 July 2010.



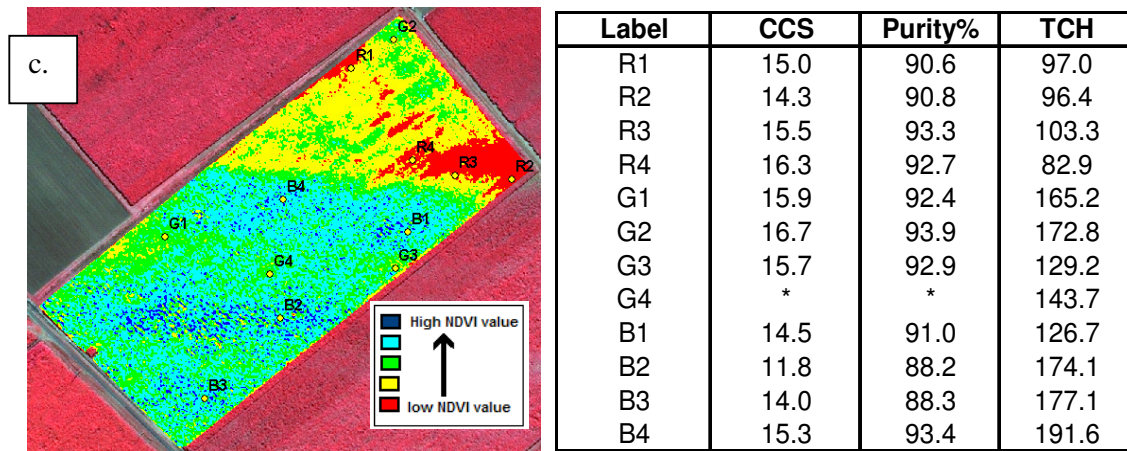


Figure 15. a. False colour IKONOS image of A.Mann crop (28 May 2010). b. NDVI image derived from IKONOS image with field sampling sites indicated. c. Classified NDVI image. Table: field sampling results.

A high resolution IKONOS image of the Burdekin (A. Mann) crop identified a large zone of reduced NDVI (red region) at the northern end (Figure 15 c). Field sampling at strategic locations identified this low region to have a substantially lower average yield (95 TCH) than that measured at high vigour zones (167.4 TCH), and a slightly higher average CCS (Figure 15 d). Soil cores taken at same locations as the plant samples, indicated that the reduced production was the result of sandy soils with low water and nutrient holding capacity. At a depth of 40- 60 cm the poor zones (red) exhibited a low average CEC (6.37 meq/ 100g) compared to 21.5 meq/ 100g measured in the blue zones, as well as lower exchangeable nutrients (incl K) and trace elements. In an attempt to mitigate this issue mid – season, the grower was encouraged to irrigate with less water but at a greater frequency in an attempt to stop nutrient leaching. Following the harvest the grower applied 15t (1.25 t/ha) of activated silica ([click icon- !\[\]\(7803df19e2f64b9d8f5d703b85a358d0_img.jpg\)](#)), 160 kg/ ha of Nitrogen and 43 kg/ ha of Sulphur. The fertilizer was coated with Aqua Boost AG100, a polycrylamide granule, in an attempt to improve moisture retention. As seen in Figure 16, these post harvest applications resulted in little visible response to the 2011 ratoon crop.

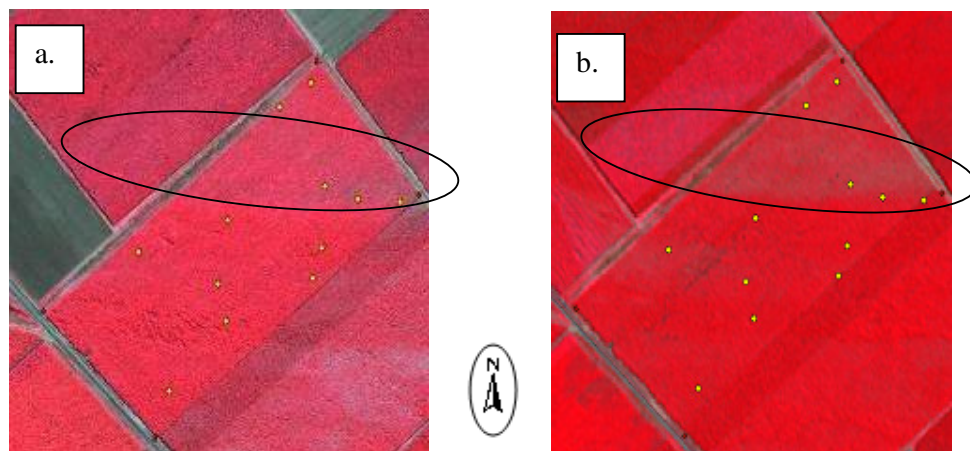


Figure 16. a. False colour IKONOS (28 May 2010) image of the A. Mann crop with sample locations and main region of reduced production identified. b. Repeat false colour image captured in 12 May 2011.

Following this lack of response it was suggested that a deep (>20cm) application of clay, road base or mill mud be applied to the sandy areas in an attempt to increase its water and nutrient holding capacity. However, as this is a highly destructive form of remedial action it would have to occur at the end of the ratoon rotations and prior to replant. Unfortunately, the impact of this remedial action could not be assessed as the grower passed away during the 2011 season.

Bundaberg site (Bullseye A9): Variety KQ200; Plant cane; Area 4.47 ha; harvested 3 Nov 2010; Row spacing 1.52 m. The block was land formed in 2008, with 2010 being the first re-plant.

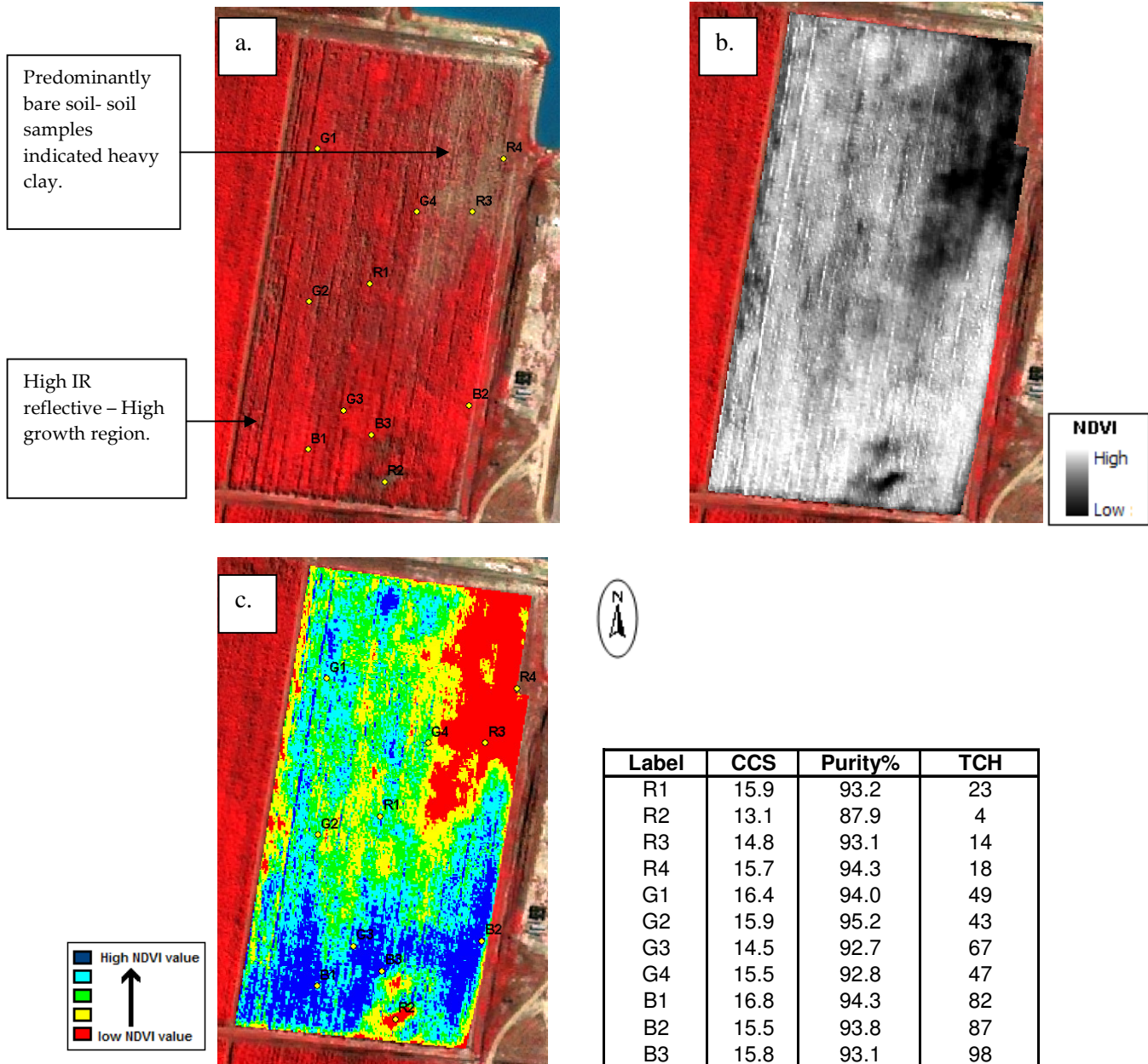


Figure 17. a. False colour IKONOS image of Bullseye A9 crop (14 May 2010). b. NDVI image derived from IKONOS image with field sampling sites indicated. c. Classified NDVI image. Table: field sampling results.

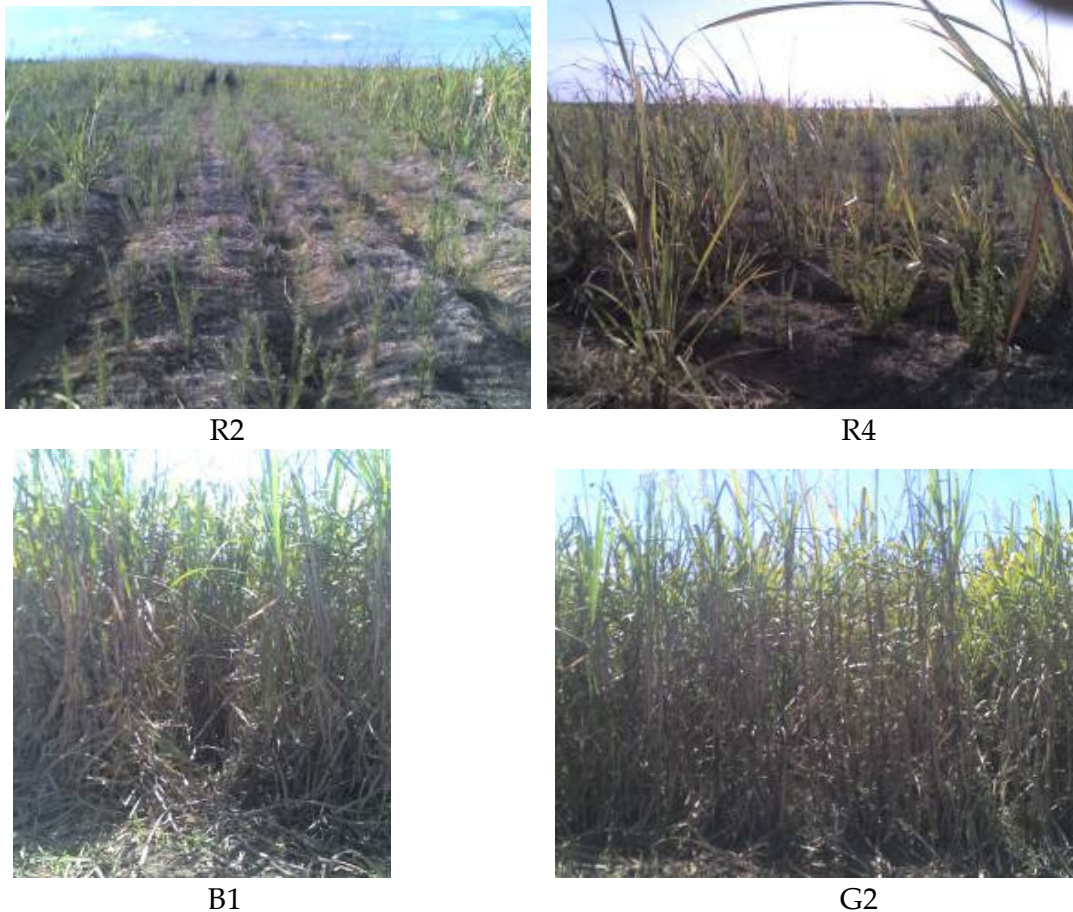


Figure 18. Photographs of cane growing at a number of the sampling locations taken prior to harvest.

The Bundaberg A9 crop displayed a large degree of spatial variability in terms of NDVI, with the low vigour region (red) dominating the north eastern corner (Figure 17c). This region was identified to have extremely poor cane with an average plant density of 10 stalks per linear metre compared to 17 measured in the blue zones (Figure 18). The measured average yield of the low NDVI zones was 15 TCH compared to 89 TCH in the blue regions, with the later also providing a slightly higher CCS (Figure 17).

Soil samples taken at depths of 0-20cm and 40- 60cm, identified low organic carbon, high salinity and sodicity to be the likely constraint to productivity. Using this information, the grower discontinued the second cane ratoon, as indicated by the bare soil in the 2011 image (Figure 19 b) and undertook remedial action on the soils. This included re-lasering, the application of 3 – 6 t/ha of gypsum based on the variability map, and a blanket application of 6 t/ha of chook manure. To further increase organic matter, a short fallow oats crop was grown and then ploughed in. For the 2011/ 2012 season, the block was re-planted with cane with only a slight improvement in growth, as inferred by an image captured on the 6 April 2012, identified along the north western edge of the crop (black circle in Figure 19 c).

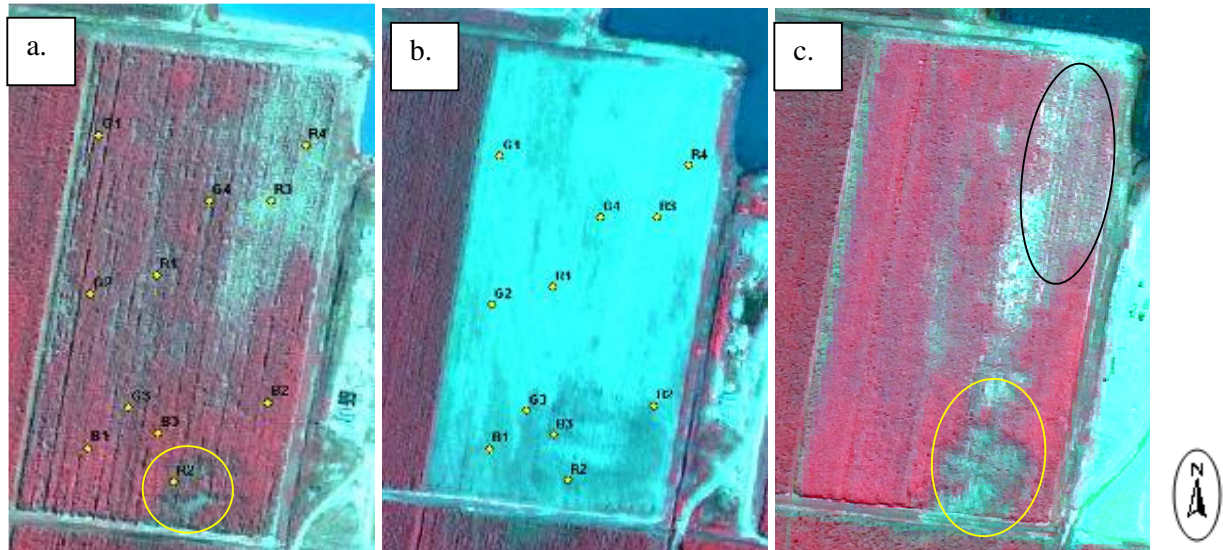
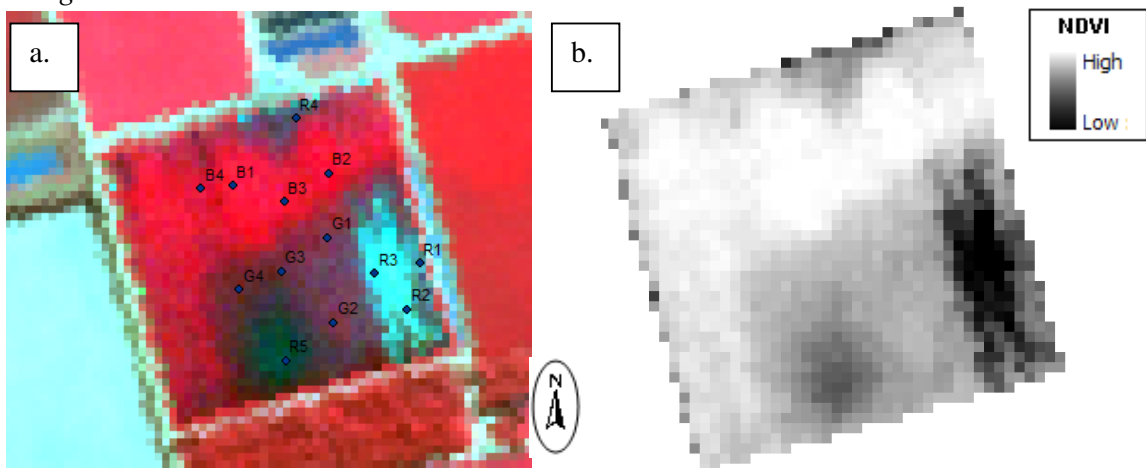


Figure 19. False colour images of Bullseye A9 block captured 14 May 2010, 23 March 2011 and 6 April 2012.

The extremely low yield measured at the R2 site (4 TCH) (yellow circle Figure 19) was believed to be the result of a saline soak with soil samples at 40 -60cm exhibiting high levels of chloride (663 mg/Kg) and exchangeable sodium (2.63 meq/110g). The subsequent increase in the poor production area surrounding this point in 2012 (Figure 19c) is believed to be the result of increased rainfall from 2010 raising the groundwater table and possibly increasing the hydraulic pressure from the dam located to the north west of the crop. It has been suggested that the grower install table drains and investigate raised beds as methods to improve drainage off the crop.

Bundaberg site (Relmay 3A): Variety Q208; Plant cane; Area 15.43 ha; harvested 25 October 2010; Row spacing 1.52 m.



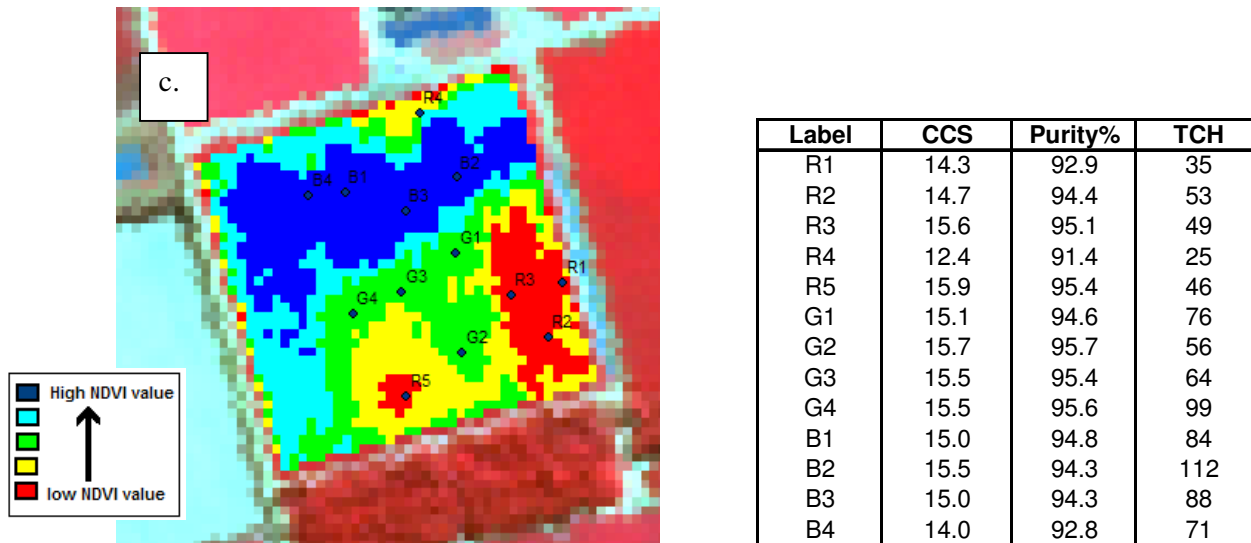


Figure 20. a. False colour SPOT5 image of Relmay 3A crop (10 May 2010). b. NDVI image derived from SPOT5. c. Classified NDVI image with field sampling sites indicated. Table: field sampling results.

Imagery of the Relmay 3A block (Figure 20) clearly identified a distinct segregation of crop vigour that was supported by similar differences in yield. Low NDVI red regions produced on average 41.6 TCH compared to 88.8 TCH in the blue high NDVI zones. There was little difference in the average CCS measured from each NDVI class, with the exception of a low value at R4 (12.4). Soil samples collected across the block identified a higher gravel content at the low NDVI regions R1 and R3, the result of prior remedial land forming where gravel was applied on sandy areas in an attempt to improve the water and nutrient holding capacity of the soil. Unfortunately as this was applied to the soil surface rather than at depth, this limited production rather than improved it. Sulphur was also identified to be at very low levels at 40- 60cm in the low NDVI regions (1.3 mg/kg) compared to (8.4 mg/kg) in the high NDVI regions. It was suggested that a test strip of higher sulphur be applied to determine if that alone would prompt a response, this unfortunately did not occur.

This block provides a good example of how imagery acquired over a number of cropping seasons can provide growers with an understanding of the inherent spatial variability within their blocks. If the spatial orientation of both high and low crop regions remains unchanged across seasons and crop age (i.e. 2005, 2008 and 2010) (Figure 21) then well informed management decisions can be made prior to planting, including the use of variable rate technologies (VRT) or more suitable cultivars. If the zones are unstable from season to season (i.e. 2005 to 2007) then the impacts of climate, management or rotational effects should be considered and managed appropriately.

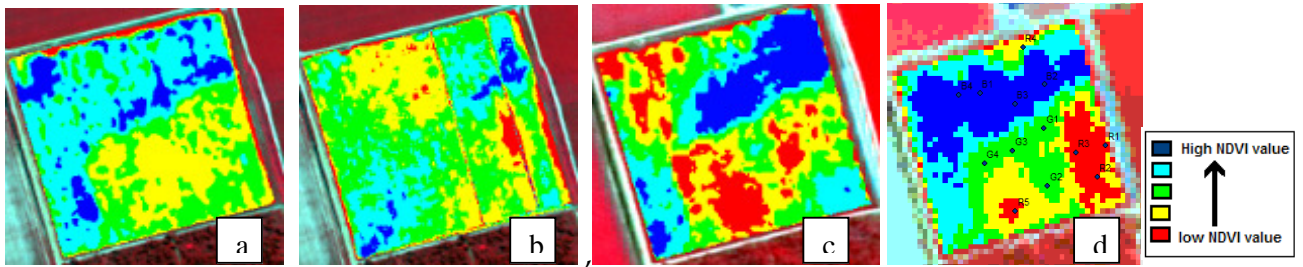


Figure 21. Classified NDVI images of cane grown within the Relmay 3A block during a. 2005 (Q188 2nd Ratoon); b. 2007 (Q205 April plant); c. 2008 (Q205 1st Ratoon) and d. 2010 (Q208 Spring replant).

Bundaberg site (Relmay 45): Variety Q183; Spring fallow plant; Area 19.5 ha; Harvested 27 September 2011; Row spacing 1.52 m.

The clustering of sample points (Figure 22 a) and cropped classified image (Figure 22 c) were the result of the northern end of the block being a different cultivar and the southern end being partially harvested prior to sample collection.

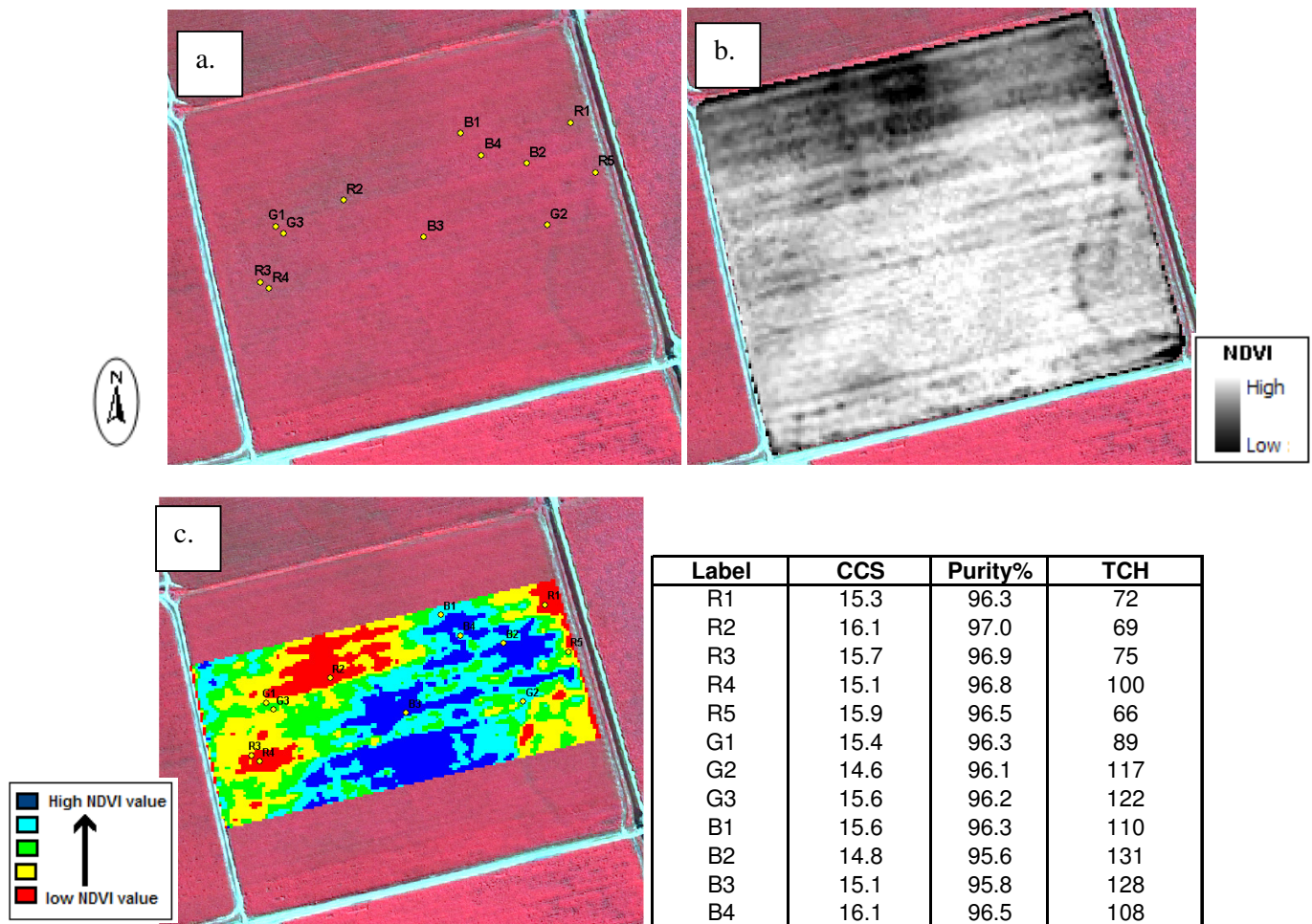


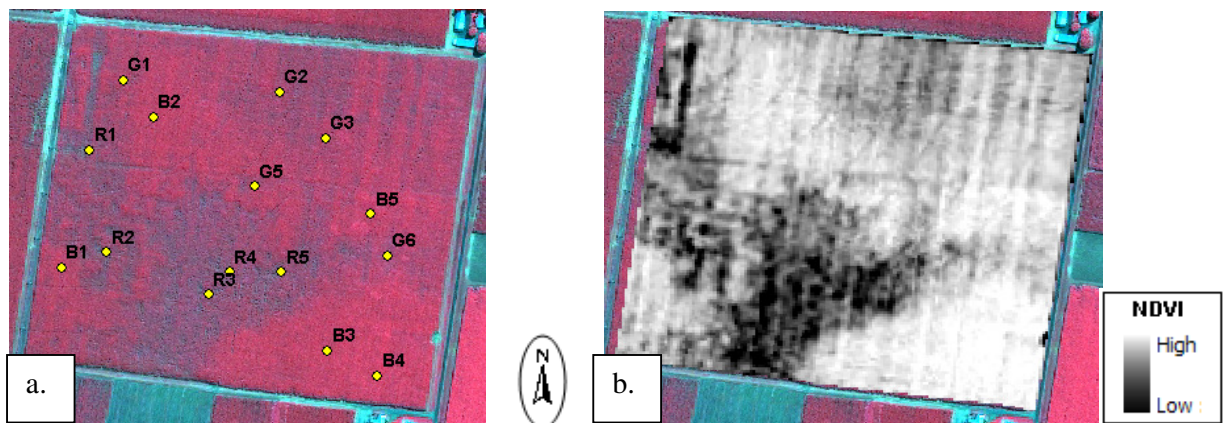
Figure 22. a. False colour IKONOS image of Relmay 45 crop (30 April 2011). b. NDVI image derived from IKONOS. c. Classified NDVI image with field sampling sites indicated. Table: field sampling results.

As with the previous examples, the Relmay cv. Q183 crop displayed a large degree of NDVI variability that was supported by differences in average yield measured in the low NDVI regions (77 TCH) to that in the high NDVI regions (120 TCH). There was little difference in average CCS between the high (15.4) and low (15.6) regions. Soil samples collected at 0-20 cm and 40-60 cm indicated critically low levels of exchangeable magnesium at depth may be limiting yield (0.16 meq/100g: 0.2 is the critical level), and that low lying crop regions may have experienced water logging following the high rainfall in January 2011. The low reflectance location R1 was attributed to extensive rat damage (Figure 23).



Figure 25. Cane stalks exhibiting extensive rat damage.

Bundaberg site (Bullseye C2): Variety KQ228; Spring fallow plant; Area 18.7 ha; Harvested 25 July 2011; Row spacing 1.5 m.



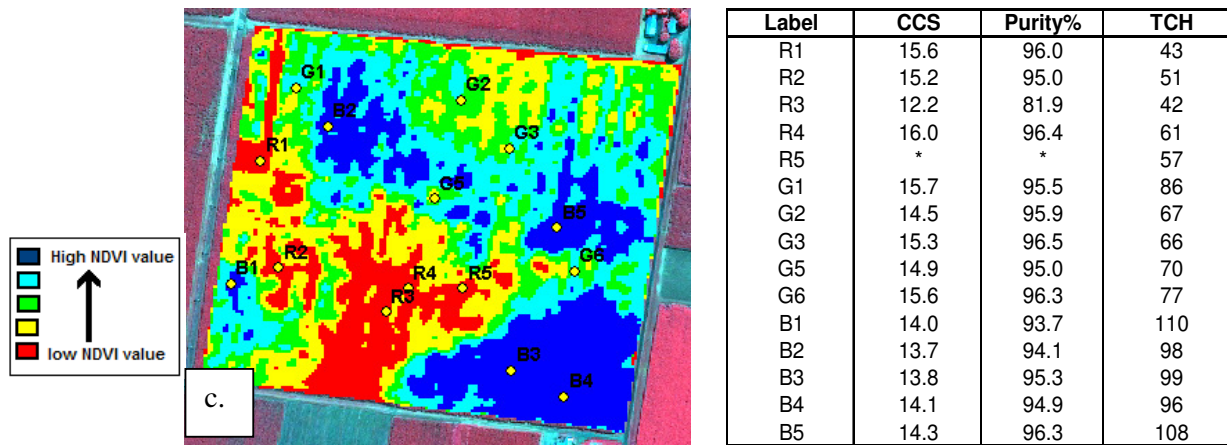
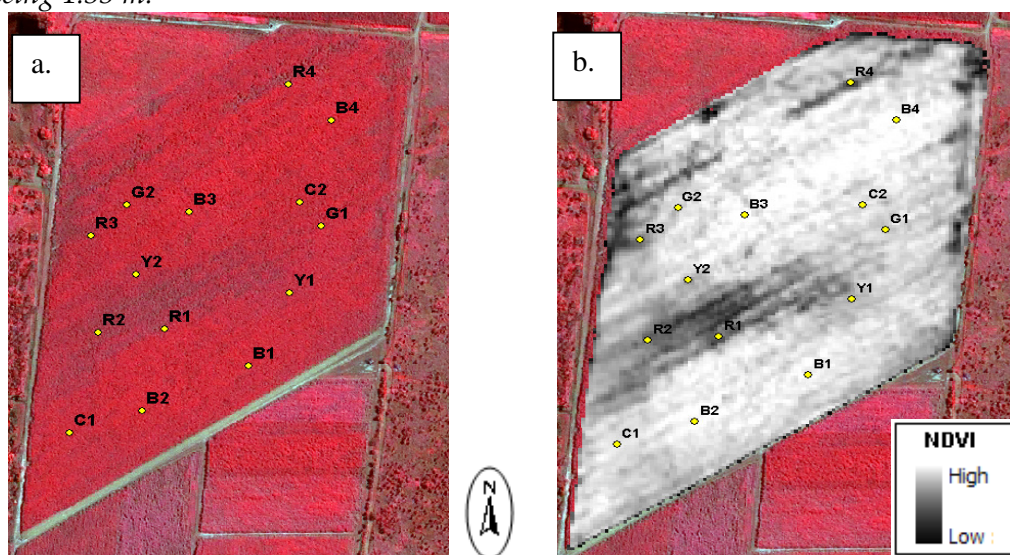


Figure 24. a. False colour IKONOS image of Bullseye C2 crop (30 April 2011). b. NDVI image derived from IKONOS. c. Classified NDVI image with field sampling sites indicated. Table: field sampling results.

Imagery of the Bullseye C2 crop (cv. KQ228) identified a large region of low NDVI extending from the southern end to the north-western corner (Figure 24c). Field sampling undertaken on the 25 July 2011, identified a 50% yield deficit between samples collected in the high NDVI (102 TCH) to that from the low NDVI regions (51 TCH). A slightly lower average CCS was measured in the high NDVI regions (14.0) compared to the low (14.7). Soil samples identified moderately sodic soils and poor drainage to be the likely drivers of reduced production, with a low ESP (0.79: 0-20cm and 3.44: 40- 60cm) measured at the high growth areas compared to 4.58 (0-20cm) and 12.92 (40-60cm) in the poor growth areas. This moderate subsoil level can prevent water infiltration, reduce oxygen availability and cause root death. It can be assumed that the poor growth areas suffered severe stunting from excessive rainfall early in the 2011 season. Both chloride and sodium levels were also higher in the poorer performing crop regions. Suggested remedial action included the application of gypsum / organic matter to increase drainage and the re-lasering of beds following the cane rotation.

Burdekin site (Pozzebon): Variety Q208; 1st ratoon cane; Area 12.4 ha; Harvested 26 November 2011; Row spacing 1.55 m.



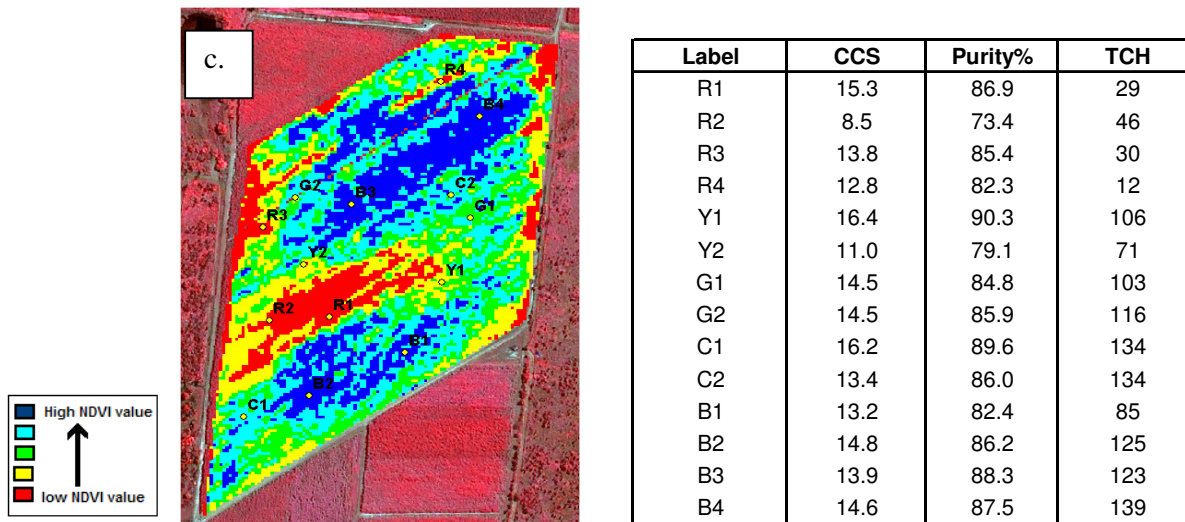


Figure 25. a. False colour IKONOS image of Burdekin Pozzebon crop (12 May 2011). b. NDVI image derived from IKONOS. c. Classified NDVI image with field sampling sites indicated. Table: field sampling results.

The Pozzebon crop, again displayed a large region of low NDVI (Figure 25 a) that when sampled yielded on average 29 TCH compared to 118 TCH from the high NDVI zones. Soil samples taken at a number of the locations indicated that the low performing regions may be attributed to saline and/ or sodic soils with low levels of potassium and phosphorus.

The agronomic group Farmacist (<http://www.farmacist.com.au/>) used the classified NDVI image (Figure 25 c) to develop a variable rate application of the liquid Nitrogen fertiliser Dundah, as well as a test strip (red strip) of 0 Nitrogen (Figure 26). A blanket application of 10- 15 kg/ ha of Sulphur was also applied. These applications were used in an attempt to verify the yield potential of cane in response to Nitrogen i.e. higher applications of N were applied to high NDVI zones, low rates applied to low NDVI zones.

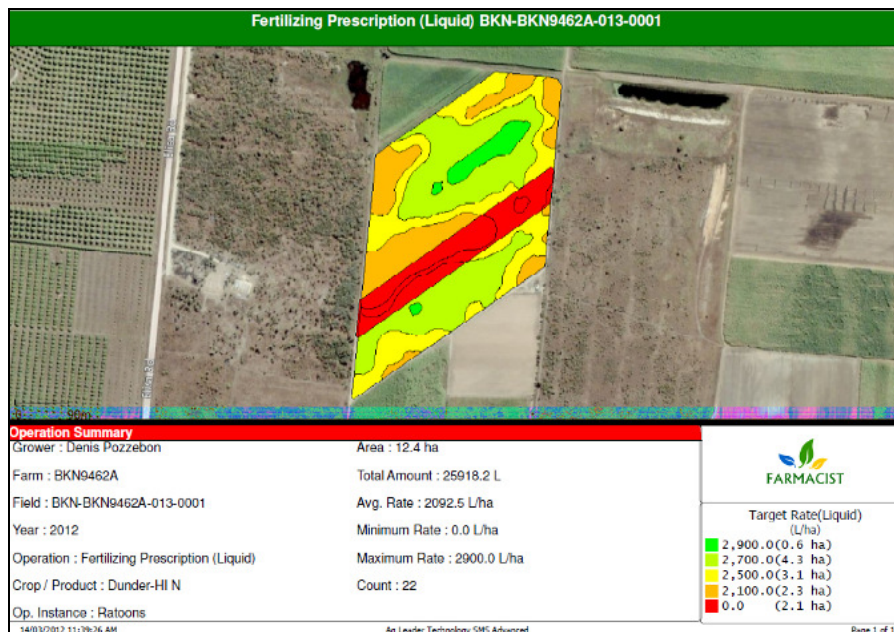


Figure 26. Variable rate fertiliser application derived from image information
SRDC Project DPI021 Final Report_without appendices.doc

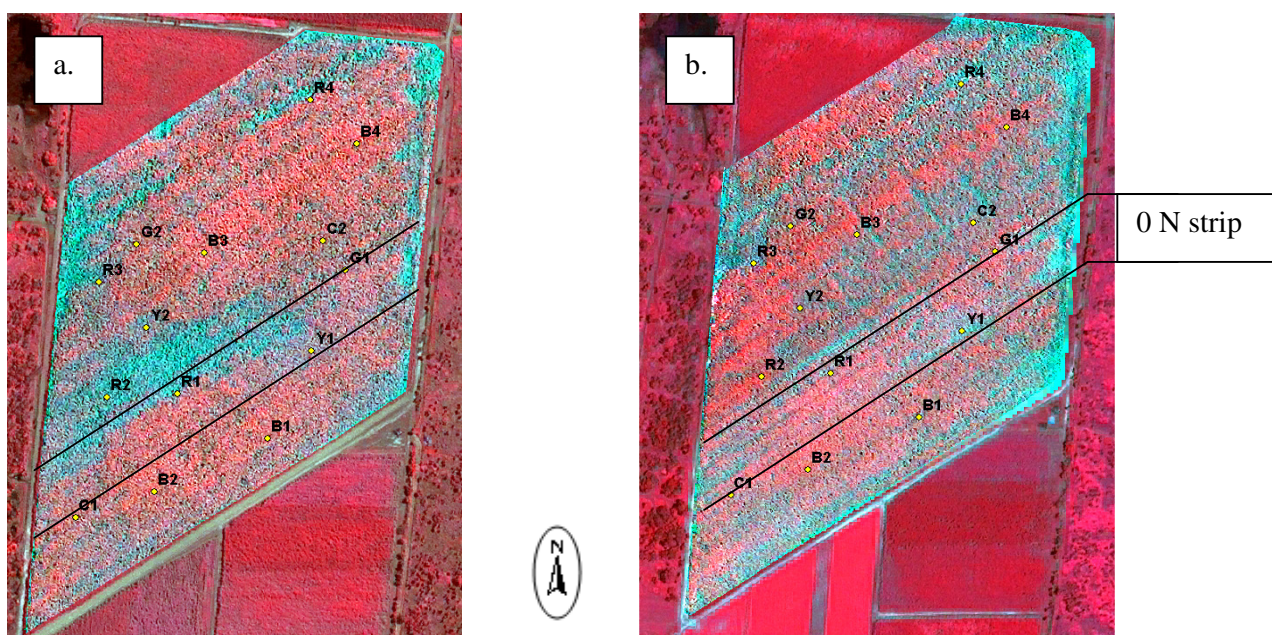


Figure 27. False colour IKONOS images captured 12 May 2011 (a) and 11 April 2012 (b), before and after the variable rate application of Dundah and the 0 N strip.

As seen in Figure 27 b, the variable N application produced little visual change in the 2012 crop, with only a minimal reduction in cane vigour observed within the 0 nitrogen strip. This result indicates that the spatial variability of the crop was not primarily driven by N deficiency but rather other constraints. Although this example did not definitively identify the driver of reduced production, it does demonstrate how imagery can be used to derive variable rate applications, and then subsequently used to monitor crop responses.

6.3. Assess the utility of this imagery for explaining the yield variability measured through the CSE022 ‘A coordinated approach to Precision Agriculture RDE for the Australian Sugar Industry’ project.

Accurate in-season predictions of regional yield are of vital importance for formulating harvesting, milling and forward selling decisions, whilst at a block scale, they provide growers with an understanding of both in-crop variability and total production. Currently, annual cane production estimates are made by visual yield assessments. Although this method can produce accuracies of up to 95% (Pitt pers. comm. 2011) it can be influenced by variable climatic conditions such as those experienced in 2010. As such, geographic information systems (GIS) and remote sensing (RS) may offer an additional tool for validating these predictions as well as potentially provide a more accurate seasonally sensitive method of prediction. The results presented within this section support this hypothesis.

As mentioned in section 5.6, a number of vegetation indices were investigated to identify that which produced the highest consistent correlation with yield (TCH), with GNDVI identified to the best suited. This result is consistent with other research that has identified

the Green visible band to be sensitive to chlorophyll content, but yet, less likely to saturate under high LAI (Gitelson et al 2002). Absorbance by the red spectral band has been identified to saturate at an LAI greater than 3, whilst research conducted by Wang *et al* (2007) identified the Green band to be sensitive to LAI beyond 5 or 6.

6.3.1. CSEO22 sites.

The following two examples were crops extensively sampled by SRDC Project CSE022, and as such only a brief overview of findings for the 2011 season are provided.

Burdekin site (CSE022 Pozzebon): Area 26.8 ha; Row spacing 1.55 m.

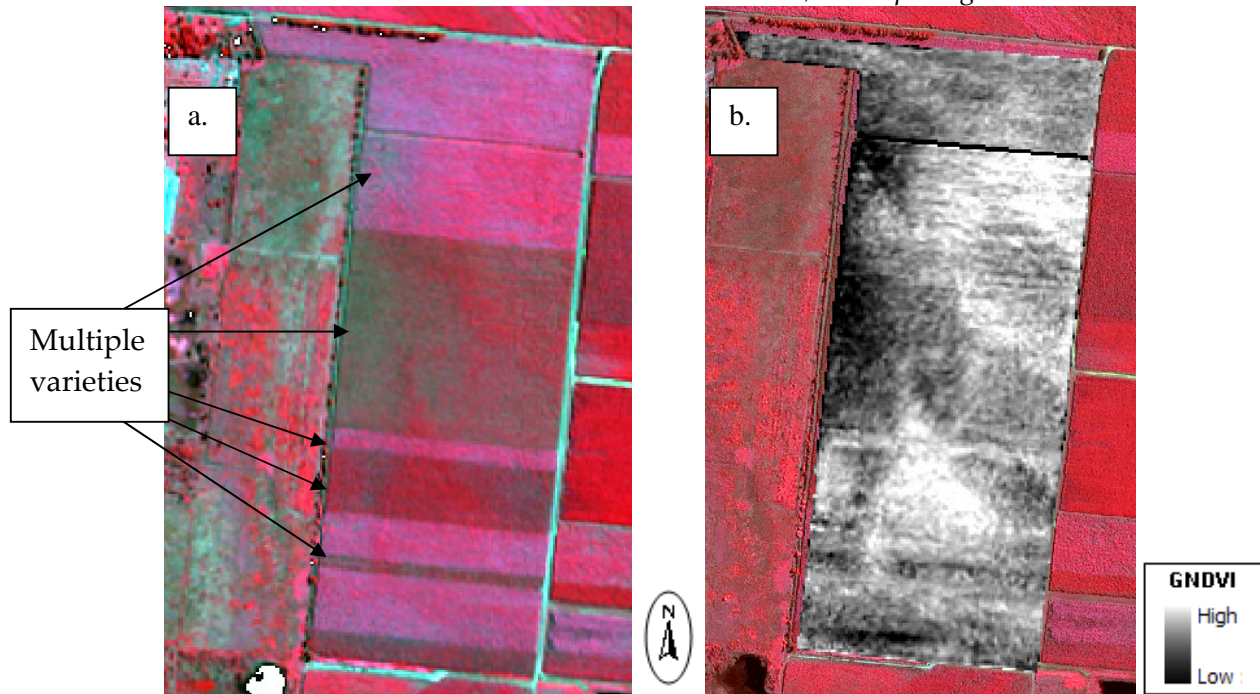


Figure 28. False colour IKONOS images captured 12 May 2011 (a) and derived GNDVI image (b)

As seen in Figure 28 a, the CSE022 Burdekin site included multiple varieties including Q183, Q208 and Tellus as well as a number of classes ranging from 3rd ratoon through to 6th ratoon. This variability within sub blocks resulted in an extended harvest period over 6 weeks. The GNDVI image (Figure 28 b) exhibited a large region of reduced vigour along the western edge, a trend that was also apparent in the yield map derived from the yield monitor and the high resolution EM38 and VERIS electromagnetic soil surveys (Bramley *et al.*, 2012) conducted after the 2011 harvest (Figure 29).

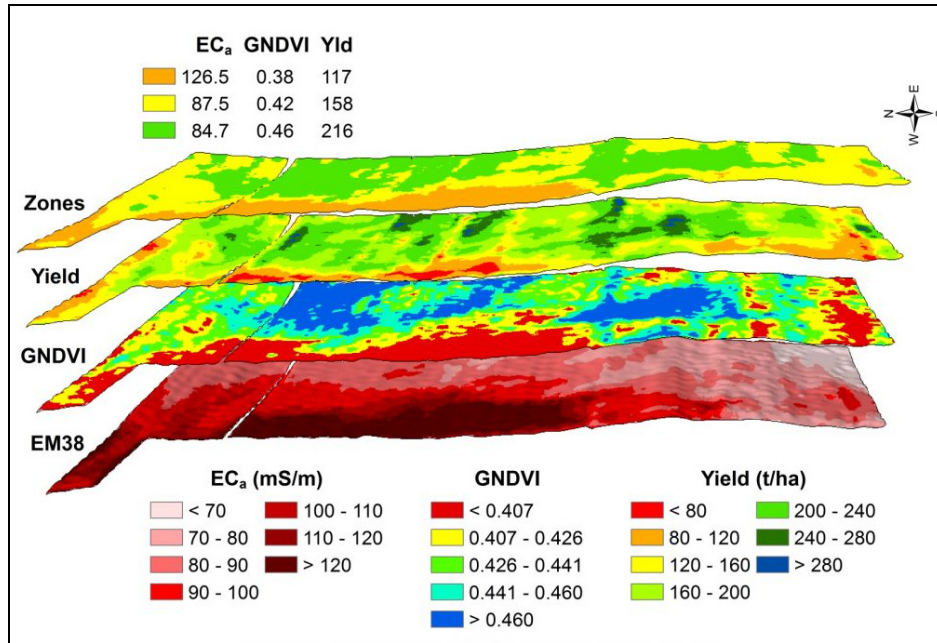


Figure 29. Comparisons of a classified GNDVI layer from an IKONOS image captured 12 May 2011; elevation and electro-conductivity (ECa) maps as well as a 3 zone classified map derived from the cluster analysis of the three layers.

The three zone layer derived from the cluster analysis (Figure 29) clearly demonstrates the consistency of spatial trends indentified by the ECa, GNDVI and yield layers. This result indicates that soil variation is the likely driver of crop variability, with topography, particularly poor drainage within low lying sodic areas contributing to reduced production.

In order to determine whether imagery could accurately explain yield variability, a direct correlation was undertaken between imagery GNDVI values and corresponding yields (TCH) for 50 specific locations extracted from the crop (Figure 30). The linear algorithm produced from this correlation was then used to convert each GNDVI pixel value into yield, allowing a surrogate yield map to be produced (Figure 31).

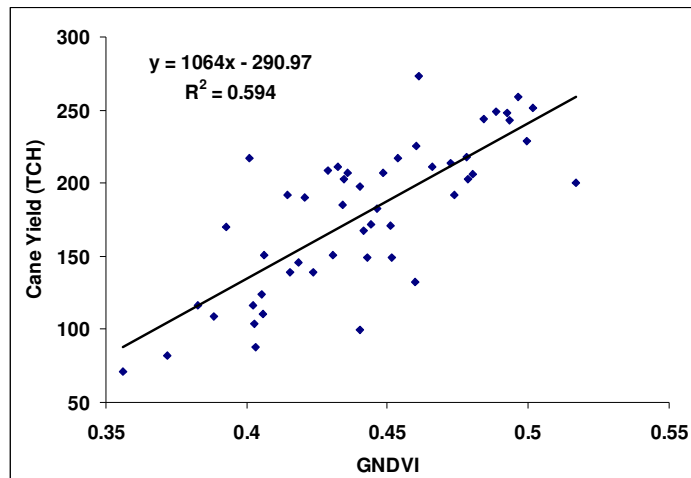


Figure 30. Correlation between yield (TCH) and GNDVI values from an IKONOS image (12 May 2011) extracted from 50 locations within the Pozzebon crop.

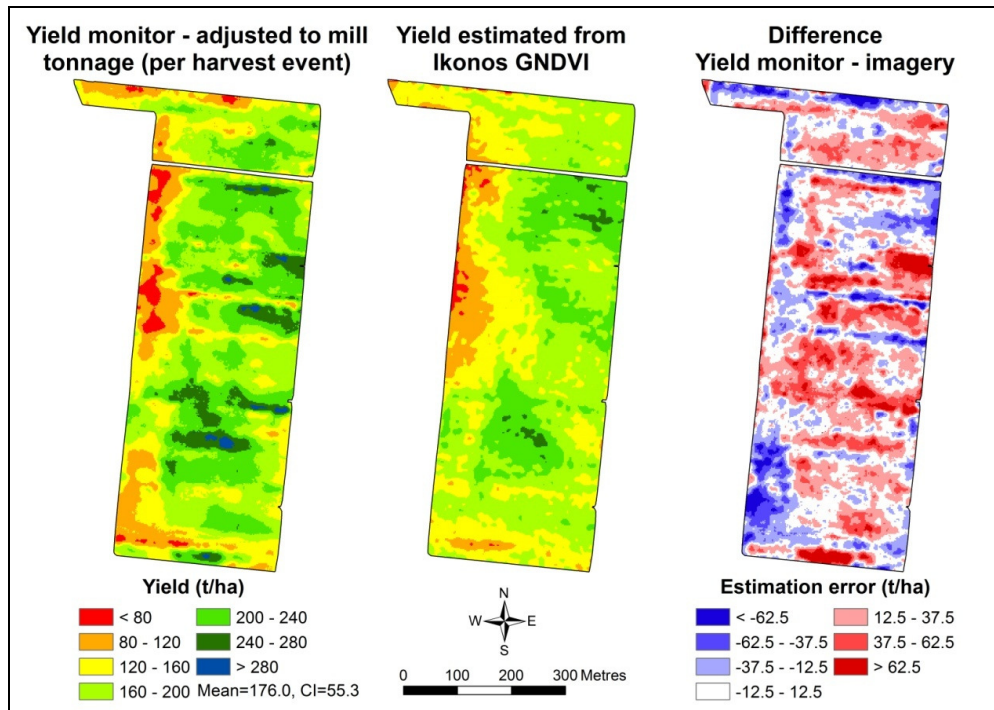


Figure 31. Classified yield maps produced from the Solfintec harvest monitor (left image) and derived from an IKONOS GNDVI image (middle image), with a difference map comparing the two provided on the right.

In order to compare the image-based yield map to that produced from the Solfintec yield monitor, a difference map was produced by subtracting one map from the other (Figure 31). The difference map identified much error between the predicted and actual yield values with large regions of over (blue) and under (red) prediction. In some case this prediction error was found to be 62.5 TCH. The yield layer derived from the Solfintec yield monitor was identified to have a confidence interval of ~55 TCH, which would have contributed to this large error. A correlation matrix undertaken on the same 50 points did provide a more encouraging comparison of the two derived yield maps, producing an R^2 of 0.59 (Figure 32).

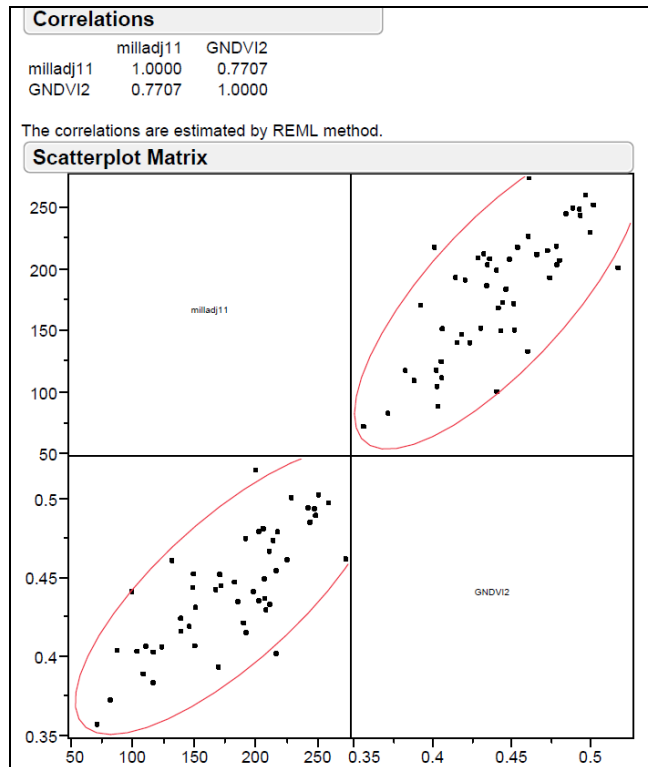


Figure 32. Correlation matrix developed between mill adjusted yield values from the Solfintec monitor to those derived from a GNDVI image.

Bundaberg site (CSE022 Hubert): Variety Q232; 1st ratoon cane; Area 6.7 ha.

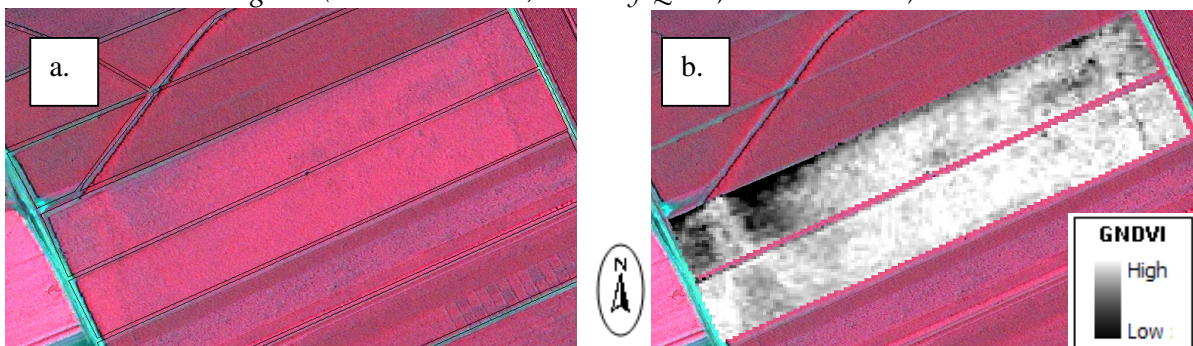


Figure 33. False colour IKONOS image of Hubert site captured 23 March 2011 (a) and derived GNDVI image (b).

The false colour and subsequent GNDVI image of the Hubert (CSE022) site for the 2011 season identified reduced crop vigour at the south- western end of the crop (Figure 33). This region of low vigour was again evident in the following April image capture, as well as within a yield map provided by from a roller opening yield sensor (Figure 34).

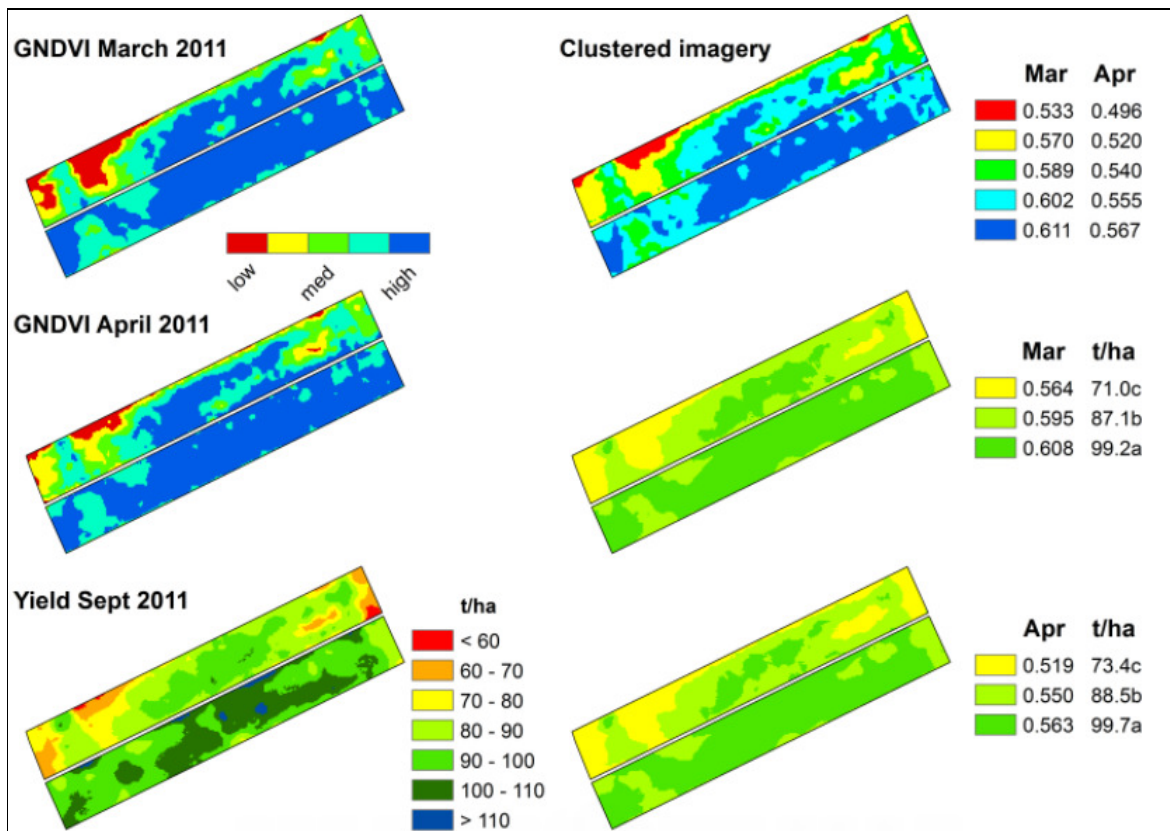


Figure 34. Comparisons of a number of spatial layers including classified GNDVI maps from IKONOS imagery captured 23 March and 30 April 2011; a classified yield map derived from CSE022 yield monitor and result of cluster analysis

A cluster analysis confirmed the consistency between the two GNDVI images (top right map in Figure 34), whilst the additional cluster analysis with yield monitor derived yield map identified a similar spatial pattern (bottom left map in Figure 34). For both image/yield cluster analyses, the mean zone yields were found to be significantly different with the 95% confidence interval for the yield map being ~ 11 t/ha. The results indicated that a potential yield difference of ~15 t/ha existed between the two sub-blocks. A correlation matrix undertaken between the two imagery derived yield maps and the monitor derived map achieved higher r values than that from the Pozzebon crop (Figure 35), a result most likely attributed to higher confidence interval ~12 t/ha of the 'roller opener' yield monitor.

	Yld3pix	April3pix	March3pix
Yld3pix	1.0000	0.8986	0.8142
April3pix	0.8986	1.0000	0.9050
March3pix	0.8142	0.9050	1.0000

The correlations are estimated by REML method.

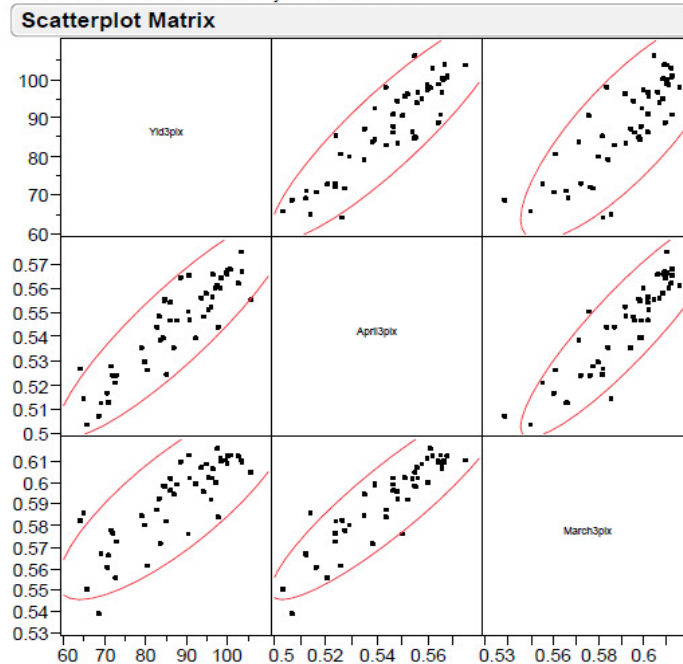


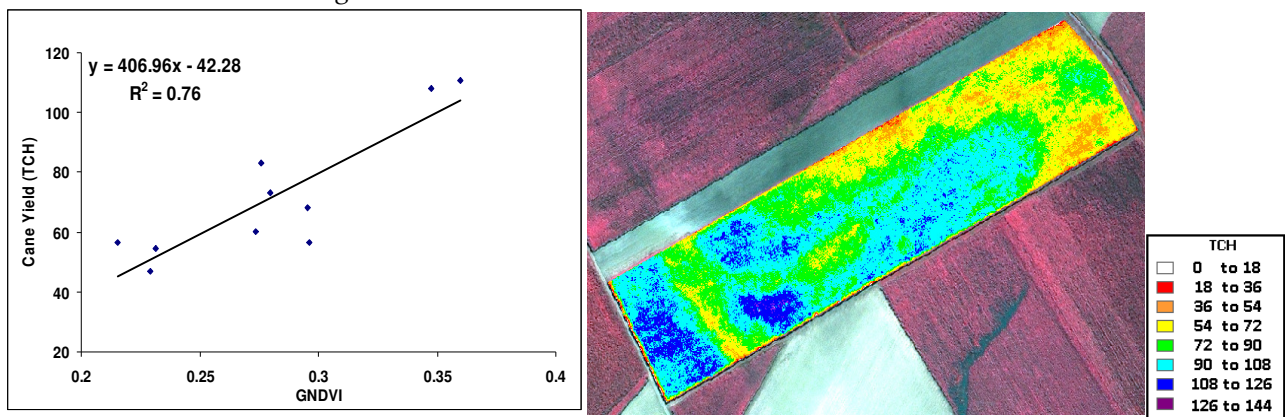
Figure 35. Correlation matrix between the harvest monitor derived yield map and the yield maps from two GNDVI IKONOS images acquired 23 March and 30 April 2011.

From the similarities observed between the classified zonal maps, it can be said that the image derived yield maps can be useful in characterising patterns of spatial variation in yield, and could therefore be a viable delineation tool for management zones. However, whether the imagery is able to predict yield with sufficient accuracy at the sub-block level requires further research and validation.

6.3.2. Additional yield validation sites.

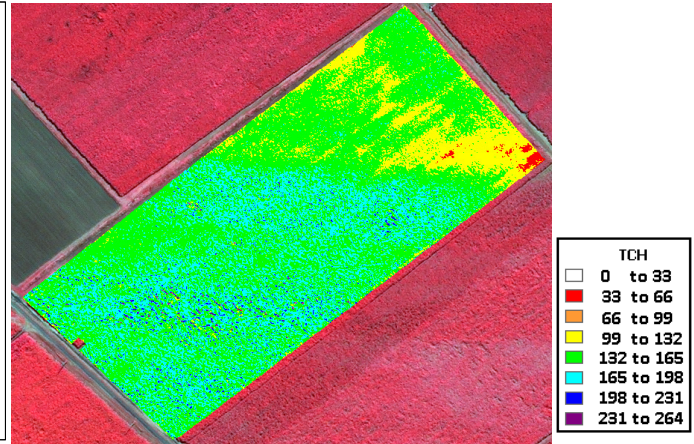
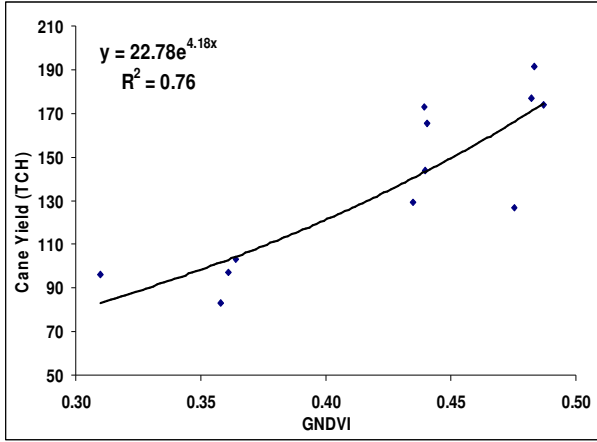
The following crops sampled for yield, coincide with those presented in section 6.2.1.

Herbert H2 IKONOS 2 August 2009.



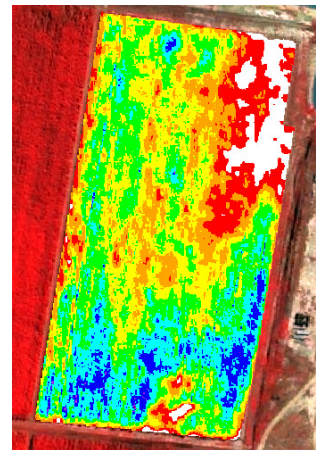
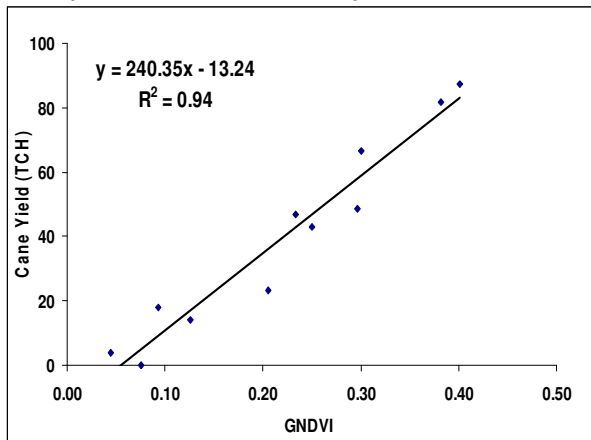
Predicted average yield= 84.7 TCH act. Ave yld = 72.4 TCH

Mann IKONOS 28 May 2010



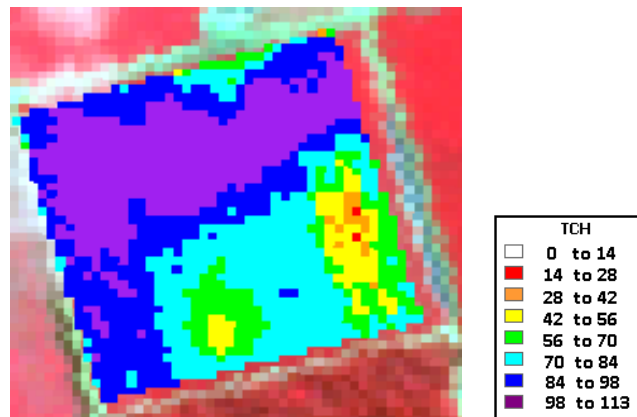
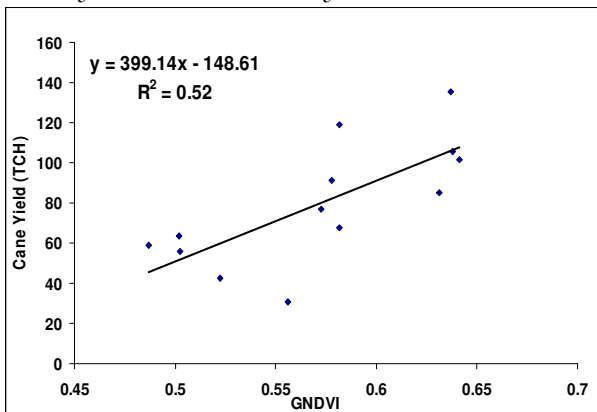
Predicted average yield= 147.2 TCH act. Ave yld = 132.5 TCH

Bullseye A9 IKONOS 14 May 2010



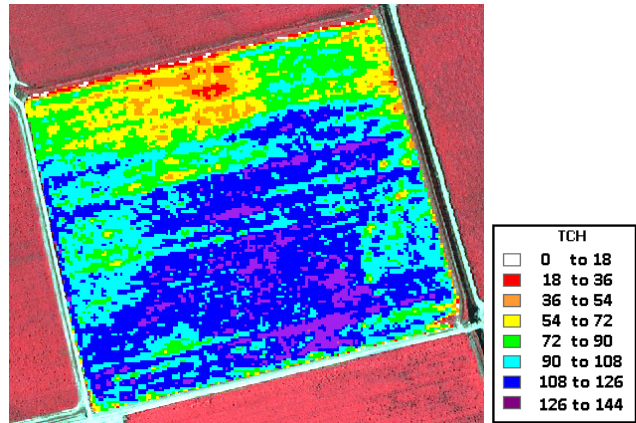
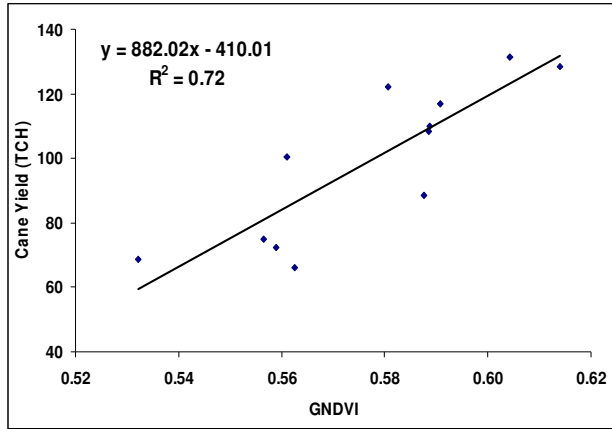
Predicted average Yield= 51.3 TCH Actual Ave yield was 40.1 TCH

Relmay 3A SPOT5 14 May 2010



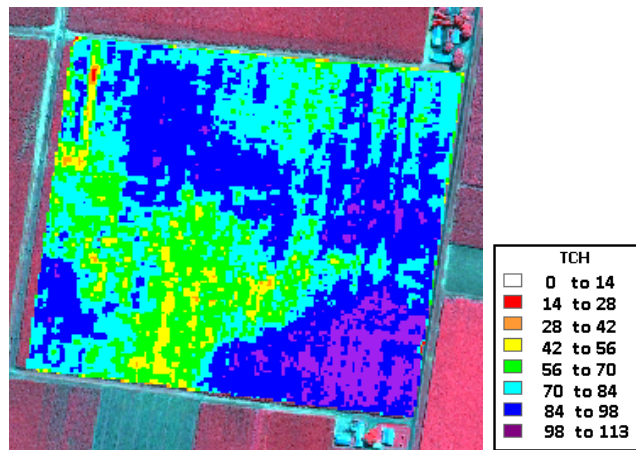
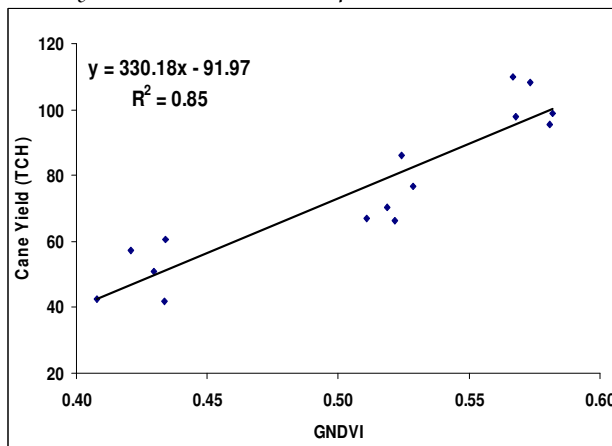
Predicted average Yield= 85.7 TCH Actual Ave yield was 93.4 TCH

Relmay 45 IKONOS 23 March 2011



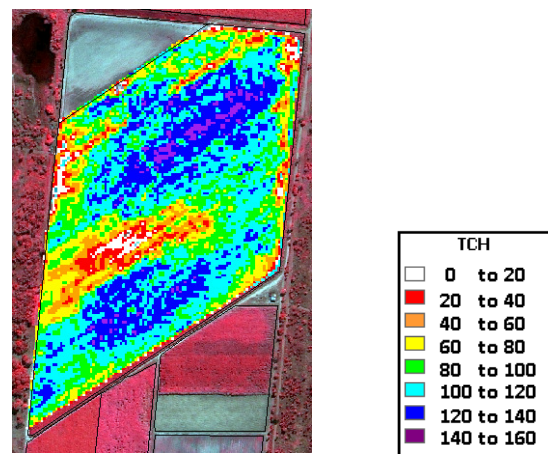
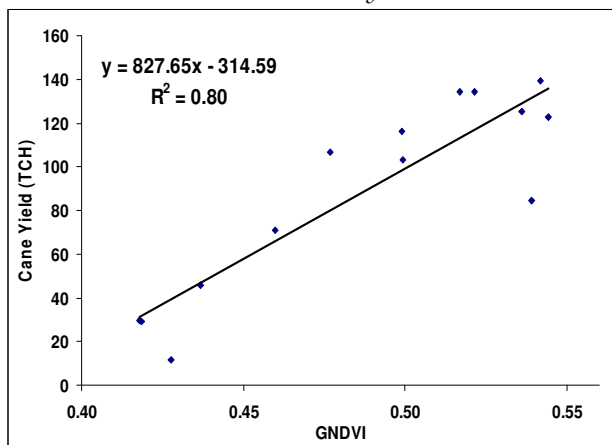
Predicted average Yield= 98.3 TCH Actual Ave yield was 100 TCH

Bullseye C2 IKONOS 30 April 2011



Predicted average Yield= 80.4 TCH Actual Ave yield was 88.7 TCH

Pozzebon 13 IKONOS 12 May 2011



Predicted average Yield= 93.2 TCH Actual Ave yield was 88.6 TCH

Figure 36. Correlation between GNDVI and crop yield (TCH) for 7 crops hand sampled during 2009, 2010 and 2011. Derivation of yield maps from each respective correlation algorithm.

The examples provided in Figure 36, demonstrate how surrogate yield maps can be derived from imagery and coordinated field sampling. At block level, predictions of average yield derived from the average GNDVI values ranged from 28% over prediction (Bullseye A9) to 9.4% under (Bullseye C2) (Figure 36). These inaccuracies may have resulted from the 5 metre linear sampling area not providing a true representative measure of actual yield found within each of the zones, or alternatively the result of errors with the consigned mill data.

In an attempt to evaluate the accuracy of the yield prediction algorithms at the within crop level, an estimate of yield was recalculated from the GNDVI value for each sampled location, using the respective crop algorithm. As seen in Figure 37, a slight under prediction of higher yield values and over prediction of low values occurred.

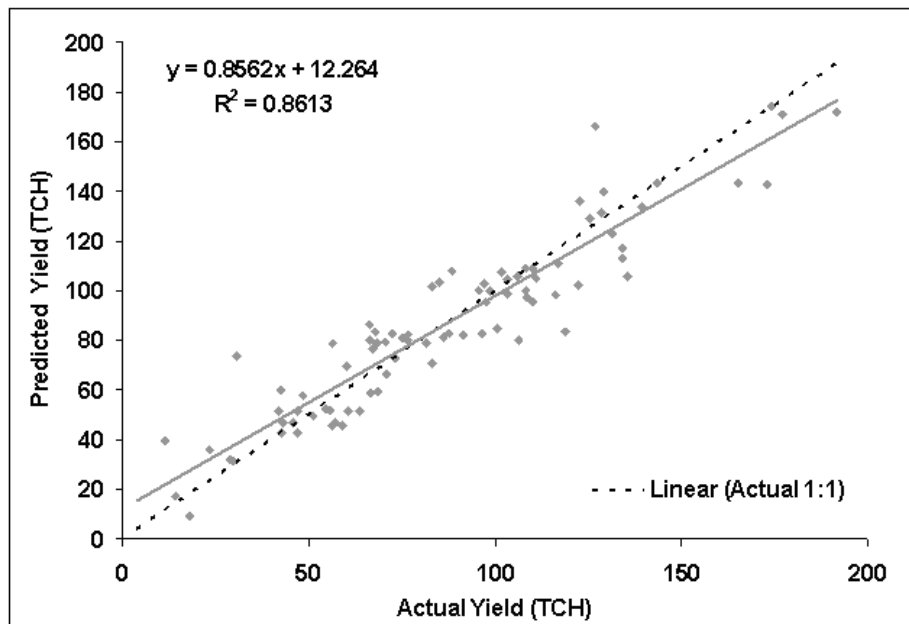


Figure 37. Comparison of actual cane yield (TCH) measured at each sample location (7 crops in Figure 36) to predicted yields derived from each respective crop algorithm.

6.3.3. Derivation of a generic algorithm.

The previous section identified imagery to be a potentially useful tool for generating surrogate yield maps. However, the need for labour and time intensive field measurements to calibrate the imagery was considered to be a major restriction to future commercial adoption. In an attempt to remove field sampling, the project team developed and evaluated a 'generic' non cultivar, non class specific algorithm. The preliminary algorithm was derived from the average GNDVI values of 112 blocks (SPOT5 image captured 10 May 2010) with corresponding average 2010 cane yields ($R^2= 0.61$). This included multiple varieties and crop classes but excluded stand over crops. The predictive ability of this algorithm was evaluated over 600 ha of cane (39 crops) grown within the Bundaberg region during the 2008 season. Using a SPOT5 image captured 31 March 2008, a predicted average yield of 66.5 TCH was achieved, 3.8% under the average actual delivered yield (69 TCH). This close estimation was

encouraging and resulted in a new algorithm being developed from both the 2008 and 2010 data (Figure 38). Although the inclusion of the 39 2008 data points did not increase the correlation coefficient of the overall equation, it did provide another season of data. It was hoped that this temporal addition would increase the algorithms ability to compensate for seasonal variability.

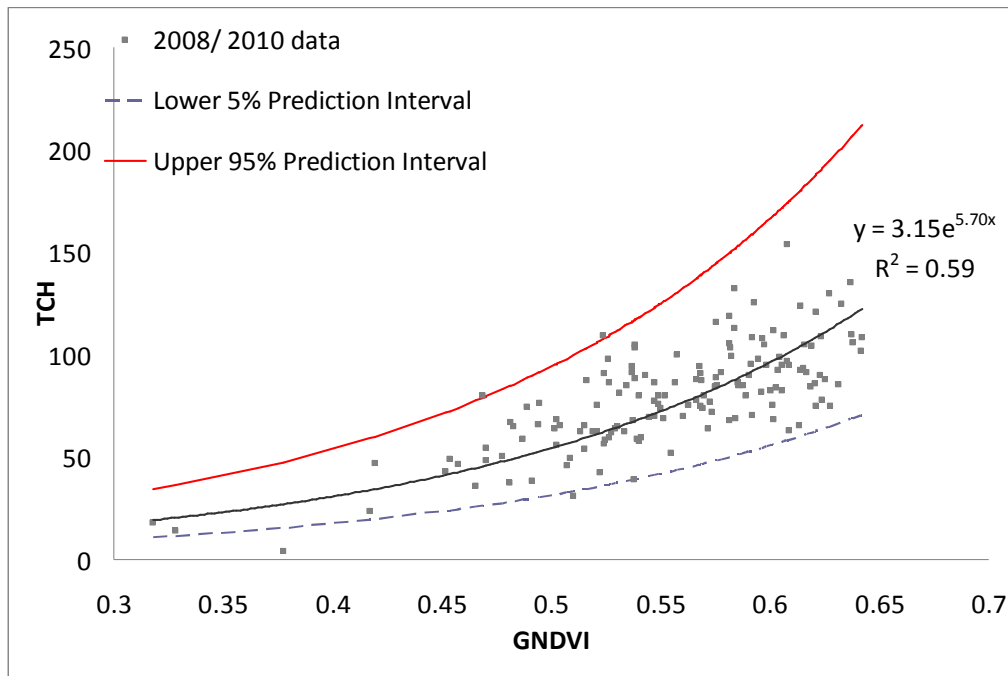


Figure 38. Correlation between GNDVI and Yield (TCH) measured during the 2008 and 2010 growing seasons (n=151). 95% prediction intervals were calculated to show error on individual predictions.

The resultant algorithm (Equation 1) was evaluated over a number of point source locations within sampled crops as well as for the prediction of average yield for the Bundaberg, Isis, Burdekin and Herbert growing regions.

Equation 1:
$$y = 3.1528 * e^{(5.6973 * x)}$$

Where y = predicted average yield (TCH)
 x = average GNDVI value extracted from TOA SPOT5 image.

6.3.4. Validation of the generic algorithm at the regional level.

For remote sensing to be considered as a useful and adoptable tool for making predictions of regional yield it has to achieve accuracies as good as or better than those achieved from the current visual assessments i.e. 95%. In order to test this; the generic algorithm was evaluated over the three main growing regions, Bundaberg/ Isis (Figure 39), Herbert (Figure 41) and Burdekin (Figure 43) during the 2010, 2011 and 2012 growing seasons. Additional regions of NSW (Condong) (Figure 45) and Mulgrave (Figure 46) were also investigated during the 2012 season.

Bundaberg/ Isis:

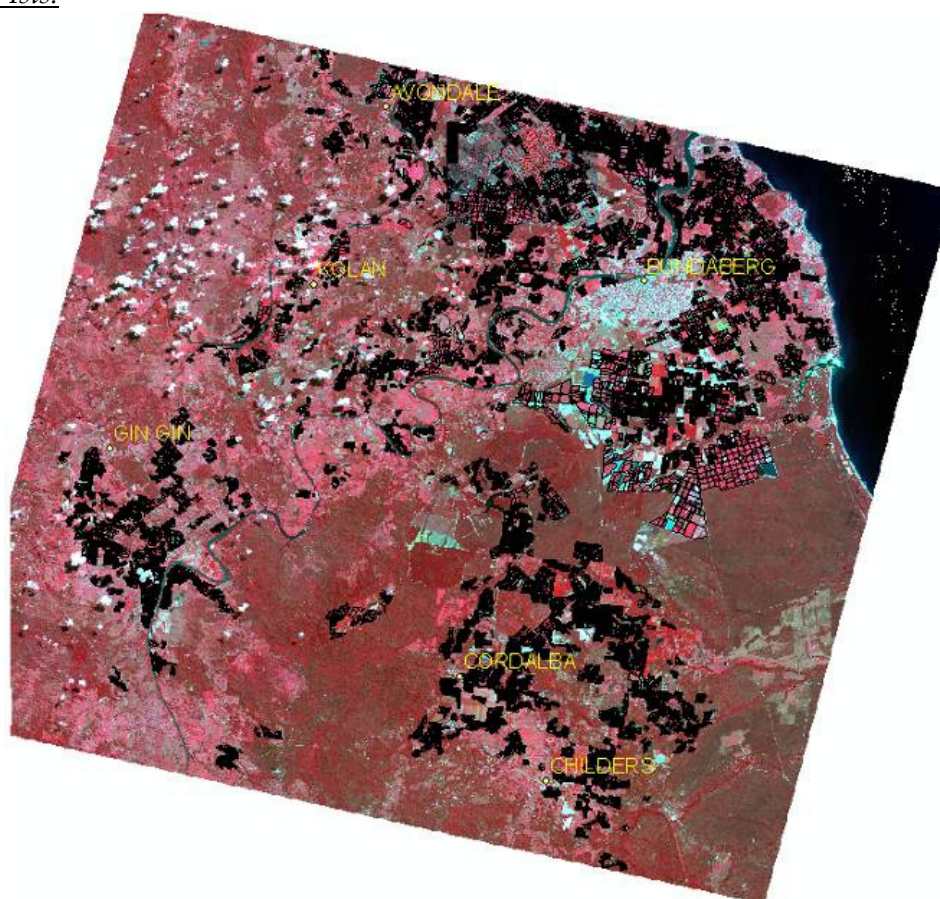


Figure 39. SPOT5 image of the Bundaberg/ Isis growing region (3600km²) overlaid with crop boundary vector file (black lines).

The evaluation of the generic algorithm over the Bundaberg and Isis growing regions during 2010- 2012, produced encouraging results in the prediction of average yield, as shown in Table 6. At the block level the accuracies were quite poor, ranging from predictions that were 89% under estimated to 494% over estimated (Isis 2012). Note 100% signifies an accurate prediction. Slight inaccuracies with Mill data as well as discrepancies with yield consignments to actual blocks also contributed to this degree of variability.

Table 6 . Predicted versus actual average yield for the Bundaberg and Isis growing regions.

Harvest year	Growing Region	Number of crops	Pred. ave. Yield (TCH)	Act. ave. Yield (TCH)	Range of Prediction at block level (% of actual)
2010	Bundaberg	3544	79.7	81.8	36 to 364
2011	Bundaberg	3824	80.1	73.3	16 to 436
2012	Bundaberg	3217	88.0	88.9	13 to 410
2010	Isis	2772	84.0	84.0	40 to 638
2011	Isis	4205	98.4	83.3	39 to 594
2012	Isis	4000	92.5	96.0	11 to 595

The obvious exception to these predictions is the 2011 season, where severe rainfall events occurring at the end of 2010, significantly reduced crop yield and therefore contributed to the over predictions (Table 6). This yield deficit can be clearly seen in Figure 40 a, with the separation of the exponential trend line representing the generic algorithm (dotted line) to that derived from 2011 crop data (green line). The high similarity between the generic trend line to that produced by the 2010 (blue line) and the 2012 (red line) data explains the close estimates achieved for those seasons. For the Isis region (Figure 40 b) a similar pattern to that of the Bundaberg region exists for the 2010 and 2011 trend lines. However, the 2012 (red line) displays a very different slope and intercept. The 4% under estimation of yield achieved for the 2012 season was due to the average GNDVI value (0.5931) for the 2012 crops (n = 4000) coinciding with the intercept between the 2012 and generic algorithm trend lines. The reason for the different 2012 trend line is unknown. It is hypothesised to be possible a seasonal effect or the result of inconsistencies with the mill vector file and consignment data.

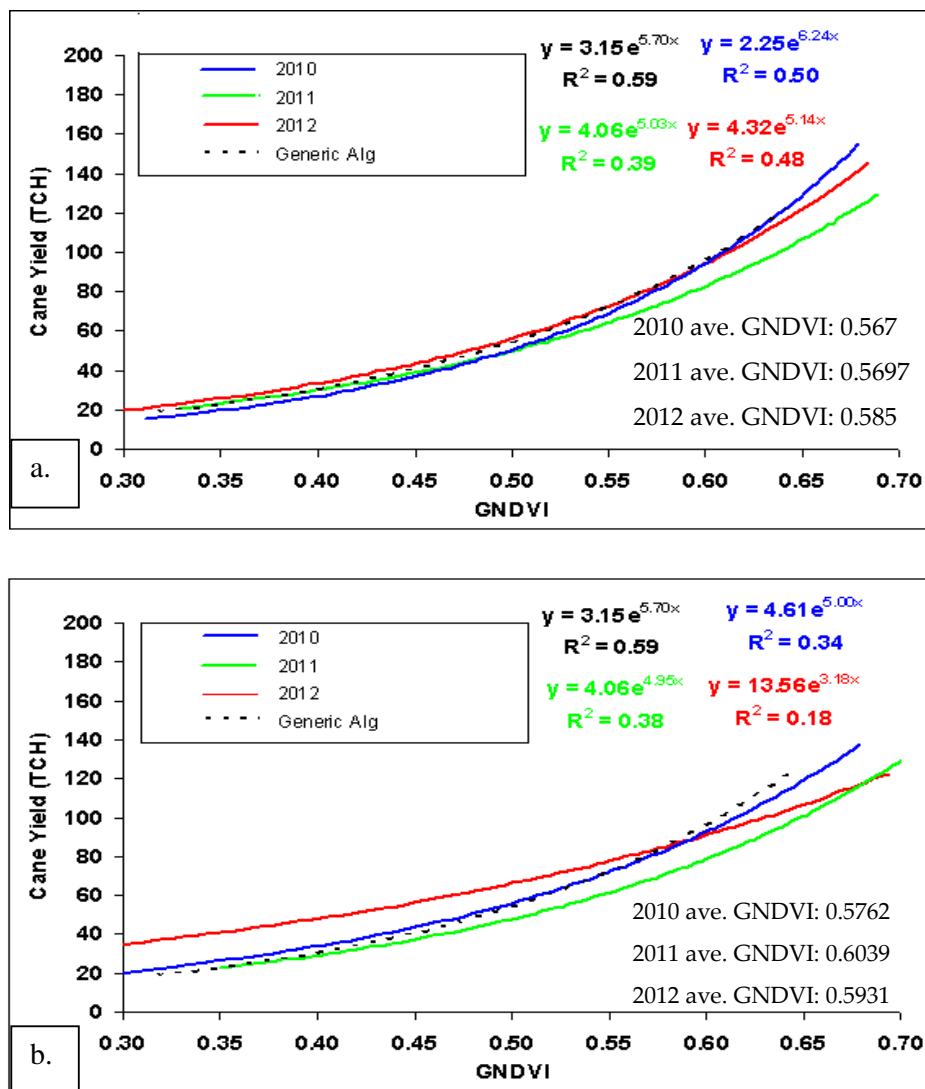


Figure 40. Exponential trend lines produced between GNDVI and yield for the generic algorithm (dashed line) as well as all crops imaged within the Bundaberg (a) and Isis (b) region during the 2010 (blue line), 2011 (green line) and 2012 (red line) growing seasons.

Herbert:

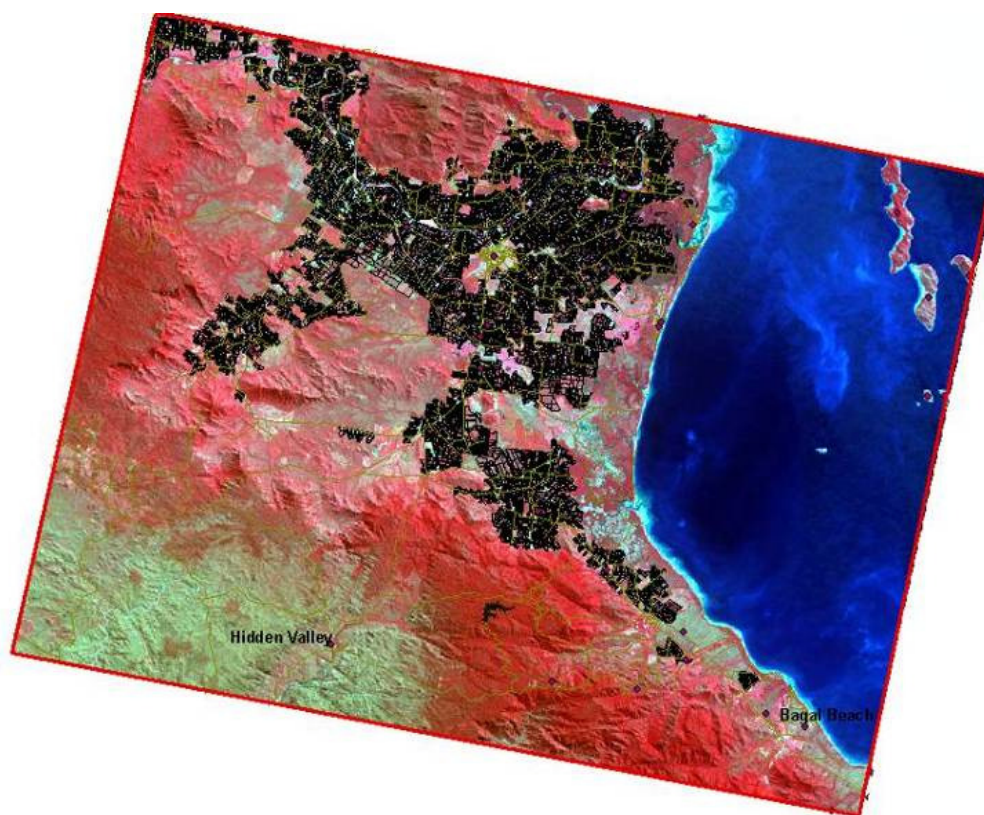


Figure 41. SPOT5 image of the Herbert growing region (3600km²) overlaid with crop boundary vector file (black lines).

The evaluation of the generic algorithm over the Herbert growing region during 2011 and 2012 also produced encouraging results (Table 7). Note no image was captured during 2010 due to continual cloud cover. Again predictions at the block level were also highly variable.

Table 7. Predicted versus actual average yield for the Herbert growing region.

Harvest year	Growing Region	Number of crops	Pred. ave. Yield (TCH)	Act. ave. Yield (TCH)	Range of Prediction at block level (% of actual)
2011	Herbert	8596	51.4	55.0	16 to 350
2011	Herbert	6481 (no SO*)	56.9	53.5	29 to 350
2012	Herbert	15463	75.0	72.0	17 to 514

* SO refers to stand over crops that were not harvested in 2010 due to severe weather events.

The influence of stand over (SO) crops was clearly identified in the prediction accuracies achieved for the 2011 growing season, with an under prediction occurring when SO crop were included and an over prediction once removed. These SO crops contributed up to 33% of the all crops imaged for this season. On average, the SO crops displayed a lower GNDVI value (SO = 0.4898; non SO = 0.5077) due mainly to being severely lodged, it did however yield slightly higher as a result of an extra season of growth. With crops denoted as SO removed for the 2012 season, an over prediction of 6.4% was achieved. A comparison of the generic algorithm trend line to those produced from the 2011 and 2012 data sets (Figure 42)

demonstrates some separation at the higher GNDVI values and therefore explanation for the over predictions. It is therefore suggested that a Herbert specific algorithm be investigated in the future.

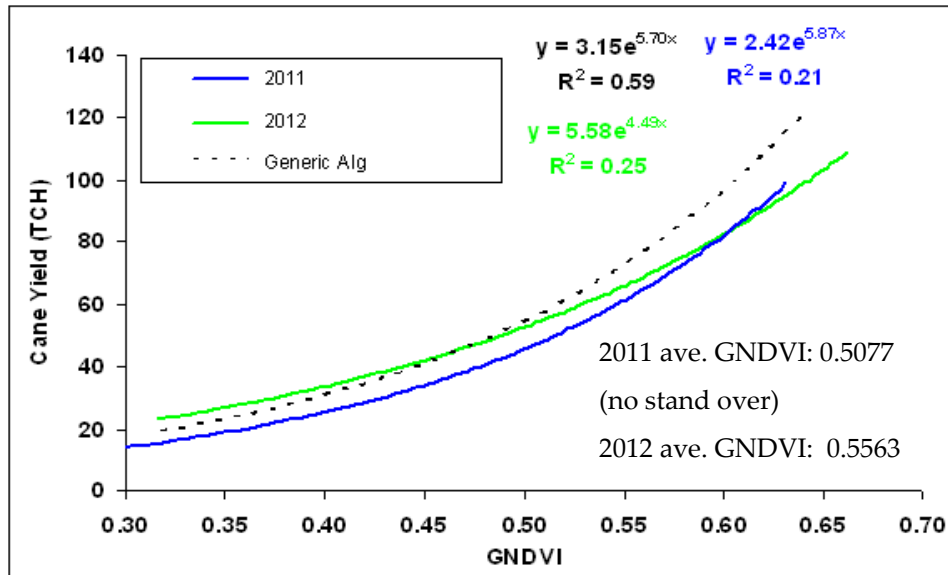


Figure 42. Exponential trend line produced between GNDVI and yield for the generic algorithm (dashed line) as well as all crops imaged within the Herbert region during the 2011 (blue line) and 2012 (green line) growing seasons.

Burdekin

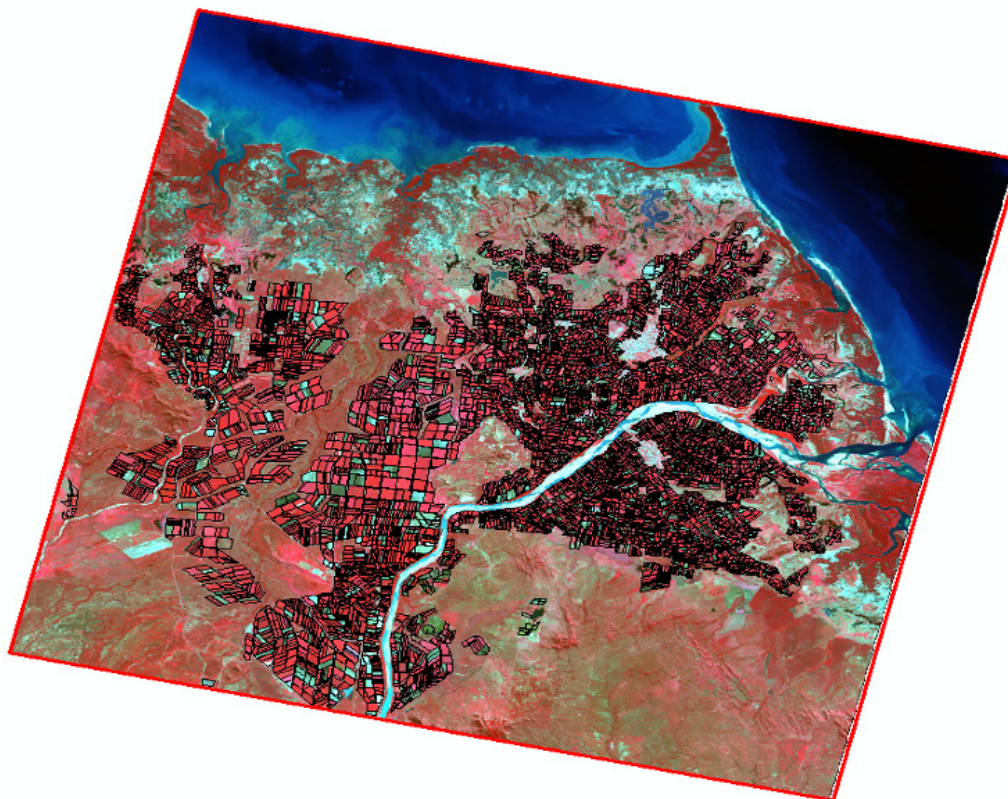


Figure 43. SPOT5 image of the Burdekin growing region (3600km²) overlaid with crop boundary vector file (black lines).

The prediction estimates for average yield produced by the generic algorithm for the Burdekin region was extremely poor for both the 2010 and 2011 season (Table 8).

Table 8 . Predicted versus actual average yield for the Burdekin growing region, generic algorithm.

Harvest year	Growing Region	Number of crops	Pred. ave. Yield (TCH)	Act. ave. Yield (TCH)	Range of Prediction at block level (% of actual)
2010	Burdekin	4573	91.9	129.6	22 to 411
2011	Burdekin	4999	83.2	120.0	17 to 360

The under predictions of 29% (2010) and 31% (2011) were attributed to the different seasonal and growing conditions experienced within this region, when compared to Bundaberg/ Isis. As such a Burdekin specific generic algorithm (equation 2) was developed from the 2010 data and then evaluated over the 2011 and 2012 seasons. This resulted in vastly improved prediction estimates (Table 9).

Equation 2:
$$y = 12.691 * e^{(3.8928 * x)}$$

Where y = predicted average yield (TCH)

x = average GNDVI value extracted from TOA SPOT5 image.

Table 9. Predicted versus actual average yield for the Burdekin growing region, Burdekin algorithm.

Harvest year	Growing Region	Number of crops	Pred. ave. Yield (TCH)	Act. ave. Yield (TCH)	Range of Prediction at block level (% of actual)
2011	Burdekin	4999	118.8	120.0	29 to 468
2012	Burdekin	6921	110.0	105.0	16 to 448

As seen in Figure 44, differing trend lines were produced from the correlations between GNDVI and yield for the three growing seasons, a result most likely attributed to seasonal variability. Considering this, it was fortunate that the prediction estimates for 2011 and 2012 were so high, i.e. 1% under prediction (2011) and 4.8% over prediction (2012). For 2011 this was the result of the average GNDVI value (0.5744) closely aligning to the 2010 and 2011 trend line intercept; while for 2012, the average GNDVI value (0.5543) corresponded to a point where both the 2010 and 2012 trend lines exhibited minor separation i.e. 5 TCH.

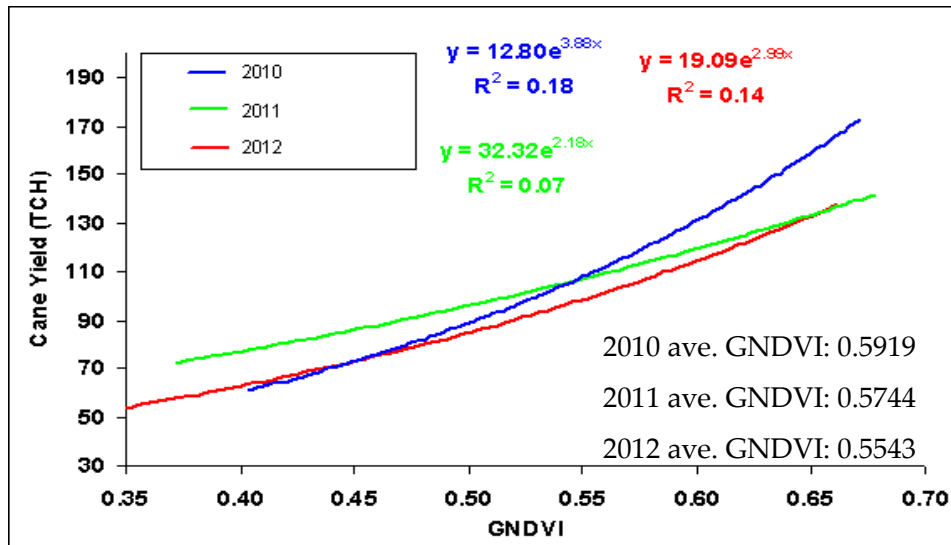


Figure 44. Exponential trend line produced between GNDVI and yield for the Burdekin generic algorithm (blue line) as well as all crops imaged within the Burdekin region during the 2011 (green line) and 2012 (red line) growing seasons.

Condong (NSW)

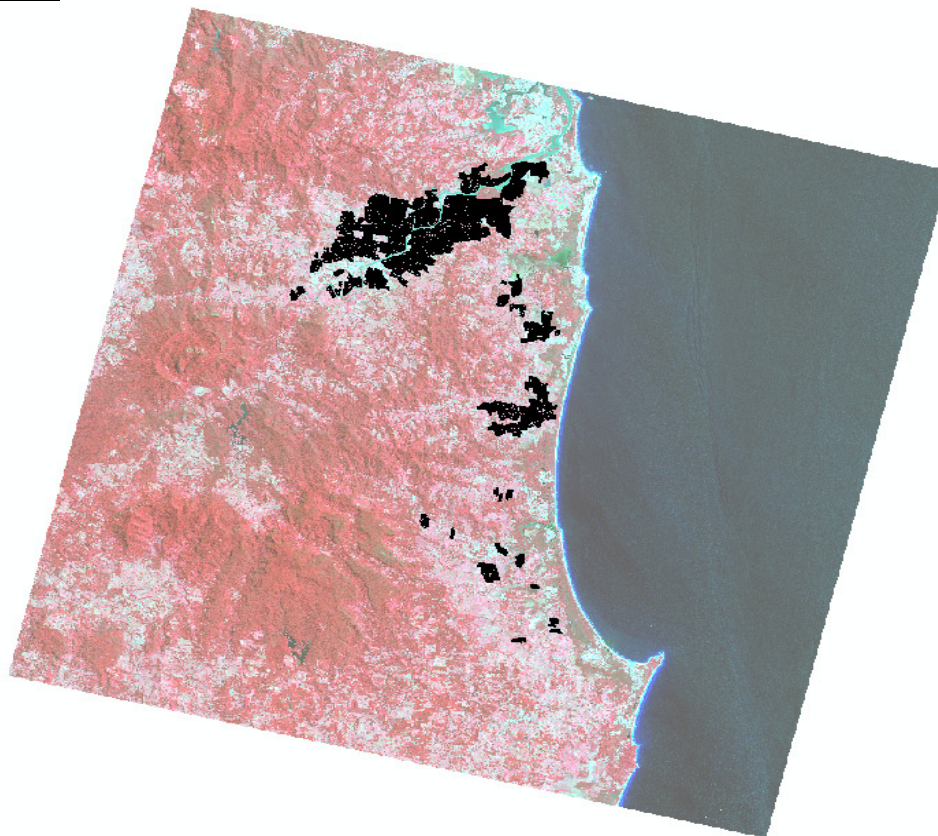


Figure 45. SPOT5 image of the Condong growing region (3600km²) overlaid with crop boundary vector file (black lines).

Following interest from the Condong (NSW) growing region, an estimate of average yield for the 2012 season was derived using the Bundaberg algorithm. The prediction produced for the 1 year cane was again encouraging (Table 10).

Table 10 . Predicted versus actual average yield for the Condong growing region.

Harvest year	Growing Region	Number of crops	Pred. ave. Yield (TCH)	Act. ave. Yield (TCH)	Range of Prediction at block level (% of actual)
2012	Condong	2087	67.6	70.0	23 to 468

As this prediction was only applied for one season, the high estimate achieved i.e. 3.4% under prediction (Table 10), may be an anomaly and as such additional research is required to further validate the algorithm. It is hypothesised that a NSW specific algorithm would be required to account for different climate within this region when compared to Bundaberg. An additional algorithm would also be required to account for the cane grown within this region over two years.

Mulgrave

An additional scoping study assessing yield prediction over the Mulgrave growing region was also undertaken during the 2012 season. Without access to a SPOT5 image the algorithm (equation 3) was derived from GNDVI values extracted from an IKONOS image captured 26 May 2010 and corresponding yield of 833 crops (coloured polygons in Figure 46 b). The prediction was applied to GNDVI values extracted from a GeoEYE image captured 4 May 2012 (1324 crops).

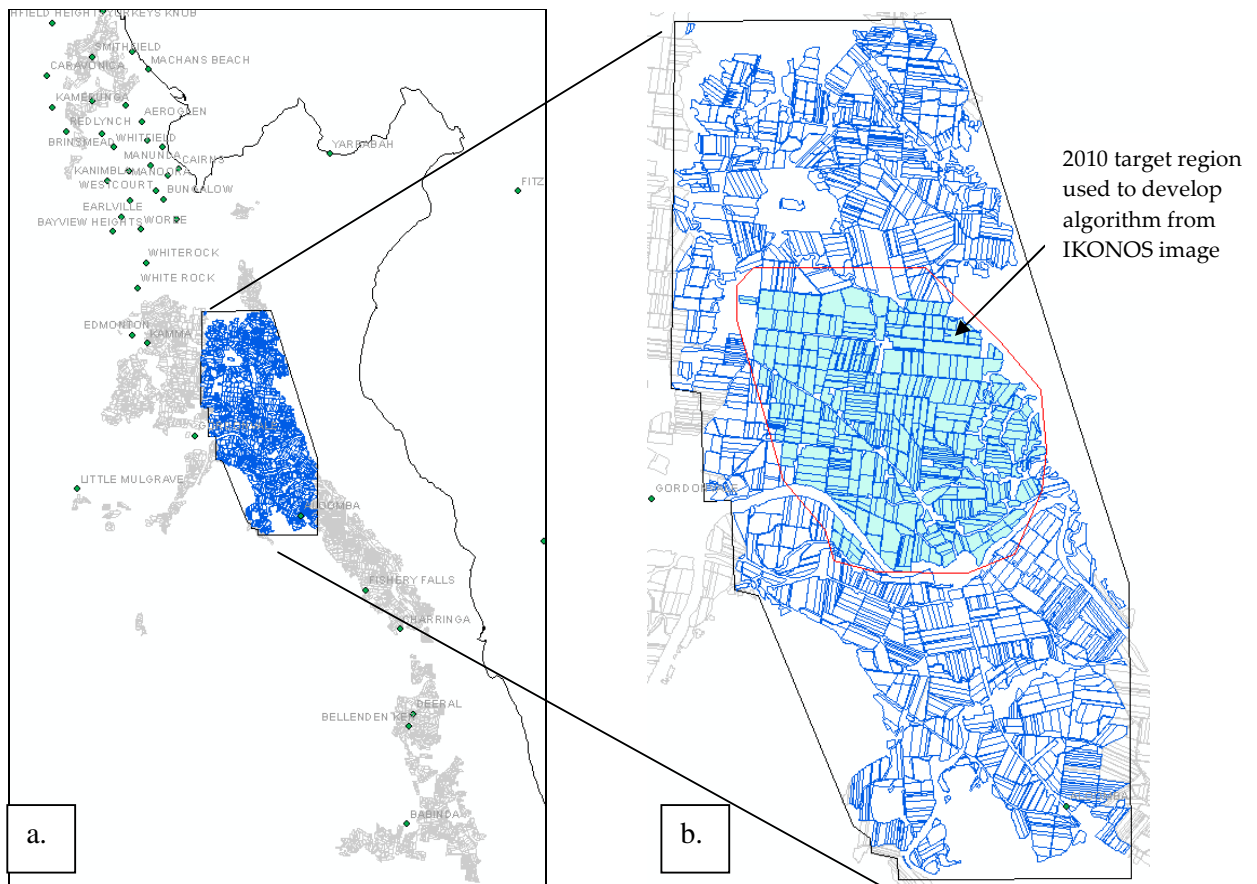


Figure 46. a. Area within the Mulgrave growing region where yield was predicted for the 2012 growing season. b. target area used to derive the 2010 yield prediction algorithm.

Equation 3:
$$y = 15.641 * e^{(3.4775 * x)}$$

Where y = predicted average yield (TCH)

x = average GNDVI value extracted from TOA SPOT5 image.

The predicted average yield for the 1324 crops closely aligned with that of the whole Mulgrave growing region for 2012 (Table 11).

Table 11 . Predicted versus actual average yield for the Mulgrave growing region

Harvest year	Growing Region	Number of crops	Pred. ave. Yield (TCH)	Act. ave. Yield (TCH)	Range of Prediction at block level (% of actual)
2012	Mulgrave	1324	86.1	84.4	33 to 388

This result, although encouraging requires additional validation over a number of growing seasons. It does however demonstrate that imagery other than SPOT5 can be used to derive yield prediction algorithms.

Summary of regional yield prediction

The estimates of regional average yield produced by this project were found to be constantly high for all growing regions investigated over the majority of growing seasons. The results are very encouraging and support remote sensing as an effective additional tool for validating seasonal estimates provided by current methods. The fact that these algorithms are non cultivar and non crop class specific, as well as in some cases regionally and seasonally insensitive reduce the complexity of analysis in the event that these protocols are adopted by industry. Between 2009- 2012, fifty-three different varieties were planted in the Herbert, twenty-six in Bundaberg and nineteen in the Burdekin growing region. If other variables such as the segregation of regions into smaller climate driven micro regions or crop class were also accounted for then the number of algorithms required would be substantial.

The regional separation of trend lines identified across some growing seasons, particularly for the Burdekin and Isis regions, does pose a concern for the future accuracy of this approach. It is therefore suggested that the implementation of an agro- meteorological model be investigated for the purpose of normalising seasonal variability. Similarly, the use of the generic algorithms was identified to have major limitations when used for the prediction of yield at the crop level, with large under and over predictions identified at all sites. This indicates that if predictions are required at this scale then it is likely that algorithms for each cultivar and possibly crop class would be required.

6.3.5. Validation of the generic algorithm at the block and within block level.

Yield maps derived from SPOT5 imagery using the generic algorithm (Figure 47 a and c) displayed similar spatial trends to those produced by the field calibrated IKONOS maps (Figure 47 b and d). However, some inconsistencies were identified particularly at the high and low range, a result consistent to that identified in Figure 37.

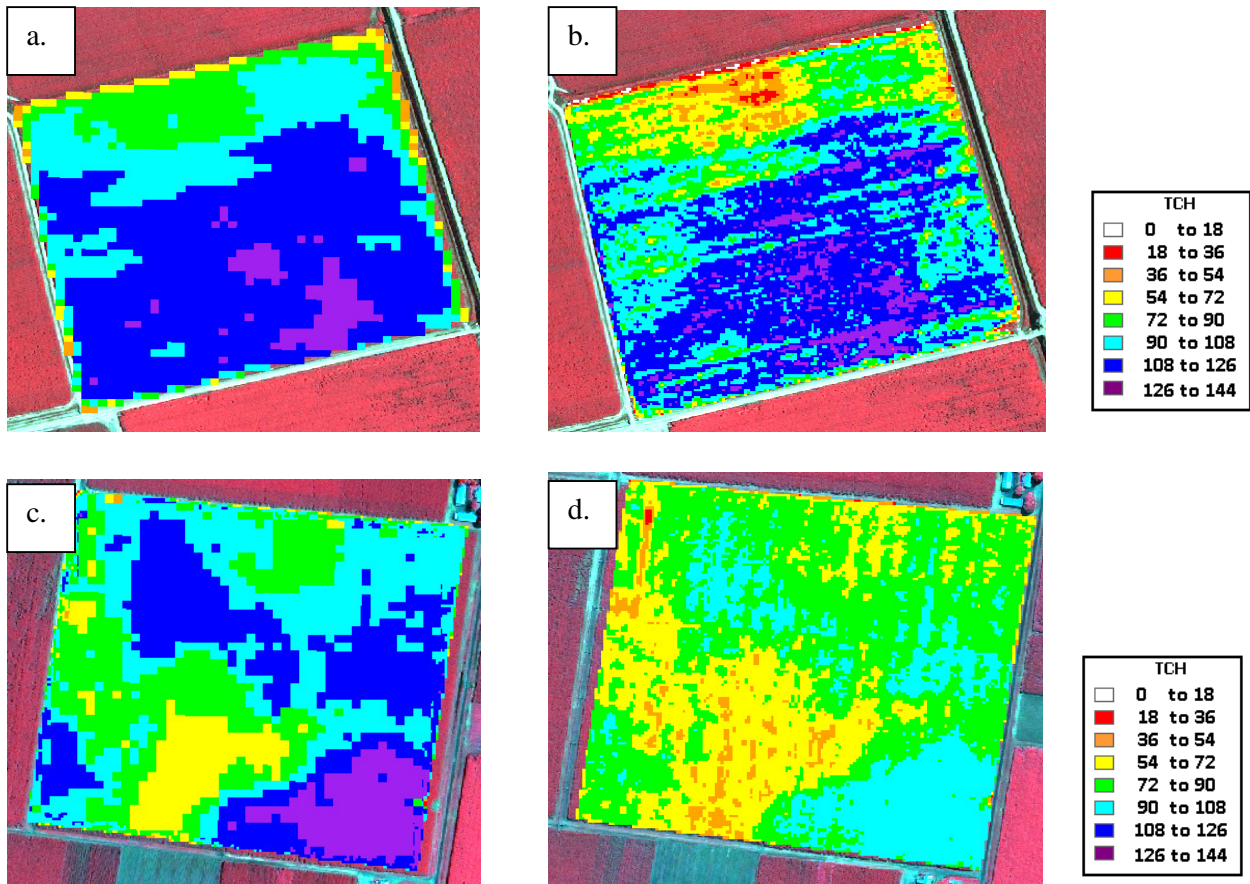


Figure 47. Classified yield map derived from SPOT5 image using the generic algorithm (a and c) and corresponding IKONOS yield map derived from field calibration samples (b and d).

A test at the within crop level identified a similar inability of the generic algorithm to accurately predict high and low yield in terms of TCH. In Figure 48, the slope (0.771) and intercept (10.369) indicate the difference between actual yield measured at a number of locations within two Bundaberg crops and predicted yield using the SPOT5 algorithm (grey markers; Figure 48). When compared to in field measurements from two crops in the Burdekin region (red markers; Figure 48), the generic algorithm was found to consistently under predict yield. This result supported the need for a Burdekin specific algorithm that could account for the substantially different growing conditions within that region.

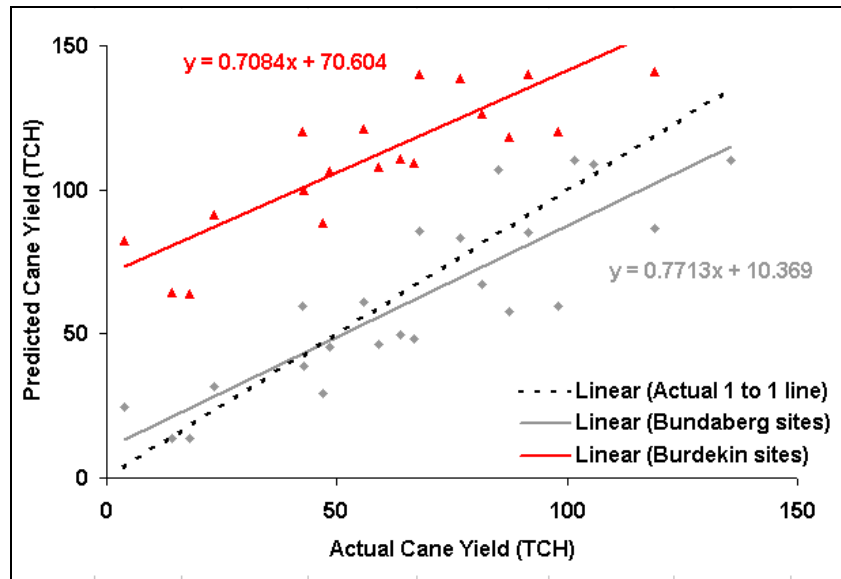


Figure 48. Comparison of actual cane yield (TCH) measured at sample locations within 2 Bundaberg and 2 Burdekin crops, to predicted yields derived from the SPOT5 generic algorithm.

A number of small growing areas within the Bundaberg region exhibited very high predictions of yield at the block level. Relmay farms for example, produced an average prediction estimate of 97%; S.D. 10% for 61 blocks, similar to that for Bullseye with also 97%; S.D. 17% (49 crops) and Cayley 87%; S.D. 11% (31 crops). A similar test in the Burdekin and Herbert region produced very poor prediction estimates (data not shown).

To further test the accuracies of yield prediction at the block level for each of the regions a simple linear regression was fitted between actual and predicted observations for each of the data sets (Bundy 2010, 2011 and 2012; Isis 2010; Burdekin 2011 and 2012 and Herbert 2011 and 2012) (Table 12). The y variables were actual yield data provided by each mill whilst the predicted values were the x variables. If the predictions were identified to be 100% accurate then the regression line would have an intercept of zero and a slope of one, with the R-square value to be 100%.

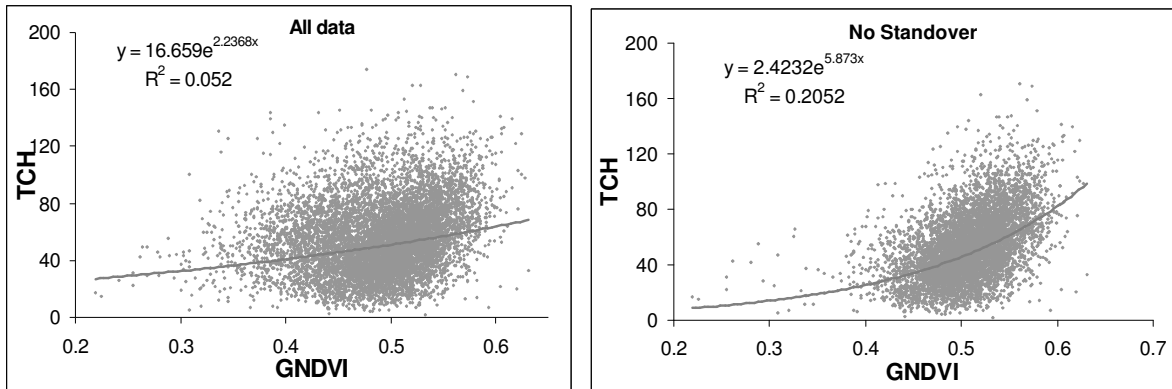
Table 12. Results of linear regressions run between actual and predicted block yields for a number of growing regions and seasons.

Location	Year	R-Square	Intercept	Slope
Bundaberg	2010	52.7	-1.6	1.0
Bundaberg	2011	38.9	7.9	0.8
Bundaberg	2012	49.8	5.9	1.0
Isis	2010	34.1	12.1	0.9
Herbert	2011	7.3	31.0	0.5
Herbert	2012	23.0	18.9	0.7
Burdekin (all data)	2011	4.2	69.9	0.4
Burdekin (without SO)	2011	32.0	-29.0	1.1
Burdekin (SO only)	2011	22.0	3.4	1.4
Burdekin	2012	14.0	25.7	0.7

From this analysis, the Bundaberg 2010 data set provided the strongest prediction estimates at the block level, with an intercept found to be non-significantly different to zero following a t-test, with a slope close to 1 (-1.6; Table 11). With the initial generic algorithm being predominantly derived from this 2010 Bundaberg data set, this result is not surprising. This also explains why high prediction accuracies were also obtained for the Bundaberg 2011 and 2012 data sets. Significant variation still existed about the regression line.

The predictions from the other data sets were poor, with the intercepts and slopes of these regression lines being far from the ideal. For Burdekin 2011 the removal of standover crops (without SO) greatly improved the prediction although the intercept was still significantly different to zero. Interestingly the analysis of the standover crops alone produced encouraging results, indicating high estimates of yield may be achieved for stand over crops as long as they are analysed independently. Note for this analysis, no data was omitted despite many data points having large residuals or high leverage.

These results indicate that although the generic algorithm has the ability to identify yield trends at the crop level; its ability to accurately predict actual tonnes of cane per hectare (TCH) was poor. It is suggested that for this to be achieved, specific algorithms would need to be developed for differing cultivars, crop class and growing region, as well as be normalised for seasonal variability. An example of how this may occur is provided in Figure 49, where the refining of data for the Burdekin 2011 season improves the correlation coefficient from $R^2 = 0.052$ when all data is used, to $R^2 = 0.205$ with the removal of stand over, $R^2 = 0.291$ with the removal of all crop classes except for plant cane and lastly $R^2 = 0.421$ with the inclusion of one variety cv. Q208.



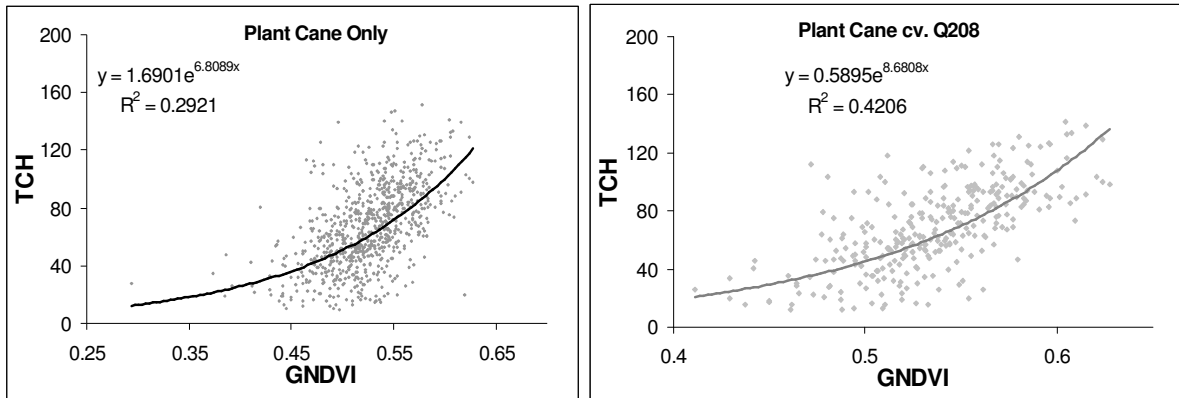


Figure 49. Burdekin 2011 example demonstrating how the refining of data in terms of stand over, crop class and variety can improve the correlation between GNDVI and cane yield (TCH).

By having access to the comprehensive Mill vector data layers, the ability to derive and then implement yield predictions based on crop class and cultivar is highly achievable. However further research is required to develop the appropriate processing steps and delivery protocols.

6.3.6. Production of classified yield maps using the generic algorithms.

Through this project, a process was established for the rapid production of classified yield maps by applying the generic algorithms to each block at the pixel level. Although the accuracies of these maps varied to some degree as discussed in section 6.3.5., the ability to access these maps and identify yield trends at the block, farm and regional level, within a growing season, offers some benefit. As seen in Figure 50, the majority of crops display yield variability, with the overall yield trend across the farm only becomes apparent when all blocks are displayed. In this case there is an obvious reduction in yield towards the south eastern corner of the farm, a result of the large dam (indicated), being filled to capacity during the late 2010 heavy rainfall event. This is believed to have increased the hydraulic pressure of the sub surface aquifers, and forced the surrounding water table to the surface producing anaerobic soils and incidences of salinity. With this information, the grower could easily identify the blocks impacted, and by having access to similar maps derived over a number of seasons, be able to determine if the area affected increases or decreases with time. In this example, the predictions of average block yields were identified to be highly accurate, so there is some confidence that accurate estimates of lost productivity can be made, thus justifying the need to apply remedial action or not.

61 blocks predicted
average yield 90 TCH,
Act. 93.4 TCH (97%)

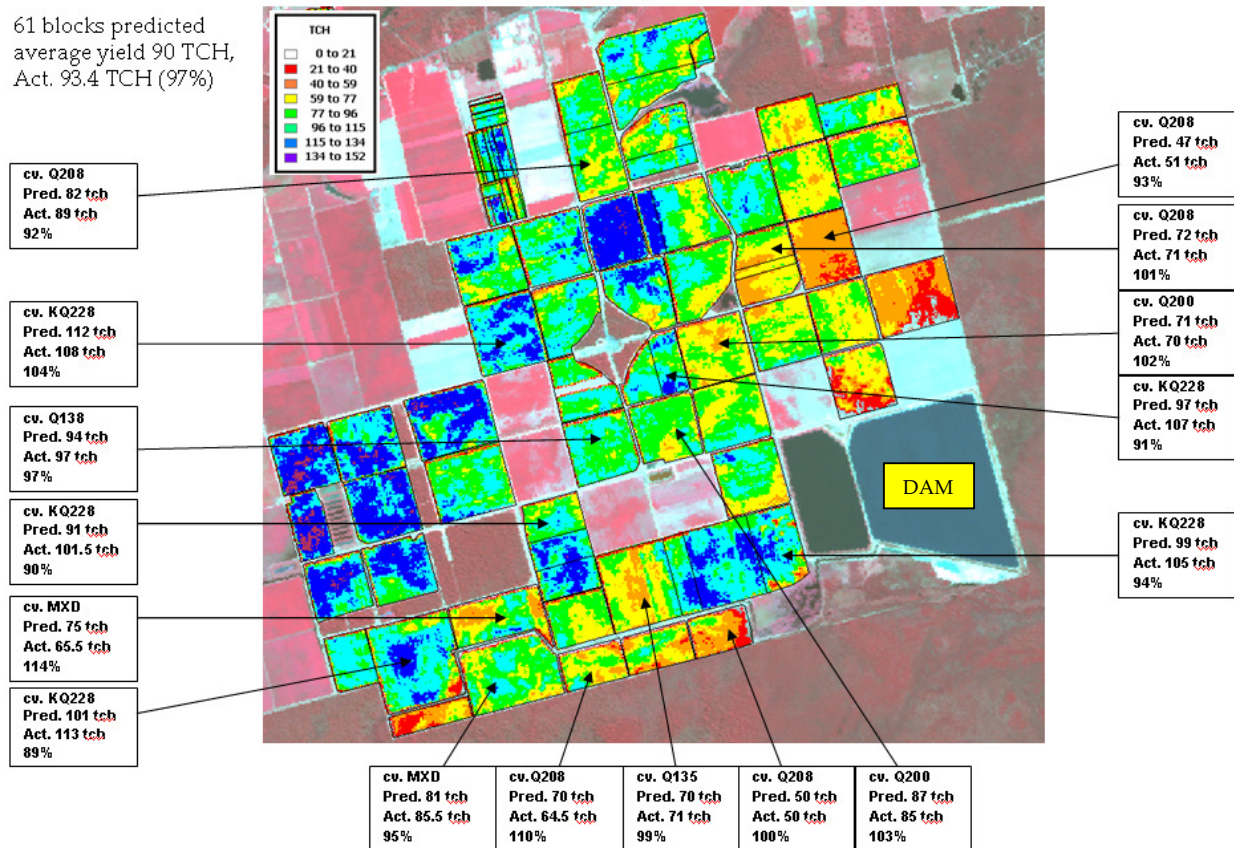


Figure 50. Classified yield maps derived from the generic algorithm overlaid on to a SPOT5 false colour image.

The ability to view these classified yield maps at the regional level also provides some indication of sub-regional trends which can assist in harvest management or support localised efforts to increase productivity. In the example below (Figure 51 a) it can be seen that there are a number of high yielding (highlighted in red) and low yielding (highlighted in black) sub regions within the Herbert growing area. These are likely to be attributed to soil type variability and topography. These same trends were also apparent in the classified image derived from actual yield values post 2012 harvest, derived by the Herbert resource information Centre (HRIC) (Figure 51b). This result gives some support to the accuracy of trends derived from the imagery based yield prediction algorithm; although again there is under prediction of higher yield values and over prediction of low values occurred.

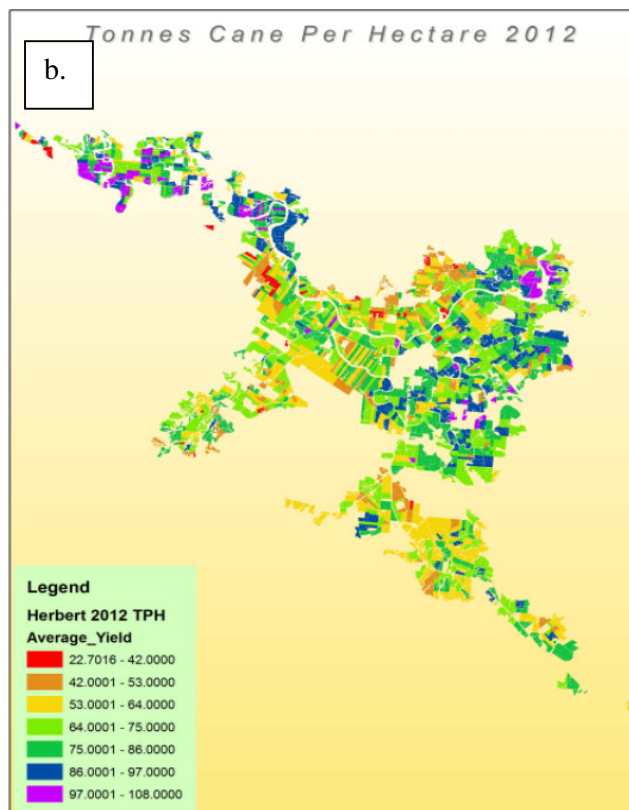
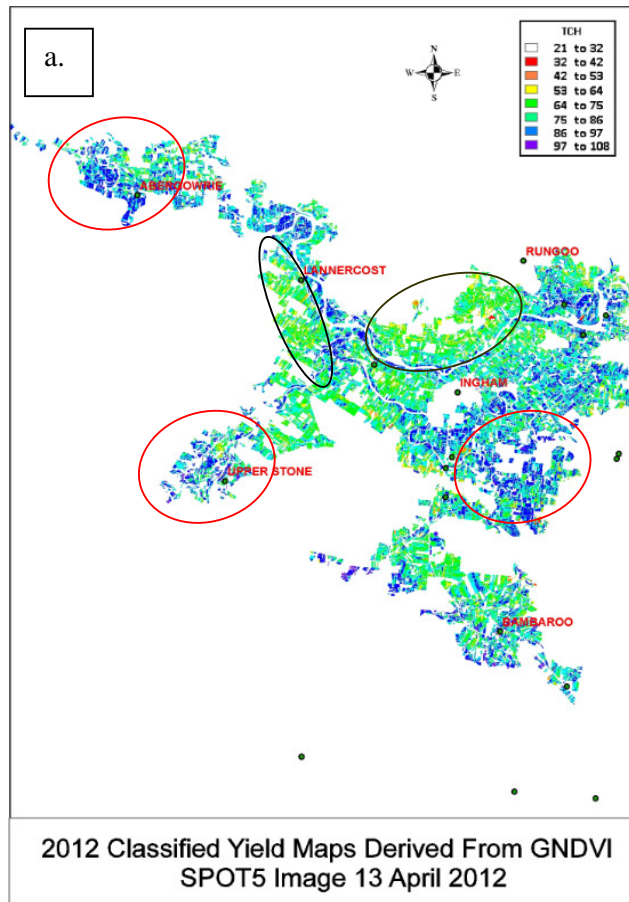


Figure 51 a. Sub regional trends of yield production as indicated by classified yield maps for the Herbert (a) and Bundaberg (b) regions.

In Figure 52, the variation between the high and low yielding sub-regions in this Bundaberg example was the result of severe flooding following the 2010 heavy rainfall event. The flood water removed top soil and nutrient from the northern side of the river which resulted in reduced yield during the 2011 season (highlighted in white).

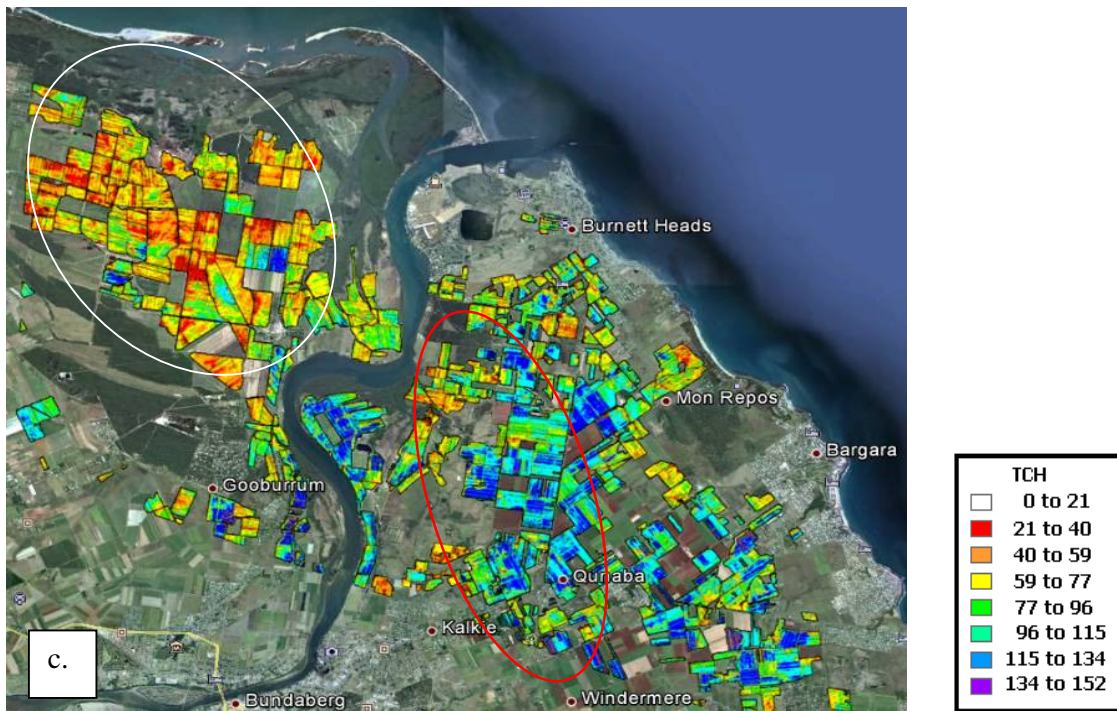


Figure 52. Sub regional trends of yield production as indicated by classified yield maps for the North Bundaberg region.

This information if generated annually can provide a strong indication of how yield trends within sub regions respond to variable seasonal conditions. This can guide where more tolerant varieties for example should be planted, when they should be planted and where crops grown in some sub-regions should be possibly discontinued due to continual poor performance.

Note: The overlaid yield maps for all regions investigated as well as the associated GoogleEarth files are not included within this report due to confidentiality agreements with the respective Mills.

6.4. Implement optimal image processing and delivery protocols for the rapid distribution of classified imagery to agronomists, growers etc.

This project successfully developed a number of processing protocols that enabled all project objectives to be achieved. The most novel of which included the derivation and then application of the regional yield prediction algorithms and classified yield maps en mass. The project identified a number of softwares suitable for achieving these objectives including ENVI, ArcGIS, Starspan GUI, and GoogleEarth with the later identified to be highly effective for the distribution of spatial information. The appendices of this report include a number of Tutorials that best demonstrate the processes developed, these include:

- *Tutorial 1:* ENVI: Converting 'At Sensor' Digital Numbers to 'Top of Atmosphere' reflectance values
- *Tutorial 2:* ENVI: Georectification of satellite imagery using an orthorectified base layer and derivation of a GNDVI image.
- *Tutorial 3:* ArcGIS: Conversion of Mapinfo (.TAB) files into ArcGIS (.SHP) files:
- *Tutorial 4:* ArcGIS: Buffering of polygons and removal of those affected by cloud before the extraction of spectral data.
- *Tutorial 5:* Starspan GUI: Extracting average spectral values and associated attribute information for multiple blocks.
- *Tutorial 6:* ENVI: Producing a classified vegetation index map of a cane crop from a 4 band satellite image.
- *Tutorial 7:* ENVI: Extracting point source spectral information from imagery using regions of interest (ROI's).
- *Tutorial 8:* ENVI: Converting VI pixel values into yield (TCH) using an exponential linear algorithm.
- *Tutorial 9:* ENVI: Creating Google Earth KMZ files from Geotiffs.

6.5. Provide recommendations to participating growers, consultants and industry representatives on the potential cost / benefit of implementing RS technologies into current agronomic management practices

The strongest indication of the cost/ benefit of the outcomes generated by this research were the increasing level of industry support and involvement experienced throughout the life of the project. From an initial target objective of three farms in the Herbert, Burdekin and Bundaberg growing regions, the project ended up collaborating and producing outcomes for 6 growing regions including the generation of over 33,000 yield maps in 2012.

The development of the accurate regional yield prediction algorithms was seen by industry as offering the greatest benefit-cost. In 2010, severe weather events caused a major discrepancy between the in season yield estimations made for each growing region to that delivered after harvest. This resulted in a sugar deficit of millions of tonnes being available to fill forward selling obligations and ultimately cost the industry, including the growers, a substantial amount of money. As a result the development of an additional tool for predicting yield, particularly one that can identify the direct impacts of within season weather anomalies, is of great benefit. As mentioned the cost for each SPOT5 scene required for each region is ~ \$AUD3800 plus processing costs, which in comparison to potential financial penalties passed on from incorrect predictions, is minimal.

At the crop level, the ability to identify low performing zones can allow an estimation of lost productivity in monetary terms to be made. The example below (Figure 53) demonstrates how a simple estimate of lost production can be made from an image derived yield map. In this example the low NDVI regions yielded on average 51 TCH, the medium 73 TCH and the high 102 TCH (based on field sampling). By multiplying the area of each of three yield classes by the average corresponding yield and then summing the results, the total crop

yield can be estimated at 1535 tonnes of cane from 18.6 ha. If the entire crop yielded at 102 TCH (average yield measured in the high NDVI zones) then the total yield would have equated to 1898 tonnes. A simple subtraction of actual total yield from optimal total yield identifies a yield deficit of 364 tonnes, or 19.6 TCH. Expressed in monetary terms this would equate to \$725 per hectare (at \$37 tonne of cane). With the low and medium yielding area extending over 10.2 ha the total monetary loss could be estimated at \$7,400 from less than optimum productivity.

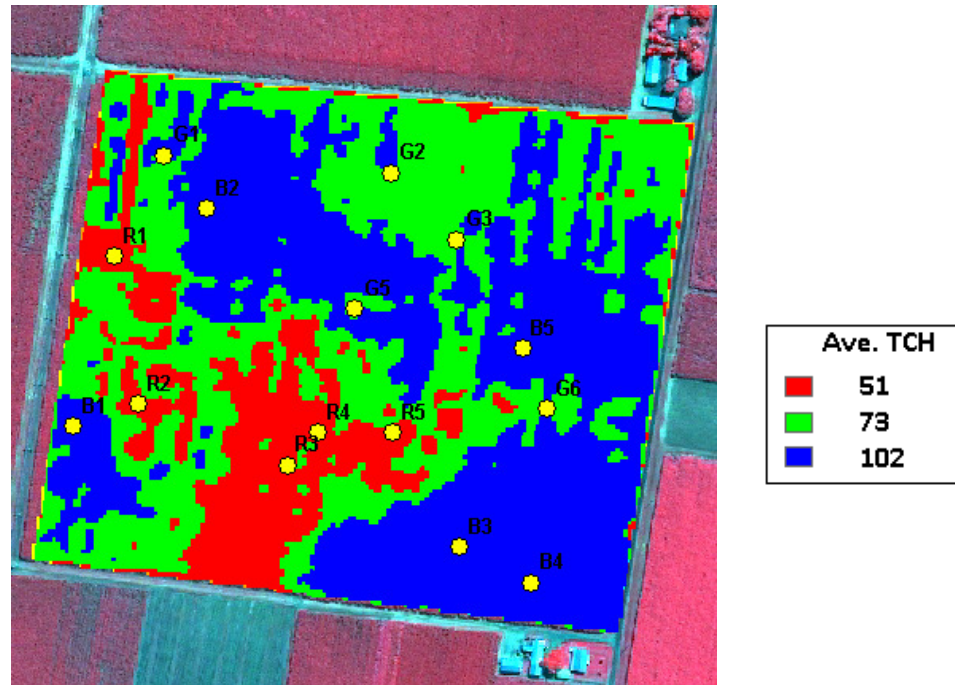


Figure 53. 3 zone yield map derived from IKONOS imagery with field sampling zones indicated by yellow markers.

By identifying the nature of the limiting factor, in this case poor drainage and sodic soils, a decision can be made on the benefit-cost of applying remedial action such as the application of gypsum / organic matter to increase drainage as well as the re-lasering of beds prior to re-plant. To further improve production costs, the 3 zone yield map can be used to direct the variable rate application of gypsum, rather than a blanket application.

As well as soil related issues the high resolution IKONOS imagery was effective in identifying additional constraints to production such as weed infestation (Figure 54a) and damage from rat, cane grub (Figure 54b), soldier fly (Figure 54c) and pig. Although these are just visual observations they do enable a grower to see what is occurring within a cane field and therefore guide within crop assessments. Again, by understanding where a constraint is occurring as well as the area affected, the grower can implement a modified management strategy such as targeted herbicide and insecticide applications.

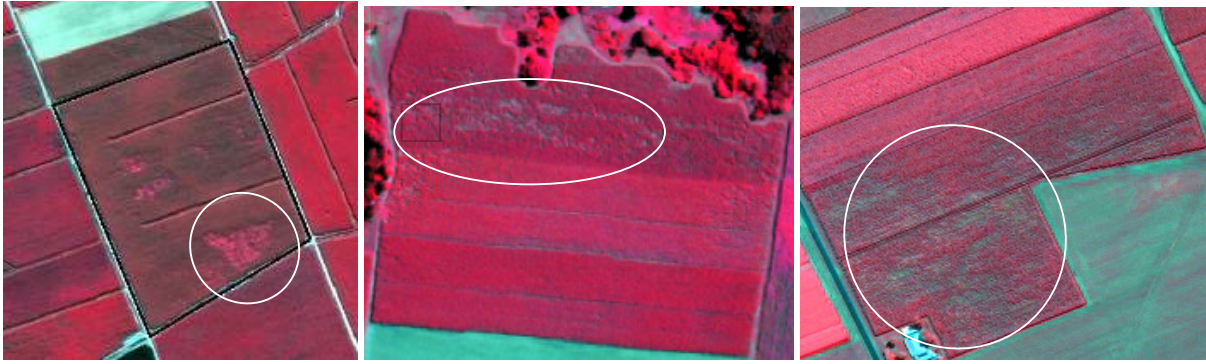


Figure 54. Occurrences of weed infestation (a), cane grub (b) and soldier fly (c) damage identified by IKONOS imagery.

Cane grubs in particular were identified to be an economically important pest and as such an additional SRDC funded project (BSS342) is being undertaken to determine if an automated image based detection and warning systems can be developed. This will incorporate both textural and spectral discrimination of imagery in an attempt to define damage specific to cane grub.

Lastly, high resolution imagery may offer some benefit to industry as a screening tool for replicated trials. Temporal imagery may indicate more homogenous locations for the placement of trials whilst imagery captured in- season can be used to identify the effects of inherent block constraints on individual replicates (Figure 55). With a surrogate measure of these external constraints such as NDVI, biometricians can add some weighting to the analysis so as to better account for non replicate specific influences. Furthermore, if trials are sampled for specific in season measure of performance (i.e. biomass, SPAD, foliar N etc) then these measures can be used to calibrate the image allowing for a trait specific map to be derived. This then could be used as a rapid screening device for the trial or possibly allow the correlations to be extrapolated over the surrounding growing area as a predictive tool. Further research will be undertaken to investigate this possibility.

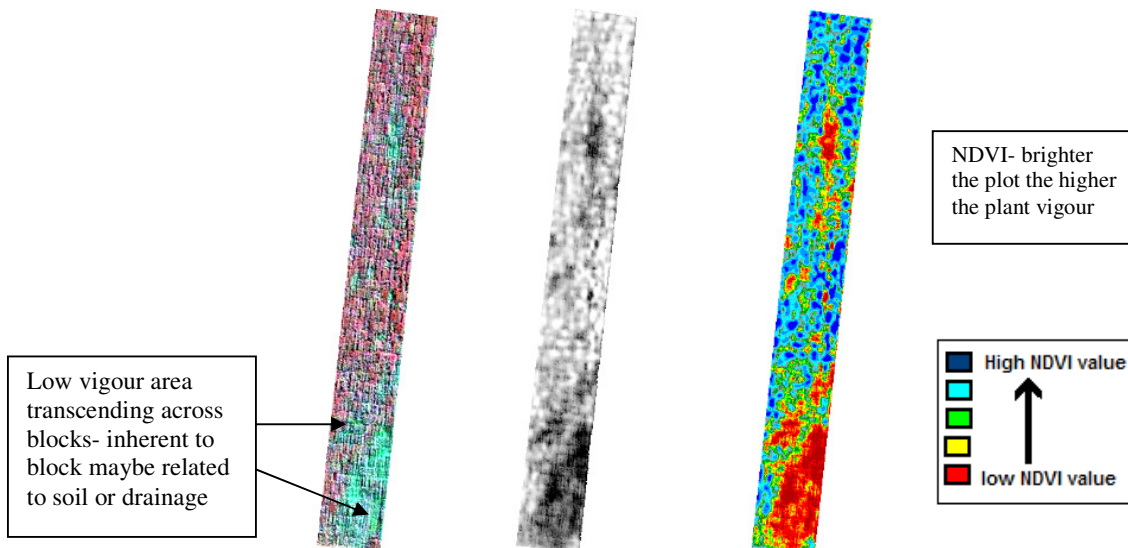


Figure 55. High resolution imagery of a replicated cane trial with the effects of an inherent block constraint i.e. soil type, drainage influencing a number of replicates.

7. Conclusion

This project successfully achieved its 5 main objectives producing applications that were directed by industry and therefore considered both relevant and adoptable. SPOT5 imagery was identified to be the best suited for coverage at the regional level due to cost, tile size, repeat capture time and spatial resolution. IKONOS was identified to provide the most feasible high resolution imagery when purchased under a multi capture deal, as well as highly effective for identifying a range of biotic and abiotic sub metre constraints. The Raptor sensor was demonstrated as a possible future provider of NDVI maps, particularly under cloud prone environments.

This project identified the effectiveness of imagery in accurately identifying within season growth variability, particularly when expressed through a vegetation index. These maps were highly effective for directing in crop sampling, with the information gained providing a useful tool for supporting modified management strategies. Although the timing of image capture, based on delays from continued cloud cover, meant the implementation of revised strategies could not occur until post harvest, due to the phenological stage and size of the crop.

The imagery captured between March and May was found to be highly correlated to final harvested yield and thus enabled surrogate yield maps to be derived from calibrated GNDVI maps using in field yield measurements. This result was consistent with previous research that also identified the stabilisation period of cane, between vegetative growth and senescence to be the best correlated to final yield. The Bundaberg and Burdekin non cultivar, non crop class specific algorithms were found to be highly accurate in predicting average yield at the regional level. This result supports the adoption of imagery as an additional tool to support existing methods, for guiding harvesting scheduling and forward selling decisions. At the crop level, only predictions within the Bundaberg region were found to be accurate. Further research will investigate if the development of crop and class specific algorithms, normalised for seasonal variability, will improve predictions accuracies of actual yield at the block level.

Analysis protocols and methodologies developed by this project will greatly assist subsequent adopters of these technologies both within Australian and overseas, particularly with the inclusion of tutorials with this final report. The identification of the freeware Starspan GUI for the rapid extraction of attribute and spectral data as well as GoogleEarth for the delivery of derived image products were both novel outputs of this project. It is hoped that further research will allow the development of a 'turn key' analysis software that will assist industry in the rapid prediction of cane yield as well as the distribution of in season yield maps.

Finally, this project received strong interest and collaboration from all facets of the Australian cane industry, a result that strongly indicates an understanding of the potential benefit that these spectral technologies offer. This support led to additional funding by

SRDC to further refine the yield prediction algorithms, particularly at the crop level, as well as investigate remote sensing as tool for the non destructive screening of breeding trials, the mapping of foliar nitrogen and as a tool for the detection of cane grub.

8. Acknowledgements

This project received over whelming support from the Australian cane industry including access to highly sensitive GIS information, essential data that allowed many of the project outcomes to be achieved. As such the project team would like to acknowledge the assistance of Bundaberg Sugar Ltd, Isis Central Sugar Mill Co. Ltd, Maryborough Sugar Factory; Mulgrave Central Mill, Mackay Sugar Mill; as well as Sucrogen and the Herbert Resource Information Centre (HRIC).

The project team would also like to acknowledge the contributions made to the project by a number of agronomic services including Farmacist, Herbert Cane Productivity Services Ltd and Burdekin Productivity Services Ltd; Research bodies including James Cook University (JCU), University of Southern Queensland (USQ) and University of Queensland (UQ); Government departments DAFFQ, DSITIA, CSIRO, Reef Catchments; Industry bodies such as BSES; and growers in particular Relmay Farming, Bullseye Precision Farming, Denis Pozzebon, Brian Tabone, Jay Hubert and the late Alan Mann.

Lastly the project team acknowledge SRDC whom in collaboration with DAFF Qld, CSIRO and University of New England (UNE) provided the funding to undertake this research.

9. References

Abdel-Rahman, EM and Ahmed, FB (2008). The application of remote sensing techniques to sugarcane (*Saccharum spp Hybrid*) production: a review of the literature. *International Journal of Remote Sensing* **29**(13), 3753- 3767.

Almeida, TIR, Filho, CR De Souza and RossettoR (2006). ASTER and Landsat ETM+ images applied to sugarcane yield forecast. *International Journal of Remote Sensing* **27**. pp 4057-4069.

Bégué, A, Lebourgeois, V, Bappel, E, Todoroff, P, Pellegrino, A, Baillarin, F, and Siegmund, B (2010). Spatio-temporal variability of sugarcane fields and recommendations for yield forecasting using NDVI. *International Journal of Remote Sensing*. **31**(20).5391-5407.

Bégué, A, Todoroff, P and Pater, J (2008). Multi-time scale analysis of sugarcane within-field variability: improved crop diagnosis using satellite time series? *Precision Agriculture* **9**.161-171.

Benvenuti, F and Weill, M (2010). Relationship between multi-spectral data and sugarcane crop yield. *Proceedings of the 19th world Congress of Soil Science Soil Solutions for a Changing World* 1-6 August 2010 Brisbane Australia.33-36.

Bramley RGV, Gobbett DL, Panitz JH, Webster AJ, McDonnell P. 2012. Soil sensing at high spatial resolution – broadening the options available to the sugar industry. Proceedings of the Australian Society of Sugar Cane Technologists, 34th Conference, Cairns. Electronic format. 8 pp.

Coventry, R.J., Hughes, J.R., Reid, A.E., McDonnell, P. (2010). Stability of spatial patterns defined by electrical conductivity mapping of soils within sugarcane paddocks. *Proceedings of the Australian Society of Sugar Cane Technologists*, **32**, 397-409.

Davis, R, Bartels, R and Schmidt, E (2007). Precision Agriculture Technologies- Relevance and application to sugarcane production. In *SRDC Technical Report 3/2007: Precision agricultural options for the Australian sugarcane industry* Eds R Bruce.60-117.

De Lai, R, Packer, G, Sefton, M, Kerkwyk, R and Wood, AW (2011). The Herbert Information Portal: Delivering real-time spatial information to The Herbert River sugar community. *Proceedings of The Australian Society of Sugar Cane Technologists* **33**.

Fernandes, JL, Rocha, JV and Lamparelli, RAC (2011). Sugarcane yield estimates using time series analysis of spot vegetation images. *Science in Agriculture* **68**(2).139-146.

Gitelson A A, Stark R, Grits U, Rundquist D, Kaufman Y, Derry D. Vegetation and soil lines in visible spectral space: A concept and technique for remote estimation of vegetation fraction. *Int J Remote Sens*, 2002, **23**(13): 2537-2562.

Huete, AR, Liu, HQ, Batchily, K and Leeuwen, W (1997). A Comparison of vegetation indices over a global set of TM images for EOS-MODIS. *Remote Sensing of Environment* **59**.440-451.

Huete, A, Didan, K, Miura, T, Rodriguez, EP, Gao, X and Ferreira, LG (2002). Overview of the radiometric and biophysical performance of the MODIS vegetation indices. *Remote Sensing of Environment* **83**.195-213.

Lee-Lovick, G and Kirchner, L (1991). Limitations of Landsat TM data in monitoring growth and predicting yields in sugarcane. *Proceedings of Australian Society of Sugar Cane Technologists* **13**.124-129.

Kishna Rao, PV, Venkateswara Rao, V, Venkataratnam, L (2002). Remote Sensing: A technology for assessment of sugarcane crop acreage and yield. *Sugar Tech* **4** (3&4). 97-101.

Markley, J Ashburner, B and Beech, M (2008). The development of a spatial recording and reporting system for productivity service providers. *Proceedings of Australian Society of Sugar Cane Technologists* **30**.10-16.

Markley, J, Raines, A and Crossley, R (2003). The development and integration of remote sensing GIS and data processing tools for effective harvest management. *Proceedings of Australian Society of Sugar Cane Technologists* **25**.2003.

Minasny, B., A.B. McBratney, and B.M. Whelan. 2005. VESPER version 1.62. Available at <http://www.usyd.edu.au/su/agri/acpa> (verified 21

Noonan, MJ (1999). Classification of fallow and yields using Landsat TM data in the sugarcane lands of the Herbert River Catchment. Herbert Resource Information Centre Qld Website link: <http://www.hric.org.au/home/JournalPublications.aspx>.

Pitt A (Pers comm). Grower Services Superintendent Bundaberg Sugar Pty Ltd.

Robson, A, Abbott, C, Lamb, D and Bramley, R (2011). Paddock and regional scale yield prediction of cane using satellite imagery Poster Abstract. *Proceedings of the Australian Society of Sugar Cane Technologists*. 33rd Conference Mackay Qld AUS 4 – 6th May 2011.

Robson, A, Abbott, C, Lamb, D and Bramley, R (2010). Remote Sensing of Sugarcane; answering some FAQ's. *Australian Sugarcane* 2011. p6-8.

Rudorff, BFT and Batista, GT (1990). Yield estimation of sugarcane based on agrometeorological- spectral models. *Remote Sensing of Environment*. **33**.183-192.

Rueda, CA, Greenberg, JA and Ustin, SL (2005). StarSpan: A Tool for Fast Selective Pixel Extraction from Remotely Sensed Data Center for Spatial Technologies and Remote Sensing (CSTARS). University of California at Davis Davis CA (Starspan GUI website link: <https://projectsatlas.cagov/frs/download.php/581/install-starspan-win32-020.jar>)

Simões, MDS, Rocha, JV and Lamparelli, RAC (2005). Spectral variables growth analysis and yield of sugarcane. *Science in Agriculture* **62**.199-207.

Simões, MDS, Rocha, JV and Lamparelli, RAC (2009). Orbital spectral variables growth analysis and sugarcane yield. *Science in Agriculture* **66**(4).451-461.

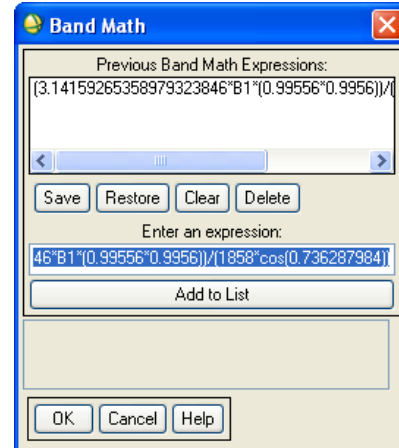
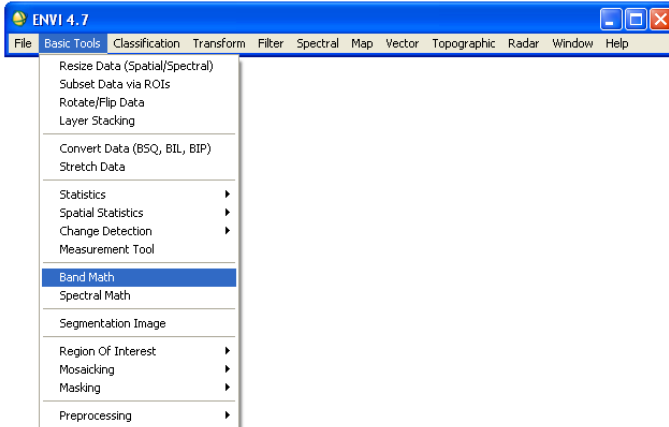
SPOT Image (2008) SPOT Image Homepage 28th April 2008. Website link <http://www.spotimage.com>.

Wang, Fu-min, Huang, Jing-feng, Tang, Yan-lin and Wang, Xiu-zhen (2007). New vegetation index and its application in estimating leaf area index of Rice. *Rice Science* **14**(3).195-203.

10. Appendix 1: Tutorials

Tutorial 1: ENVI: Converting 'At Sensor' Digital Numbers to 'Top of Atmosphere' reflectance values

On the main toolbar open: -Basic Tools- Band Math



In the Band Math window type the expression:

$$\rho_i^* = \frac{\pi \cdot d^2 \cdot L_i^t}{\cos \theta_s \cdot E_{s,i}^e}$$

In this example (IKONOS image) the text will appear like this:

(3.14159265358979323846*1.0307122576*((10000*float(b1))/(728*71.3)))/(cos(0.851987187)*1930.9)

Where:

π = 3.14159265358979323846 (double precision)

d^2 = 1.0307122576

L_i^t = ((10000*float(b1))/(728*71.3))

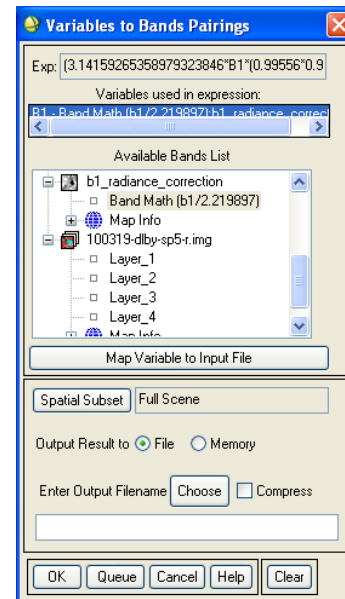
θ_s = 0.851987187

$E_{s,i}^e$ = 1930.9

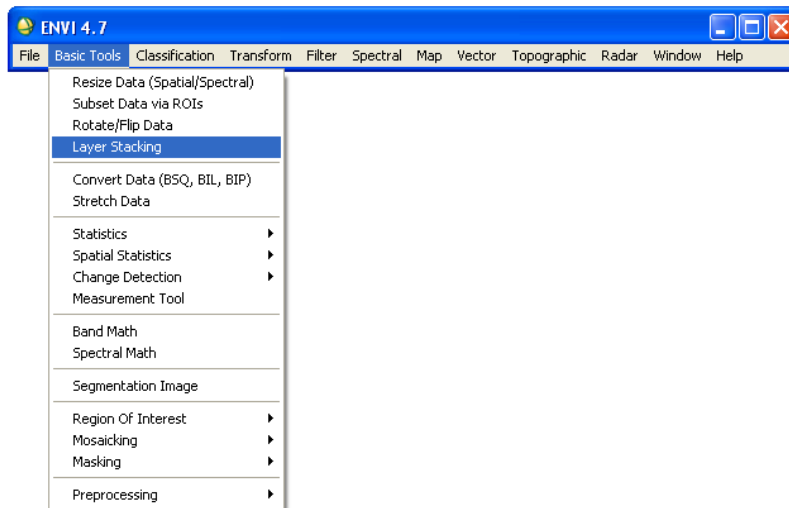
A new window will open asking to link B1 to an appropriate band. Choose the suitable Band to transform.

Choose an appropriate file name identifying the band in the output. In the next step, several of these will be layer stacked together to form one file.

Repeat for each band.

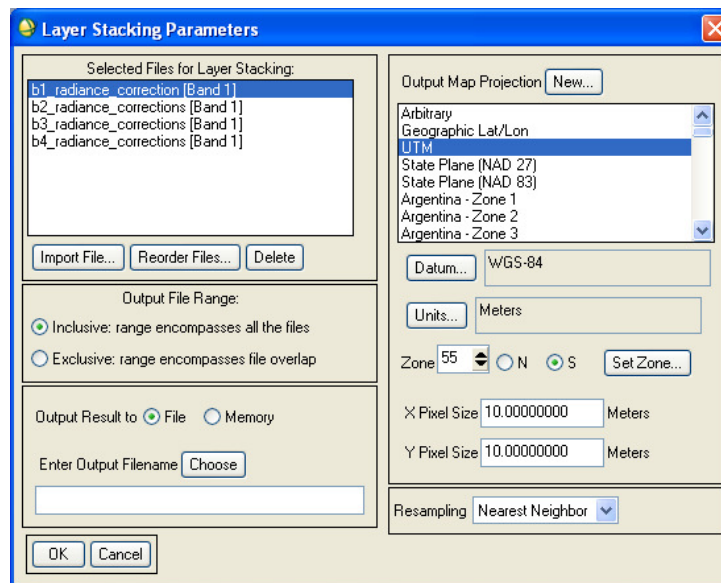


To create one data file from the transformation outputs use the 'Layer Stacking' tool.
 On the main toolbar open- Basic Tools - Layer Stacking



Choose the appropriate layers for the new data file using the 'Import File' button. The order in which the individual files are selected, denotes their subsequent order in the final layer stacked image.

Choose a filename and projection – press OK to finish the process.



Theory

Converting 'At Sensor' digital numbers to 'Top of Atmosphere' reflectance values.

Equation 1:

$$\rho_i^* = \frac{\pi \cdot d^2 \cdot L_i^e}{\cos \theta_s \cdot E_{s,i}^e}$$

Where:

- ρ^* = Top of Atmosphere Reflectance (Unitless Planetary Reflectance)
- d = Earth-Sun distance Factor (ratio of the actual distance to the mean distance)
- θ_s = Solar Zenith angle in degrees (converted to radians)
- L_i^e = Spectral radiance at the sensor's aperture
- $E_{s,i}^e$ = Mean solar exoatmospheric irradiances

Finding d

d = Earth-Sun distance factor (ratio of the actual distance to the mean distance)

This value is a ratio of the distance of the Earth to the Sun on the individual day of image capture to the mean distance of the Earth to the Sun for every day in the year.

Earth-Sun distance (d) in astronomical units for Day of the Year (DOY)+ Day of the Month (DOM) for Non-Leap Years. For leap years add 1 DOY to dates after 28 February. (January 1 = Julian Day 1)

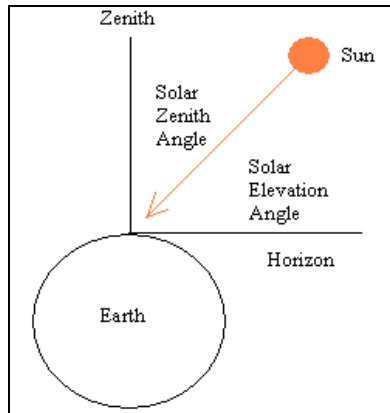
Earth-Sun distance (d) in astronomical units for Day of the Year (DOY)											
DOY	d	DOY	d	DOY	d	DOY	d	DOY	d	DOY	d
1	0.98331	62	0.99133	123	1.00806	184	1.01670	245	1.00898	306	0.99228
2	0.98330	63	0.99158	124	1.00831	185	1.01670	246	1.00874	307	0.99202
3	0.98330	64	0.99183	125	1.00856	186	1.01670	247	1.00850	308	0.99177
4	0.98330	65	0.99208	126	1.00880	187	1.01670	248	1.00825	309	0.99152
5	0.98330	66	0.99234	127	1.00904	188	1.01669	249	1.00800	310	0.99127
6	0.98332	67	0.99260	128	1.00928	189	1.01668	250	1.00775	311	0.99102
7	0.98333	68	0.99286	129	1.00952	190	1.01666	251	1.00750	312	0.99078
8	0.98335	69	0.99312	130	1.00975	191	1.01664	252	1.00724	313	0.99054
9	0.98338	70	0.99339	131	1.00998	192	1.01661	253	1.00698	314	0.99030
10	0.98341	71	0.99365	132	1.01020	193	1.01658	254	1.00672	315	0.99007
11	0.98345	72	0.99392	133	1.01043	194	1.01655	255	1.00646	316	0.98983
12	0.98349	73	0.99419	134	1.01065	195	1.01650	256	1.00620	317	0.98961
13	0.98354	74	0.99446	135	1.01087	196	1.01646	257	1.00593	318	0.98938
14	0.98359	75	0.99474	136	1.01108	197	1.01641	258	1.00566	319	0.98916
15	0.98365	76	0.99501	137	1.01129	198	1.01635	259	1.00539	320	0.98894
16	0.98371	77	0.99529	138	1.01150	199	1.01629	260	1.00512	321	0.98872
17	0.98378	78	0.99556	139	1.01170	200	1.01623	261	1.00485	322	0.98851
18	0.98385	79	0.99584	140	1.01191	201	1.01616	262	1.00457	323	0.98830
19	0.98393	80	0.99612	141	1.01210	202	1.01609	263	1.00430	324	0.98809
20	0.98401	81	0.99640	142	1.01230	203	1.01601	264	1.00402	325	0.98789
21	0.98410	82	0.99669	143	1.01249	204	1.01592	265	1.00374	326	0.98769
22	0.98419	83	0.99697	144	1.01267	205	1.01584	266	1.00346	327	0.98750
23	0.98428	84	0.99725	145	1.01286	206	1.01575	267	1.00318	328	0.98731
24	0.98439	85	0.99754	146	1.01304	207	1.01565	268	1.00290	329	0.98712
25	0.98449	86	0.99782	147	1.01321	208	1.01555	269	1.00262	330	0.98694
26	0.98460	87	0.99811	148	1.01338	209	1.01544	270	1.00234	331	0.98676
27	0.98472	88	0.99840	149	1.01355	210	1.01533	271	1.00205	332	0.98658
28	0.98484	89	0.99868	150	1.01371	211	1.01522	272	1.00177	333	0.98641
29	0.98496	90	0.99897	151	1.01387	212	1.01510	273	1.00148	334	0.98624
30	0.98509	91	0.99926	152	1.01403	213	1.01497	274	1.00119	335	0.98608
31	0.98523	92	0.99954	153	1.01418	214	1.01485	275	1.00091	336	0.98592
32	0.98536	93	0.99983	154	1.01433	215	1.01471	276	1.00062	337	0.98577
33	0.98551	94	1.00012	155	1.01447	216	1.01458	277	1.00033	338	0.98562
34	0.98565	95	1.00041	156	1.01461	217	1.01444	278	1.00005	339	0.98547
35	0.98580	96	1.00069	157	1.01475	218	1.01429	279	0.99976	340	0.98533
36	0.98596	97	1.00098	158	1.01488	219	1.01414	280	0.99947	341	0.98519
37	0.98612	98	1.00127	159	1.01500	220	1.01399	281	0.99918	342	0.98506
38	0.98628	99	1.00155	160	1.01513	221	1.01383	282	0.99890	343	0.98493
39	0.98645	100	1.00184	161	1.01524	222	1.01367	283	0.99861	344	0.98481
40	0.98662	101	1.00212	162	1.01536	223	1.01351	284	0.99832	345	0.98469
41	0.98680	102	1.00240	163	1.01547	224	1.01334	285	0.99804	346	0.98457
42	0.98698	103	1.00269	164	1.01557	225	1.01317	286	0.99775	347	0.98446
43	0.98717	104	1.00297	165	1.01567	226	1.01299	287	0.99747	348	0.98436
44	0.98735	105	1.00325	166	1.01577	227	1.01281	288	0.99718	349	0.98426
45	0.98755	106	1.00353	167	1.01586	228	1.01263	289	0.99690	350	0.98416
46	0.98774	107	1.00381	168	1.01595	229	1.01244	290	0.99662	351	0.98407
47	0.98794	108	1.00409	169	1.01603	230	1.01225	291	0.99634	352	0.98399
48	0.98814	109	1.00437	170	1.01610	231	1.01205	292	0.99605	353	0.98391
49	0.98835	110	1.00464	171	1.01618	232	1.01186	293	0.99577	354	0.98383
50	0.98856	111	1.00492	172	1.01625	233	1.01165	294	0.99550	355	0.98376
51	0.98877	112	1.00519	173	1.01631	234	1.01145	295	0.99522	356	0.98370
52	0.98899	113	1.00546	174	1.01637	235	1.01124	296	0.99494	357	0.98363
53	0.98921	114	1.00573	175	1.01642	236	1.01103	297	0.99467	358	0.98358
54	0.98944	115	1.00600	176	1.01647	237	1.01081	298	0.99440	359	0.98353
55	0.98966	116	1.00626	177	1.01652	238	1.01060	299	0.99412	360	0.98348
56	0.98989	117	1.00653	178	1.01656	239	1.01037	300	0.99385	361	0.98344
57	0.99012	118	1.00679	179	1.01659	240	1.01015	301	0.99359	362	0.98340
58	0.99036	119	1.00705	180	1.01662	241	1.00992	302	0.99332	363	0.98337
59	0.99060	120	1.00731	181	1.01665	242	1.00969	303	0.99306	364	0.98335
60	0.99084	121	1.00756	182	1.01667	243	1.00946	304	0.99279	365	0.98333
61	0.99108	122	1.00781	183	1.01668	244	1.00922	305	0.99253	366	0.98331

<http://landsathandbook.gsfc.nasa.gov/handbook/handbook.htmls/chapter11/chapter11.html>

Finding θ_s

θ_s = Solar Zenith angle in degrees (converted to radians)

This is the angle between the sun and the zenith or the vertical direction above any particular location.



Visual representation of solar zenith and solar elevation angle.

Equation 2: *Solar Zenith angle = $90^\circ - \text{solar altitude (solar elevation)}$*

This value is in degrees and therefore needs to be converted into radians before being entered into the formula.

Equation 3: *Angle in Radians = (Angle in degrees * $\pi / 180$)*

The solar elevation can be located in the image metadata as shown below.

Metadata from SPOT5, GeoEYE and Digital Globe defining sun angle elevation.

SPOT (SPOT # & Pleiades)	metadata.dim or associated *.pdf files	<div style="border: 1px solid black; padding: 5px;"> <p style="text-align: center;">Scene Extract Parameters</p> <p>Scene ID 5 386-405 1003/19 23:45:18 1 J K.J identification 386-405 Date 2010-03-19 23:45:18.2 Instrument HRG 1 Shift Along Track 0.8 Preprocessing level 1A Spectral mode J Number of spectral bands 4 Spectral band indicator H11 H12 H13 H14 Gain number 7 7 6 4 Absolute calibration gains (1/W²*sr*µm) 2.219897 2.747822 2.380254 8.145173 Orientation angle 15.57868 degree Incidence angle 830.76554 degree Sun angles (degree) Azimuth: 57.031816 Elevation: 47.813806 Number of lines 6000 Number of pixels per line 6000</p> </div>
GeoEye (IKONOS & Pleiades)	*.metadata.txt	<div style="border: 1px solid black; padding: 5px;"> <p style="text-align: center;">ps_421321_metadata.txt Notepad</p> <p>File Edit Format View Help</p> <hr/> <p>Source Image Metadata</p> <p>Number of Source Images: 1</p> <p>Source Image ID: 2010062200330360000011621467 Product Image ID: 000 Sensor: IKONOS-2 Acquired Nominal GSD Pan Cross Scan: 0.8355299830 meters Pan Along Scan: 0.8293969031 meters MS Cross Scan: 3.3421199122 meters MS Along Scan: 3.3175879141 meters scan Azimuth: 321.7673104416 degrees Scan Direction: Forward Panoramic: TOI Mode: 13 Nominal Collection Azimuth: 46.2872 degrees Nominal Collection Elevation: 82.98949 degrees Sun Angle Elevation: 40.64167 degrees Acquisition Reference Time: 2010-06-22 00:00:00 GMT Percent Cloud cover: 3</p> <hr/> <p>Product Space Metadata</p> <p>Number of Image components: 1</p> </div>

If not available in the metadata file, it can be calculated using: the date, the time of day and the longitude and latitude of the centre pixel of the image. An on-line calculator can be found at: <http://www.unitconversion.org/angle/degrees-to-radians-conversion.html>)

Finding $E_{s,i}^e$

$$E_{s,i}^e = \text{Mean solar exo-atmospheric irradiances (Esun } \lambda)$$

This is the solar irradiance for each spectral band measured at the top of the atmosphere before it is influenced by sun angles, atmospheric scattering etc. Each spectral band encompasses a range of wavelength irradiance values derived from detector sensitivity, signal to measurement transfer etc. To compensate for this, the wavelength irradiance values within a spectral band are weighted by a response function at each wavelength, summed and then averaged. A list of Esun λ values for a range of platforms are supplied below.

Sensor Esun λ values for a range of satellite platforms and band widths.

IKONOS		GeoEye-1	
Band (λ)	Esun λ (W/m ² /μm)	Band (λ)	Esun λ (W/m ² /μm)
Panchromatic	1375.8	Panchromatic	161.7
Blue	1930.9	Blue	196
Green	1854.8	Green	185.3
Red	1556.5	Red	150.3
Near-Infrared	1156.9	Near-Infrared	103.9

Band (λ)	Esun λ (W/m ² /μm)					
	SPOT 2		SPOT 4		SPOT 5	
	HRV1	HRV2	HRV1	HRV2	HRG1	HRG2
Panchromatic	1075	1670	1568	1586	1762	1773
Green	1865	1865	1843	1851	1858	1858
Red	1620	1615	1568	1586	1573	1575
Near-Infrared	1085	1090	1052	1054	1043	1047
Mid-Infrared			233	240	236	234

Finding L_i^e

$$L_i^e = \text{Spectral radiance at the sensor's aperture (commonly referred to as 'At-Sensor Radiance')} - \text{calculated from the Digital Numbers of the raw image}$$

Each platform sensor has its own equation for calculating L_i^e , as shown below:

IKONOS

$$\text{Equation 4: } L_i^e \text{ (Radiance)} = \frac{10^4 \cdot DN_\lambda}{\text{CalCoef}_\lambda \cdot \text{Bandwidth}_\lambda}$$

Where:

$CalCoef_{\lambda}$ = Radiometric calibration coefficient [DN/(mW/cm²-sr)].
 Bandwidth _{λ} = Bandwidth of spectral band λ (nm).
 Radiance = equivalent irradiance at the input of the sensor [W/m²/μm/sr].

IKONOS radiometric calibration coefficients

IKONOS Band (λ)	CalCoef _{λ} Pre 22/2/2001 [DN/(mW/cm ² -sr)]	CalCoef _{λ} Post 22/2/2001 [DN/(mW/cm ² -sr)]	Bandwidth _{λ} (nm)
Pan	161	161	403
Blue	633	728	71.3
Green	649	727	88.6
Red	840	949	65.8
NIR	746	843	96.4

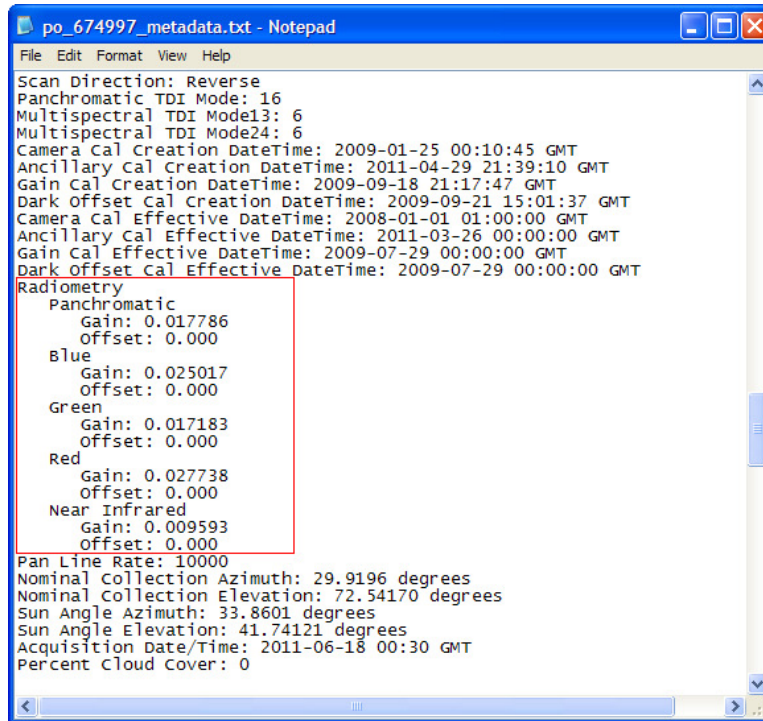
GeoEye-1

Equation 5: L_i^{λ} (Radiance) = (DN*Absolute calibration gain) +Absolute calibration Offset

Where:

Radiance = equivalent irradiance at the input of the sensor [W/m²/μm/sr].

Each image has its own unique ‘Gain’ and ‘Offset’ values and can be found in the *po_#####_metadata.txt* file of the image. Note that the Offset values were 0 for this image (refer below).



GeoEye-1 radiance offset and gains.

SPOT:

Equation 6: L_i^{λ} (Radiance) = (DN/Absolute calibration gain) +Absolute calibration Offset

Where:

Radiance = equivalent irradiance at the input of the sensor [W/m²/μm/sr].

Each image has its own unique 'Gain' and 'Offset' values and can be found in the 'metadata.dim' file or associated PDF files (refer below). Note that the 'Offset' values were 0 for this image.

Scene Extract Parameters				
Scene ID	5 386-405 10/03/19 23:45:18 1 J			
K-J identification	386-405			
Date	2010-03-19 23:45:18.2			
Instrument	HRG 1			
Shift Along Track	0 8			
Preprocessing level	1A			
Spectral mode	J			
Number of spectral bands	4			
Spectral band indicator	HI1	HI2	HI3	HI4
Gain number	7	7	6	4
Absolute calibration gains (1/W*m2*sr*µm)	2.219897	2.747822	2.380254	8.145173
Orientation angle	15.577808 degree			
Incidence angle	R30.765254 degree			
Sun angles (degree)	Azimut: 57.033816 Elevation: 47.813806			
Number of lines	6000			
Number of pixels per line	6000			

SPOT radiance absolute calibration offset and gains.

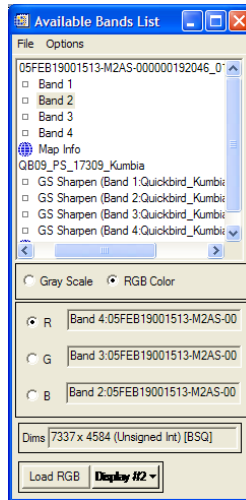
Technical Sheet References for further reading:

- **IKONOS:** Taylor (2005) "IKONOS Planetary reflectance and mean solar exo-atmospheric irradiance.
- **Quickbird:** Krause (2005) "Radiometric Use of Quickbird Imagery"
- **Worldview 2:** Updike and Comp (2010) "Radiometric Use of WorldView-2 Imagery" .
- **SPOT:** "Technical Information": <http://www.spotimage.com/web/en/584-faq.php>
- **Landsat 7:** Landsat 7 Science Data Users Handbook: Chapter 11: http://landsathandbook.gsfc.nasa.gov/handbook/handbook_htmls/chapter11/chapter11.html
- **RapidEye:** RapidEye (2011) "RapidEye Standard Image Product Specifications" : http://www.rapideye.de/upload/documents/PDF/RE_Product_Specifications_ENG.pdf

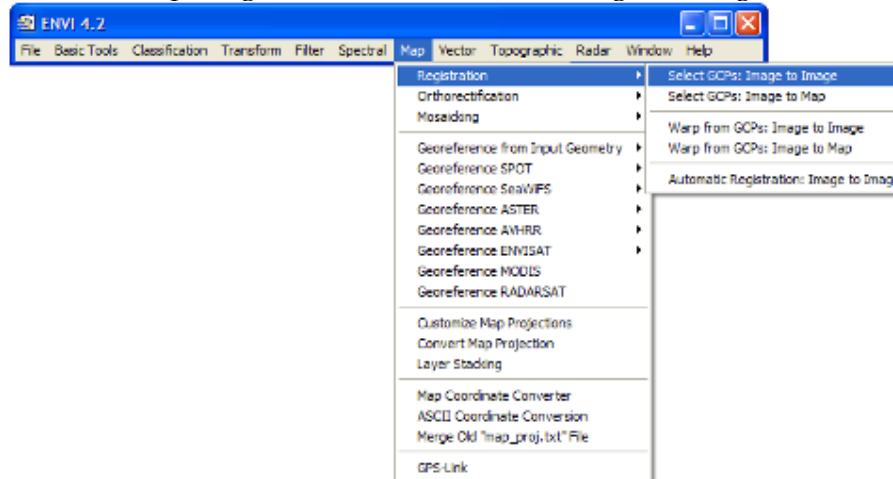
Tutorial 2: ENVI: Georectification of satellite imagery using an orthorectified base layer and derivation of a GNDVI image.

Selecting ground control points (GCPs).

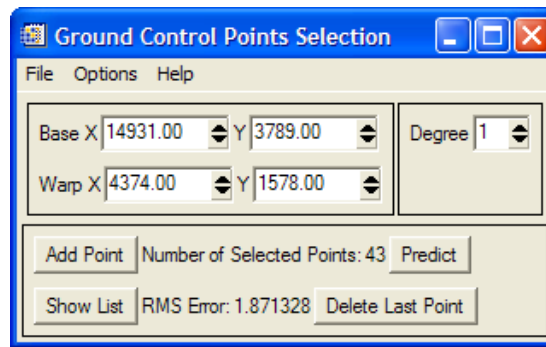
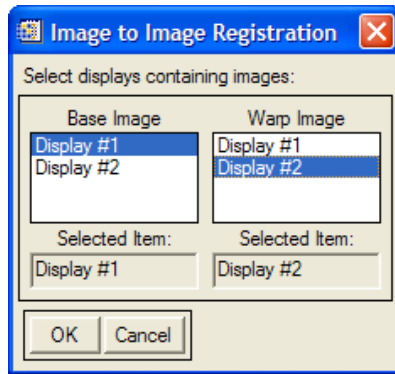
Open the orthorectified base image as well as the new image to be warped using the main menu toolbar, select File- Open image. This will list both images in the “Available band List” window. Load the images into two different displays.



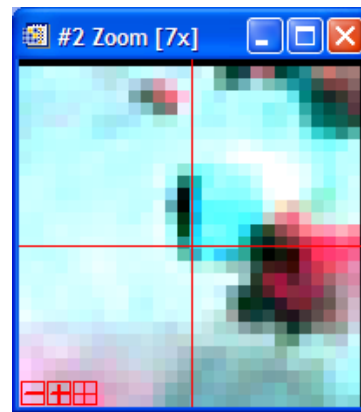
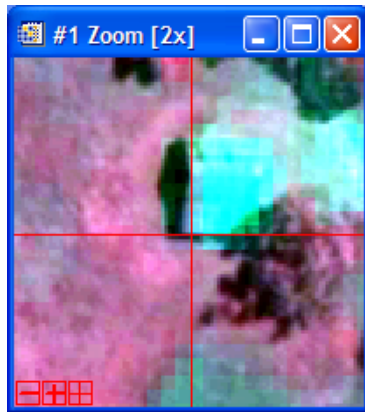
To select GCPs select Map- Registration- Select GCPs: Image to Image from the ENVI toolbar



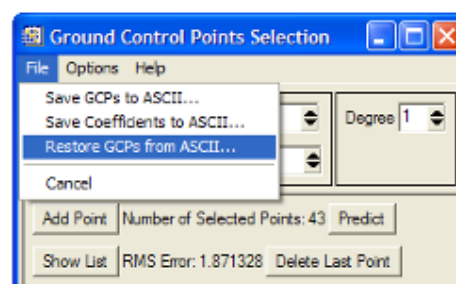
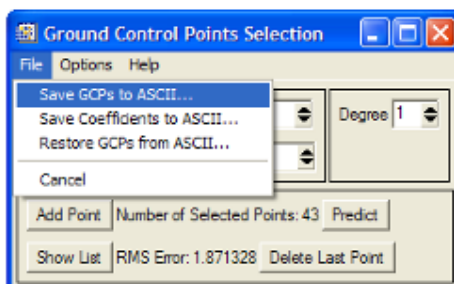
From the ‘image to image registration’ window select the orthorectified image as the base image ‘Display 1’ and the image to be warped as the Warp image ‘Display 2’. Select OK to open the ‘Ground Control Points Selection’ window.



Using the cross hair in the 'Zoom' displays identify pixels that represent the same target within each image. Press "Add Point" to record the GCPs. Try to avoid targets that may have changed over time such as the edge of a water bodies or crop boundaries. Road intersections or corners of roof structures are favourable.



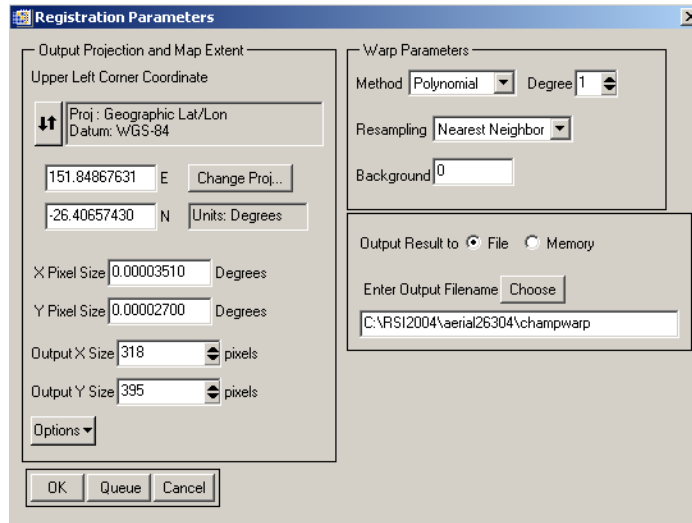
Once four GCPs have been selected, ENVI will provide a Root Mean Square (RMS) error so that the accuracy of the existing GCPs as well as those subsequently added can be determined. The ability to predict the location of where the next GCP will be in the Warp Image will also be activated. Select a target in the Base Image, press 'Predict', and the Warp Image will display a corresponding location. The cross hairs can then be moved to the required pixel. The list of GCPs can be saved and then restored for later use by using the 'Ground Control Points Selection' window.



It is recommended that at least 80 GCP's are selected to warp an image, and that RMS error is as close to 0 as possible, particularly when warping high resolution images such as IKONOS (3.2m).

Image warping.

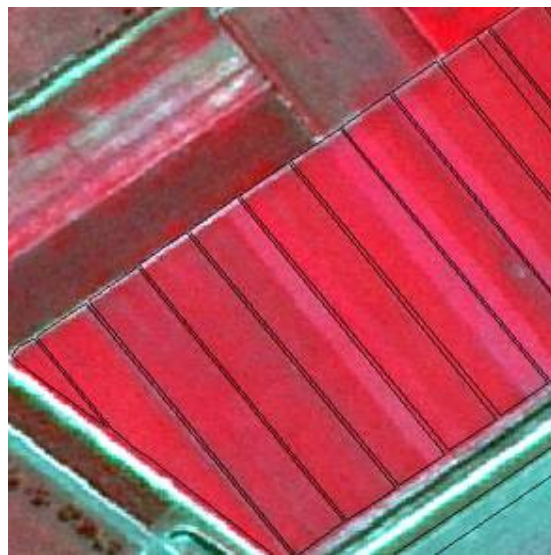
Once GCPs have been entered, select 'Options'- 'Warp File' from the 'Ground Control Points Selection' window (above). Select the image too be warped (generally this will be the image that is opened), Select 'Registration Parameters' window- output name- 'OK'.



The accuracy of the georectification can be assessed by overlaying the orthorectified image or an accurate vector layer i.e. crop boundaries, using software such as ArcGIS, to see how they align.

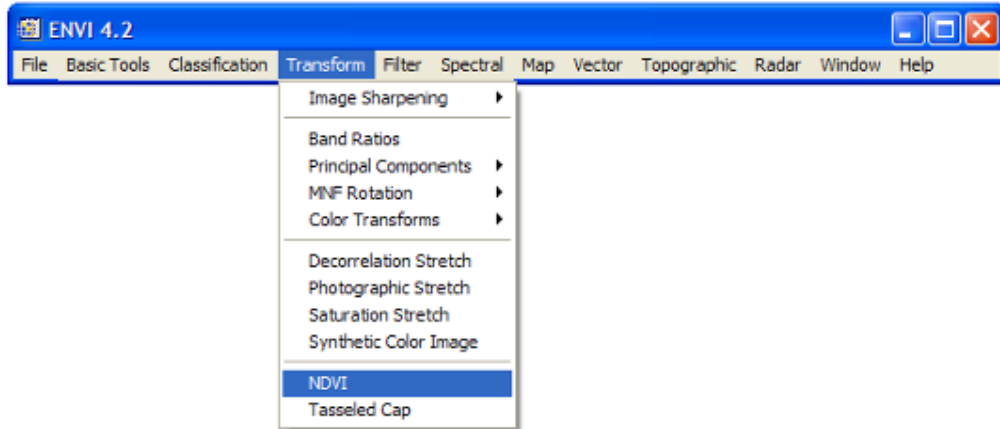


Some misalignment between vector data and imagery

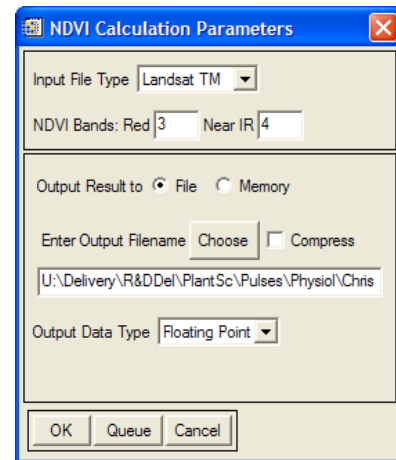
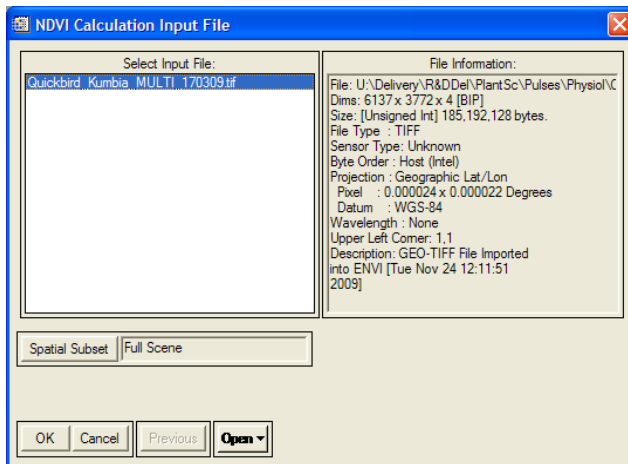


Alignment after georectification

Producing a GNDVI image.



Under the 'Transform' option in the main ENVI title bar select NDVI (above), this will open the 'NDVI Calculation Input File' window (below). Select the name of the image to be transformed- then 'OK'. This will open the 'NDVI Calculation Parameters' window- select the 'Input File Type'; the corresponding bands for Green (instead of Red) and NIR in 'NDVI Bands' and 'Output data type' as shown. Select an output file location and name (eg. QB09_17march09_Kumbia_GNDVI) this identifies the satellite used, acquisition date, location and vegetation index used.



On the completion of the index transformation the new GNDVI file will automatically appear in the 'Available Band List' window.

Tutorial 3: ArcGIS: Conversion of Mapinfo (.TAB) files into ArcGIS (.SHP) files.

This section is relevant to ArcGIS users whom need to open mill data created in MapInfo as a .TAB file. The ArcGIS user can either purchase a copy of MapInfo, or download the free spatial software package “FW Tools” (<http://fwtools.maptools.org/>).

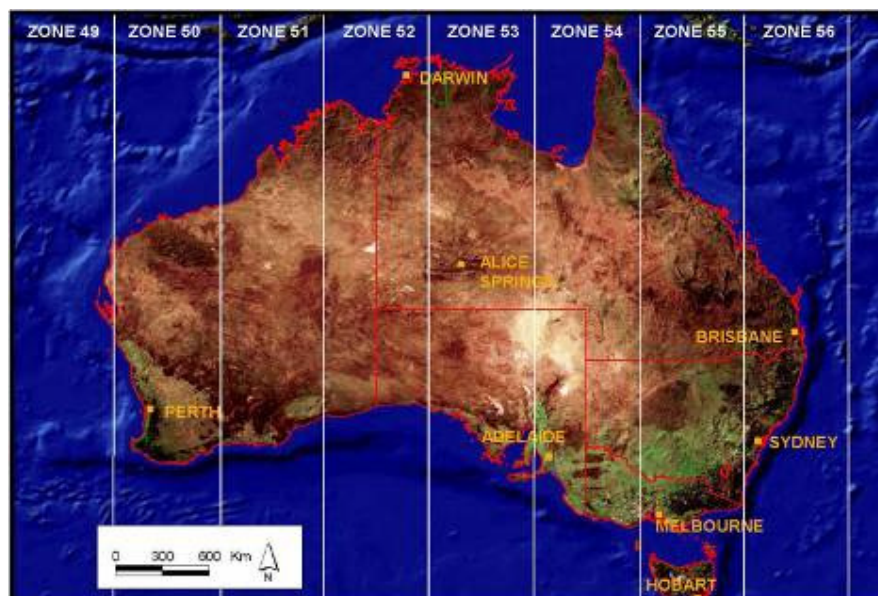
In the C:\Program Files\FWTools directory create a new folder named 'Mapinfo2Shp' and unzip the MapInfo file; This includes four extensions: .DAT, .ID, .MAP and .TAB

Open the 'FWTools Shell' command window. Copy and paste the following command into the window, inserting the required file names (indicated in red: the first file is the output shape file, while the second is the original TAB file) and press 'Enter'

```
ogr2ogr -f "ESRI Shapefile" Mapinfo2Shp\FILENAME.shp Mapinfo2Shp\FILENAME.tab
```

The ESRI shape file set will appear in the selected directory and available for input into an Arc project. (Note: ensure there are no spaces in either the TAB or Shp file name as this will prevent the conversion.

Although effective, the output .SHP file from FW Tools can sometimes display a projection error where files are misaligned by approximately 200m. If this error does occur, the projection of the newly created shape file needs to be defined and then reprojected. Import the SHP file into ArcMAP- within the ArcToolbox select 'Data management tools'- 'Projections and Transformations'- 'Define Projection', select the .SHP file. Select the coordinate system icon in the 'Define Projection' window- 'Select' in the 'Spatial Reference Properties' window- then in the 'Browse for Coordinate System'- select 'Projected Coordinate Systems'- 'National Grids'- 'Australia'- 'AGD 1984 AMG Zone (and the appropriate zone i.e. 55 or 56, refer below)'- name the output file and then 'OK'.

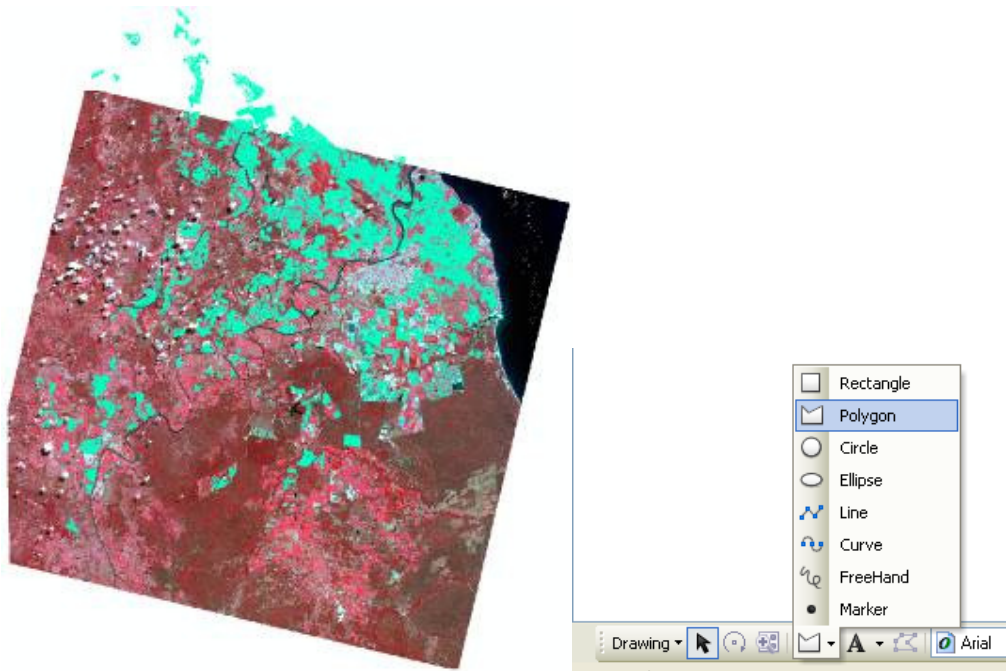


Grid zones of Australia (<http://www.environment.gov.au/ssd/publications/ir/pubs/ir473.pdf>)

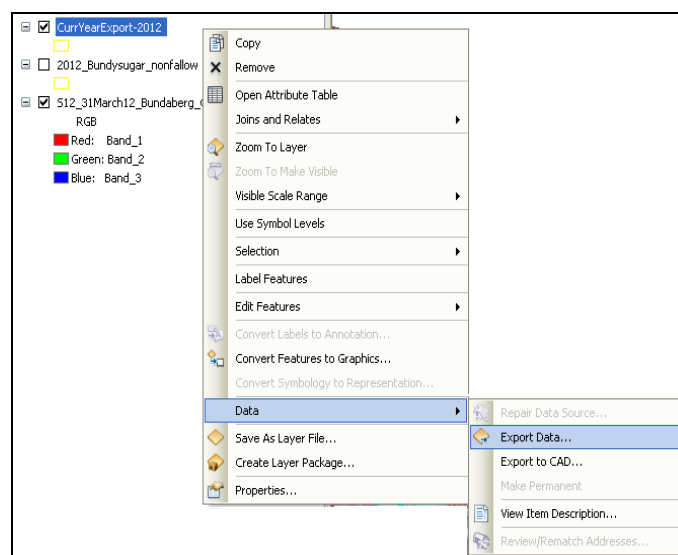
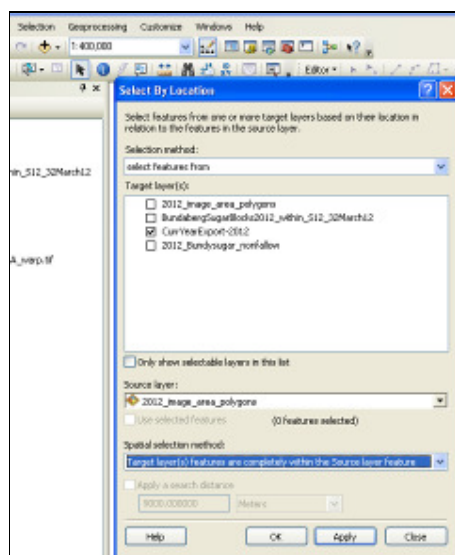
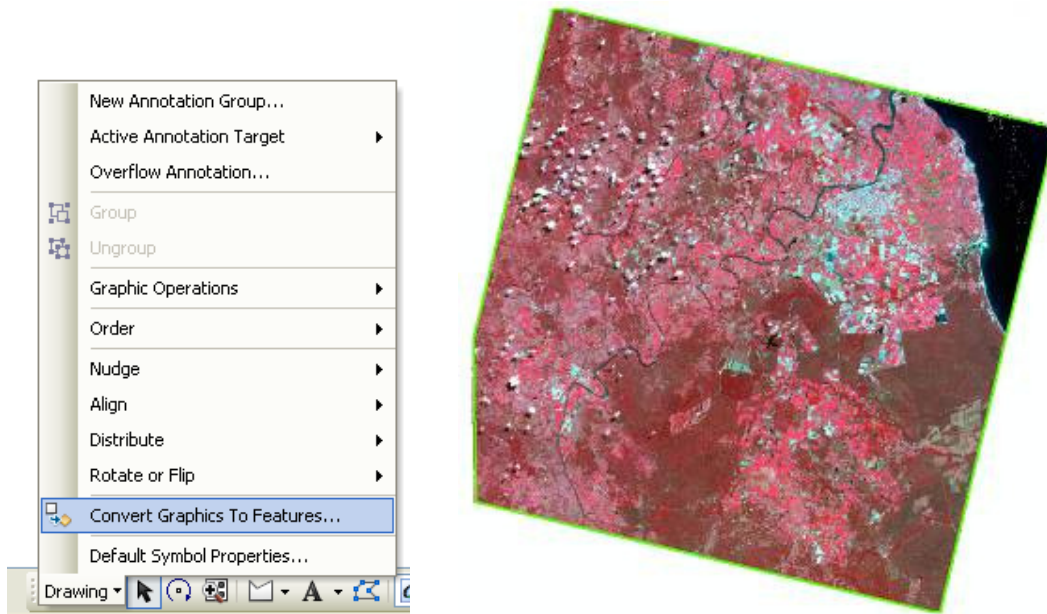
With the projection of the shape file now defined it needs to be reprojected into a common coordinate system. In 'Arctoolbox', select 'Data management tools'- 'Projections and Transformations'- 'Feature'- 'Project', input shape file, define the name and location of the output file, and select output coordinate system. 'Select' in the 'Spatial Reference Properties' window- then in the 'Browse for Coordinate System'- select 'Projected Coordinate Systems'- 'National Grids'- 'Australia'- GDA 1994 MGA and appropriate zone. The out put file will now align with the georectified imagery.

Tutorial 4: ArcGIS: Buffering of polygons and removal of those affected by cloud before the extraction of spectral data.

Within ArcGIS open both the georectified image (.TIF format) and mill vector file (.SHP). As seen below some crop boundaries extend beyond the image coverage area and therefore they require removal prior to additional analysis. This is achieved by creating a new shape that denotes the extent of the image.



Then after drawing convert the graphic into a shapefile.



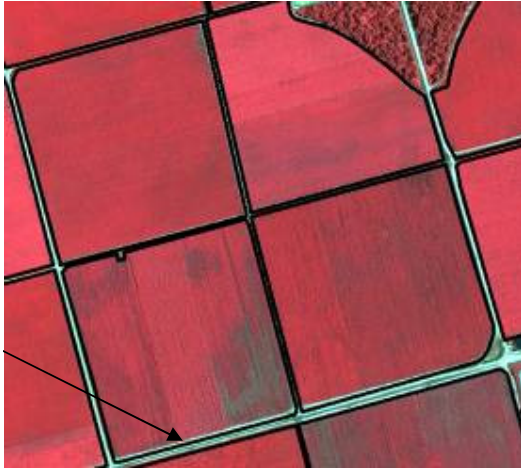
Create a new file name that denotes the removal of crop boundaries outside the extent of the image.

For the removal of clouds repeat the process defined above, with a polygon defining the area of cloud cover rather than the extent of the satellite image.

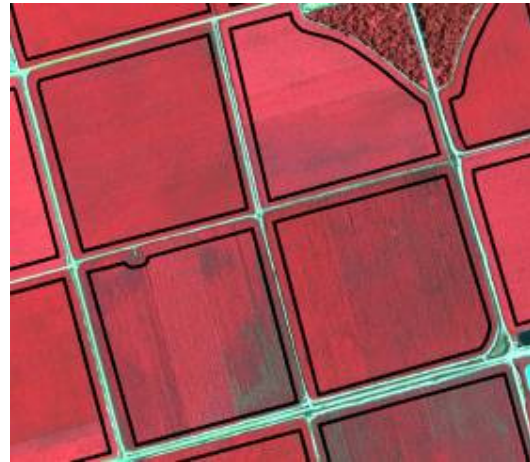
Buffering of crop boundaries.

Even with accurately georeferenced imagery and vector layers, some crop boundaries can include spectral information that is not specific to cane such as head lands, roads etc. To eliminate this 'spectral contamination' an internal buffer is applied to the boundary of each crop. For SPOT 5 imagery an internal buffer of 20m (2 pixels) was applied whilst for higher resolution imagery a 10m buffer was used.

Crop boundary includes non cane related pixels

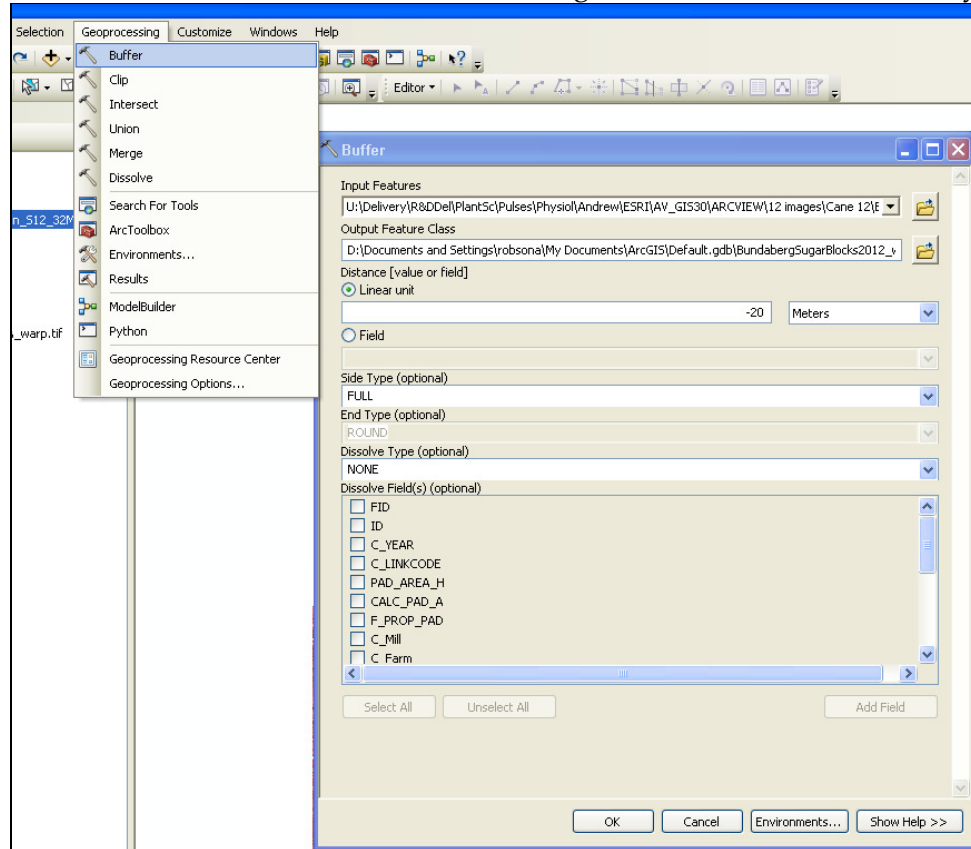


Imagery overlaid with a crop boundary vector layer (from Mill data)



Crop boundaries buffered by 10m (IKONOS imagery)

The ArcGIS software The internal buffering was undertaken achieved by



A negative effect of buffering process particularly for the SPOT 5 imagery is the loss of spectral information from small crops or small sub-blocks of differing varieties. In some cases the buffering removes all pixel information, ultimately negating that block from all further analysis.

Tutorial 5: Starspan GUI: Extracting average spectral values and associated attribute information for multiple blocks.

In order to identify the correlation between average GNDVI value and average block yields (as supplied in mill GIS layers) a rapid method for extracting imagery data for every block and aligning it with mill attribute data was required. The freeware program *Starspan GUI* was identified to be highly effective for completing this task.

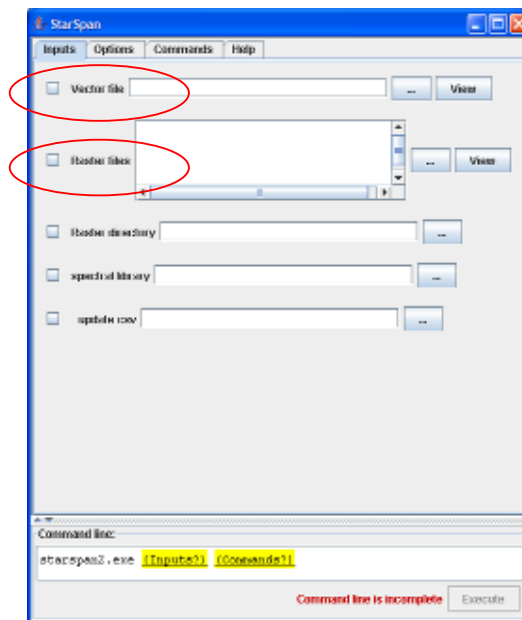
Datasets required:

- Ortho-rectified remotely sensed imagery that includes separate spectral bands that allow the calculation of GNDVI, or alternatively a layer stacked multispectral image that includes a derived GNDVI layer.
- Accurate vector file outlining crop boundaries as well as associated attribute information such as crop variety, class, yield, CCS etc.

Download StarSpan from:

<https://projects.atlas.ca.gov/frs/download.php/581/install-starspan-win32-0.2.0.jar>

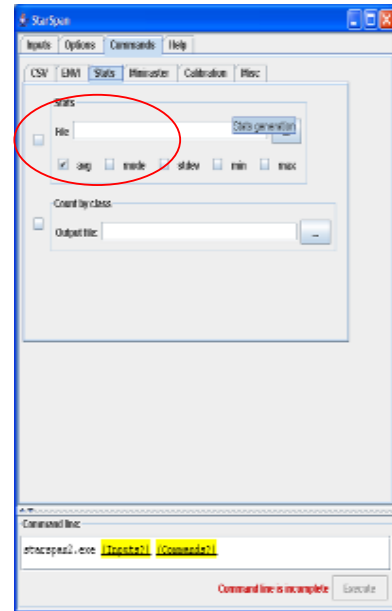
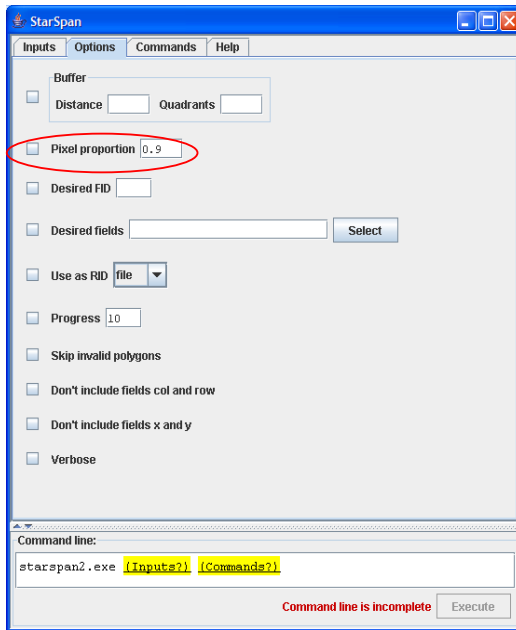
Within the StarSpan 'Inputs' screen add the 'Vector file' (mill GIS layer) and 'Raster file' (image).



To extract GNDVI values:

Within the 'Options' screen- Change pixel proportion to 0.9

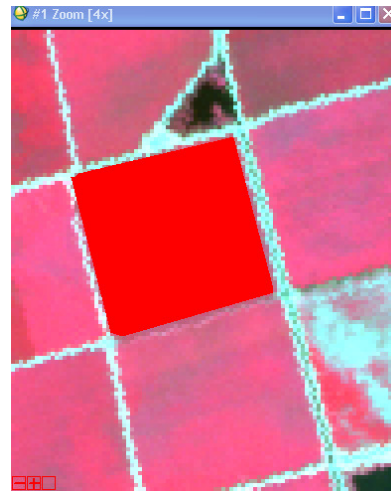
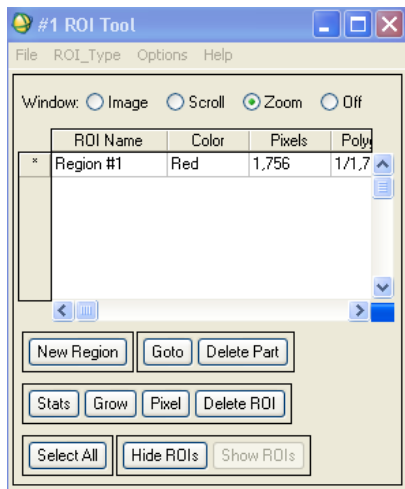
With in the 'Commands' screen - select 'avg' as the output statistic and name the output file a name and directory. Select 'Execute' to complete task.



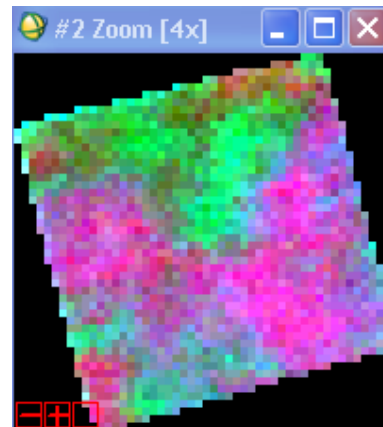
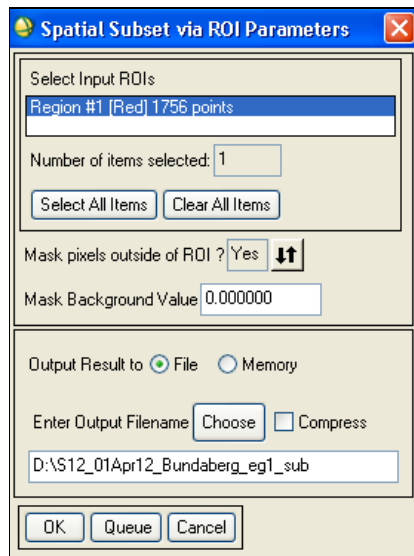
The output file that includes all attribute information from the vector file and spectral data extracted for each corresponding block will be in a .CSV that can be opened in Microsoft Excel.

Tutorial 6: ENVI: Producing a classified vegetation index map of a cane crop from a 4 band satellite image.

With the required multispectral image opened in ENVI, from the main toolbar select 'Basic Tools' - 'Region of Interest' - 'ROI Tool' and then outline the required crop (below).

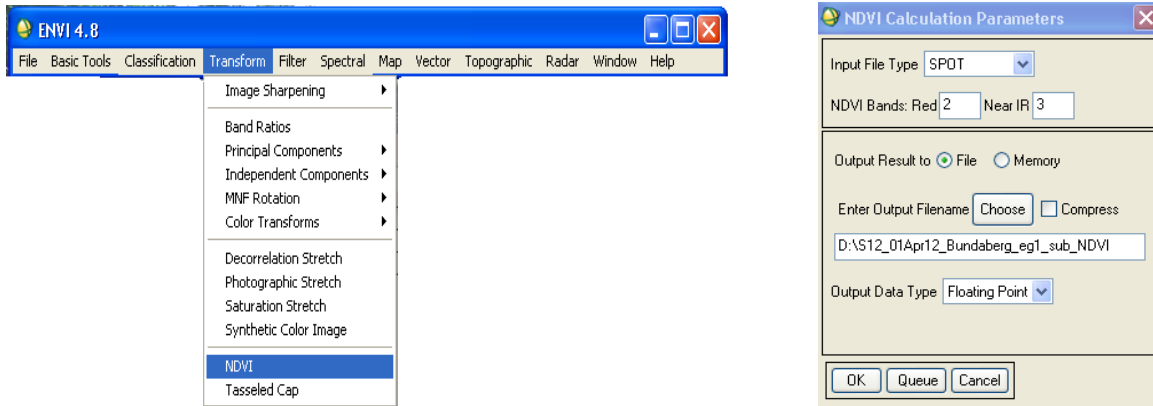


From the 'ROI Tool' - 'File' menu select 'Subset Data via ROIs'. This will activate the 'Select input File to Subset via ROI' window. Select all four spectral bands from the 'File Spectral Subset' window, then 'OK'. From the 'Spatial Subset via ROI Parameters' window (below left) select the ROI, 'Yes' to 'Mask pixels outside of ROI', '0.0000' as the 'Mask Background Value', name the output file and then 'OK'. Open the output file within a new display (below right).

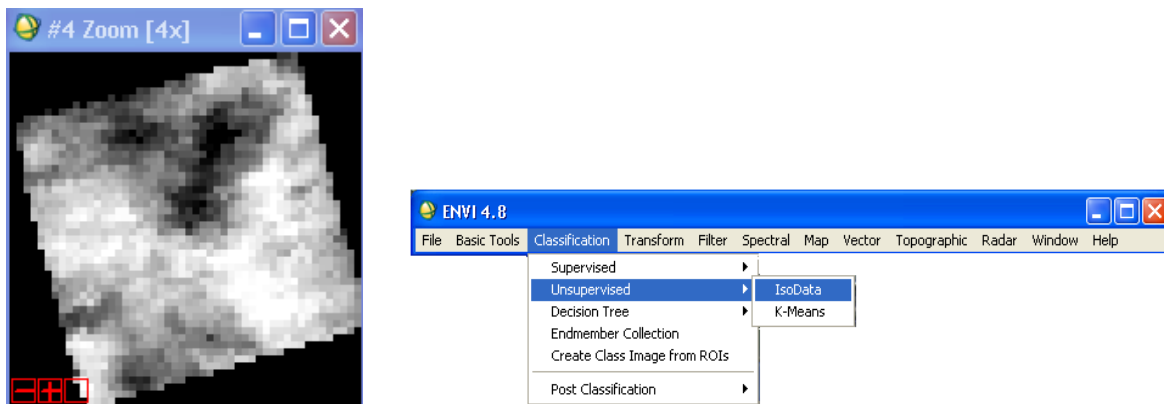


To apply a vegetation index to the 4 band satellite image of the crop, select 'Transform' - 'NDVI' from the main ENVI Toolbar (below left). Select the input image from the 'NDVI Calculation Input File' window and 'OK' to activate the 'NDVI Calculation Parameters' window (below right). Select the sensor type, in this example 'SPOT' and the appropriate bands. Note: although this method is for NDVI, a GNDVI index can be applied by selecting

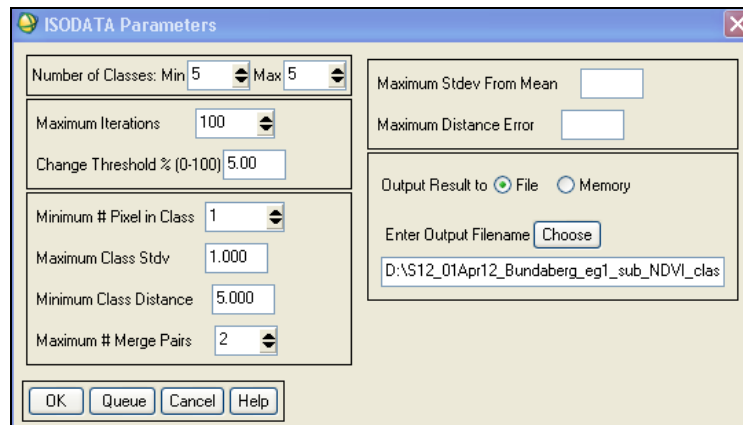
the corresponding band (1) for the 'Green' bandwidth rather than (2) for the 'Red'. Select 'Output data Type' as 'Floating Point' and then 'OK'



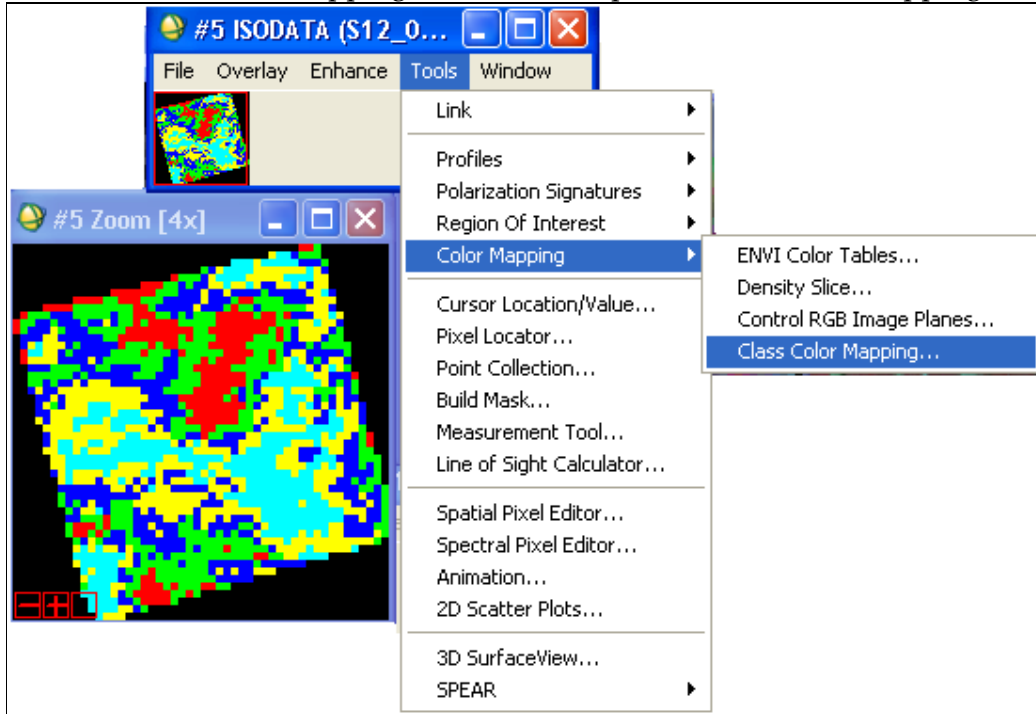
Open the indexed image as a new display (below left). From the main ENVI Toolbar select 'Classification' - 'Unsupervised' - 'Isodata' (Below right).



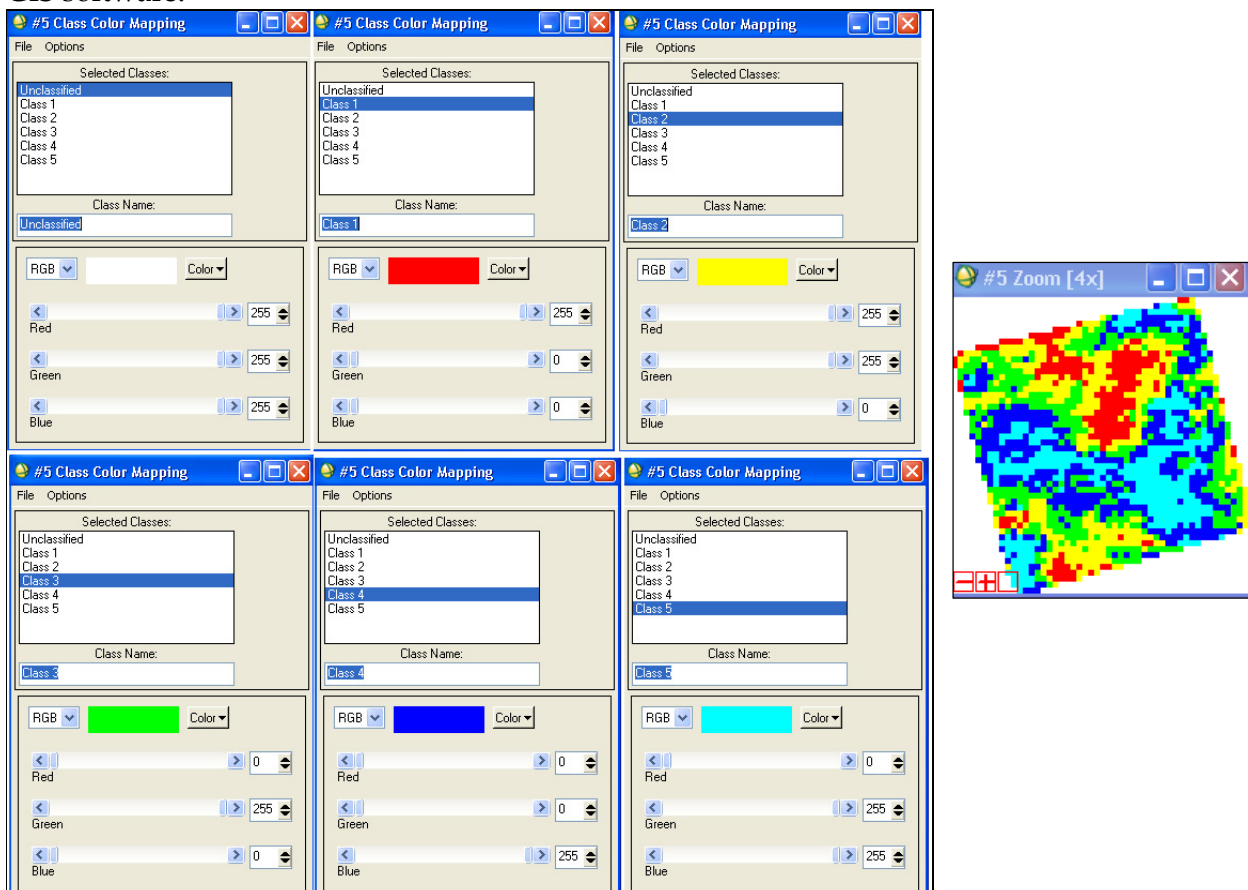
This will open the 'Classification Input File', select the image to be classified as well as the mask band, which can be any band from the original image, select 'OK'. From the 'ISODATA Parameters' window (Below) select the 'Number of Classes' to 'Min' 5 and 'Max' 5, 'Maximum Iterations' to 100 and name the output file, select 'OK'.



Open the classified image as a new display. Using the classified image display toolbar, select 'Tools'- 'Color Mapping' – which will open a 'Class Color Mapping' window.

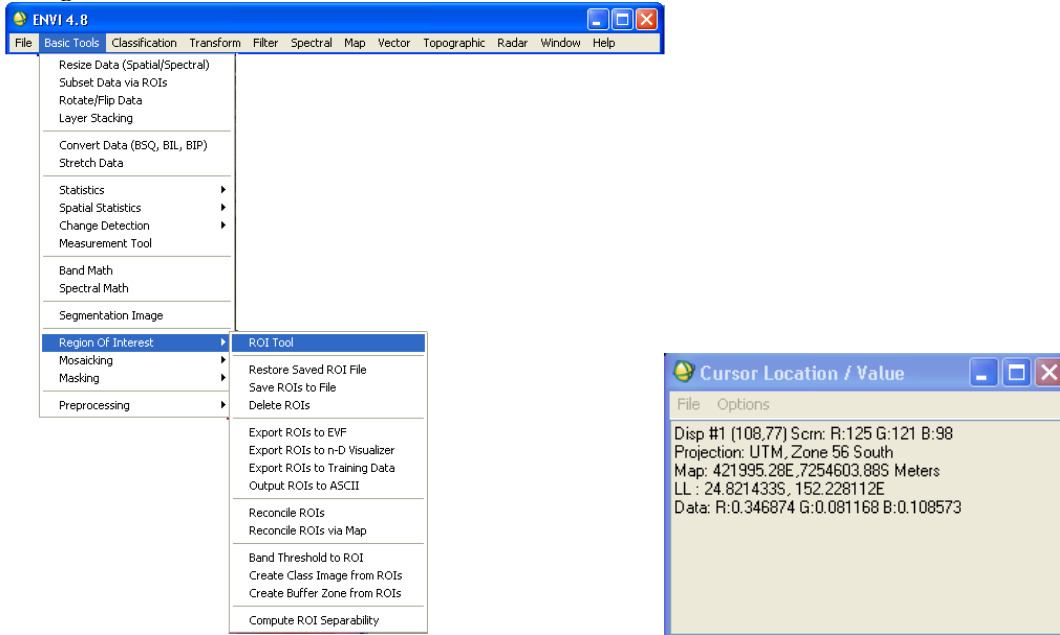


Using this window change the colour scheme to that of the SPAA standard (as below), then File save changes. The classified image can then be saved as a TIF file and imported into any GIS software.

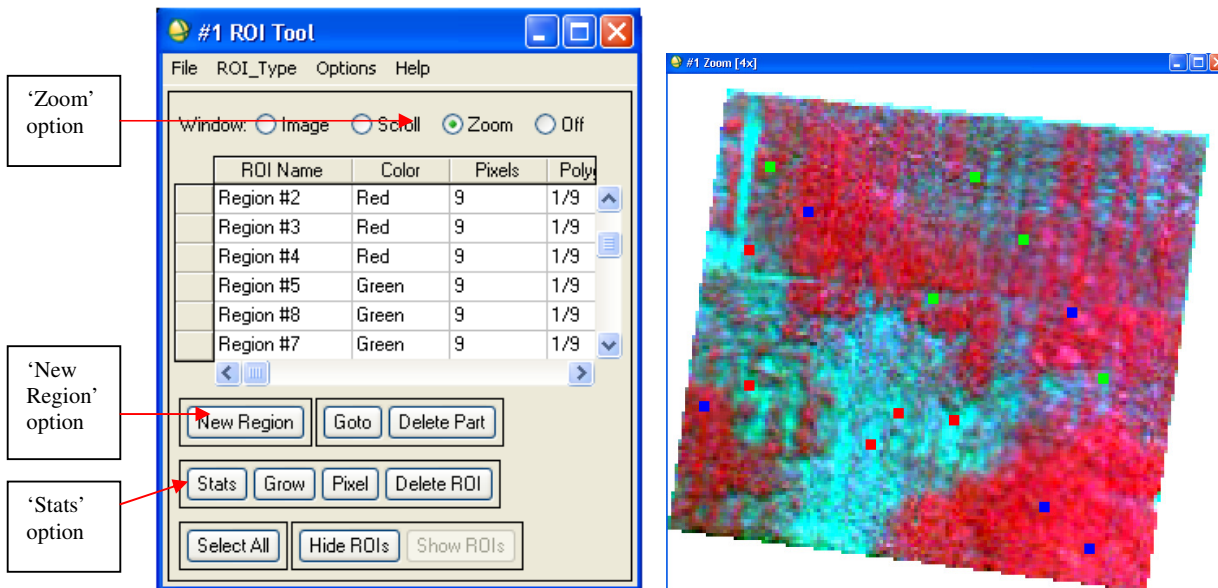


Tutorial 7: ENVI: Extracting point source spectral information from imagery using regions of interest (ROI's).

With the required multispectral image opened in ENVI, from the main toolbar select 'Basic Tools' - 'Region of Interest' - 'ROI Tool'.



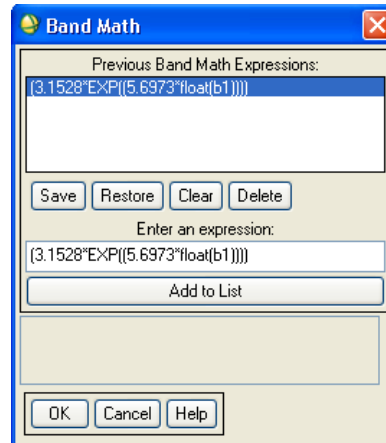
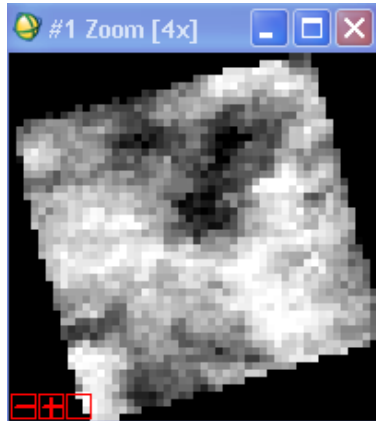
Use the 'cursor location/ value' window (above right) from the main image tool bar- 'Tools' option, to locate the sampling point coordinates within the image. These points can also be directly overlaid on to image if stored as a shape file. Once the points have been located, select the 'Zoom' option in the 'ROI Tool' window (below left) and then in the zoom window (below right) manually draw the ROI around the sampling coordinate. We suggest a 3*3 pixel array for IKONOS and 2*1 pixels for SPOT5. After each ROI is drawn select 'New Region' in the 'ROI Tool' window.



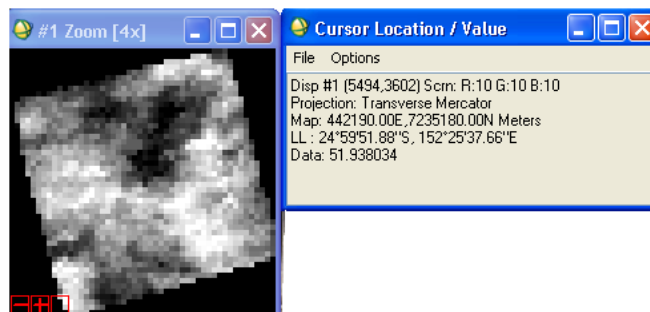
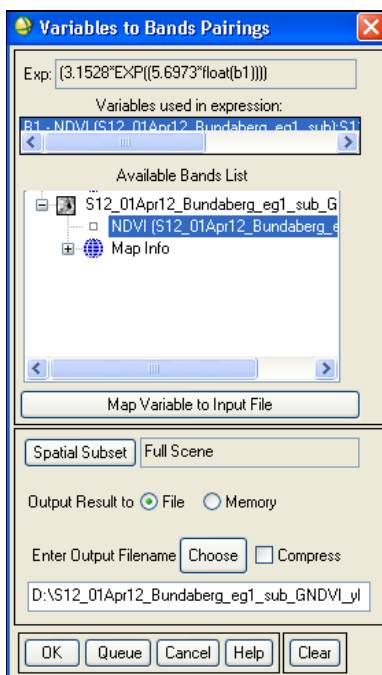
Once all ROI's have been drawn, the mean spectral values for each ROI can be viewed by selecting the 'Stats' option in the 'ROI Tool' window. Record these values in Excel for further analysis.

Tutorial 8: ENVI: Converting VI pixel values into yield (TCH) using an exponential linear algorithm.

For this example a GNDVI image developed through the process described in Tutorial 6 will be used. From the main ENVI Toolbar open the indexed single band image as a new display (below left). From the 'Basic Tools' option select 'Band Math', which will open a 'Band Math window' (below right). For this example, enter the exponential equation developed from the correlation between TCH and GNDVI. Note the use of 'float' in the equation, this ensures the 8-bit GNDVI values are seen as a floating point value and therefore are not rounded up to the nearest whole number. Select 'OK'.

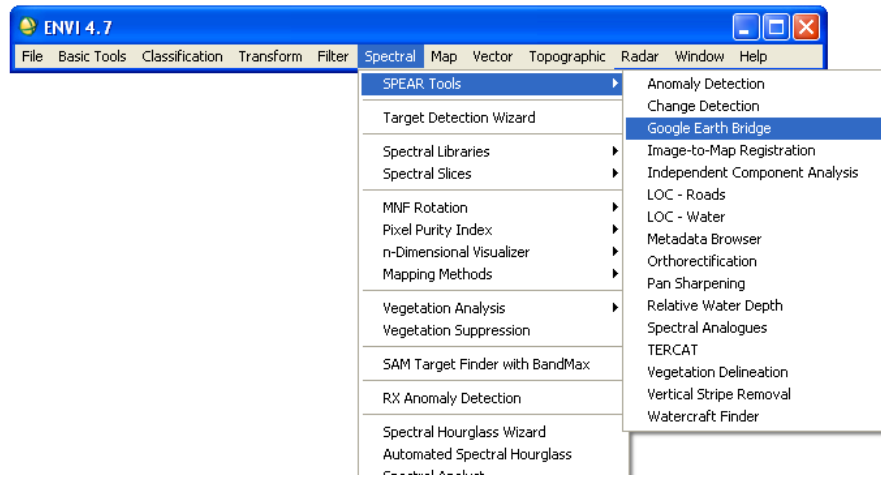


Select the GNDVI band from the 'Variables to Band Pairings' window name the output yield file and select 'OK' (Below left). To identify if the conversion has worked correctly open the derived yield map and double click the cursor on the main image, the values shown as 'Data' should correspond with expected yield values.

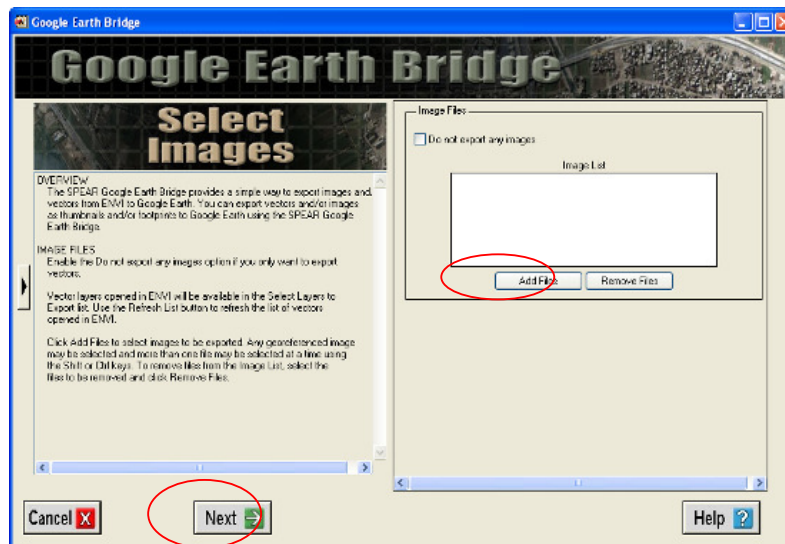


Tutorial 9: ENVI: Creating Google Earth KMZ files from Geotiffs.

With the required 3 band Geotiff opened in ENVI, select 'Spectral'- 'SPEAR Tools'- 'Google Earth Bridge' from the main ENVI menu bar (refer below).



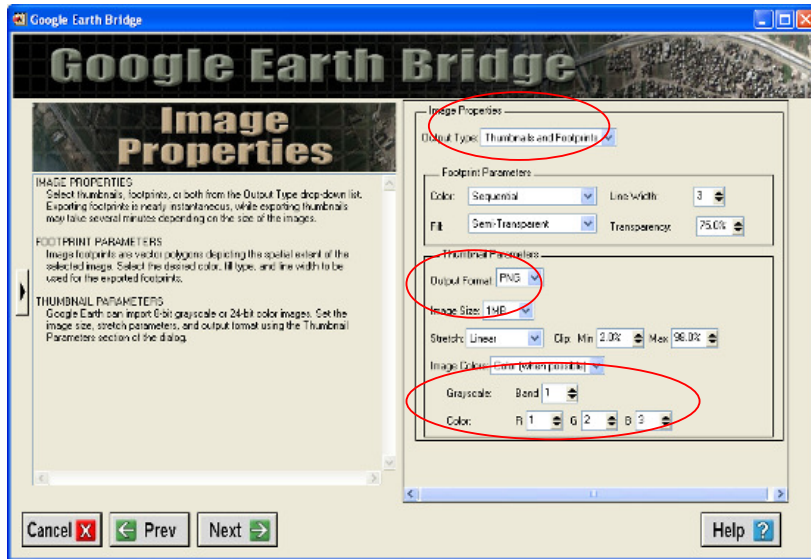
Within the Google Earth bridge window select 'Add Files' and locate the required files from the drop down list and select 'Next'.



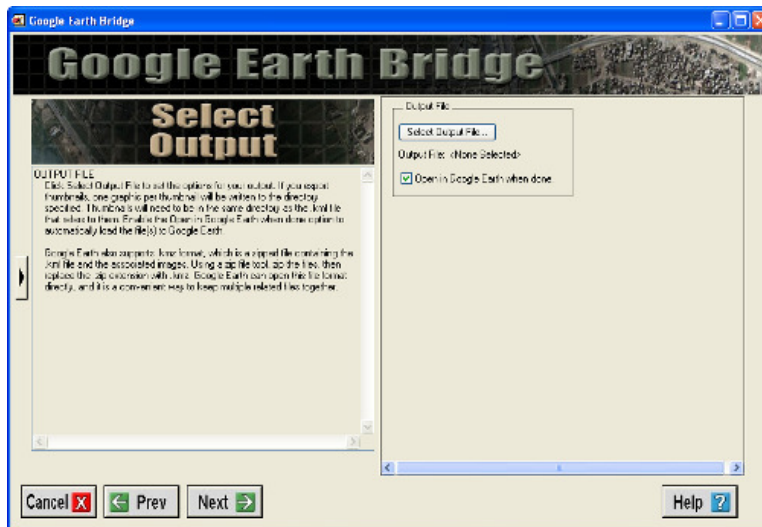
A warning (as below) may be displayed. Select 'OK' as this does not influence the conversion process. Google Earth allows images to be displayed in a time series but for this exercise it is unnecessary.



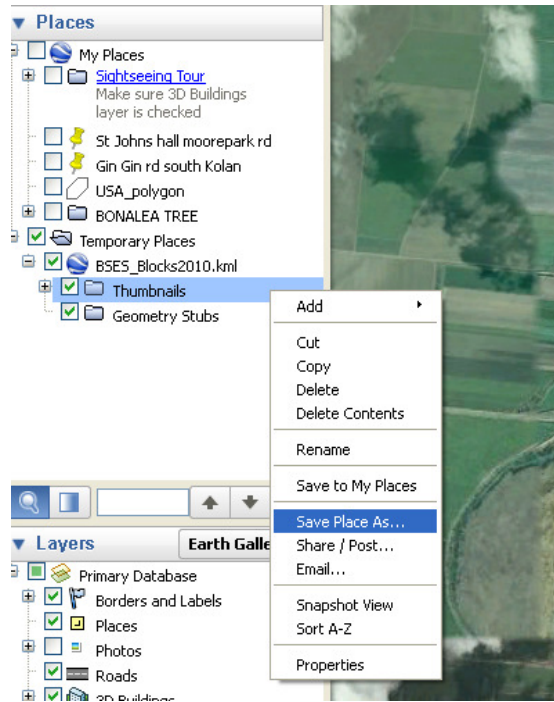
From the following window (as below), select 'Thumbnails' from the 'Output Type'; 'PNG' as the 'Output Format'; '1MB' as the 'Image Size'; and 'R3' 'G2' and 'B1' as 'Color'. Then select 'Next'.



From the following window, select the box for 'Do not export any vectors', then 'Next'. From the subsequent window select 'Select Output File', name the KML file and save it to the desired directory. Select 'Open in Google Earth when done' box if you want to view the file immediately after it is created. Click 'Next' to create the image.



Once opened in Google Earth, right mouse click on the 'Thumbnails' legend option of the image (refer to image below) and select 'Save place As'. The 'Save file' window that opens will allow the KML file to be saved as a KMZ.



11. Appendix 2: Media/ Publications

2012 ASSCT presentation.

AG 24. DEVELOPING SUGAR CANE YIELD PREDICTION ALGORITHMS FROM SATELLITE IMAGERY

By

ANDREW ROBSON¹, CHRIS ABBOTT¹, DAVID LAMB², ROB BRAMLEY³

¹Department of Employment Economic Development and Innovation, Kingaroy.

²University of New England, Armidale

³CSIRO, Adelaide, SA

andrew.robson@deedi.qld.gov.au

KEYWORDS: Yield forecasting, satellite imagery, SPOT5, GNDVI

Abstract

The research presented in this paper discusses the accuracies of remote sensing and GIS as yield prediction tools at both a regional and crop scale over three Australian cane growing regions; Bundaberg, Burdekin and the Herbert. For the Burdekin region, the prediction of total tonnes of cane per hectare (TCH) produced from 4999 crops during the 2011 season was 99% using an algorithm derived from 2010 imagery (green normalised difference vegetation index) and average yield (TCH) data extracted from 4573 crops. Similar accuracies were produced for the Bundaberg region during 2010 (95.5% from 3544 blocks) and 2011 (91.5% for 3824 crops) using a Bundaberg specific algorithm derived from 2008/2010 imagery and yield data. The Bundaberg algorithm was also accurate in predicting yield at specific in-crop locations (91.5% accuracy; SE = 0.028).

1. Introduction

Accurate in-season predictions of regional yield are of vital importance for formulating harvesting, milling and forward selling decisions, whilst at a block scale, they provide growers with an understanding of both in-crop variability and total production. Currently, annual cane production estimates are made by quantifying the area of cane grown within a region by visual in-season yield assessments. Although this method can produce accuracies of up to 95% (Pitt pers. comm. 2011) it can be influenced by variable climatic conditions such as those experienced in 2010. As such geographic information systems (GIS) and remote sensing (RS) may offer an additional tool for validating these predictions as well as potentially provide a more accurate seasonally sensitive method of prediction.

1.1 GIS and Remote Sensing in the Sugar Industry

Geographic information systems (GIS) have been widely adopted by the Australian sugar industry as an essential tool for the recording and managing spatial data (Davis *et al.* 2007). One such system developed for the Mackay and Burdekin region has greatly increased the integration of mill and productivity datasets, thus enabling greater efficiencies in data retrieval and analysis of client information (Markley *et al.* 2008). Similarly, the development of a whole-of-community GIS system by the Herbert River sugar district has created the capacity to record real-time cane harvester operations via GPS, enabling improvements in the coordination and planning of the cane harvest, efficient reporting of harvest performance and the identification of consignment errors. This

information has also been used to improve rail transport infrastructure safety and efficiency (De Lai *et al.* 2011).

Globally, satellite imagery has been identified as an effective tool for predicting sugar cane yield (Fernandes *et al.* 2011; Benvenuti and Weill 2010; Bégué *et al.* 2010; Simões *et al.* 2009; Abdel-Rahman and Ahmed 2008; Bégué *et al.* 2008; Almeida *et al.* 2006; Simões *et al.* 2005; Krishna Rao *et al.* 2002; and Rudorff and Batista 1990), although such research has been limited in Australia (Noonan. 1999; Markley *et al.* 2003; Robson *et al.* 2011; Robson *et al.* 2010; Lee-Lovick and Kirchner 1991). For the last decade, Mackay Sugar Ltd has been the predominant adopter of satellite imagery as a commercial yield forecasting tool for the Mackay region, utilising yield prediction algorithms derived from SPOT imagery (Markley *et al.* 2003). The research presented in this paper investigates the development and validation of similar algorithms over three additional Australian growing regions including Bundaberg, Burdekin and Herbert.

1.2 Yield Predictions using Remote Sensing Techniques

The amount of electro-magnetic radiation (EMR) reflected from a sugarcane canopy is positively correlated to the leaf area index (LAI), which in turn may correspond to the amount of biomass within the crop, and therefore yield (Bégué *et al.* 2010). However, this relationship can be influenced by variations in canopy architecture, foliar chemistry, agronomic parameters and sensor and atmospheric conditions (Abdel-Rahman and Ahmed 2008). More specifically, variety, crop class (plant or ratoon), date of crop planting or ratooning, duration of harvest period and environmental variability are all factors that have been shown to influence the accuracies of yield prediction algorithms developed from remotely sensed imagery (Zhou *et al.* 2003; Singels *et al.* 2005; Inman-Bamber 1994).

In an attempt to remove influences such as spectral interference or ‘noise’, previous researchers have investigated a number of vegetation indices. The most commonly used Normalised Difference Vegetation Index (NDVI), does address some measurement errors associated with atmospheric attenuation and shading, however it can saturate in large biomass crops such as sugar cane with a LAI greater than 3 (Benvenuti and Weill 2010; Bégué *et al.* 2010; Xiao 2005; Xiao *et al.* 2004b; Xiao *et al.* 2004a; Huete *et al.* 2002; Huete *et al.* 1997). To reduce the effects of saturation, a number of additional indices have been employed including the Green Normalised Difference Vegetation Index (GNDVI) (Gitelson *et al.* 1996; Benvenuti and Weill 2010).

Timing of image capture has also been identified to be an important consideration when predicting cane yield, especially when compared to the growth phase of the crop. Sugar cane undergoes three distinct growth phases including germination or establishment and tillering, vegetative development or stalk growth and stabilisation, senescence or maturation (Bégué *et al.* 2010; Simões *et al.* 2005; Fernandes *et al.* 2011; Krishna Rao *et al.* 2002). During the vegetative growth stage NDVI can increase from 0.15 to 0.7, before remaining relatively stable (if unstressed) during the maturation phase, until harvest (Bégué *et al.* 2010). Almeida *et al.* (2006) identified this time period to be 3-6 months prior to harvest, whilst Simões *et al.* (2005) suggested 240 days after planting or ratooning. As well as a stabilisation period of NDVI, a ‘synchronisation’ of NDVI was also observed across various plant and ratoon ages due to climatic factors such as rain and temperature. This synchronisation and stabilisation of NDVI is important as it indicates that there is likely to be an extended window of image capture where variability in the canopies spectral response as well as differences across crops is minimalised (Bégué *et al.* 2010; Almeida *et al.* 2006; Krishna Rao *et al.* 2002; Rudorff and Batista 1990).

Bundaberg2010_caneblocks_withinSPOT							
FID	Shape *	ID	C_YEAR	AREA_HA	VARIETY	CLASS	IRRIGATE
0	Polygon	1	2010	2.52	Q208	Autumn Plant	Furrow
1	Polygon	2	2010	2.44	Q208	Autumn Plant	Furrow 2nd Row
2	Polygon	3	2010	2.47	KQ228	Spring Fallow Plant	Furrow
3	Polygon	4	2010	1.22	KQ228	Spring Fallow Plant	Furrow 2nd Row
4	Polygon	5	2010	1.23	Q205	5 Ratoon	Furrow 2nd Row
5	Polygon	7	2010	3.19	Q205	4 Ratoon	Furrow 2nd Row
6	Polygon	8	2010	3.09	Q135	Spring Fallow Plant	Furrow
7	Polygon	10	2010	4.22	Q188	3 Ratoon	Water Winch
8	Polygon	11	2010	9.55	Q188	3 Ratoon	Water Winch

Figure 1: SPOT5 images captured over each growing region (a). Burdekin, (b). Herbert and (c). Bundaberg. (d). closer view of agronomic information provided within the GIS attribute table.

2.4 Vegetation Indices

To identify the best correlations between satellite imagery and crop yield (TCH), a number of vegetation indices were examined including the Normalised Difference Vegetation Index (NDVI), Green Normalised Difference Vegetation Index (GNDVI) (equation 1), The Soil Adjusted Vegetation Index (SAVI) and the Two-band Enhance Vegetation Index (EVI_2). These indices were calculated for every cane block defined by a GIS paddock boundary within each image capture area. Using harvested tonnes of cane per hectare (TCH) supplied by the respective mills, the index that provided the highest correlation coefficient were identified. For all regions the GIS attribute data was used to separate the spectral information on the basis of variety, crop class (plant or ratoons) and age of crop, in an attempt to improve the correlations.

$$\text{GNDVI} = (P_{\text{NIR}} - P_{\text{GREEN}}) / (P_{\text{NIR}} + P_{\text{GREEN}}) \quad (1)$$

Where P_{GREEN} , and P_{NIR} are the TOA reflectance values measured in the green and near infrared spectral bands.

Additionally, predictions of average yield were made for 3544 (2010) and 3,824 (2011) cane crops within the Bundaberg region using an algorithm derived from the linear relationship between 2008 and 2010 crop yield and corresponding SPOT5 data (Robson *et al.* 2011) (equation 2). The accuracy of this algorithm was also evaluated against point source locations within a single crop and validated within field measurements. Sampling coincided with the commercial harvest of the crop and consisted of 5m linear cane rows hand cut at replicated locations representing high, medium and low GNDVI values, located with a non- differential GPS unit.

$$\text{GNDVI yield prediction algorithm (Bundaberg)} \quad y = 3.1528 * \text{EXP}(5.6973 * x) \quad (2)$$

Where y = predicted average yield (TCH) and x = average GNDVI value extracted from TOA SPOT5 image. (n= 150 crops)

A similar prediction was also undertaken for 4999 cane crops grown within the Burdekin region (2011 season) using an algorithm derived from the correlation between 2010 Burdekin crop yields and corresponding 2010 imagery (equation 3).

$$\text{GNDVI yield prediction algorithm (Burdekin)} \quad y = 12.691 * \text{EXP}(3.8928 * x) \quad (3)$$

Where y = predicted average yield (TCH) and x = average GNDVI value extracted from TOA SPOT5 image. (n= 4573 crops)

3. Results

The initial aim of this research was to develop a generic image-based yield algorithm for all Queensland growing regions that was non-specific to variety, growth stage, and even seasonal variability. However, it was quickly identified that one algorithm would be insufficient due to the large range of varieties planted as well as variation in growing and climate conditions across each region. As such, each growing region was evaluated separately.

3.1 Bundaberg

The correlation between TCH and spectral data extracted for 3824 cane crops grown within the Bundaberg region during 2011 (including 26 varieties with nine ratoon stages, plant, replant and standover classes) was promising with all vegetation indices producing correlation coefficients above 0.6, with GNDVI producing the highest ($r = 0.63$) (Table 1). This correlation was further improved by segregating the data into plant and ratoon classes.

Table 1: Correlation coefficients (r) identified between TCH and individual spectral bands/vegetation indices for the Bundaberg district, 2011 growing season.

Band/VI	Bundaberg District									
	All Blocks	Plant Cane	1 st Ratoon	2 nd Ratoon	3 rd Ratoon	Variety Q208		Variety KQ228		
						Plant	1 st Rat	Plant	1 st Rat	
Green	0.20	0.23	0.17	0.15	0.16	0.51	0.50	0.41	0.50	
Red	0.42	0.40	0.44	0.47	0.48	0.58	0.55	0.45	0.58	
NIR	0.58	0.70	0.62	0.60	0.57	0.64	0.60	0.74	0.63	
SWIR	0.37	0.28	0.37	0.38	0.38	0.45	0.44	0.44	0.47	
NDVI	0.61	0.67	0.68	0.69	0.66	0.68	0.65	0.66	0.66	
GNDVI	0.63	0.71	0.71	0.70	0.66	0.68	0.68	0.72	0.70	
SAVI	0.61	0.71	0.66	0.65	0.62	0.68	0.64	0.73	0.66	
EVI_2	0.61	0.72	0.66	0.65	0.62	0.68	0.64	0.74	0.66	

The stability of correlation across varieties for both GNDVI and NDVI is important as it indicates that a ‘generic’ algorithm which is not cultivar specific may be possible for the Bundaberg region, a finding that supports initial results presented by Robson *et al.* (2011). To further investigate the consistency of GNDVI values across varying classes, variety and seasons, the 2011 data (n= 3824) were overlaid with similar data used to develop the 2008/ 2010 algorithm (n= 150)(Figure 2). From Figure 2 it can be seen that although there is variance around the line of best fit, the overall trend between GNDVI and TCH is relatively consistent across the two data sets.

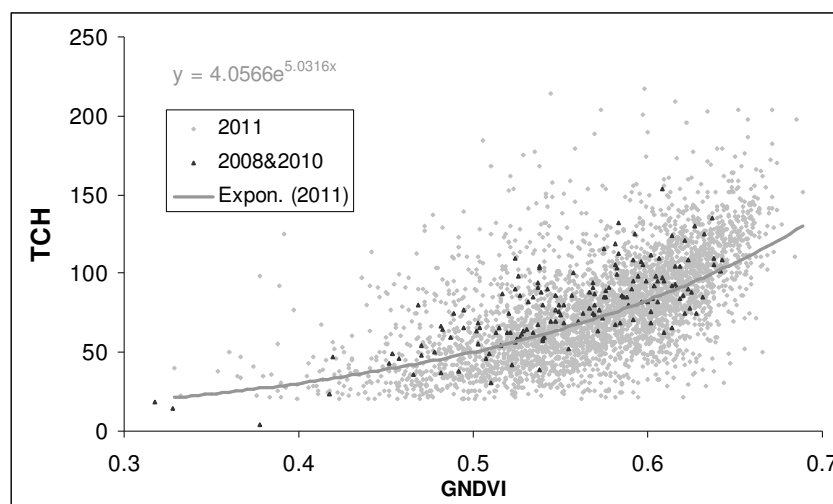


Figure 2. Correlation between GNDVI (SPOT 5) and TCH from Bundaberg cane blocks during the 2008/2010 (black points) and 2011 (grey points) seasons.

The calculation and then subsequent substitution of average GNDVI value (0.567) from 3544 crops grown during 2010 into the 2008/ 2010 algorithm produced an estimated average yield of 78.1 TCH, highly comparable to the actual milled yield of 81.8 TCH (95.5% accurate). For the 2011 harvest season, an average yield of 80.1 TCH was predicted following the substitution of average GNDVI value (0.57) sourced from 3824 crops into 2008/2010 algorithm. This prediction was within 9% of actual milled harvest yield of 73.3 TCH (91.5%). The accuracy of overall prediction, and the fact that the data was not segregated into variety or growth stage, indicates that this technology has the potential to predict regional cane yield within the Bundaberg growing region, a result that differs from previous findings by Lee-Lovick and Kirchner (1991).

To coincide with regional forecasting, the development of such an algorithm offers the potential for predicting individual crop yield as well as the derivation of surrogate yield maps, prior to harvest. To test this, the accuracy of the GNDVI yield algorithm was also evaluated over point source locations within an individual Bundaberg cane crop (area 18.7 ha, var. KQ228) harvested 25 July 2011 (Figure 3). This analysis identified a strong relationship between predicted yield from a SPOT5 image captured on the 27 March 2011, and final yield measured on the 25 July 2011.

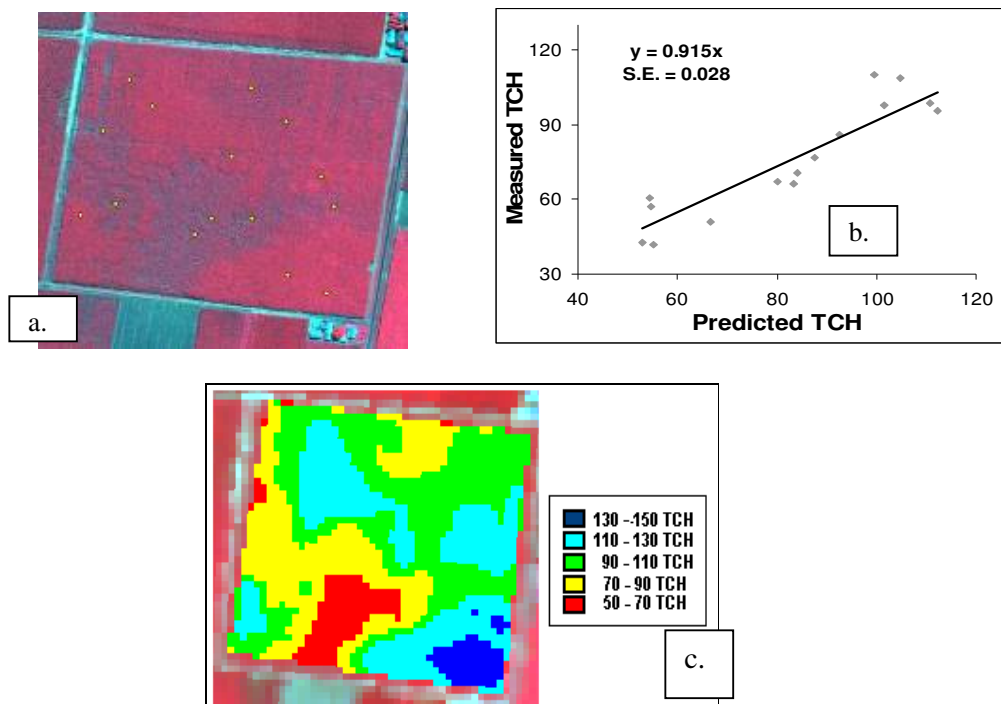


Figure 3. (a). False colour image of Bundaberg cane crop (area 18.7 ha, var. KQ228) harvested 25 July 2011, with yellow markers indicating field sampling locations. (b). measured verse predicted cane yield at the locations identified in (a). (c). Classified yield map generated by applying the 2008/2010 GNDVI yield algorithm to the SPOT5 (27 March 2011) pixel values.

The generation of a classified yield map (Figure 3c) and subsequent accurate prediction of total crop yield from the average crop GNDVI value (predicted of 92 TCH, actual delivered yield of 88.7 TCH) further supports the potential of this technology for producing in-season yield variability maps.

3.2 Burdekin

For the Burdekin region, correlation coefficients produced between TCH and SPOT5 derived vegetation indices (captured 14 May 2010) for all 4573 crops were relatively consistent ranging from $r=0.39$ (NDVI) to $r=0.44$ (SAVI and EVI_2) (Table 2). This correlation remained relatively

unchanged when data was segregated into the different cultivars Q208 and KQ228, indicating that a yield prediction algorithm for this region may not be required to be cultivar specific.

Table 2: Correlation coefficients (r) identified between TCH and individual spectral bands/vegetation indices for the Burdekin district.

Band/VI	Burdekin District									
	All Blocks	Plant Cane	1 st Ratoon	2 nd Ratoon	3 rd Ratoon	Variety Q208		Variety KQ228		
						Plant	1 st Rat	Plant	1 st Rat	
Green	0.12	0.08	0.11	0.10	0.18	0.20	0.16	0.02	0.04	
Red	0.18	0.19	0.15	0.17	0.11	0.27	0.23	0.13	0.12	
NIR	0.41	0.40	0.39	0.28	0.20	0.36	0.36	0.50	0.42	
SWIR	0.19	0.18	0.12	0.11	0.06	0.28	0.10	0.07	0.06	
NDVI	0.39	0.42	0.35	0.29	0.21	0.39	0.35	0.41	0.31	
GNDVI	0.43	0.44	0.40	0.29	0.21	0.41	0.35	0.45	0.35	
SAVI	0.44	0.44	0.41	0.31	0.23	0.39	0.37	0.50	0.40	
EVI_2	0.44	0.43	0.41	0.31	0.23	0.39	0.37	0.50	0.40	

Unlike the Bundaberg analysis however, there was a noticeable drop in the correlation coefficients with ratoon age, especially 2nd and 3rd ratoon (Table 2). This variation indicates that an algorithm that is not crop class specific may be inaccurate, especially when predicting point source yield within individual crops such as that displayed in Figure 3.

At a regional level the predicted average crop yield of 4999 crops grown during the 2011 season using the 2010 algorithm (equation 3) was 99% (actual average yield of 120 TCH, predicted 118.8 TCH). Although highly accurate, the result is not considered robust, due to the large spread of data ($r^2 = 0.07$) produced particularly with standover crops (grey markers in Figure 4). This predictive accuracy will however be further validated during the 2011/2012 season.

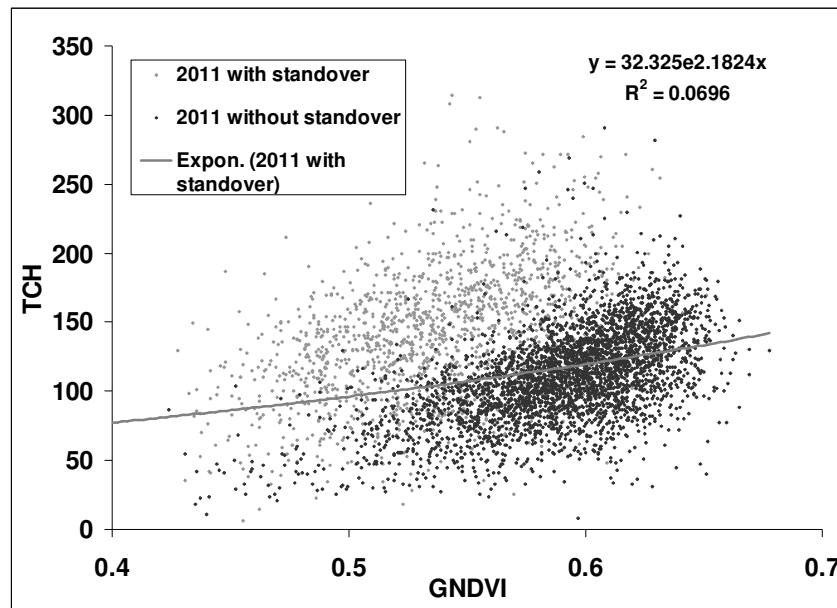


Figure 4. Correlation between GNDVI (SPOT 5) and TCH from 2011 Burdekin cane blocks with black points indicating non-standover crops whilst grey points indicating standover.

3.2 Herbert

The initial correlation between TCH and spectral data (SPOT 5 captured 2 June 2011) for 8596 cane crops grown in the Herbert region (including 53 varieties, multiple ratoon stages, plant, replant and standover) was poor (Table 3). This result is believed to be attributed to severe climatic conditions experienced towards the end of 2010 and start of 2011. The Herbert region had around 25% of the 2011 crop as ‘stand over’ i.e. not harvested from 2010, with the remainder exhibiting

various degrees of flood related damage. The removal of standover blocks did improve the coefficients. The highest regression coefficients were identified by segregating the data into crop class and then variety, for example KQ228 plant crop $r=0.65$ (GNDVI).

Table 3: Correlation coefficients (r) identified between TCH and individual spectral bands/vegetation indices for the Herbert district.

Herbert District												
Band/VI	All Blocks	Standover removed	Plant Cane	1 st	2 nd	3 rd	Variety Q208		Variety KQ228		Variety Q200	
				Ratoon	Ratoon	Ratoon	Plant	1 st Rat	Plant	1 st Rat	Plant	1 st Rat
Green	0.01	0.03	0.01	0.15	0.15	0.35	0.03	0.13	0.01	0.31	0.06	0.02
Red	0.10	0.09	0.10	0.05	0.05	0.16	0.17	0.17	0.07	0.20	0.17	0.09
NIR	0.23	0.46	0.54	0.45	0.40	0.46	0.65	0.55	0.59	0.49	0.50	0.39
SWIR	0.38	0.42	0.37	0.35	0.05	0.46	0.53	0.48	0.30	0.29	0.35	0.33
NDVI	0.22	0.40	0.47	0.34	0.31	0.37	0.60	0.16	0.47	0.36	0.50	0.33
GNDVI	0.23	0.45	0.54	0.42	0.42	0.44	0.65	0.55	0.58	0.45	0.50	0.37
SAVI	0.23	0.45	0.54	0.42	0.37	0.46	0.65	0.56	0.57	0.45	0.51	0.37
EVI_2	0.24	0.46	0.54	0.42	0.37	0.46	0.65	0.56	0.58	0.46	0.51	0.37

These results indicate that for the accurate prediction of yield within the Herbert region a number of algorithms representing different growth stages and even varieties may be required. This hypothesis requires further validation over subsequent growing seasons, particularly seasons that are not influenced by extreme climatic conditions.

Discussion

The undertaking of this research over the three distinct growing regions was highly beneficial considering the array of success identified. Results from the Bundaberg region, and to a lesser extent the Burdekin, indicated that a ‘generic’ yield prediction algorithm may be developed and then used to accurately predict regional production and even within crop yield variability. Although improved correlations were produced following the segregation of data into different groups such as crop class (Burdekin) and variety (Herbert) some consideration has to be made on the number of algorithms developed. In regards to variety, fifty-three were planted in the Herbert, twenty-six in Bundaberg and nineteen in the Burdekin in the years encompassed by this study. If other variables such as the segregation of regions into smaller climate driven micro regions or crop class are also accounted for then the number of algorithms required would grow substantially. One method to address this may be to develop algorithms for only the dominant varieties. For example, only three varieties (of nineteen) in the Burdekin accounted for 83% of the total number of planted blocks. Alternatively, varieties could be categorised into groups based on their spectral signatures. The use of multiple algorithms may increase the flexibility of the predictive models for the season upon which it is applied, allowing it to better compensate for changing percentages of varieties and classes throughout a district and the addition of new varieties.

In the past, the adoption of remote sensing as a yield prediction tool by the Australian Sugar industry has been severely hampered by a number of limitations including: a lack of yield data from the mills due to privacy issues, an extended harvesting period resulting in a patchwork of different varieties, growth and ratoon stages in close proximity and, seasonal or climatic variability, constant cloud cover, insufficient computational demands for image processing, a shortage of skilled analysts and concerns regarding the benefit-cost of adopting the technology. Irrespective of these concerns the research presented in this paper identified satellite imagery and associated GIS data as useful tools for supporting current methods of yield forecasting, with the potential of improving both regional and in-crop yield predictions in the future following further validation.

Acknowledgements.

The authors would like to acknowledge SRDC for providing funding for this research as well as those growers and industry partners whom have collaborated, particularly Bundaberg Sugar Pty Ltd, Herbert Resource Information Centre, Sucrogen and Farmacist Pty Ltd.

References:

- Abdel-Rahman, EM and Ahmed, FB (2008). The application of remote sensing techniques to sugarcane (*Saccharum* spp Hybrid) production: a review of the literature. *International Journal of Remote Sensing* **29**(13), 3753- 3767.
- Almeida, TIR, Filho, CR De Souza and RossettoR (2006). ASTER and Landsat ETM+ images applied to sugarcane yield forecast. *International Journal of Remote Sensing* **27**. pp 4057-4069.
- Bégué, A, Lebourgeois, V, Bappel, E, Todoroff, P, Pellegrino, A, Baillarin, F, and Siegmund, B (2010). Spatio-temporal variability of sugarcane fields and recommendations for yield forecasting using NDVI. *International Journal of Remote Sensing*. **31**(20).5391-5407.
- Bégué, A, Todoroff, P and Pater, J (2008). Multi-time scale analysis of sugarcane within-field variability: improved crop diagnosis using satellite time series? *Precision Agriculture* **9**.161-171.
- Benvenuti, F and Weill, M (2010). Relationship between multi-spectral data and sugarcane crop yield. *Proceedings of the 19th world Congress of Soil Science Soil Solutions for a Changing World* 1-6 August 2010 Brisbane Australia.33-36.
- Davis, R, Bartels, R and Schmidt, E (2007). Precision Agriculture Technologies- Relevance and application to sugarcane production. In *SRDC Technical Report 3/2007: Precision agricultural options for the Australian sugarcane industry* Eds R Bruce.60-117.
- De Lai, R, Packer, G, Sefton, M, Kerkwyk, R and Wood, AW (2011). The Herbert Information Portal: Delivering real-time spatial information to The Herbert River sugar community. *Proceedings of The Australian Society of Sugar Cane Technologists* **33**.
- Fernandes, JL, Rocha, JV and Lamparelli, RAC (2011). Sugarcane yield estimates using time series analysis of spot vegetation images. *Science in Agriculture* **68**(2).139-146.
- Huete, AR, Liu, HQ, Batchily, K and Leeuwen, W (1997). A Comparison of vegetation indices over a global set of TM images for EOS-MODIS. *Remote Sensing of Environment* **59**.440-451.
- Huete, A, Didan, K, Miura, T, Rodriguez, EP, Gao, X and Ferreira, LG (2002). Overview of the radiometric and biophysical performance of the MODIS vegetation indices. *Remote Sensing of Environment* **83**.195-213.
- Inman-Bamber, NG (1994). Temperature and seasonal effects on canopy development and light interception of sugarcane. *Field Crops Research* **36**.41-51.
- Kishna Rao, PV, Venkateswara Rao, V, Venkataratnam, L (2002). Remote Sensing: A technology for assessment of sugarcane crop acreage and yield. *Sugar Tech* **4** (3&4). 97-101.
- Lee-Lovick, G and Kirchner, L (1991). Limitations of Landsat TM data in monitoring growth and predicting yields in sugarcane. *Proceedings of Australian Society of Sugar Cane Technologists* **13**.124-129.

Markley, J Ashburner, B and Beech, M (2008). The development of a spatial recording and reporting system for productivity service providers. *Proceedings of Australian Society of Sugar Cane Technologists* **30**.10-16.

Markley, J, Raines, A and Crossley, R (2003). The development and integration of remote sensing GIS and data processing tools for effective harvest management. *Proceedings of Australian Society of Sugar Cane Technologists* **25**.2003.

Noonan, MJ (1999). Classification of fallow and yields using Landsat TM data in the sugarcane lands of the Herbert River Catchment. Herbert Resource Information Centre Qld Website link: <http://www.hric.org.au/home/JournalPublications.aspx>.

Pitt A (Pers comm). Grower Services Superintendent Bundaberg Sugar Pty Ltd.

Robson, A, Abbott, C, Lamb, D and Bramley, R (2011). Paddock and regional scale yield prediction of cane using satellite imagery Poster Abstract. *Proceedings of the Australian Society of Sugar Cane Technologists*. 33rd Conference Mackay Qld AUS 4 – 6th May 2011.

Robson, A, Abbott, C, Lamb, D and Bramley, R (2010). Remote Sensing of Sugarcane; answering some FAQ's. *Australian Sugarcane* 2011. p6-8.

Rudorff, BFT and Batista, GT (1990). Yield estimation of sugarcane based on agrometeorological-spectral models. *Remote Sensing of Environment*. **33**.183-192.

Rueda, CA, Greenberg, JA and Ustin, SL (2005). StarSpan: A Tool for Fast Selective Pixel Extraction from Remotely Sensed Data Center for Spatial Technologies and Remote Sensing (CSTARS). University of California at Davis Davis CA (Starspan GUI website link: <https://projectsatlas.cagov/frs/download.php/581/install-starspan-win32-020.jar>)

Simões, MDS, Rocha, JV and Lamparelli, RAC (2005). Spectral variables growth analysis and yield of sugarcane. *Science in Agriculture* **62**.199-207.

Simões, MDS, Rocha, JV and Lamparelli, RAC (2009). Orbital spectral variables growth analysis and sugarcane yield. *Science in Agriculture* **66**(4).451-461.

Singels, A, Smit, MA, Redshaw, KA and Donaldson, RA (2005). The effect of crop start date crop class and cultivar on sugarcane development and radiation interception. *Field Crops Research* **92**.249-260.

SPOT Image (2008) SPOT Image Homepage 28th April 2008. Website link <http://www.spotimage.com>.

Xiao, X, Hollinger, D, Aber, J, Goltz, M, Davidson, E, Zhang, Q and Moore, B (2004a). Satellite-based modelling of gross primary production in an evergreen needleleaf forest. *Remote Sensing of Environment* **89**.519-534.

Xiao, X, Zhang, Q, Braswell, B, Urbanski, S, Boles, S, Wofsy, S, Moore, B and Ojima, D (2004b). Modelling gross primary production of temperate deciduous broadleaf forest using satellite images and climate data. *Remote Sensing of Environment* **91**.256-270.

Xiao, X, Zhang, Q, Saleska, Huttyra, L, De Camargo, P, Wofsy, S, Frohking, S, Boles, S, Keller, M and Moore, B (2005). Satellite-based modelling of gross primary production in a seasonally moist tropical evergreen forest. *Remote Sensing of Environment* **94**.105-122.

Zhou, MM, Singels, A and Savage, MJ (2003). Physiological parameters for modelling difference in canopy development between sugarcane cultivars. *In Proceedings of the South African Sugar Technologist Association* 7.610-621.

Article in Australian Sugarcane. February- March 2011.

Remote Sensing of Sugarcane; answering some FAQ's.

Andrew Robson¹, Chris Abbott¹, David Lamb² and Rob Bramley³.

¹Department of Employment Economic Development and Innovation. Kingaroy, QLD. 4610.

²University of New England. Armidale NSW. 2351.

³CSIRO, Adelaide. SA. 5064.

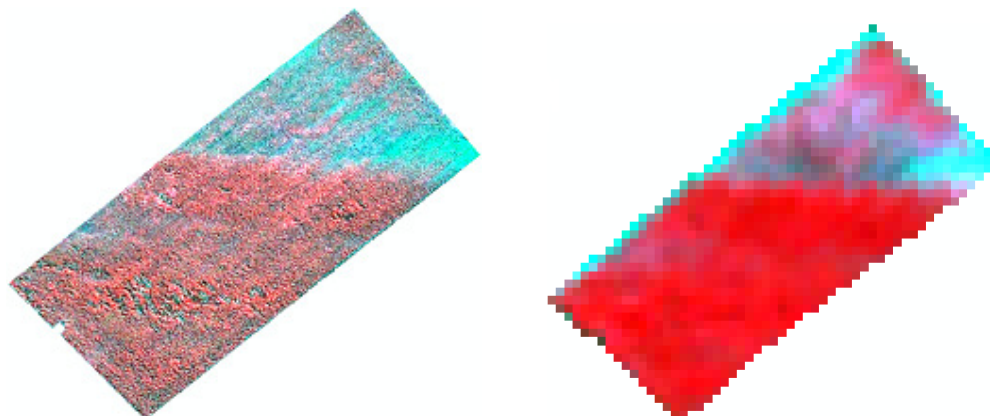
Remote sensing technologies have the potential to drastically improve the monitoring of spatial variability within Australian Sugarcane crops aiding in the better implementation of inputs and the optimisation of crop yields. Applications such as the detection of crop damage from pest, disease and poor nutrition, as well as the prediction of yield and its stability over time, have been investigated within many agricultural systems including sugarcane. However, grower adoption in the sugar industry remains low. This is likely attributed to a poor understanding of what technologies are available, who provides them, what they cost and the cost/benefit of implementation, as well as an overall shortage of knowledge and skills in the interpretation and then dissemination of the data to end users. This article addresses some of these issues in an attempt to inform consultants and growers of the potential benefits of adopting these technologies, particularly with the ongoing pressures of maintaining economical and environmental sustainability.

What is Measured?

For the assessment of agricultural crops, remote sensing platforms measure the amount of solar electro-magnetic radiation (EMR) reflected and transmitted by a plant canopy. The measurement of EMR within the Near-Infrared (NIR) region (700 – 1300nm) provides an indication of a plant's internal canopy structure as predominantly influenced by leaf water content and morphology and therefore is specific to plant stress or desiccation. The Red region (600-700nm) is specific to chlorophyll concentration. Ratios of NIR and Red reflectance such as NDVI (Normalised Difference Vegetation Index = $\text{NIR} - \text{Red} / \text{NIR} + \text{Red}$) or Plant Cell Density ($\text{PCD} = \text{NIR} / \text{Red}$) when mapped across a crop are commonly used to emphasise spatial variability in plant structure and condition. The greater the NDVI or PCD value at a given location the more vigorous the plant and generally the higher the associated crop yield.

What is the best Spatial Resolution?

Currently available commercial satellites offer a wide range of spatial resolutions, defined by the size of the on ground image picture element or pixel. These range from 0.5m² to 1km² with the optimum resolution determined by the required application i.e. plant, farm or landscape scale. Using too low a spatial resolution may limit the ability to define specific crop features such as disease or pest 'hot spots' or even crop boundaries as each pixel displays multiple features smoothing out actual variability. Conversely, too high a spatial resolution may complicate the definition of larger management zones due to a 'salt and pepper' effect where each pixel is providing a measure of independent features such as plant canopy, trash, soil and shadow. In general, high resolution imagery is better suited for measuring localised plant stress such as that from cane grubs or nematode damage, weed and disease, as well as overall spatial variability within smaller crops. Mid resolution imagery i.e. 10m to 20m, could be considered to be more suitable for identifying variability trends across whole crops, farms and catchments including those arising from soil variability, topography or prior history. An example of a single cane block captured at two different spatial resolutions is included below.



False colour image of plant cane as identified by 0.8m IKONOS imagery (left) and 10m SPOT5 imagery (right). The brighter the red colour, the higher the infrared reflectance and the more vigorous the crop.

Commercially available satellite options and their associated cost:

Selection of the most cost-effective imagery ultimately depends on the intended application, with spatial resolution as well as the minimum capture area having the greatest influence. In general, higher spatial resolution images are more expensive per hectare than lower resolution images, but generally have a lot smaller minimum required capture area i.e. 47km² compared to 5000km². If an individual grower is purchasing an image directly from a provider, they will generally have to pay for an area greater than their farm, resulting in the cost for useable imagery on a hectare basis increasing. This can be minimised by including a number of neighbouring growers to share the cost, have a consultant provide the imagery as part of their agronomic service or use an image on-seller who can purchase whole scenes and then on-sell each property as required. The latter may result in a slight increase in imagery cost. However, the resultant product is likely to be correctly processed for geographic accuracy and have vegetation indices such as NDVI applied. Also worth noting is the image revisit time, where the higher the frequency the more chance that imagery will be successfully captured in regions with continued cloud cover. Other platforms such as LIDAR, Radar and aerial imagery are available but are not covered in this article. A list of commercially available satellite imagery platforms and associated costs is provided below.

Commercially available satellite imagery options for assessing within-field variability.

Attribute	SPOT	GeoEye		Digital Globe		RapidEye
		IKONOS	GeoEye-1	Quickbird	Worldview-2	
Spatial Resolution	10m, 20m	3.2m	2m	2.4m	2m	5m
Panchromatic Band	2.5m, 5m	0.8m	0.5m	0.6m	0.5m	none
Min Area	1800km ²	1*100km ² or 3*50km ²	1*100km ² or 3*50km ²	78km ²	47km ²	5000km ²
Min Cost	\$4,800	1*\$2383 or 3*\$1100	1*\$2383 or 3*\$1100	\$1980USD	\$1980USD	\$13,500
Cost/total km ²	\$2.70	1*\$24 or 3*\$22	1*\$29 or 3*\$27.5	\$25	\$42	\$2.70
Dynamic Range	8-bit	11-bit	11-bit	11-bit	11-bit	12-bit
Image Revisit	2-3 Days	1-3 Days	3 Days	1-3.5 Days	3.5 Days	0.5 Days
Band 1	NIR	Blue	Blue	Blue	Ocean	Blue
Band 2	Red	Green	Green	Green	Blue	Green
Band 3	Green	Red	Red	Red	Green	Red
Band 4	MIR	NIR	NIR	NIR	Yellow	Red-edge
Band 5					Red	NIR
Band 6					Red-edge	
Band 7					NIR1	
Band 8					NIR2	

Some commercial providers and on-sellers of satellite imagery:

AAM: www.aamgroup.com

Geoimage: www.geoimage.com.au

SPOT imaging Services: www.spotimage.com.au.

Sinclair Knight and Merz: www.skmconsulting.com

Precision Agriculture.com: www.precisionagriculture.com.au

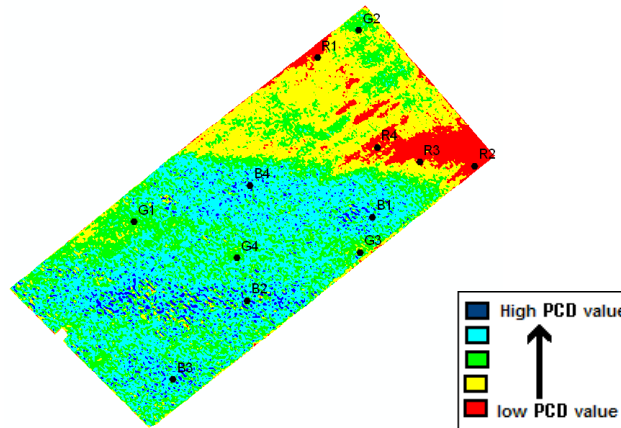
CTF solutions: www.ctfsolutions.com.au

Terranean mapping technologies: www.terreanean.com.au

Agrecon: <http://www.agrecon.com>.

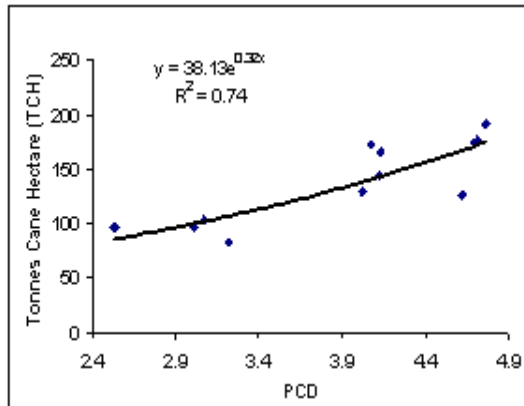
What applications can imagery be used for?:

Growers generally have a good understanding of inherent spatial variability within their cane blocks. Satellite imagery can improve this awareness by indicating the exact location and area affected by a cropping constraint, as well as identifying those events such as pest incursion or lodging that do not persist from season to season. From the following example, a large degree of variability within a plant cane crop can be seen, with high vigour or PCD shown as Blue and low vigour or PCD as Red (like NDVI, PCD gives an indication of the size and health of the plant canopy). From this map, GPS guided agronomic and yield assessments can be made to determine the nature of the constraints as well as their impact on productivity. In this example yield, commercial cane sugar (CCS) and soil samples were collected to coincide with commercial harvest.

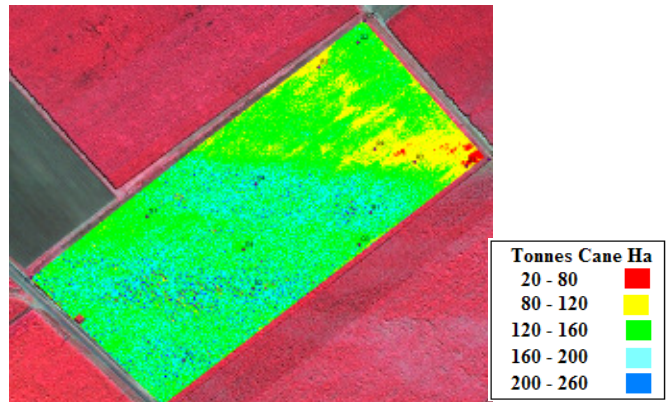


Classified PCD IKONOS 0.8m image of plant cane crop with sample locations. (Area =11.5ha)

The low PCD regions within this crop yielded 90 tonnes of cane per hectare (TCH) compared to 170TCH in the high areas. The relationship between the point source measurement of cane yield and the corresponding image information can allow a surrogate yield map to be developed as well as provide an estimate of total yield.



Correlation between PCD and TCH



Surrogate yield map derived from PCD/ TCH correlation

<i>Prediction of average crop yield</i>	= 38.13 * EXP(0.32*PCD crop average)
	= 38.13 * EXP(0.32*4.123)
	= 142.6 TCH
<i>Prediction of Total yield</i>	= 11.52 ha * 142.6 TCH
	= 1643 Tonnes
<i>Actual yield harvested</i>	= 1526.6 t (prediction over by 8%).

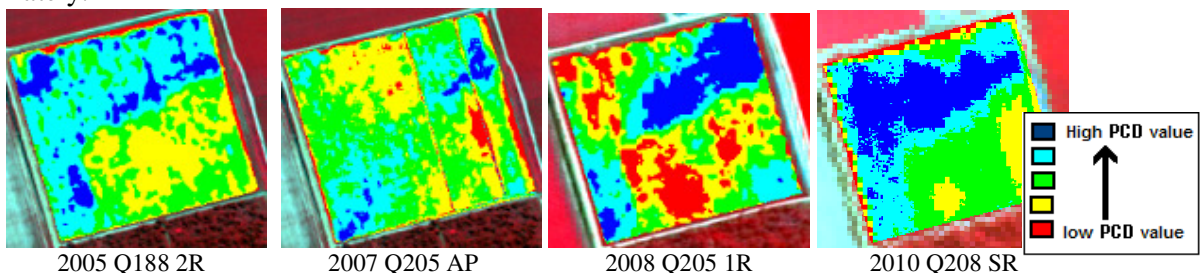
The development of a generic yield algorithm that can accurately predict total yield as well as yield variability without the need for crop sampling would be of great benefit to the Australian sugar industry. This would not only assist growers with management decisions but, as Mackay Sugar Ltd has demonstrated, can also allow more accurate regional decisions regarding forward selling, handling and storage to be made prior to harvest.

Cost-benefit of informed decisions regarding remedial action:

By identifying the area of reduced productivity as well as the resulting yield deficit, an estimation of lost productivity in monetary terms can be made. From the example above the low vigour regions yielded 10 tons of harvestable sugar per hectare less than the high yielding areas. Expressed in monetary terms this would equate to \$4,500 (at \$450t) per hectare. With the low yielding area extending over 4ha this would equate to \$18,000 of less than optimum productivity. By identifying the nature of the limiting factor, in this case sandy subsoil with reduced water holding capacity, low EC, exchangeable nutrients and trace elements, a decision can be made on the cost/ benefit of applying remedial action such as the deep application of mill mud or clay.

Understanding your blocks inherent variability:

Imagery acquired over a number of cropping seasons can allow growers to understand the inherent spatial variability within their blocks. If the spatial orientation of both high and low crop regions remains unchanged across seasons and crop age (i.e.2005, 2008 and 2010 below) then well informed decisions can be made on the management of these blocks prior to planting including the use of variable rate technologies (VRT). If the zones are unstable from season to season (i.e. 2005 to 2007) then the impacts of climate, management or rotational effects should be considered and managed appropriately.



Conclusion

Pioneers of remote sensing technologies such as independent precision agricultural services and some industry groups have long understood the benefits of satellite imagery. However, for industry wide adoption it is imperative that all facets obtain some understanding of what technologies are available and what possible applications and cost/benefits they can provide. To increase overall adoption there is an obvious need to address the limitations of imagery accessibility, availability and minimum area; A web based framework linked to commercial image provider could possibly provide a solution. This method of accessing imagery, aligned with integrated farm management software would enable growers to form management decisions based on a culmination of spatial information including yield and soil maps, elevation etc. This would aide better data compatibility, recording and interrogation, resulting in the improved management of crop inputs and ultimately increased productivity. Although this is not a new concept, the availability of new commercial platforms and a greater awareness of what the technology can offer may improve adoptability and enable Australian cane growers to maintain economic and environmental sustainability.

Acknowledgements.

The authors would like to acknowledge SRDC for providing funding for this research as well as those growers and industry partners whom have collaborated. Also DERM for providing access to imagery over a number of the target sites. For more information please contact Andrew Robson (andrew.robson@deedi.qld.gov.au) or Chris Abbott (chris.abbott@deedi.qld.gov.au).

2011 ASSCT Poster presentation.

PADDOCK AND REGIONAL SCALE YIELD PREDICTION OF CANE USING SATELLITE IMAGERY

Andrew Robson¹, Chris Abbott¹, David Lamb² and Rob Bramley³.

¹*Department of Employment Economic Development and Innovation, Kingaroy, QLD. 4610.*

²*Precision Agriculture Research Group, University of New England, Armidale NSW. 2351.*

³*CSIRO Ecosystem Sciences, Adelaide. SA. 5064.*

KEYWORDS: Yield prediction, NDVI.

Abstract

The pre-harvest forecasting of regional cane production within any given season is of great importance to the Australian cane industry. If inaccurate, significant financial penalties can be incurred by marketers with roll on effects for mills and growers. The use of remote sensing to predict yield is not a new concept, with progressive mills such as Mackay Sugar using SPOT satellite imagery for a number of years. However other regions are yet to implement this technology. Current research, funded by SRDC, has developed a preliminary algorithm for the Bundaberg region that has demonstrated accurate yield predictions for both large cropping regions and within individual crops.

The algorithm was developed from the correlation between NDVI (normalised difference vegetation index) values derived from a SPOT 5 image captured on the 10th May 2010, with 2010 cane yields measured from whole blocks and from point source locations within individual crops ($R^2 = 0.61$; $n = 112$). These data included 12 varieties and 15 planting stages. To assess the robustness of the algorithm, it was applied to 2008 season imagery captured on the 31st March 2008. For 600ha of cane, a yield of 39,707 tonnes of harvested cane or 66.5 tonnes cane per hectare (TCH) was predicted which was 3.8% under the actual delivered yield (41,255 t at 69 TCH). The development of a subsequent

algorithm using both 2008/2010 data ($R^2 = 0.6$; $n = 151$) did not improve the accuracy of the prediction, indicating that the relationship between yield and NDVI for the Bundaberg region may be consistent across seasons; this requires further validation using expanded datasets.

The production of potential yield maps prior to harvest is also of great benefit to cane growers. To test whether such maps could be developed from the regional yield prediction algorithm, the predicted yields of point source locations (area 200m^2) within two crops from the 2010 season were validated against measured hand cut samples. When compared to a one to one relationship between actual and predicted yield, the predicted yields showed a tendency to over-predict in low yielding areas and under-predict in high yielding areas. Again, further refinement and validation of the algorithm in the 2011 season is expected improve the prediction accuracy.

Paddock and regional scale yield prediction of cane using satellite imagery

Andrew Robson¹, Chris Abbott¹, David Lamb² and Rob Bramley³.

¹Department of Employment, Economic Development and Innovation, Kingsgrove, QLD, 4810. ²Precision Agriculture Research Group, University of New England, Armidale, NSW, 2351. ³CSIRO Ecosystem Sciences, Adelaide, SA, 5084.

Introduction

Pre-harvest forecasting of regional cane production is of great importance to the Australian cane industry. If inaccurate, significant financial penalties can be incurred by marketers, mills and growers. Current research, funded by SRDC, has developed a preliminary algorithm for the Bundaberg region that has been shown to be accurate in the prediction of yield over a large cropping area and within individual blocks.

Development of the yield algorithm

The algorithm was developed from the correlation between NDVI (normalised difference vegetation index) values from a SPOT 5 image captured 10 May 2010 with 2010 whole block and point source yield data (blue markers in Figure 1) ($R^2 = 0.61$; $n = 112$). This includes 12 varieties and 15 ratoon stages. The overlaying of 2008 NDVI and yield data from 2008 (red markers- Figure 1) produced a similar trend to that identified from 2010 indicating consistency across growing years.

Validation of algorithm

The 2010 prediction algorithm was applied to NDVI values from a 2008 SPOT 5 image captured 31 March 2008. From a 600ha area a total yield of 39,707 tonnes of harvested cane at 66.5 tonnes cane per hectare (TCH) was predicted (Figure 2). This prediction was 3.8% under the actual delivered yield, indicating that an accurate pre-season prediction could be made over a larger growing region and across seasons.

Prediction of 2008 Yield from 2010 algorithm:

Validation Area = 600 ha sugarcane
 Predicted TCH = $3.3424 \times e^{4.6294 \times 0.648915} = 66.2$ TCH
 Total Yield = $66.2 \text{ TCH} \times 600 \text{ ha} = 39,707$ tonnes
 Actual Yield (Mill Harvest Report) = 41,255 tonnes (at 69 TCH)

Under prediction of 3.8%

Derivation of crop specific yield maps

At an individual crop level, predicted yields of 24 point source locations (each area 200m²) were made within two Bundaberg crops from the 2010 season (black markers Figure 3). The predicted yields were comparable to the actual 'one to one' measured yield line (dotted line- Figure 2).

To test the predictive accuracy of the Bundaberg algorithm within other growing regions it was also applied to a SPOT 5 image captured 14 May 2010 over the Burdekin. This produced a consistent over prediction of yield when compared to a 'one to one' line (Red markers- pink outline). This result indicates that either a unique yield prediction algorithm is required for each growing region, or a standardised weighting factor needs to be applied to the basic algorithm to account for regional variability.

Note: An algorithm for the Burdekin region is currently being developed.

The authors would like to acknowledge SRDC for funding the research as well as collaborating industry members, namely Reimay and Bullseye Farming enterprises.

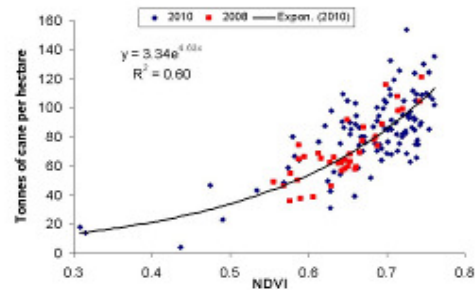


Figure 1. Correlation between NDVI and Yield (TCH) for the 2010 growing seasons (blue dots). Corresponding data from the 2008 season (red dots) shows stability of relationship across years.

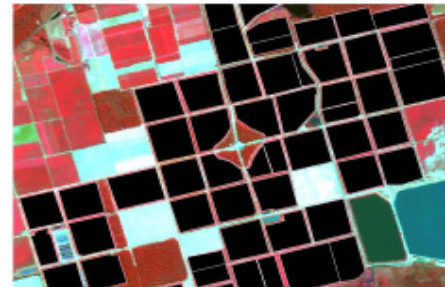


Figure 2. Whole cane blocks (Black polygons) where whole crop yields and corresponding NDVI values were sourced for the algorithm

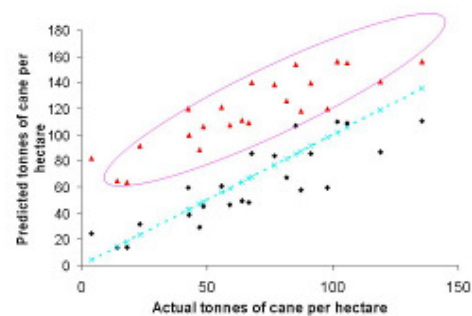


Figure 3. Actual measured Yield (TCH) of numerous locations within 2 Bundaberg crops plotted against predicted yield using the 2010 Bundaberg algorithm (black markers). Actual measured yield (TCH) of a Burdekin crop plotted against predicted yield using the same 2010 Bundaberg algorithm (red markers).

More information

Department of Employment,
Economic Development and Innovation

Name: Dr Andrew Robson
 Phone: +61 7 4160 0735
 Email: andrew.robson@deedi.qld.gov.au

www.deedi.qld.gov.au



2010 ASSCT Poster presentation.

USING SPATIAL MAPPING LAYERS TO UNDERSTAND VARIABILITY IN PRECISION
AGRICULTURAL SYSTEMS FOR SUGARCANE PRODUCTION.

By

JR HUGHES¹, RJ COVENTRY², A ROBSON³

¹*Department of Employment, Economic Development, and Innovation, Mackay*

²*Soil Horizons Pty Ltd, Townsville*

³*Department of Employment, Economic Development, and Innovation, Kingaroy*

John.Hughes@deedi.qld.gov.au

KEYWORDS: Soil Variability, EC Mapping, Crop Yield, Yield Monitoring, NDVI, Site-specific Management

Abstract

Precision agriculture (PA) has been identified as an effective tool for identifying and then managing crop production across a wide range of farming systems, globally. The implementation of such technologies within the Australian Sugar cane industry also holds much potential however it is imperative that a strong cohesion between sound agronomy and PA technologies is first achieved. Intensive yield observations across five study sites in the Mackay, Burdekin, and Herbert districts identified that to manage within-paddock variability, improved strategies must consider the multifaceted interactions of variables including nutritional issues, seasonal conditions, management practices, and biological factors such as plant disease and pest damage. It therefore follows that there is also a need to combine a number of existing PA tools, quantified with corresponding field samples, to ensure a more accurate and robust diagnosis of crop production is achieved. The following example from the Herbert cane growing region demonstrates how the interaction of spatial data layers (satellite imagery, EC mapping, yield monitoring) can be used effectively to identify the spatial variability of crop production, including the use of strategic soil and yield sampling and for the prediction of lost production resulting from underperforming regions. The infrared reflectance images of plant cane crops, derived from high resolution satellite images captured just before harvest, identified in-season crop variability that related well with the expected variability driven by contrasting soil properties portrayed through soil EC mapping. A linear algorithm developed between Normalised Difference Vegetation Index (NDVI) values with strategically located manually harvested yield samples, was shown to be a reliable predictor of spatial variability as well as total crop yield when compared to final harvest weights and results obtained from a yield monitor on a commercial sugarcane harvester. These results indicate how decisions based on multiple mapping layers are likely to underpin new farm management strategies in the further development of a precision agricultural framework for the sugar industry.

Using spatial mapping layers to understand variability in precision agriculture systems for sugarcane production

Andrew Robson¹, John Hughes², Ross Coventry³, Lawrence Di Bella⁴, Enrique Ponce⁵, Michael Sefton⁶
¹DEEDI, Kingaroy ²DEEDI, Mackay ³Soil Horizons, Townsville ⁴Terrain NRM, Ingham ⁵Techagro Pacific, Macknade ⁶HCPSSL, Ingham

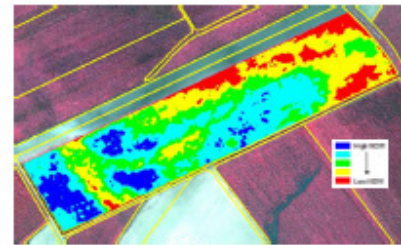
Crop reflectance: NDVI

Crop reflectance was measured from a high resolution IKONOS satellite image, enhanced through the calculation of a normalised difference vegetation index (NDVI) for each pixel, classified, and mapped (right).

$$NDVI = (NIR - Red) / (NIR + Red)$$

where 'NIR' indicates the reflectance measured within the near infrared region of the electromagnetic spectrum (757 – 853 nm) and 'Red' within the visible region (632 – 698 nm).

A high NDVI value generally indicates healthy, vigorous plants while a low value indicates reduced vigour.

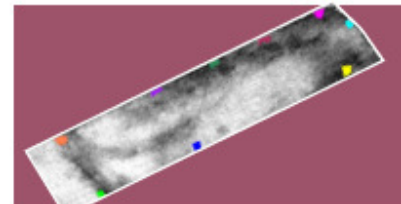


Classified NDVI based on an IKONOS image captured 2 August 2009



Yield validation samples

To assess the correlation between NDVI and yield variability, ten 5 metre rows of cane were manually sampled from areas with a range of NDVI values and weighed via a portable weigh trailer. These samples were collected on the 21 August 2009, 19 days after image capture and three days before the commercial harvest of the crop on 24 August 2009.



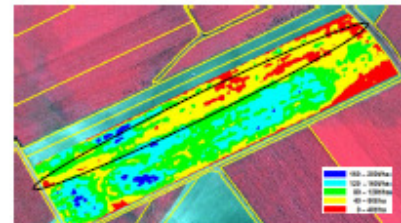
Field sampling locations manually harvested 21 August 2009

Harvester yield monitor

TechAgro yield monitor data and NDVI map data were geo-referenced and set to the same 7x7 metre grid.

A significant correlation was identified between Techagro yield monitor data with NDVI ($R^2=0.60$, $n=1807$; blue points).

The removal of yield monitor values (black ellipse, right) suspected to be spurious (yellow points; $n=226$) improved the correlation to ($R^2=0.66$, $n=1581$).



Classified yield map (Techagro): harvest 24 August 2009

Yield prediction

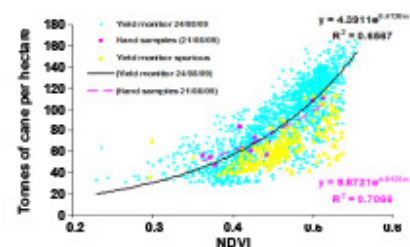
The manually sampled data (pink dots and curve, right) show a close fit to the exponential linear algorithm developed between the Techagro and NDVI correlation (black curve). Total yield prediction using both the Techagro/ NDVI algorithm (714 t) and manually harvested samples/ NDVI algorithm (684 t) were comparable, with the later being more accurate to the actual final yield (594 t). The over prediction of 13% may be explained by harvest losses.

Average NDVI over the whole of the crop = 0.465747

Manual yield Mean yield = $(8.8721 \cdot \text{EXP}(4.8123 \cdot 0.465747)) = 83.448 \text{ t/ha}$
 $83.448 \text{ t/ha} \cdot 8.2 \text{ ha} = 684 \text{ tonnes from paddock (over estimate: 13.3\%)}$

Yield monitor Mean yield = $(4.3911 \cdot \text{EXP}(6.4136 \cdot 0.465747)) = 87.068 \text{ t/ha}$
 $87.068 \text{ t/ha} \cdot 8.2 \text{ ha} = 714 \text{ tonnes from paddock (over estimate: 16.7\%)}$

Actual paddock yield (cane delivered over mill weighbridge) = 594 t



Correlation between Techagro yield data and curve spanning NDVI values (blue points); suspected spurious points (to be removed) shown as yellow points. Pink points are manually harvested data. Black ellipse marks area removed from data.

These results indicate that the spatial variability of cane yield can be predicted using satellite imagery, if validated with either accurate yield monitor data or strategically located manually harvested samples. Further research is required, however, to identify if accurate algorithms can be developed to predict yield with out the need for intensive field sampling, as well as optimal timing for image capture.

More information



Department of Employment, Economic Development and Innovation
 Name: Dr Andrew Robson
 Phone: +61 7 4160 0735
 Email: andrew.robson@deedi.qld.gov.au
 www.deedi.qld.gov.au



Article in the Burdekin 'The Advocate' Newspaper promoting the presentation at Burdekin Productivity Services Annual General Meeting 16th August 2011.

SATELLITES SENSE VARIABILITY IN BURDEKIN CANE CROPS

Using satellite imagery to boost effective yield prediction in sugar cane

The latest innovations in satellite technology for the Queensland cane industry, will be highlighted at the Burdekin Productivity Services AGM on 16 August in Ayr.

Currently, collaborative research across Australian cane growing regions by the Department of Employment, Economic Development and Innovation (DEEDI), University of New England and CSIRO has identified a number of applications using satellite imagery, ranging from regional yield prediction to identifying the stability and drivers of variability within individual crops.

The three-year Sugar Research Development Corporation (SRDC) funded project has involved all facets of the sugar industry to determine where imagery can provide a feasible and efficient tool for improving current management and decision-making processes.

DEEDI project leader Dr Andrew Robson is working directly with end users such as growers, mills, productivity services and research bodies (i.e. BSES), to identify the optimal commercial satellite, capture timing, appropriate resolution, and most importantly cost vs. benefit that will provide the best result.

The imagery can be used for the detection of crop limiting factors, including soil nutrition, drainage issues and cane grubs.

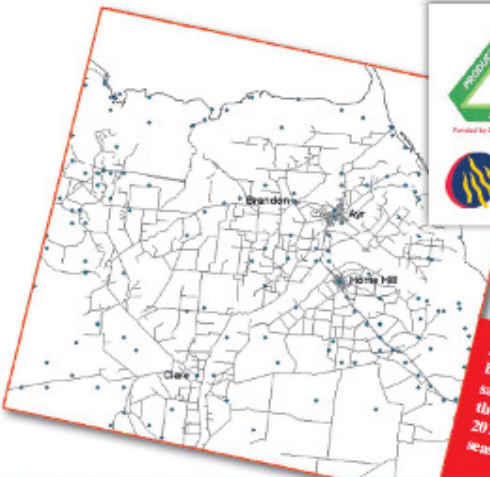
This research is inspiring greater adoption of this technology. Following Cane Productivity Initiative (CPI) meetings in February 2011, more than 20 Burdekin growers have requested image derived variability maps for the 2010 season.

The development of yield prediction algorithms from SPOT 5 imagery have proven highly accurate for the Bundaberg region. With further refinement, these could provide a useful tool for mill owner/managers when forming harvest management and on-selling decisions prior to harvest. A similar algorithm will be developed for the Burdekin and Herbert region this season.

For more details or for imagery of your own properties please contact Dr Andrew Robson on (07) 4160 0735 or Chris Abbott (07) 4160 0733.

Dr Robson will be the guest speaker at Burdekin Productivity Services (BPS) AGM on 16 August at Delta Cinemas, 7.30pm start.

BPS provides agricultural services and technical advice to growers in the Burdekin cane-growing, in order to maximise farm productivity, profitability and sustainability.





Area imaged by the SPOT 5 satellite during the 2010 and 2011 growing seasons.



SRDC promotion of DPI021 involvement in the Herbert Resource Information Centre Spatial Community in Action Conference. Ingham (18-19 August 2011)

Spatial community in action - Grow your business conference - 18th & 19th August 2011



The Herbert Resource Information Centre will host the [Spatial Community in Action: Grow your business](#) conference in Ingham on 18th and 19th August 2011. This conference will look at the use of GIS technology and information management and its role in developing sustainable communities into the future. During the conference, delegates will hear the latest on GIS mapping and agriculture research from industry experts and visit a Project Catalyst trial farm to see technology demonstrations.

Some guest speakers include:
 Andrew Wood - Landscape and soils issues
 Peter McDonnell - Variable rate fertilizer applications
 Trevor Parker - Salinity mapping

- Mario Torrisi (BoM) - Weather and climate forecasting
- Solinftec Pacific Pty Ltd - Use of GIS in Brazil - JetPatcher
- Yvette Everingham (JCU) - Long term climate forecasting
- Andrew Robson - Satellite Imagery in the sugar, cotton and pulse industries
- Ross Coventry - Soil Mapping: how does the industry use the info?
- Mark Poggio - FarmWorks management and financial accounting
- Lachlan Thomson - Townsville Port Authority: Sugar export
- Lawrence Di Bella - Future of spatial applications in agriculture

Venue: Conference Centre, MacRossan St, Ingham QLD
 Date: 18th and 19th August 2011

Cost: \$100 for conference plus \$60 for dinner at Kupmurri at Mungalla Station

Register: Contact Rod Nielson at the HRIC for [registration](#) details and payment methods. Phone: 07 4776 4779 or email: RNielson@hinchinbrook.qld.gov.au view full [conference program](#) or read [event flyer](#)

[Back to top](#)

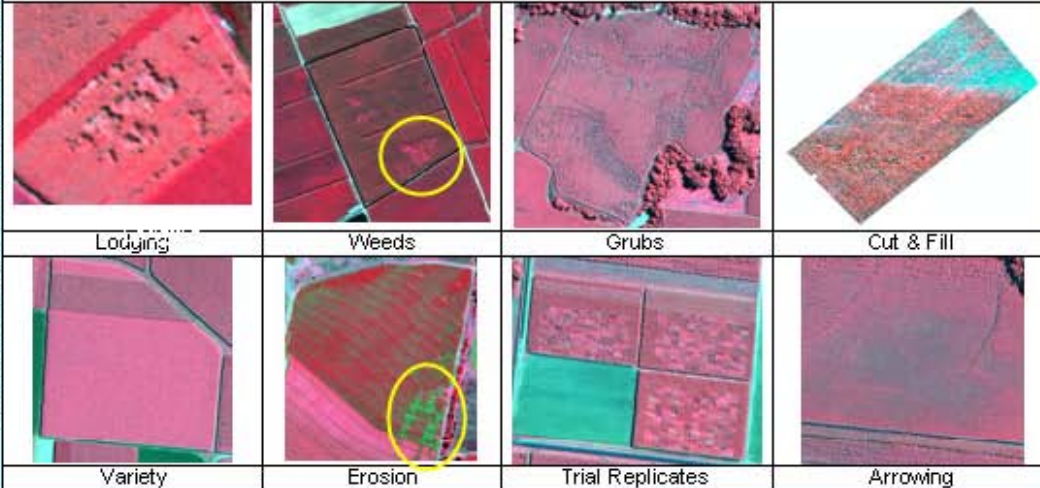
Hand out for BSES cane talks

Department of Employment, Economic Development and Innovation

Developing Remote Sensing Applications in Cane

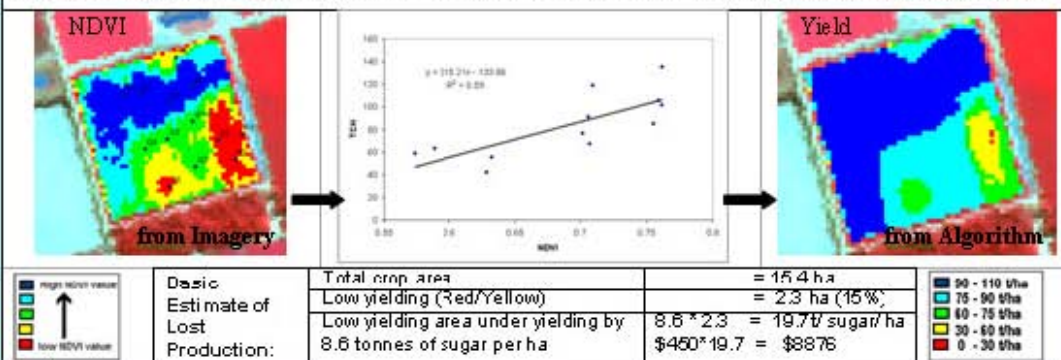
Department of Employment, Economic Development and Innovation; Kingaroy Queensland

What can be identified from remotely sensed Imagery:

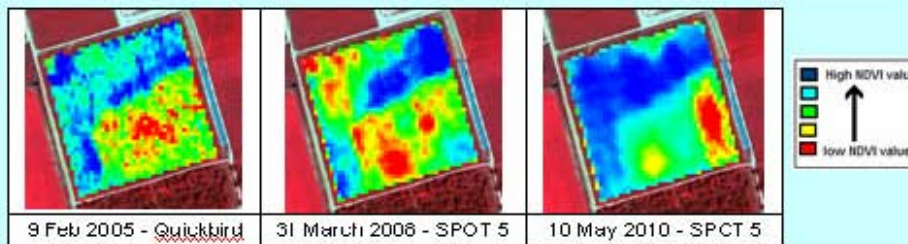


Predicting Yield:

Field sampling in high & low vigour areas allowed a predictive yield algorithm to estimate yield across a block.



Recurring spatial patterns over time: Inherent block features can create similar high and low vigour patterns every year. By identifying these patterns, low vigour areas can be targeted for remedial action. The estimate of lost production enables a cost-benefit assessment of remedial action.



Department of Employment Economic Development and Innovation		
Dr Andrew Robson	andrew.robson@deedi.qld.gov.au	+61 7 41600735
Chris Abbott	chris.abbott@deedi.qld.gov.au	+61 7 41600733



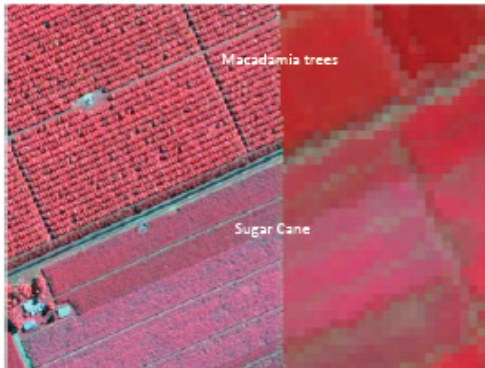
The SRDC sugar cane project (DPI021) featured in a Department of Innovation, Industry, Science, and Research (DIISR): Space Policy Unit (SPU) handout promoting Earth Observation R&D being conducted in Australia ([click icon- !\[\]\(92cb3c8a4d3e1523fd158b46a2e3f73e_img.jpg\)](#)).

How Much Sugar?

Sugar is the second largest export crop in Australia. Over five million tonnes of raw sugar are produced per year, with an economic value of around \$2 billion. The vast majority of Australia's sugar is grown in Queensland, where 20% of the total crop area—500,000 ha—is devoted to sugar cane.

To optimise the management of sugar cane crops, high resolution satellite imagery is being used to monitor crop area, growth, and health. Current research is identifying the most appropriate imagery and analyses to characterise mid-season variability within sugar cane crops, in terms of:

- Image scale, frequency and cost;
- Optimal timing for image acquisition;
- Reliability of analyses;
- Efficient processing and distribution; and
- Costs and benefits to industry.



High resolution satellite imagery is available with spatial resolutions from 0.5 m to 10m. The false colour composite image above shows IKONOS data (0.8 m resolution—left) compared with SPOT imagery (10 m resolution—right)

An accurate in-season prediction of yield is of vital importance to the Australian sugar cane industry. At a regional level, such forecasts are essential for optimising harvesting, milling, marketing and forward selling of produce. At a paddock scale, yield forecasts provide growers with an understanding of both in-crop variability and total production. By using GIS framework to extract image data from all crops within a growing region, correlations between image-based greenness maps and actual yield have been established. This correlation has been used to effectively predict regional yield as well as generate

Further information is available from:
andrew.robson@deedi.qld.gov.au

Research Partners:
DEEDI (Queensland), UNE, CSIRO
Industry Partners (BSES, Bullseye Farming, Bundaberg Sugar, ISIS Mill, Herbert Cane Productivity Services Ltd, Herbert Resource Information Centre, Burdeking Productivity Services, Mackay Sugar)

Research Grants:
Sugar Research and Development Corporation (SRDC FPP818)
CSIRO (CSEO22 project)

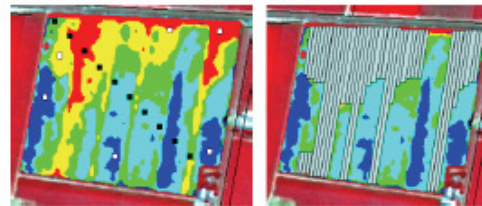
Additional Information:
<http://www.hric.org.au/home/OnlineMapping.aspx>



Variability in cane crops can occur for many reasons, including soil nutrition, plant and soil pests and diseases, irrigation deficiencies, erosion and weed infestation. By using high resolution satellite imagery to monitor crop variability during the growing season, the exact location and extent of a



As well as allowing production to be maximised, detailed information about crop growth enables prudent use of water, fertilisers and agricultural chemicals. Monitoring crop variability over several growing seasons allows growers to better understand the inherent variability within blocks, and concentrate intensive analyses, such as soil sampling, in identified problem areas.



Traditional soil sampling (black dots) did not identify soil nutrient constraints, while strategic sampling based on image greenness maps (white dots) identified calcium deficiency in low vigour areas (shown as red/yellow). Targeted application of lime and dolomite (above right) only required one third the volume and reduced fertiliser costs by more than \$200/ha.

Earth Observation Data Sources

Satellite	Sensor	Supplier	Country
IKONOS	IKONOS	GeoEYE	USA
GeoEYE-1	GeoEYE-1	GeoEYE	USA
QuickBird	BGIS 2000	DigitalGlobe	USA
WorldView-2	WorldView-2	DigitalGlobe	USA
SPOT 5	HRG	Astrium	France

What's new

Cane monitoring made easy with new sensor

In what is a world first, the University of New England (UNE)'s Precision Agriculture Research Group has completed its initial trials of a new type of crop sensor dubbed the "Raptor".

Attached underneath a low-flying aircraft (see below), the Raptor enables rapid scanning of crop biomass over entire paddocks.

The sensor works by directing rapid pulses of red and near-infrared light onto the crop plants and measuring the light reflected back to the aircraft.

"The relative reflectance of plants in these two wavelengths is an excellent indicator of plant vigour – be it in terms of actual biomass, or water or nutrient status," said the project leader, Professor David Lamb.

Developed by Kyle Holland of Holland Scientific based in Nebraska in the United States, the sensor is the culmination of extensive testing involving a prototype sensor that was flown in 2009 by the Armidale-based company Superair.

"At that time we had only enough optical power to fly the sensor at four metres above the crop canopy – something the pilots really enjoyed, but not really the safest option," Professor Lamb said.



Professor David Lamb (right) and UNE Technical Officer Derek Schneider with the Raptor crop sensor attached to the bottom of the Superair fertiliser plane used to test the system.

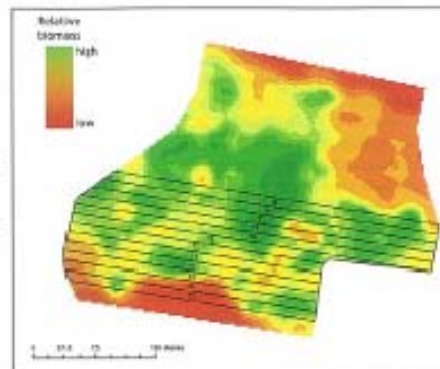
"It was also limited to level fields."

The Raptor involves more powerful optics and extra-sensitive detection electronics, and can be operated at heights of 50 metres or more above the crop. This allows deployment over hilly country.

Funded by the Cooperative Research Centre for Spatial Information (CRCSI) as part of its 'Biomass Business' project, the Raptor system was developed to address key limitations in the traditional methods of using satellite or aerial imagery to map crop vigour; the biggest of these being the difficulty in getting imagery when you actually need it.

The sensor can be easily retro-fitted to any standard crop duster or agricultural spray plane, so that crop scans can be carried out when spraying or fertiliser applications are being done.

"But by far the biggest advantage is its flexibility in the collection of data," Professor Lamb said. "As it uses its own light sources, the Raptor system is able



The sugar biomass map was produced by the Raptor system on a plane flying 50 metres above the ground.

to capture data under cloud and even at night. Conventional aerial or satellite imagery can only be obtained on clear days, and this can be a real problem during peak cane growing seasons."

Following a recent successful trial over wheat in NW NSW, the UNE team recently conducted a test flight over sugarcane near Maclean in north east New South Wales.

"Our aim was to test whether the sensor could cope with the large biomass levels we see in cane fields – especially mature ones," said Professor Lamb.

Bob Aitken, Senior Extension Officer for BSES Limited coordinated three fields to test the system over and the UNE team were encouraged by the results.

The Raptor Sensor detected plenty of spatial variability in the fields and the data is being verified by some follow up ground truthing.

Moreover, the UNE team also ordered a satellite image of the same fields (on a clear day) to check the results are consistent. All being well with this initial data, the Raptor Sensor will be involved in Joint Department of Employment, Economic Development and Innovation (DEEDI)/CSIRO trials, funded by the Sugar Research and Development Corporation, in the Bundaberg region early next year. ▶

SRDC Webinar conducted 22 February 2013.

<http://www.vision6.com.au/ch/31388/1qn8f/1877656/1ca609hx9.wmv>



Australian Government
Sugar Research and Development Corporation

SRDC Webinar

Making sense of remote sensing-based precision agriculture

Presented by

Dr Andrew Robson, Senior Agricultural Remote Sensing Officer,
QLD Department of Agriculture, Fisheries and Forestry



Dr Andrew Robson and Chris Abbott at the Queensland Department of Agriculture, Fisheries and Forestry, have recently completed an SRDC funded research project aimed at increasing adoption of remote sensing across the sugarcane industry. This project was in partnership with the University of New England and CSIRO, and involved the invaluable input from a wide range of industry collaborators.

The project, *'Remote sensing-based precision agriculture tools for the sugar industry'* investigated the use of remotely sensed imagery to assist in managing yield variability, make yield predictions at regional and field scales, deliver protocols for rapid distribution of technology, and provide guidance to industry on the benefits and then adoption of remote sensing technologies.

The industry response to this research has been very encouraging, with the majority of Australian growing regions becoming actively involved, providing full GIS data layers to assist in the development of the applications.

The remote sensing team in collaboration with BSES are also developing remote sensing applications for the detection of cane grubs and will begin a new SRDC funded project entitled *'Developing remote sensing as an industry wide yield forecasting, nitrogen mapping and research aide'* (DPI025) later this year.

Dr Andrew Robson has been involved in agricultural research since 1996, concentrating for the last 10 years on developing spatial applications across a number of cropping systems. He will be presenting an update on his current project, and insight into the benefits and methodologies of remote sensing for the Australian Sugar cane industry.

For those people who are not available to join the webinar, a recording of Dr Andrew Robson's presentation will be available from SRDC's website within 48 hours of the webinar.

INVITATION

SRDC WEBINAR

Friday 22 February 2013

11pm – 12:00 noon
(QLD time)

Contact: Carolyn Martin
Ph: (07) 3210 0495
cmartin@srdc.gov.au

WEBINAR INSTRUCTIONS FOR PARTICIPANTS

1. To register for the next SRDC webinar, register via the Redback conference invitation page:
<http://www.vision6.com.au/em/forms/subscribe.php?db=404014&s=116004&a=31388&k=dc9613>
2. Complete the registration form by entering your name, phone and email address.
3. You will then receive an email confirming your registration and instructions on how to join the presentation by phone and a website link.

If you have any questions about the SRDC webinar please contact SRDC Communications Manager, Carolyn Martin on phone: 07 3210 0495 or mobile: 0439 399 886 or email cmartin@srdc.gov.au

Investing in sugar research innovation

www.srdc.gov.au

12. Appendix 3: Project Contracts and variations

 Australian Government Sugar Research and Development Corporation	SRDC FUNDING APPLICATION 2008		
	<i>Version 20050317 PMS4</i>		
	Research Project Proposal Form		
Enter responses in white cells.			
Your Internal Project ID			
Important: consult the "Project Application Kit" document provided with this Form			
-			
Title of Project	Remote Sensing- based Precision Agriculture Tools for the Sugar Industry		
Start Date	1/07/2009	All dates to be 1st of month. This date copied to be first Milestone date.	
End Date	1/08/2012	All dates to be 1st of month. This date copied to be final Milestone date.	
	SRPN	Surname, Initial	email
Research Contact	126438	Robson, AJ	andrew.robson@dpi.qld.gov.au
Administrative Contact	133242	Kamel, H	helen.kamel@dpi.qld.gov.au
Org. Code		Use the SRDC org code list or leave blank	
Organisation:			
Our Sugar Research Personal Number (SRPN) Contacts database provides all required contact details for Project Investigators. Previous researchers have an SRPN already. If you do not provide your SRPN here your Name and details do not appear on the proposal.			
-			
Use F2 to change Excel into Edit mode prior to paste of prepared paragraph(s) from a Word document. Use Alt/Enter to insert new/blank lines. Use Alt/Enter then an asterisk for text only dot points. N.B. Bullet points from MS Word will convert to small dots in Excel and these are OK in our database.			
OBJECTIVES			
What does the research seek to achieve? [150 words maximum]			

The project will produce practical and relevant benchmarks, protocols and recommendations for the adoption of remote sensing technologies for improved in season management and therefore production within the Australian sugar cane industry. This will be achieved through:

- * benchmarking and identifying the most feasible and suitable commercial imagery (i.e. spatial resolution, repeat time and economic feasibility) for identifying crop variability and thus directing targeted mid-season management within the Australian cane industry.

- * Also the optimum time of image capture that will accurately depict mid- season crop variability whilst avoiding seasonal times most prone to cloud cover, across key Australian cane farming regions.

- *Assess the utility of this imagery for explaining the yield variability measured through the CSE022 project.

- *Implement optimal image processing and delivery protocols for the rapid distribution of classified imagery to agronomists, growers etc.

- *Provide recommendations to participating growers, consultants and industry representatives on the potential cost / benefit of implementing RS technologies into current agronomic management practices.

RESEARCH CLASSIFICATION

Specify the SRDC Investment Horizon code for the project application. The three SRDC Investment Horizons are defined on page 20 of the SRDC R&D Plan 2007-2012.

Investment Horizon	1	Shorter term delivery of benefits through implementation underpinned by integration of existing technologies
	Horizon	Horizon Description
	1	Shorter term delivery of benefits through implementation underpinned by integration of existing technologies
	2	Medium term delivery of benefits through implementation underpinned by emerging technologies
	3	Longer term delivery of benefits through strategic research

Specify the SRDC Investment Arena for the project application. The three SRDC Investment Arenas are defined in pages 15-17 of the SRDC R&D Plan 2007-2012.

Program	B	Regional Futures
	Code	Program Title
	A	Not used
	B	Regional Futures
	C	Emerging Technologies
	D	People Development

Invalid response - must be one of Programs listed

Specify the Theme code for the project application. There are 7 Themes within the Investment Arenas outlined on page 22 of the SRDC R&D Plan 2007-2012.

Strategy	B2	Farming and Harvesting Systems	
Program	Strategy	Code	Program Strategy Description
A	1	A1	Not used
A	2	A2	Not used
B	1	B1	Value Chain Integration
B	2	B2	Farming and Harvesting Systems
B	3	B3	Transport, Milling and Marketing Systems
C	1	C1	Genetics and Breeding Systems
C	2	C2	Farming, Harvesting, Transport, Milling and Marketing Systems
C	3	C3	Not used
D	1	D1	Individual Capacity
D	2	D2	Social Capacity
D	3	D3	Not used
D	4	D4	Not used
D	5	D5	Not used

R&D Approach (i): Succinctly explain how the project will be conducted to address the issue. Indicate what is innovative and different to previous R&D. [150 words maximum]

*This project will evaluate high resolution satellite imagery as an effective tool for identifying mid-season crop variability and in particular underperforming crop regions, thus aiding in the future implementation of PA through strategies such as targeted soil sampling, targeted agronomy for improved detection of in season constraints and zonal management.

* It will operate in close collaboration with CSE022 with a focus on that project's key sites (Bundaberg, Burdekin, Herbert)

* Imagery will be by acquired from a number of commercial providers (SPOT 5, IKONOS, QuickBird, RapidEye, potentially ALOS and Radar) and used to identify the optimum spatial and spectral resolution, repeat time and capture time to facilitate mid-season management of the cane crop.

* Assess the cost: benefit of using such imagery for improved production.

* Imagery captured during this project will compliment existing RS applications undertaken by relevant industry parties as well as existing imagery data sets.

R&D Approach (ii): Indicate the extent of collaboration and/or partnerships, especially with end users. [100 words maximum]

* CSE022 project team, key stakeholders and collaborating growers/ industry groups.

* linkages with existing projects in the same regions and imagery captured by GRDC/ DAQ 00129 - Improving the integration of legumes in grain and sugar cane farming systems, and ACIAR ASEM/ 2004/041- Peanut project to quantifying the impacts of pulse or legume crops on cane production.

* SRDC/ BPS001- value adding existing data and facilitating the implementation of the technology over larger regions and for a wider spectrum of constraints.

* industry partners (i.e. BSES, Bullseye Farming, Bundaberg Sugar, ISIS Mill, PCA).

* University-based research (Yvette Everingham/ UQ).

END

OUTPUTS AND OUTCOMES

List the Outputs (knowledge, skills, processes, practices, products and technology) that will be derived from this project. [150 words maximum]

Key outputs include:

- * An evaluation of available remote sensing technologies including the identification of optimal imagery acquisition time, resolution, cost, etc. will be conducted.
- * Classified satellite images depicting in season crop variability for each study site.
- * Further development of RS technologies for a broader range of applications so as to maximise useability.
- * Streamlined, accurate and reproducible image processing techniques identified
- * Existing imagery data sets incorporated with high resolution captures to increase the usability of imagery.
- * Cost/ benefit analysis of implementing remote sensing technologies into existing agronomic practices. This includes the interpretation of images against measured field parameters useful for management changes and yield variability.
- * Improved delivery of remotely sensed imagery to growers/ agronomists (via internet, e-mail) to increase adoption.
- * Results widely communicated to industry via field days (at least 1 p.a.), ASSCT conferences (at least 2 publications), publication of results at international conferences (at least 1 publication will be submitted).

List the Outcomes (impacts that benefit the industry and community) that will be derived from this project and estimate the extent (including an estimate of \$ value) of economic, environmental and social benefits. [150 words maximum]

Outcomes generated from this project will increase the capacity and knowledge of Australian cane growers/ consultants / companies (ISIS Mill, BSES, Bundy Sugar, Bullseye Farming, and Mackay Sugar) within three cane growing regions in the use of remote sensing technologies for:

- * Identifying mid season crop variability, particularly underperforming regions.
- * The location and extent of a growth constraint (including irrigation, drainage, disease, and pest) that can then be quantified in terms of yield deficit.
- * Strategic soil sampling locations that correspond with high and low crop growth regions, offering significant reduction in soil mapping ie, quantity, collection and analysis costs, to that of current costs of \$340/ ha for 100ha (Coventry et al (2009).
- * Climatic/seasonal impacts on spatial variability of crop performance, allowing for improved long term management strategies.
- * Impact of legume rotations (crop vigour response and disease/ pest suppression).
- * The resulting improvement in agronomic management will generate both cost and environmental benefits by allowing zonal management, including a more coordinated and efficient use inputs (a recent ex

BENEFITS

Indicate social, environmental and economic dimensions of expected outcomes of the project. Percent

Social Human capacity and capability building (change, learning, innovation etc), occupational health and safety, partnerships with rural and regional communities	10%
Environmental Mitigation of climate change, water quality, water use efficiency, environmental flows, salinity, soil health, sediment losses, biodiversity, air quality, sustainable natural resource management	35%
Economic Profitability, quality and product differentiation, capital utilisation, unit costs of production	55%

The light yellow cell will automatically recalculate so that all three values add to 100%

RISK ASSESSMENT

Indicate the nature and magnitude of the risk factors associated with conducting the project and delivering the target outcomes, including, but not necessarily limited to, Research Risk and the risk of causing environmental harm. [150 words maximum].

Cloud cover preventing the successful capture of remotely sensed imagery is a major risk to the success of this project and as such a number of steps will be taken to ensure results. These are further explained in the accompanying attachment 'Addressing the issues raised by the SRDC project review panel regarding RPE818.doc'. The steps are -

- 1) Using multiple sites so if cloud is an issue there is a greater chance that at least one site will yield data.
- 2) Optimizing image capture timing to avoid times most prone to cloud cover will be investigated.
- 3) Undertaking some desktop analysis, including inherent variability within cane crops etc, from imagery already acquired by QDPI&F (2007/08) and from the BPS 001 project, if continued cloud cover persists. These analyses can be undertaken to coincide with yield data collected by the CSE 022 project.
- 4) QDPI&Fs aerial multispectral imaging system can be deployed across trial locations if required.
- 5) Investigating additional technologies such as Radar (assisted by UQ) that can look through cloud.also active sensors such as Greenseeker.

Please note that the paragraphs below do not refer to Risk Assessment issues.

Accompanying Drawings

Figure(s), drawings, flow diagrams or other graphical supplement. (Optional)

Optional self contained drawings of up to two A4 pages may be supplied as an electronic Acrobat Reader (.pdf) file only. This may be generated by any means available.

For auditing purposes during the printing and evaluation of submission proposals please enter the number of pages (1 or 2) and filename you have chosen for the .pdf file in the cell below.

Pages
(1 or 2)

Filename

RESEARCHERS

Our Sugar Research Personal Number (SRPN) data base provides all required contact details for Project Investigators. Previous researchers have an SRPN already. If you do not enter the SRPN in this form your Name and details will not appear on the proposal. Do not enter Support Staff on this sheet. Include total of Support Staff salaries on the next sheet in row 22.

Please choose one of the Chief Investigators to be designated as the Research Contact and enter details on Title sheet row 12. The same data will be copied below into row 21. The Research Contact will be listed in all SRDC publications, and will be contacted by SRDC in all communications.

Please enter the annual salary including on costs and average percentage of time to be applied to this project in each year. Percentage time refers to this project only.

ALL DOLLAR values on all budget sheets to be expressed in 2009 values.

An inbuilt inflation factor of **3%** will be applied to data in following years.

Annual Salary to be expressed in **2009 values**

Financial years are designated by the year in which July 1 falls.

Investigators	SRPN	Surname, Initial	Annual Salary including on-costs	SRDC Org. Code	2009		2010		2011		2012		2013		2014		Surname, Initial	#
					% time funded by SRDC project	% time funded in kind by host	% time funded by SRDC project	% time funded in kind by host	% time funded by SRDC project	% time funded in kind by host	% time funded by SRDC project	% time funded in kind by host	% time funded by SRDC project	% time funded in kind by host				
Research Contact					0%	0%	0%	0%	0%	0%	0%	0%	0%	0%	0%	0%		
Chief Investigator 1	126438	Robson, AJ	\$93,465.78		0%	30%	0%	30%	0%	30%	0%	0%	0%	0%	0%	0%	Robson, AJ	1
Chief Investigator 2	137113	Lamb, D	\$162,000		5%	5%	5%	5%	5%	5%	5%	5%	5%	5%	5%	5%	Lamb, D	2
Chief Inv. 3	132127	Bramley, R	\$158,000		0%	0%	0%	0%	0%	0%	0%	0%	0%	0%	0%	0%	Bramley, R	3
Investigator 4	0	PO2(4) TBA	\$70,021		70%	30%	70%	30%	70%	30%	70%	30%	70%	30%	70%	30%	PO2(4) TBA	4
Investigator 5	0				0%	0%	0%	0%	0%	0%	0%	0%	0%	0%	0%	0%		5
Investigator 6	0				0%	0%	0%	0%	0%	0%	0%	0%	0%	0%	0%	0%		6
Investigator 7	0				0%	0%	0%	0%	0%	0%	0%	0%	0%	0%	0%	0%		7
Investigator 8	0				0%	0%	0%	0%	0%	0%	0%	0%	0%	0%	0%	0%		8
Investigator 9	0				0%	0%	0%	0%	0%	0%	0%	0%	0%	0%	0%	0%		9
Investigator 10	0				0%	0%	0%	0%	0%	0%	0%	0%	0%	0%	0%	0%		10
Investigator 11	0				0%	0%	0%	0%	0%	0%	0%	0%	0%	0%	0%	0%		11
Investigator 12	0				0%	0%	0%	0%	0%	0%	0%	0%	0%	0%	0%	0%		12
Investigator 13	0				0%	0%	0%	0%	0%	0%	0%	0%	0%	0%	0%	0%		13
Investigator 14	0				0%	0%	0%	0%	0%	0%	0%	0%	0%	0%	0%	0%		14
Investigator 15	0				0%	0%	0%	0%	0%	0%	0%	0%	0%	0%	0%	0%		15
Investigator 16	0				0%	0%	0%	0%	0%	0%	0%	0%	0%	0%	0%	0%		16
Investigator 17	0				0%	0%	0%	0%	0%	0%	0%	0%	0%	0%	0%	0%		17
Investigator 18	0				0%	0%	0%	0%	0%	0%	0%	0%	0%	0%	0%	0%		18
Investigator 19	0				0%	0%	0%	0%	0%	0%	0%	0%	0%	0%	0%	0%		19
Investigator 20	0				0%	0%	0%	0%	0%	0%	0%	0%	0%	0%	0%	0%		20

END

Chief Investigators:

One Chief Investigator is normally designated from each organisation involved in a project.

If more than 3 Chief Investigators, change relevant "Investigator Y" to "Chief Investigator Y". Except for the Research Contact who must be in the first position any position can be changed to "Chief"

The uploading software is merely checking for the word Chief in first 5 characters of A column cells in order to set a database flag indicating a particular person is a Chief Investigator. Thus apart from number 1 the order will not matter. What is the difference between Chief and non Chief? The Chief Investigators are all listed in the submission papers sent to the board (and in the agreement if funded) complete with contact details of Postal address, phone number, fax number and email address. The other investigators are merely listed by Name, Position, Organisation and City. In all cases the contact details are taken from the SRPN contacts database not from this spreadsheet - missing SRPN means missing contact details. For a Full Project Proposal (PPP) ALL SRPN fields must be valid.

Cells below this line are only intermediate calculations - they are excluded from the print range. They must NOT be tampered with or the budget calculations will break.

CALCULATION OF SALARY TO BE FUNDED BY SRDC

POSITION	SRPN	Surname, Initial	Annual Salary	2009	2010	2011	2012
Research Contact							
Chief Investigator 1	126438	Robson, AJ	93465.78	\$0	\$0	\$0	\$0
Chief Investigator 2	137113	Lamb, D	162000	\$8,100	\$8,100	\$8,100	\$0
Chief Inv. 3	132127	Bramley, R	158000	\$7,900	\$7,900	\$7,900	\$0
Investigator 4	0	PO2(4) TBA	70021	\$49,015	\$49,015	\$0	\$0
Investigator 5	0		0	\$0	\$0	\$0	\$0
Investigator 6	0		0	\$0	\$0	\$0	\$0
Investigator 7	0		0	\$0	\$0	\$0	\$0
Investigator 8	0		0	\$0	\$0	\$0	\$0
Investigator 9	0		0	\$0	\$0	\$0	\$0
Investigator 10	0		0	\$0	\$0	\$0	\$0
Investigator 11	0		0	\$0	\$0	\$0	\$0
Investigator 12	0		0	\$0	\$0	\$0	\$0
Investigator 13	0		0	\$0	\$0	\$0	\$0
Investigator 14	0		0	\$0	\$0	\$0	\$0
Investigator 15	0		0	\$0	\$0	\$0	\$0
Investigator 16	0		0	\$0	\$0	\$0	\$0
Investigator 17	0		0	\$0	\$0	\$0	\$0
Investigator 18	0		0	\$0	\$0	\$0	\$0
Investigator 19	0		0	\$0	\$0	\$0	\$0
Investigator 20	0		0	\$0	\$0	\$0	\$0
TOTAL SALARIES EACH YEAR				\$65,015	\$65,015	\$65,015	\$0

These results are transferred to the Budget sheet.

CALCULATION OF "IN-KIND" CONTRIBUTIONS BASED ON CONSTANTS

POSITION	SRPN	Surname, Initial	Salary including on-costs	2009	2010	2011	2012
Chief Investigator 1	126438	Robson, AJ	93465.78	\$72,903	\$72,903	\$72,903	\$0
Chief Investigator 2	137113	Lamb, D	162000	\$34,020	\$34,020	\$34,020	\$0
Chief Inv. 3	132127	Bramley, R	158000	\$12,640	\$12,640	\$12,640	\$0
Investigator 4	0	PO2(4) TBA	70021	\$133,040	\$133,040	\$133,040	\$0
Investigator 5	0		0	\$0	\$0	\$0	\$0
Investigator 6	0		0	\$0	\$0	\$0	\$0
Investigator 7	0		0	\$0	\$0	\$0	\$0
Investigator 8	0		0	\$0	\$0	\$0	\$0
Investigator 9	0		0	\$0	\$0	\$0	\$0
Investigator 10	0		0	\$0	\$0	\$0	\$0
Investigator 11	0		0	\$0	\$0	\$0	\$0
Investigator 12	0		0	\$0	\$0	\$0	\$0
Investigator 13	0		0	\$0	\$0	\$0	\$0
Investigator 14	0		0	\$0	\$0	\$0	\$0
Investigator 15	0		0	\$0	\$0	\$0	\$0
Investigator 16	0		0	\$0	\$0	\$0	\$0
Investigator 17	0		0	\$0	\$0	\$0	\$0
Investigator 18	0		0	\$0	\$0	\$0	\$0
Investigator 19	0		0	\$0	\$0	\$0	\$0
Investigator 20	0		0	\$0	\$0	\$0	\$0
TOTAL IN KIND CONTRIBUTION EACH YEAR				\$252,603	\$252,603	\$252,603	\$0

These yearly IN-KIND results are multiplied by inflation factor as they are transferred to the Budget sheet.

BUDGET JUSTIFICATION

Salary

Provide an overview of the role of each researcher and the relevant skills they bring to the project (in dot point form).

Excel cells are limited to 150 words maximum - extra words will not display or print. Maximum 30 words per person and 300 words in total. [If more than 10 investigators use fewer than 30 words per person on average] Put the first 150 words in cell A4, then use cell A5 if needed. SRDC will upload cells A4, A5 to the database using simple concatenation with one blank line between each of the cells.

Dr Andrew Robson has over 7 years experience in the development of practical remote sensing applications for improved in-season management and harvest segregation across a number of cropping systems including peanut, cotton and grains in addition to helping develop improved surveillance techniques for biosecurity risks such as citrus canker and sugar cane smut. In the sugar farming systems Dr Robson recently identified high resolution satellite imagery, captured over 6 intensive cane cropping regions, as an effective tool for guiding targeted soil sampling and strategic agronomy (LWA healthy soils project).

As project leader, Dr Robsons' responsibilities will include the capture and analysis of imagery over a number of key cane growing locations, assisting and training the newly appointed scientist (TBA) in the ground sampling of field trials for imagery validation, building on collaborative linkages with other projects, industry, agronomists, etc and presenting results at appropriate forums and publications. The allocation of 70% FTE for the newly appointed scientist will enable them to:

- Meet with industry representatives from each of the key regions to identify areas of interest for image collection (each
- Create shapefiles for each image area (up to 9 per annum) for ordering.
- Analyse each image on collection, including image georectification, applying a number of vegetation indices, sub- sett
- Identifying improved distribution methods of imagery to project collaborators, including internet.
- Identify strategic locations for ground sampling crops to determine nature of limiting constraints.
- Sample selected crops within each image area (plant, soil, disease etc) for up to 36 crops per annum (3 key regions*
- Process field samples for data collection (i.e. soil drying, grinding, packaging for chemical analysis)
- Data entry and spatial analysis of processed imagery versus field sample data.
- Production of maps, presentations, reporting for work undertaken to be presented at relevant forums.

Dr David Lamb has an extensive record of industry-focussed R&D related to PA, and the development of remote and proximal sensing for the wine, rice, cotton and grain industries.

Rob Bramley has over 12 years experience in PA research in the wine, sugar and grains industries, has given numerous invited presentations on PA at international meetings and leads CSE022.

Drs Bramley and Lamb collaborated closely and successfully on the recent CRC Viticulture vineyard variability project which provided the basis for the profitable adoption of PA in the wine industry.

As part of this project both scientists will be required to provide expertise, advice and consultation on all project activities, including RS analysis and field observations. As project leader of the current CSE022 project, Rob Bramley will have significant input in identifying trial site locations and provision of crop yield data from different zones in monitored fields.

Travel

Explain why the travel is necessary for the project, who is to travel, when or how often, and how the fares and other charges have been costed. [150 words maximum]

Travel costs include:

- * Travel per diems and fares (where appropriate) are required for the ground sampling of field sites in the Burdekin, Bundaberg and Herbert districts from Kingaroy Qld by Dr Robson and an additional project officer (TBA). Sampling trips will coincide with image captures and will cost \$23,000 per year (8K fares and 15K allowance).
- * Vehicle lease costs (\$8000/ pa) represents a 1/2 share of a 4wd dual cab utility necessary to run the field program at the selected localities, particularly within the Bundaberg region.
- * Fares and per diems have been included for travel to and from selected localities (i.e. Bundaberg or Brisbane) for 6 month project meetings with industry representatives by David Lamb (2 trips a year @\$1600/ trip from Armidale NSW) and Rob Bramely (2 trips a year@\$2,500 from Adelaide SA) (note- trip and allowance costs included within 5% salary component for both David and Rob)

Operating

Justify the items and the costings [150 words maximum]

- * RS imagery is the essential data source required for the proposed project.
- * Currently available high resolution multispectral satellite imagery can be obtained at relatively low cost. SPOT 5 images (2.5m spatial resolution) cost 5c/ha for a minimum area of 1800km²; QuickBird images (60cm resolution) cost 43c/ha for a minimum area of 78km²; and IKONOS images (1m resolution) cost 50c/ha for a minimum area of 100km².
- * Through collaborative linkages it is hoped that additional multispectral imagery as well as radar and active sensor data can be obtained and analysed as part of the project.
- * The collection of aerial imagery will incur aircraft hire costs that are currently \$360/hr for a Cessna 187.

BACKGROUND

**Review existing knowledge and linkages to other research, and highlight gaps in knowledge / tools / integration / implementation which provide the rationale for conducting this project. [300 words maximum]
Do NOT repeat information presented in the Issue and R&D Approach sections (Issue sheet).**

Only the first 150 words per cell will display or print. SRDC will concatenate cells A3 and A4. If more than 150 words are required simply move into cell A4 - a paragraph break will be automatically inserted.

SRDC recently committed \$1.5M to a major R&D project aiming to develop and deliver improved precision agriculture (PA) technologies to the sugar industry (CSE022). This did not include remote sensing (RS). While RS technologies are not a new concept in sugar cane, its broad scale adoption and implementation as an efficient agronomic tool has been limited. Multispectral RS work in Brazil and USA has been limited to yield estimation and monitoring, using only low resolution imagery (20- 30m) (Bramley, 2009), whilst South African researchers used low resolution imagery to coordinate plant tissue and soil sampling regimes. Temporal SPOT (10 and 20m) imagery has also been used in the French West Indies to identify seasonal and growth stage trends in cane variability (Begue et al 2008), whilst research in Mauritius has indicated high resolution QuickBird imagery (visible colour bands only) as strong indicators of canopy variability, soil condition and yield (Autrey et al 2006).

Although useful applications these examples are only concentrated on specific parameters restricted by the high spatial resolution of the imagery used, do not use the imagery for identifying in-season and in-crop variability for the purpose of coordinating in-crop agronomic checks to improve in-season management strategies. Through the use of strategic in-field sampling, based on high and low reflective zones, this project offers the opportunity to identify a wider array of specific constraints including cane grubs, weeds, disease 'hot spots' potentially Smut, as well as more regional issues such as soil nutrition and irrigation efficiency. The detection of many of these parameters has never been attempted through remote sensing technologies and therefore the outcomes generated from this project will be unique both domestically and internationally. Further more with the Australian sugar industry being under increasing pressure to improve crop management practices this technology creates the opportunity of implementing variable rate technology and minimise offsite impacts through improved input use efficiencies.

With a number of new satellites being deployed each year (ie. RapidEye, ALOS), global sugar industries do

RESEARCH PLAN

Broadly specify methodology, activities and project management to deliver outputs and outcomes. Key stages and deliverables during the project should be reflected in the Milestone Achievement Criteria. [600 words maximum]

Excel cells are limited to 150 words maximum - extra words will not display or print. Since larger projects will require more than one cell, SRDC will upload cells A3, A4, A5, A6 to the database using simple concatenation with one blank line between the text of each of the cells.

*Research will be undertaken over three intensive cane growing regions (Herbert, Burdekin and Bundaberg) to identify the optimal timing for image acquisition that will maximise the usefulness of imagery for making early or mid-season agronomic decisions, to explore the underlying causes of yield variability, and minimise exposure to seasonal times prone to continued cloud cover.

*The capture of imagery will be attempted over 3 consecutive seasons at a maximum acquisition rate of 3 images per year, per site, to coincide with 3 key phenological stages of cane development. This will be dependant on the persistence of continued cloud cover. In the event that cloud cover does become a major impediment, a number of protocols have been established to ensure results are achieved (as stated in Risk section).

*The optimum imagery (list provided below) for each site will be decided on the total area of cane cropped within each of the three main project areas and the level of cloud risk.

Satellite	Cost per image	minimum area	resolution	repeat time	operating
SPOT 5	\$9600AUS	1800km ²	2.5m	1- 4 days	sampled once a year
QuickBird	\$2200USD	78km ²	0.6m	1- 3.5 days	sampled after each image
IKONOS	\$3420USD	100km ²	0.8m	1- 3 days	sampled after each image
Rapid Eye	\$13500AUS	5000km ²	5.0m	2 per day	sampled once a year
ALOS	\$3300AUS	900km ²	2.5m	when available	sampled after each image

*Imagery obtained from the majority of commercially available satellite will be evaluated with the high resolution QuickBird (0.6m) or IKONOS (1m) satellites predominantly used with an additional SPOT 5 and RapidEye image captured to compare data quality, usefulness (i.e. spectral and spatial resolution), repeat capture time and cost. Imagery from the ALOS satellite will also be investigated if available.

*It is proposed that the larger coverage, more expensive options be attempted at least once over the larger area

*Radar and airborne multispectral imagery will be acquired in the event of continued cloud cover, with the lat

*Historical imagery will be sourced from QDPI&F and NRW databases, relevant industry participants (i.e. mills) and current projects such as BSP 001, allowing for more intensive analysis to be undertaken on identifying inherent spatial variability occurring across ratoons and in rotation crops.

*Multispectral imagery will be processed using existing software (ENVI, Imagine) with proven vegetation indices such as normalised vegetation difference index (NDVI), nitrogen reflectance index (NRI) and photochemical reflectance index (PRI) and accepted methods of classification (i.e. supervised and unsupervised).

*Classified images of trial sites depicting crop variability will enable direct agronomic assessment and sample collection to be made to quantify variability in useable terms (i.e. crop condition, yield variability, pest and disease incidence, soil health).

*Integration of on-ground PA data including yield (CSE022) with processed RS imagery will facilitate predictions of crop and yield variability, assist in understanding causal factors behind yield performance, enable the extent of lost production to be quantified and allow an economic assessment of lost production from under performing regions to be made

*Cost: benefit analyses regarding both the application of remedial action (zonal management to improve underperforming regions) as well as the adoption of RS technology will be made.

*Improved delivery of imagery (i.e. internet, e-mail) will also be investigated to ensure useable data is delivered to project participants in a timely manner, demonstrating possibilities for future adoption.

*Industry recommendations will be delivered via workshops, key industry engagements, technical reference groups, project reports and additional publications.

Communication and Implementation Strategies

Indicate plans for communication and implementation of project outputs both during and after the project. [Maximum 150 words].

This project will address industry demand for further validation, application development and education of remote sensing technologies as well as to offer value adding information the current yield mapping project (CSE 022). As such the active involvement and direction from industry representatives, consultants and growers at each of the project locations (Burdekin, Herbert and Bundaberg) is encouraged and will provide the main on-ground conduit of project communication.

On a broader scale the results will also be reported through industry gatherings such as field days, conferences and relevant media including ASSCT and industry wide publications such as canegrowers, as well as through communication activities stated in the CSE 022 communication plan.

For the continued implementation of RS technologies following the projects completion it would be considered necessary to include some commercial providers of RS into the final year of the project.

EVALUATION

Baseline Evaluation: Document the baseline by which the outputs and outcomes of this project can be evaluated. [150 words maximum]

Baseline

A baseline evaluation for the proposed project will involve an estimation of the Australian cane industries current awareness of available remote sensing technologies, including actual adoption levels, current skills base in ordering and analysing imagery and general interest via results presented in the recent CSE 018 project as well as additional questioning of growers and other stakeholders within the first year of the project.

The current use of the technology will be assessed to determine its current benefit and problems. This will include collection of current images and understanding the current use of these technologies in the sugar industry.

**Performance Evaluation:
Specify method(s) to evaluate performance in delivery of outputs and outcomes.
[150 words maximum]**

Performance in this project will be determined by its effectiveness to address project goals and milestones, and more specifically:

- * A measured increase via survey, in industry awareness of commercially available RS technologies, including knowledge of optimal platforms and capture times that maximise useability and probability of data collection.
- * A firm understanding of potential applications and cost- benefit of adopting RS technologies into existing farming management practices.
- * Ability for the Australian cane industry to 'stand alone' in the implementation of RS technologies following the completion of the project, via education and training of relevant industry parties where required and/or through the establishment of linkages with existing commercial providers of RS imagery.
- * Develop protocols to ensure the best use of RS technologies in the management of yield variability and for improving in season management practices. This will be achieved by identifying optimal technologies, image analysis methodologies, and predictive accuracy.
- * Increased adoption of RS technologies both within study sites and those external to the project, assessed

MILESTONES

Specify significant, measurable events (outputs) at approximately 6 monthly intervals. Use dot point format. All dates to be first of the month. (Excel accepts mm/yyyy).

Use Milestone #12 as the Final Report Milestone. The amount should be 20% of the final full year of the project.

MS #	Date	\$	Title	Achievement Criteria
1	1/7/2009	\$0	Signing of Agreement	All parties to have signed project agreement and agreed to milestones and achievement criteria
2	1/10/2009	\$45,000	Group Liaison	<ul style="list-style-type: none"> - Reporting arrangements with SRDC agreed and documented. - Initial project group meeting conducted and research plan agreed by the participants. - Industry representatives and consultants identified and consulted. - Imaging program for year 1 agreed and documented. - Selection of target sites and sampling protocols established - Project Officer 2, entry level scientist appointed - Base line information collected from all three sites. - Parameters and KPIS identified to assess implications on management practices.
3	1/03/2010	\$86,516	First imaging/ground sampling	<ul style="list-style-type: none"> - Window opens for continued imaging attempts over key sites (CSE 022), with emphasis on key phenological periods i.e. early to mid January (early closure) to a maximum of 3 images per site. - First set of Images collected from all three sites (max. 3 images per site) using both high and low resolution imagery. - Ground sampling of key CSE 022 sites as well as those identified by industry to be 'of interest in regards to abiotic or biotic stresses' undertaken with results compared with corresponding processed imagery. - Interpretation of imagery collected against field parameters (soil and plant) from crops of interest as specified by industry representatives (established for
4	1/10/2010	\$45,000	Review of results	<ul style="list-style-type: none"> - First annual meeting (notes provided) and recommendations made for improvement of the research approach used. - Report on ability to conduct imagery at each site including issues affecting the experiments and potential changes. - Recommendations on remedial action to improve underperforming crops (i.e. test strips) to be monitored in the second season of imagery. - Imaging and sampling program for year 2 agreed and documented. - Reporting of results at relevant forums including a component of field days at each region, grower liaisons, and promotional material published in industry wide publications.
5	1/03/2011	\$89,461	second imaging/ground sampling	<ul style="list-style-type: none"> - ASSCT papers submitted and accepted. - Second set of images collected from all three sites (max. 3 images per site) with attempts over key sites (CSE 022), with emphasis on key phenological periods i.e. early to mid January (early closure) to a maximum of 3 images per site. - Ground sampling of key CSE 022 sites as well as those identified by industry to be 'of interest in regards to abiotic or biotic stresses' undertaken with results compared with corresponding processed imagery. - Interpretation of imagery collected against field parameters (soil and plant) from crops of interest as specified by industry representatives (established for
6	1/10/2011	\$32,095	Review of results	<ul style="list-style-type: none"> - Initial assessment of year 2 imagery and its integration with other spatial data collected in CSE022. - Second annual meeting held (notes provided) and recommendations made for improvement of the research approach used. - Discussion on the inclusion of commercial imagery providers to be involved in the last year of the project so as to offer RS support following completion of the project. - Imaging and sampling program for year 3 agreed and documented. - Recommendations on remedial action to improve underperforming crops (i.e. test strips) to be monitored in the second season of imagery.
7	1/04/2012	\$69,704	third imaging/ground sampling	<ul style="list-style-type: none"> - ASSCT papers submitted and accepted. Submission of paper to international journal. - Window for continued imaging attempts over key sites (CSE 022), with emphasis on key phenological periods i.e. early to mid January (early closure) to a maximum of 3 images per site. - Ground sampling of key CSE 022 sites compared with imagery, as well as to quantify different management practices applied after the second years imagery. - Final assessment of all data collected, including cost/ benefit analysis. - Final review meeting conducted and notes provided.
12	1/8/2012	\$27,905	Final Report	Submission of final report. Final report accepted by SRDC.
END		\$395,681	TOTAL DOLLARS	

Less than 12 milestones : simply leave cells in columns B-E blank in all unwanted rows.

Cell C17 above (Total all Milestones) should equal the relevant figure below taken from the Budget sheet.

Check MS total =	\$395,681	Total Milestone payments (in row 17 above) if cash funds from others (Budget sheet row 22) are provided through SRDC.
Check MS total =	\$395,681	Total Milestone payments (in row 17 above) if cash funds from others (Budget sheet row 22) are provided directly to your organisation.



Australian Government
Sugar Research and Development Corporation

Telephone: 07 3210 0495 Web: www.srdc.gov.au Email: srdc@srdc.gov.au
Facsimile: 07 3210 0506 PO Box 12050, Brisbane George Street Q 4003, Australia

ABN 41 343 997 980

28 June 2012

Ms Helen Kamel
DAFFQ
PO Box 102
TOOWOOMBA QLD 4350

Dear Helen,

Project: DPI021 - Remote sensing-based Precision Agriculture tools for the sugar industry

SRDC agrees to the variation of the above project described below, as requested by or arranged with the Chief Investigators. A copy of the revised list of milestones is also attached.

Would you please arrange for the appropriate person in each Research Organisation (if more than one) to sign all pages of the attached duplicate(s) of this letter and attachments, as acknowledgment of the changes, and return one copy to SRDC.

Could you please forward a copy to the Chief Investigator(s).

Variation

M8 Milestone 8

- Biometric analysis of data to improve yield prediction algorithms particularly within the Burdekin and Herbert growing regions. This would also allow an accuracy of prediction to be calculated for each block within all three locations and across multiple years;
- Provide additional time to interact and train potential end users of the technology, such as mills and productivity services thus supporting future adoption.
- Ability to run initial investigations on additional mill areas that have shown an interest to be involved such as Isis and Mulgrave central.
- Assess the commercial costs and acquisition benefits of using an airborne multispectral camera (DuncanTech) instead of satellite imagery.

Delay due date from 1/6/2012 to 1/8/2012

Yours sincerely,


for Annette Sugden
Executive Director

Investing in Sugarcane Industry Innovation

			<p>to be 'of interest in regards to abiotic or biotic stresses' undertaken with results compared with corresponding processed imagery.</p> <ul style="list-style-type: none"> - Interpretation of imagery collected against field parameters (soil and plant) from crops of interest as specified by industry representatives (established for management practices). - Report on ability to conduct imagery at each site including issues affecting the experiments and potential changes - Report on the use on Airborne system.
1/10/2011	6.1	\$40,202	<p>Review of results</p> <p>Achievement Criteria:</p> <ul style="list-style-type: none"> - Initial assessment of year 2 imagery and its integration with other spatial data collected in CSE022. - Second annual meeting held (notes provided) and recommendations made for improvement of the research approach used. - Discussion on the inclusion of commercial imagery providers to be involved in the last year of the project so as to offer RS support following completion of the project. - Imaging and sampling program for year 3 agreed and documented. - Recommendations on remedial action to improve underperforming crops (i.e. test strips) to be monitored in the second season of imagery. - Reporting of results at relevant forums including field days at each region, grower liasons, and promotional material published in industry wide publications. -Draft protocols in use of the technology including one training session for interested representatives from the three key regions in the use of technology including training in image analysis software. Evaluation of the increased capacity of participants at training session documented - Assessment of airborne system in assessing the optimum capture timing and its correlation to yield
1/04/2012	7	\$69,704	<p>third imaging/ ground sampling</p> <p>Achievement Criteria:</p> <ul style="list-style-type: none"> - ASSCT papers submitted and accepted. Submission of paper to international journal. - Window for continued imaging attempts over key sites (CSE 022), with emphasis on key phenological periods i.e. early to mid January (early closure) to a maximum of 3 images per site. - Ground sampling of key CSE 022 sites compared with imagery, as well as to quantify different management practices applied after the second years imagery. - Final assessment of all data collected, including cost/ benefit analysis. - Final review meeting conducted and notes provided. - Reporting of results at relevant forums including field days, grower liasons and promotional material published in industry wide publications.
1/08/2012	8.2	\$30,000	<p>Milestone 8</p> <p>Achievement Criteria:</p> <ul style="list-style-type: none"> * Biometric analysis of data to improve yield prediction algorithms particularly within the Burdekin and Herbert growing regions. This would also allow an accuracy of prediction to be calculated for each block within all three locations and across multiple years; * Provide additional time to interact and train potential end users of the technology, such as mills and productivity services thus supporting future adoption. * Ability to run initial investigations on additional mill areas that have shown an interest to be involved such as Isis and Mulgrave central. * Assess the commercial costs and acquisition benefits of using an airborne multispectral camera (DuncanTech) instead of satellite imagery.
1/12/2012	9.1	\$27,905	<p>Final Report</p> <p>Achievement Criteria:</p> <ul style="list-style-type: none"> Submission of final report. Final report accepted by SRDC.

Xiao, X, Hollinger, D, Aber, J, Goltz, M, Davidson, E, Zhang, Q and Moore, B (2004a). Satellite-based modelling of gross primary production in an evergreen needleleaf forest. *Remote Sensing of Environment* **89**.519-534.

Xiao, X, Zhang, Q, Braswell, B, Urbanski, S, Boles, S, Wofsy, S, Moore, B and Ojima, D (2004b). Modelling gross primary production of temperate deciduous broadleaf forest using satellite images and climate data. *Remote Sensing of Environment* **91**.256-270.

Xiao, X, Zhang, Q, Saleska, Hutryra, L, De Camargo, P, Wofsy, S, Frohking, S, Boles, S, Keller, M and Moore, B (2005). Satellite-based modelling of gross primary production in a seasonally moist tropical evergreen forest. *Remote Sensing of Environment* **94**.105-122.